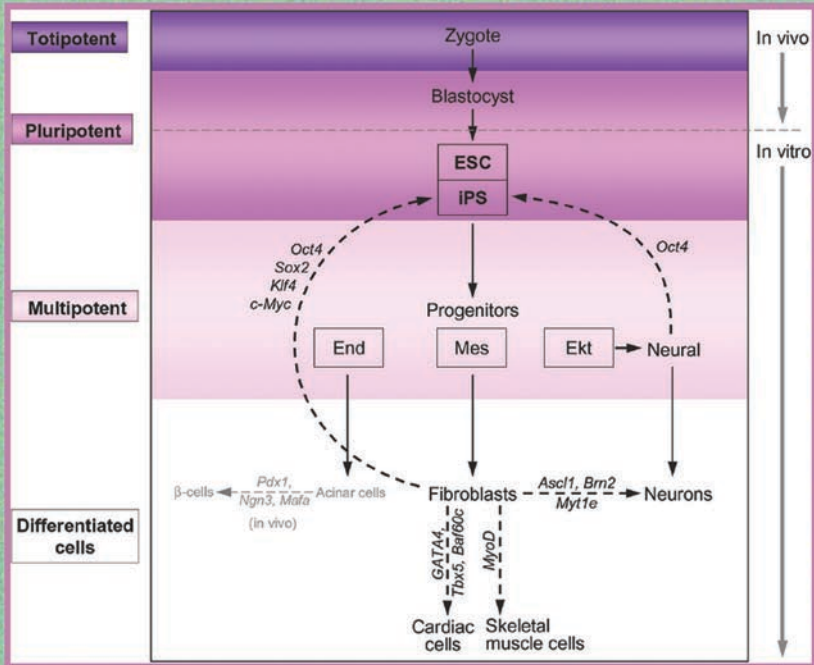


# Innovative Strategies in Tissue Engineering



Editors  
Mayuri Prasad  
Paolo Di Nardo



River Publishers

---

# **Innovative Strategies in Tissue Engineering**

---

# **RIVER PUBLISHERS SERIES IN RESEARCH AND BUSINESS CHRONICLES: BIOTECHNOLOGY AND MEDICINE**

Volume 2

---

*Series Editors*

**ALAIN VERTES**

*Sloan Fellow, London*

*Business School, Switzerland*

**PAOLO DI NARDO**

*Rome Tor Vergata, Italy*

**PRANELA RAMESHWAR**

*Rutgers University, USA*

Combining a deep and focused exploration of areas of basic and applied science with their fundamental business issues, the series highlights societal benefits, technical and business hurdles, and economic potentials of emerging and new technologies. In combination, the volumes relevant to a particular focus topic cluster analyses of key aspects of each of the elements of the corresponding value chain.

Aiming primarily at providing detailed snapshots of critical issues in biotechnology and medicine that are reaching a tipping point in financial investment or industrial deployment, the scope of the series encompasses various specialty areas including pharmaceutical sciences and healthcare, industrial biotechnology, and biomaterials. Areas of primary interest comprise immunology, virology, microbiology, molecular biology, stem cells, hematopoiesis, oncology, regenerative medicine, biologics, polymer science, formulation and drug delivery, renewable chemicals, manufacturing, and biorefineries.

Each volume presents comprehensive review and opinion articles covering all fundamental aspect of the focus topic. The editors/authors of each volume are experts in their respective fields and publications are peer-reviewed.

For a list of other books in this series, [www.riverpublishers.com](http://www.riverpublishers.com)

[http://riverpublishers.com/series.php?msg=Research and Business Chronicles:  
Biotechnology and Medicine](http://riverpublishers.com/series.php?msg=Research and Business Chronicles: Biotechnology and Medicine)

---

# Innovative Strategies in Tissue Engineering

---

**Editors**

**Mayuri Prasad**

Haematological Research Laboratory  
Department of Haematology at  
Aalborg University Hospital, Denmark

**Paolo Di Nardo, MD**

Laboratorio Cardiologia Molecolare & Cellulare  
Dip. Scienze Cliniche e Medicina Traslazionale  
Università di Roma Tor Vergata, Italy





**Published 2015 by River Publishers**  
River Publishers  
Alsbjergvej 10, 9260 Gistrup, Denmark  
www.riverpublishers.com

**Distributed exclusively by Routledge**  
4 Park Square, Milton Park, Abingdon, Oxon OX14 4RN  
605 Third Avenue, New York, NY 10017, USA

*Innovative Strategies in Tissue Engineering* / by Mayuri Prasad, Paolo Di Nardo.

© River Publishers 2015. This book is published open access.

#### **Open Access**

This book is distributed under the terms of the Creative Commons Attribution-Non-Commercial 4.0 International License, CC-BY-NC 4.0) (<http://creativecommons.org/licenses/by/4.0/>), which permits use, duplication, adaptation, distribution and reproduction in any medium or format, as long as you give appropriate credit to the original author(s) and the source, a link is provided to the Creative Commons license and any changes made are indicated. The images or other third party material in this book are included in the work's Creative Commons license, unless indicated otherwise in the credit line; if such material is not included in the work's Creative Commons license and the respective action is not permitted by statutory regulation, users will need to obtain permission from the license holder to duplicate, adapt, or reproduce the material.

The use of general descriptive names, registered names, trademarks, service marks, etc. in this publication does not imply, even in the absence of a specific statement, that such names are exempt from the relevant protective laws and regulations and therefore free for general use.

The publisher, the authors and the editors are safe to assume that the advice and information in this book are believed to be true and accurate at the date of publication. Neither the publisher nor the authors or the editors give a warranty, express or implied, with respect to the material contained herein or for any errors or omissions that may have been made.

Printed on acid-free paper.

Routledge is an imprint of the Taylor & Francis Group, an informa business

ISBN 978-87-93237-09-4 (print)

While every effort is made to provide dependable information, the publisher, authors, and editors cannot be held responsible for any errors or omissions.

---

# Contents

---

<b>Preface</b>	<b>xi</b>
<b>List of Figures</b>	<b>xiii</b>
<b>List of Abbreviation</b>	<b>xxi</b>
<b>1 Bioactive Nanocomposites with Applications in Biomedicine</b>	<b>1</b>
C.-G. Sanporean, Z. Vuluga and et al.	
1.1 Introduction . . . . .	1
1.2 Factors that Influence the Quality of a Biomaterial . . . . .	3
1.3 Layered Silicate Nanocomposites for Biomaterials . . . . .	5
1.3.1 Layered Silicate Properties . . . . .	5
1.3.2 Layered Silicate Purification . . . . .	7
1.3.3 Layered Silicate in Drug Release Systems . . . . .	8
1.3.4 Biopolymers Properties . . . . .	9
1.4 Routes for Obtaining Bio-Nanocomposites . . . . .	10
1.5 Biomaterials Development . . . . .	12
1.6 Conclusions . . . . .	16
<b>2 Cerium Dioxide Nanoparticles Protect Cardiac Progenitor Cells against the Oxidative Stress</b>	<b>25</b>
Francesca Pagliari, Giorgia Nardone and et al.	
2.1 Interaction of Cerium Oxide Nanoparticles with Biological Systems . . . . .	26
2.2 Cerium Oxide Nanoparticles Shield Cardiac Precursor Cells against the Oxidative Stress . . . . .	27
<b>3 Animals Models and <i>In Vitro</i> Alternatives in Regenerative Medicine: Focus on Biomaterials Development</b>	<b>37</b>
Monika Kozak Ljunggren, DVM, PhD and May Griffith, PhD	

3.1	Introduction . . . . .	37
3.1.1	Animals in Medical Research . . . . .	37
3.1.2	Ethical Considerations of Animal Use . . . . .	37
3.2	Designing Animal Experiments . . . . .	38
3.2.1	Randomization and Blinding . . . . .	38
3.2.2	Control Groups . . . . .	39
3.2.3	Statistical Analysis . . . . .	39
3.2.4	Design Stages . . . . .	39
3.3	Limitations of Animal Models . . . . .	39
3.3.1	Animal Species . . . . .	39
3.3.2	Health and Age Status . . . . .	40
3.3.3	Reproducibility . . . . .	40
3.4	Examples of Animal Models for Cardiac and Corneal Regenerative Medicine Testing . . . . .	41
3.4.1	Myocardial Infarct and Other Ischemic Models . . . . .	41
3.4.1.1	Myocardial coronary artery ligation . . . . .	41
3.4.1.2	Cryoinjury . . . . .	42
3.4.1.3	Hind-limb ischemia . . . . .	43
3.4.2	Corneal Transplantation Models . . . . .	43
3.4.2.1	Animal species . . . . .	43
3.4.2.2	Lamellar and penetrating keratoplasty . . . . .	44
3.4.2.3	Infectious models . . . . .	44
3.5	<i>In Vitro</i> Systems as Alternatives to Animal Testing . . . . .	45
3.5.1	<i>In Vitro</i> Corneal Equivalents for Screening Biomaterials as Potential Implants . . . . .	45
3.5.2	<i>In Vitro</i> Angiogenesis Models . . . . .	47
3.6	Conclusion . . . . .	49

**4 Differentiation Plasticity of Germline Cell-Derived Pluripotent Stem Cells and Their Potential Application in Regenerative Medicine 53**

Sharmila Fagoonee, Letizia De Chiara and et al.		
4.1	Introduction . . . . .	54
4.2	Hepatocytes Derived from GPSCs . . . . .	56
4.3	Cardiac Cells Derived from GPSCs . . . . .	57
4.4	Neuronal Cells Derived from GPSCs . . . . .	58
4.5	Hematopoietic Cells from GPSCs . . . . .	58
4.6	Vascular Cells Derived from GPSCs . . . . .	59

<b>5</b>	<b>Mechanical Stimulation in Tissue Engineering</b>	<b>67</b>
	John Rasmussen, Cristian Pablo Pennisi and et al.	
5.1	Background and Introduction . . . . .	67
5.1.1	Mechanical Theories of Material Damage . . . . .	67
5.1.2	Damage of Living Tissue . . . . .	70
5.2	Mechanical Loading in Two Dimensions . . . . .	71
5.2.1	Hertz-inspired Tissue Deformation . . . . .	72
5.2.2	Preliminary Results of Cell Straining . . . . .	75
5.3	Conclusions and Outlook . . . . .	76
<b>6</b>	<b>Immune Properties of Mesenchymal Stem Cells in the Translation of Neural Disorders</b>	<b>79</b>
	Garima Sinha, Sarah A. Bliss and et al.	
6.1	Introduction . . . . .	80
6.2	MSC Immunology . . . . .	81
6.3	MSCs and Cancer . . . . .	82
6.3.1	Role in Tumor Growth . . . . .	82
6.3.2	MSCs in Tumor Suppression . . . . .	83
6.3.3	MSC and Brain Cancer . . . . .	83
6.4	Regenerative Potential . . . . .	86
6.5	Safety . . . . .	88
6.6	Conclusion . . . . .	89
<b>7</b>	<b>Novel Design of Manufacturing Bioreactor and Facility of Cell-Based Health Care Products for Regenerative Medicine</b>	<b>97</b>
	Masahiro Kino-oka	
7.1	Introduction . . . . .	97
7.2	Bioreactor Design for Cell Processing . . . . .	98
7.3	Facility Design for Cell Processing . . . . .	100
7.4	Flexible Modular Platform Technology . . . . .	103
7.5	Acknowledgments . . . . .	104
<b>8</b>	<b>Insight into Melanoma Stem Cells: The Role of the Hedgehog Signaling in Regulating Self-Renewal and Tumorigenicity</b>	<b>107</b>
	Barbara Stecca and Roberta Santini	
8.1	Introduction . . . . .	107

8.2	Evidence for the Existence of Melanoma Stem Cells with Self-Renewing and Tumorigenic Properties . . . . .	108
8.3	The Hedgehog Signaling Pathway . . . . .	110
8.4	Role of the Hedgehog Signaling in Regulating Self-Renewal and Tumorigenicity of Melanoma Stem Cells . . . . .	112
8.5	Conclusions . . . . .	113
8.6	Acknowledgement . . . . .	114
<b>9</b>	<b>A Quest for Refocussing Stem Cell Induction Strategies: How to Deal with Ethical Objections and Patenting Problems</b>	<b>117</b>
	Hans-Werner Denker	
9.1	Introduction . . . . .	118
9.2	Potential for Autonomous Pattern Formation: Embryoid Bodies . . . . .	120
9.3	Potential for Assisted Development: Tetraploid Complementation . . . . .	121
9.4	Pluripotency, an Obstacle for Patenting . . . . .	124
9.5	Alternative Approaches . . . . .	125
9.6	Conclusions . . . . .	127
9.7	Acknowledgments . . . . .	129
<b>10</b>	<b>Constitutive Equations in Finite Viscoplasticity of Nanocomposite Hydrogels</b>	<b>135</b>
	A.D. Drozdov and J. deClaville Christiansen	
10.1	Introduction . . . . .	135
10.2	Constitutive Model . . . . .	137
	10.2.1 Kinematic Relations . . . . .	137
	10.2.2 Free Energy Density of a Hydrogel . . . . .	140
	10.2.3 Derivation of Constitutive Equations . . . . .	141
10.3	Simplification of the Constitutive Equations . . . . .	146
10.4	Fitting of Observations . . . . .	151
	10.4.1 Nanocomposite Hydrogels Subjected to Drying and Swelling . . . . .	151
	10.4.2 As-Prepared Poly(Dimethylacrylamide)–Silica Hydrogels . . . . .	153
	10.4.3 As-Prepared Polyacrylamide–Clay Hydrogels . . . . .	160
	10.4.4 Discussion . . . . .	166

10.5 Concluding Remarks . . . . . 168  
10.6 Acknowledgement . . . . . 169

**11 Regulatory Issues in Developing Advanced Therapy  
Medicinal Products with Stem Cells in Europe 173**

Maria Cristina Galli, B.Sc., Ph.D.

11.1 Introduction . . . . . 173  
11.2 European Regulatory Frame for ATMP . . . . . 174  
11.3 Stem Cell-Based ATMP . . . . . 177  
11.4 Quality Issues for Stem Cell-Based  
Product Development . . . . . 178  
11.5 Non Clinical Issues for Stem Cell-Based  
Product Development . . . . . 179  
11.6 Clinical Issues for Stem Cell-Based  
Product Development . . . . . 180  
11.7 Conclusion . . . . . 181

**Index 183**

**Editor's Biographies 185**





**Taylor & Francis**

Taylor & Francis Group

<http://taylorandfrancis.com>

---

## Preface

---

In spite of intensive investments and investigations carried out in the last decade, many aspects of the stem cell physiology, technology and regulation remain to be fully defined. After the enthusiasm that characterized the first decade of the discovery that, when given the right cue, stem cells could repair all the different tissues in the body; it is now time to start a serious and coordinated action to define how to govern the stem cell potential and to exploit it for clinical applications. This can be achieved only with shared research programs involving investigators from all over the world and making the results available to all.

The Disputationes Workshop series (<http://disputationes.info>) is an international initiative aimed at disseminating stem cell related cutting edge knowledge among scientists, healthcare workers, students and policy makers. The present book gathers together some of the ideas discussed during the third and fourth Disputationes Workshops held in Florence (Italy) and Aalborg (Denmark), respectively. The aim of this book is to preserve those ideas in order to contribute to the general discussion on organ repair and to bolster a fundamental scientific and technological leap towards the treatment of otherwise incurable diseases.

### **Editors**

Mayuri Prasad  
Paolo Di Nardo, MD



**Taylor & Francis**

Taylor & Francis Group

<http://taylorandfrancis.com>

---

## List of Figures

---

<b>Figure 1.1</b>	Montmorillonite structure . . . . .	5
<b>Figure 1.2</b>	Scheme flow for obtaining layered silicate nanocomposites . . . . .	11
<b>Figure 1.3</b>	Scheme flow for obtaining collagen based nanocomposites . . . . .	12
<b>Figure 1.4</b>	Microscopic analysis of osteoblast culture samples sowed on CG/ PB/ MA-MMA ternary nanocomposite . . . . .	13
<b>Figure 1.5</b>	Microscopic analysis of human dermal fibroblast culture samples sowed on collagen/clay/bioactive substance membranes . . . . .	14
<b>Figure 1.6</b>	Water vapour adsorption for nanocomposite membranes with quebracho and methylene blue . . . . .	14
<b>Figure 1.7</b>	Microscopic analysis of human dermal fibroblast culture samples sowed on collagen/clay/gentamicine membrane . . . . .	15
<b>Figure 1.8</b>	Gentamicin release concentration in time from collagen/layered silicate membranes . . . . .	16
<b>Figure 2.1</b>	Transmission (A) and Scanning (B) electron micrographs of CeO <sub>2</sub> nanoparticles. . . . .	29
<b>Figure 2.2</b>	Representative TEM micrograph showing CeO <sub>2</sub> NPs inside the cytoplasm of a CPC at 7 days from the administration of 50 µg/mL CeO <sub>2</sub> <i>in vitro</i> . . . . .	29
<b>Figure 2.3</b>	A) CPC proliferation assessed at 1 d, 3 d, and 7 d after 24 h CeO <sub>2</sub> exposure. The values are expressed as means ± SD of three independent experiments. (#= p > 0.05). B) Effect of H <sub>2</sub> O <sub>2</sub> on intracellular ROS levels in Lin- Sca-1pos CPCs at 7 days after CeO <sub>2</sub> treatment. ROS production, measured using a DCFH probe, decreased with all NPs concentrations tested.	

(#= H<sub>2</sub>O<sub>2</sub> treated cells vs. CeO<sub>2</sub>-H<sub>2</sub>O<sub>2</sub> treated cells). The values are expressed as means ± SD of the fold change in DCF fluorescence intensity with respect to H<sub>2</sub>O<sub>2</sub>-untreated control (ctr-) from three different tests (p < 0.05). . . . . 30

**Figure 3.1** Ischemia resulting from ligation of the LAD in a rat model. . . . . 42

**Figure 3.2** *In vivo* confocal microscopy is used after transplantation as a non-invasive means to track in-growth or overgrowth of cells and nerves into the implant, and also to detect any undesired issues, e.g. neovascularisation, inflammatory cell invasion. . . . . 44

**Figure 3.3** *In vitro* model of “cornea” with surrounding “sclera” with a nerve source embedded within the “sclera”. This allows for in-growth of neuritis into the cornea, mimicking albeit in a highly simplistic manner, the *in vivo* situation where the nerves enter the cornea from the limbal area just beyond the cornea. . . . . 46

**Figure 3.4** A) A potential hydrogel constructed is “implanted” into a 3D human corneal equivalent model to evaluate the potential for that biomaterial formulation to support growth, differentiation and stratification of corneal epithelial cells. B) Examples of poor and good epithelial growth on two different hydrogel formulations. C) After implantation of the hydrogels that supported good epithelial development into a mini-pig model, the hydrogel did indeed support epithelial re-growth with the formation of a basement membrane complex including anchoring fibrils. . . . . 47

**Figure 3.5** A) A corneal construct is “implanted” into a 3D human corneal equivalent that is supplied with a nerve source, e.g. from a ganglion. B) Nerve growth patterns within the a collagen-polyamide hydrogel as viewed by confocal microscopy. The pseudo-coloured image shows surface located neurites that are coloured red, and neurites inside the polymer, coloured green

	and blue are at depths of 5 $\mu\text{m}$ and 15 $\mu\text{m}$ , respectively. Bar, 20 $\mu\text{m}$ . . . . .	47
<b>Figure 3.6</b>	(A–E) Images of human umbilical vein endothelial cells cultured on various hydrogels after 2 days. Capillary-like networks were formed on (A) 5:1 and (B) 10:1 ratio collagen–chitosan hydrogels. (F) The average complete tube length on the different hydrogels. * $p \leq 0.003$ versus collagen; $\{p \leq 0.04$ versus all other groups. Scale bar $1/475$ mm. (G) The average complete area of tubule structure formation on the different hydrogels. * $p \leq 0.005$ versus collagen; $\{p \leq 0.0004$ versus all other groups. Reproduced from Deng C et al. (2010) . . . . .	48
<b>Figure 5.1</b>	Draping the membrane over a post by means of vacuum. The colors on the right-hand picture are membrane shear strains simulated by a 3-D model. Notice that the strain field is uniform over the post. . . . .	71
<b>Figure 5.2</b>	Finite element simulation of maximum shear strains on a membrane draped over posts with varying degrees of ovality. . . . .	72
<b>Figure 5.3</b>	Indentation of a sphere into a planar surface. The strain state will be symmetrical about the z axis, and the strain tensor at a given (r, z) position can be predicted. . . . .	73
<b>Figure 5.4</b>	Experimental setup. . . . .	74
<b>Figure 5.5</b>	Axisymmetric, nonlinear finite element model of sphere indentation into an alginate gel. . . . .	74
<b>Figure 5.6</b>	Maximum shear stress as a function of radius (r) and height (z) in a gel under compression of a circular indenter. The strain is at its maximum at (r, z) = (0, 0) i.e. directly below the center of pressure and decreases radially. . . . .	75
<b>Figure 5.7</b>	Necrosis of cells over time with different compression forces applied. . . . .	75
<b>Figure 6.1</b>	Shown is the differentiation of MSCs into neurons. <b>A.</b> MSCs are cultured from bone marrow aspirates and then subjected to differentiation to neurons. <b>B.</b> As the	



	MSCs differentiate, <i>REST</i> expression is decreased. If REST protein is rapidly decreased this could cause cell transformation. . . . .	88
<b>Figure 7.1</b>	Intelligent bioreactor system for passage automation. A; overview of the system, B; culture vessel, and C; monitoring system. . . . .	99
<b>Figure 7.2</b>	Chip bioreactor system for maturation of retina pigment epithelial cells. A; overview of the system, B; medium supplement (arrow a) unit and incubation unit (arrow b), C; chip culture vessel, and D; culture image in chip. . . . .	100
<b>Figure 7.3</b>	Proposal of manufacturing system based on flexible Modular Platform (fMP) . . . . .	104
<b>Figure 7.4</b>	Automation system of sheet assembly based on the fmp technology . . . . .	104
<b>Figure 8.1</b>	Schematic diagram of the Hh signaling pathway. In the absence of the ligand (left), the Ptch receptor suppresses the function of Smo. Full-length Gli proteins (Gli, yellow) are converted to a C-terminally truncated repressor form (Gli-R, red). Formation of the Gli-R is promoted by sequential phosphorylation of full-length Gli by GSK3 $\beta$ , PKA and CKI, which creates binding sites for the adapter protein $\beta$ -TrCP, becoming subject of ubiquitination. The Gli-R mediates transcriptional repression of target genes. In presence of the ligands (right), binding inhibits Ptch's function, which results in activation of Smo. Active Smo promotes the activation of full-length Gli proteins (Gli, green), which enters the nucleus and promotes transcription of target genes. . . . .	111
<b>Figure 9.1</b>	Strategies for stem and progenitor cell derivation and cell reprogramming. The "traditional" strategy includes a pluripotent state of cells (ESC, iPSC; above); from these pluripotent stem cells multipotent lineage-specific progenitors and finally the various differentiated cell types are derived. In case of iPSC, the cells of origin are differentiated cells (e.g. fibroblasts) which are reprogrammed by activation of the four pluripotency-associated genes Oct4, Sox2,	

Klf4 and c-Myc (Yamanaka factors; left part of diagram). The *alternative strategy* (lower part of the diagram) avoids the induction of the ethically problematic pluripotent state (*direct reprogramming, bypassing pluripotency*): In this strategy, transcription factor-induced lineage reprogramming results either in cells remaining within the same cell lineage (i.e. mesoderm), or may produce functional cells of other lineages (converting mesodermal fibroblasts into ectodermal neurons). This transcription factor-induced lineage reprogramming not only avoids the ethical problem posed by a self-organizing and cloning capability gained (e.g. TC capability) but possibly also reduces tumor-formation risks (from [48] with permission). . . . . 127

**Figure 10.1** Stress  $\sigma$  versus elongation ratio  $k$ . Symbols: experimental data in tensile tests on DMAA-NC hydrogel subjected to drying down to various  $Q_{\text{dry}}$  and subsequent re-swelling up to  $Q = 7.2$  ( $\circ$  – as-prepared;  $\bullet$  –  $Q_{\text{dry}} = 3.0$ ;  $*$  –  $Q_{\text{dry}} = 1.7$ ;  $\star$  –  $Q_{\text{dry}} = 0.8$ ;  $\diamond$  –  $Q_{\text{dry}} = 0.06$ ). Solid lines: results of simulation. . . . . 152

**Figure 10.2** Parameters  $f$  and  $J$  versus solvent content after drying  $Q_{\text{dry}}$ . Circles: treatment of observations on DMAA-NC hydrogels. Solid lines: approximation of the data by Equation (10.69). . . . . 153

**Figure 10.3** Stress  $\sigma$  versus elongation ratio  $k$ . Symbols: experimental data in tensile tests on DMAA-Si hydrogels with  $\phi_p = 142$  g/L and various  $\phi_f$  g/L ( $\circ$  – 710.5;  $\bullet$  – 284.4;  $*$  – 142.7;  $\star$  – 71.4). Solid lines: results of simulation. . . . . 154

**Figure 10.4** Parameters  $G$  and  $\tilde{G}$  versus concentration of solid phase  $\phi_s$ . Circles: treatment of observations in tensile tests on DMAA-Si hydrogels with  $\phi_p = 142$  g/L and various  $\phi_f$  g/L. Solid lines: approximation of the data by Equation (10.70). . . . . 155

**Figure 10.5** Elongation ratio for plastic deformation  $k_p$  versus elongation ratio  $k$ . Symbols: results of simulation

	for tensile tests on DMAA-Si hydrogels with $\phi_p = 142$ g/L and various $\phi_f$ g/L ( $\circ - 710.5$ ; $\bullet - 284.4$ ; $* - 142.7$ ; $\star - 71.4$ ). . . . .	156
<b>Figure 10.6</b>	Stress $\sigma$ versus elongation ratio $k$ . Symbols: experimental data in tensile tests with various strain rates $\dot{\epsilon} \text{ s}^{-1}$ ( $\circ - 0.06$ ; $\bullet - 0.6$ ) on DMAA-Si hydrogels with $\phi_p = 142.2$ g/L and $\phi_f = 142.7$ g/L (A), $\phi_f = 710.5$ g/L (B). Solid lines: results of simulation. . . . .	156
<b>Figure 10.7</b>	Dimensionless stress $\tilde{\sigma}$ (*) versus relaxation time $t'$ and moduli $G$ ( $\circ$ ), $\tilde{G}$ ( $\bullet$ ) versus loading time $t'$ . Symbols: observations on DMAA-Si hydrogels with $\phi_n = 142.2$ g/L, $\phi_f = 142.7$ g/L (A), and $\phi_f = 710.5$ g/L (B). Asterisks: experimental data in tensile relaxation test with strain $\epsilon = 0.5$ . Circles: treatment of experimental data in tensile tests with strain rates $\dot{\epsilon} = 0.06$ and $0.6 \text{ s}^{-1}$ . Solid lines: results of simulation. . . . .	157
<b>Figure 10.8</b>	Stress $\sigma$ versus elongation ratio $k$ . Symbols: experimental data in cyclic tests on DMAA-Si hydrogels with $\phi_p = 142$ g/L and various $\phi_f$ g/L ( $\circ - 710.5$ ; $\bullet - 284.4$ ; $* - 142.7$ ). Solid lines: results of simulation. . . . .	158
<b>Figure 10.9</b>	Parameters $\tilde{G}$ and $S$ versus concentration of solid phase $\phi_s$ . Circles: treatment of observations under retraction in cyclic tests on DMAA-Si hydrogels with $\phi_p = 142$ g/L and various $\phi_f$ g/L. Solid lines: approximation of the data by Equation (10.71). . . . .	159
<b>Figure 10.10</b>	Elongation ratio for plastic deformation $k_p$ versus elongation ratio $k$ . Symbols: results of simulation for cyclic tests on DMAA-Si hydrogels with $\phi_p = 142$ g/L and various $\phi_f$ g/L ( $\circ - 710.5$ ; $\bullet - 284.4$ ; $* - 142.7$ ). . . . .	159
<b>Figure 10.11</b>	Stress $\sigma$ versus elongation ratio $k$ . Symbols: observations in tensile tests with various strain rates $\dot{\epsilon} \text{ s}^{-1}$ on PAM-NC hydrogels with $\phi_p = 200$ g/L and $\phi_f = 20$ g/L ( $\circ - \dot{\epsilon} = 0.083$ ; $\bullet - \dot{\epsilon} = 0.83$ ; $\star - \dot{\epsilon} = 1.67$ ). Solid lines: results of simulation. . . . .	160

- Figure 10.12** Stress  $\sigma$  versus elongation ratio  $k$ . Symbols: observations in tensile tests with various strain rates  $\dot{\epsilon}$  s<sup>-1</sup> on PAM-NC hydrogel with  $\phi_p = 250$  g/L and  $\phi_f = 20$  g/L ( $\circ - \dot{\epsilon} = 0.083$ ;  $\bullet - \dot{\epsilon} = 0.83$ ;  $\star - \dot{\epsilon} = 1.67$ ). Solid lines: results of simulation. . . 161
- Figure 10.13** Stress  $\sigma$  versus elongation ratio  $k$ . Symbols: observations in tensile tests with various strain rates  $\dot{\epsilon}$  s<sup>-1</sup> on PAM-NC hydrogel with  $\phi_p = 100$  g/L and  $\phi_f = 40$  g/L ( $\circ - \dot{\epsilon} = 0.083$ ;  $\bullet - \dot{\epsilon} = 0.83$ ;  $\star - \dot{\epsilon} = 1.67$ ). Solid lines: results of simulation. . . 161
- Figure 10.14** Dimensionless stress  $\bar{\sigma}$  ( $\star$ ) versus relaxation time  $t'$  and modulus  $G$  versus loading time  $t'$ . Symbols: observations on PAM-NC hydrogels with  $\phi_p = 200$  g/L,  $\phi_f = 20$  g/L (A),  $\phi_p = 250$  g/L,  $\phi_f = 20$  g/L (B),  $\phi_p = 100$  g/L,  $\phi_f = 40$  g/L (C). Stars: experimental data in tensile relaxation test with strain  $\epsilon = 0.005$ . Circles: treatment of experimental data in tensile tests with various strain rates. Solid lines: results of simulation. . . . . 162
- Figure 10.15** Parameter  $S$  versus strain rate  $\dot{\epsilon}$ . Circles: treatment of observations in tensile tests on PAM-NC hydrogels with  $\phi_p = 200$  g/L,  $\phi_f = 20$  g/L (A),  $\phi_p = 250$  g/L,  $\phi_f = 20$  g/L (B),  $\phi_p = 100$  g/L,  $\phi_f = 40$  g/L (C). Solid lines: approximation of the data by Equation (10.72). . . . . 163
- Figure 10.16** Parameter  $\tilde{G}$  versus strain rate  $\dot{\epsilon}$ . Circles: treatment of observations in tensile tests on PAM-NC hydrogels with  $\phi_p = 200$  g/L,  $\phi_f = 20$  g/L (A),  $\phi_p = 250$  g/L,  $\phi_f = 20$  g/L (B),  $\phi_p = 100$  g/L,  $\phi_f = 40$  g/L (C). Solid lines: approximation of the data by Equation (10.73). . . . . 163
- Figure 10.17** Stress  $\sigma$  versus elongation ratio  $k$ . Circles: experimental data in cyclic tensile tests on PAM-NC hydrogels with  $\phi_f = 20$  g/L and  $\phi_p = 200$  g/L (A),  $\phi_p = 250$  g/L (B). Solid lines: results of simulation. . . . . 164
- Figure 10.18** Stress  $\sigma$  versus elongation ratio  $k$ . Circles: experimental data in cyclic tests on PAM-NC hydrogels with  $\phi_n = 100$  g/L and  $\phi_f = 30$  g/L (A),

	$\phi_f = 40$ g/L (B). Solid lines: results of simulation. . . . .	165
<b>Figure 10.19</b>	Parameters $G, \tilde{G}, S, J$ versus concentration of solid phase $\phi_s$ . Circles: treatment of observations under tension in cyclic tests on PAM-NC hydrogels. Solid lines: approximation of the data by Equation (10.74). . . . .	165
<b>Figure 10.20</b>	Parameters $\tilde{G}, S, K$ versus concentration of solid phase $\phi_s$ . Circles: treatment of observations under retraction in cyclic tests on PAM-NC hydrogels. Solid lines: approximation of the data by Equation (10.75). . . . .	166
<b>Figure 10.21</b>	Elongation ratio for plastic deformation $k_p$ versus elongation ratio $k$ . Symbols: results of simulation for cyclic tests on PAM-NC hydrogels ( $\circ - \phi_p = 200$ g/L, $\phi_f = 20$ g/L; $\bullet - \phi_p = 250$ g/L, $\phi_f = 20$ g/L; $* - \phi_p = 100$ g/L, $\phi_f = 30$ g/L; $\star - \phi_p = 100$ g/L, $\phi_f = 40$ g/L). . . . .	167

---

## List of Abbreviations

---

3D	three dimensional
ABCB5	ATP-binding cassette sub-family B member 5
ABCG2	ATP-binding cassette sub-family G member 2
AIFA	Agenzia Italiana del farmaco (Italian Medicine Agency)
ALDH	Aldehyde dehydrogenase
AM	acrylamide
APA	aseptic processing area
APC	Antigen Presenting Cells
ATMP	Advanced Therapy Medicinal Products
BWP	Biologics Working Party
CAPS	cell aseptic processing system
CAT	Committee for Advanced Therapy
CeO <sub>2</sub>	cerium dioxide
CHMP	Committee for Human Medicinal Products
CKI	Casein kinase 1
CPCs	cardiac progenitor cells
CPF	cell processing facility
CPWP	Cell Products Working Party
CSC	Cancer stem cells
CTMP	Cell Therapy Medicinal Products
DKK-1	Dickkopf-related protein -1
DMAA	N,N-dimethylacrylamide
DPTE	Double Porte de Transfert Etanche
EATRIS-	European Advanced Translational Research
ERIC	Infrastructure-European Research Infrastructure Consortium
EB	embryoid body
ECM	extracellular matrix
EMA/EMEA	European Medicine Agency
ESC	embryonic stem cell
EU	European Union
EU-CJ	European Court of Justice
FACS	Fluorescence-activated cell sorting



xxii *List of Abbreviations*

fMP	flexible Modular Platform
GBM	Glioblastoma multiforme
GCV	Ganciclovir
GFP	green fluorescent protein (GFP)
GSK3 $\beta$	Glycogen synthase kinase 3 beta
GTMP	Gene Therapy Medicinal Products
GTWP	Gene Therapy Working Party
HDF	human dermal fibroblast cells
hESC	Human Embryonic Stem Cells
Hh	Hedgehog
hiPSC	human induced pluripotent stem cell
HSC	Hematopoietic Stem Cells
HSV-1	herpes simplex virus type 1
IFN $\gamma$	Interferon gamma
iPSC	Induced Pluripotent Stem Cells
ISO	International Organization for Standardization
IVF-ET	<i>in-vitro</i> fertilization – embryo transfer
KPS	potassium peroxydisulfate
LAD	left anterior descending
LK	lamellar keratoplasty
MD	Medical Devices
MHC-II	Major Histocompatibility Complex II
MI	myocardial infarct
MITF	Microphthalmia-associated transcription factor
MMT	montmorillonite
MS	Member State
MSC	Mesenchymal Stem Cell
MSC	Mesenchymal/Stromal Stem Cells
NC	nanocomposite
NOD/SCID	Non-obese diabetic/severe combined immuno de?ciency disease
NPs	nanoparticles
PAM	polyacrylamide
Pax3	Paired box 3
PDMS	Polydimethylsiloxane
PGA	poly(glycolic acid)
PK	penetrating keratoplasty
PKA	Protein kinase A
PLA	poly(lactic acid)
PLGA	poly(DL- lactic-co-glycolic acid)
PLGA	poly(lactic-co-glycolic acid)

PS	primitive streak
PSC	pluripotent stem cell
Ptch	Patched
RANK	Receptor Activator of Nuclear Factor kB
RAS	Rat sarcoma
ROS	reactive oxygen species
RTP	rapid transfer port
SC	Stem Cells
Sca-1	Stem cell antigen-1
shRNA	Short hairpin RNA
Si	silica
SME	Small Medium Enterprises
Smo	Smoothened
SOD	superoxide dismutase
Sox2	Sex-determining region Y (SRY)-Box 2
Sufu	Suppressor of Fused
TC	tetraploid complementation
TEMED	tetramethylenediamine
TEP	Tissue Engineered Medicinal Products
TiO <sub>2</sub>	titanium oxide
TNF	Tumor Necrosis Factor
TSE	Transmissible Spongiform Encephalitis
VEGF	Vascular Endothelial Growth Factor



**Taylor & Francis**

Taylor & Francis Group

<http://taylorandfrancis.com>

## Bioactive Nanocomposites with Applications in Biomedicine

---

C.-G. Sanporean<sup>1</sup>, Z. Vuluga<sup>2</sup>, J.deC. Christiansen<sup>1</sup>

<sup>1</sup>Aalborg University, Department of Mechanical and Manufacturing Engineering, Aalborg, Denmark

<sup>2</sup>National Research and Development Institute for Chemistry and Petrochemistry-ICECHIM, Bucharest, Romania

Corresponding author: C.-G. Sanporean <gabi@m-tech.aau.dk>

### Abstract

Nowadays one of the big challenges is to obtain materials that can find applications in biomedicine. In order to develop tailor-made biomaterials different aspects need to be considered such as selection of materials in terms of purity, toxicity and biocompatibility, manufacturing process and final application of the new material. For such materials to be used in biomedicine, certain mechanical properties are typically desired (i.e., low friction coefficient, wear resistance, thermal stability). Nanocomposites materials have been tested for biomedical use and especially those based on layered silicates have shown great properties. Due to special properties that layered silicates possess, and by dispersing them into different polymer matrices, bioactive materials can be obtained which can find applications as: drug delivery systems and targeting into sites of inflammation or tumours, wound healing patches, covers for implants biointegration, tissue engineering, bone repair, a.s.o.

**Keywords:** Nanocomposites, biomaterials, bioactive, biocompatibility, layered silicates, collagen, scaffolds, drug delivery systems.

### 1.1 Introduction

Research in biomaterials has increased in the last years, due to promising results that have been observed and due to the versatility within these materials.

*Mayuri Prasad and Paolo Di Nardo (Eds.), Innovative Strategies in Tissue Engineering, 1–24.*

© 2014 River Publishers. All rights reserved.

## 2 *Bioactive Nanocomposites with Applications in Biomedicine*

Materials developed in this sense are important for drug delivery systems and tissue engineering approaches and can play a key role in developing of artificial organs or on growing organs.

Many types of polymers can be used as carrier systems due to their ability to provide delivery of active substances to specific sites. Moreover, such biomaterials can deliver cells to the surrounding tissue, which makes them excellent candidates for controlling the attachment, growth and differentiation of the cells [1].

Bioactive ceramics can form a mechanically strong interfacial bond with bone depending on the conditions. Thus, bioactive composites present excellent biochemical compatibility, but less optimal biomechanical compatibility. To be an ideal bone replacement material, composite biomaterials have to combine bioactivity with biomechanical properties [2].

Biomaterials can find applications in biomedicine as soft or hard implants and can be used as: joint replacements, bone cements, artificial ligaments, dental implants, blood vessels, heart valves, skin repair, contact lenses, and cochlear replacement [3].

Considering the various types of implants that can be engineered and their functions, they need to be designed with appropriate geometry, size and weight for a given patient. To obtain tailored made prosthesis, many researchers have incorporated different features to promote tissue ingrowth [4], several described rapid prototyping [5, 6] to create artificial tissue by means of computer numerical controlled machining and others used electron beam melting [7] to fabricate complex shape implants. In the future years it is overseen a dramatically increase in use of biomaterials and development of advanced materials in medical-device industry due to materials complex properties and shapes [8].

At the beginning, the only requirement for materials when they were used for the first time in biomedical applications was to be “inert” so as to reduce the inflammatory response [9]. These type of materials were classified as “first – generation” and had to possess proper combination of physical properties as for the replaced tissue with a low toxic response of the body.

The second-generation of biomaterials appeared between 1980 and 2000. They were completely opposite to the first generation in terms of interaction to the human body. These materials had the ability to interact with the biological environment, to improve their biointegration and some were bioabsorbable; they undergo degradation while the new tissue was regenerated.

The third-generation of biomaterials combines bioactivity and biodegradability with the ability to stimulate cellular response [10]. Moreover,

three-dimensional porous structures are being developed that can stimulate cell proliferation or can act as drug delivery systems [11–13]. Tissue engineering and the third-generation of biomaterials appeared approximately at the same time as a potential solution to tissue transplantation and grafting [14–16]. Regenerative medicine is a recent research area, which explores ways to repair and regenerate organs and tissues using combination of stem cells, growth factors and peptide sequences with synthetic scaffolds [17, 18].

## 1.2 Factors that Influence the Quality of a Biomaterial

Polymer matrices used in therapeutic applications are often resorbed or degraded in the body. In this case, two key challenges can be identified. First, the degradable polymers used in tissue engineering were selected from materials used for other surgical uses and thus such materials may have deficiencies in terms of mechanical and degradation properties [19]. To overcome this, new classes of polymers and biopolymers are being developed. The second major challenge concerns tailoring these polymers into scaffolds with defined and complex porous shapes, which can undergo cell attachment and proliferation [20, 21].

Biodegradable three-dimensional scaffolds play an important role in maintaining the cell functions. The cells adhere to the porous scaffold in all three directions, proliferate and replace the temporary scaffold. Moreover, the scaffold should be biodegradable, biocompatible, and highly porous with a large surface area, with a specific mechanical strength and shape to permit cell attachment, proliferation and maintaining of differentiated cell functions [22].

When obtaining a biomaterial several factors need to be considered starting with selection of raw materials in terms of purity, toxicity and biodegradability, the obtaining process and last but not least the mechanical and structural properties of the final material.

Polymer purity as well as purity of other additives is important for biocompatibility of medical devices and drug delivery systems. Residual monomers, catalyst residue or impurities strongly affect cell viability; a special consideration must be given also to the biodegradability compounds. Therefore, quality assurance of productions processes must be taken into account especially for biocompatibility of newly obtained biomaterials [23].

Many natural polymers have been extensively used in biomaterials in tissue repair and regeneration, for example collagen, gelatine and

#### 4 *Bioactive Nanocomposites with Applications in Biomedicine*

chitosan [24–27]. The use of natural polymers in tissue engineering as scaffolds or biomaterials is limited by poor mechanical properties and by the loss of biological properties during processing [28]. Thus, natural polymers in general are chemically treated or mixed with other materials to improve their mechanical properties and maintain their biological activity. However, some problems were observed in the chemical treatment of some biopolymers i.e. when collagen was modified with glutaraldehyde, which promoted calcification of heart valve [29, 30].

Implants in general are used for several years, thus they must perform adequately, must not cause locally abnormal reactions and should not produce toxic or carcinogenic effects inside the body. Similar, biodegradable scaffolds should not release toxic products or affect the healing process anyhow, while serving their intended function [31].

New approaches are needed for processing the polymers to make implants with complex architectures and macroscopic shapes, allowing the composition to change to accommodate changes in tissue development. A great challenge arises in tissue engineering from materials issues, that the biological processes are not yet well understood to set the design parameters specifically. The development of materials and understanding of biological processes take place simultaneously. The development of new materials gives indications about the complexity of biological processes, which consequently improves the design of scaffolds. From tissue engineering great challenges and opportunities arise for material science in terms of materials design and processing. Scaffolds must be designed in three-dimensional configuration and direct the cells proliferation to form the desired tissue structure, especially in a way that can be reproducible and on a large scale. From molecular point of view it is important that the new materials interact with cells controlling adhesion and proliferation phenomena [32].

Usually, implanted devices are subjected to high stresses and cycle loading; consequently, the materials used are exposed to environmental aggressive conditions inside the body, which often leads to failure. During erosion of an implanted device, fragments can be detached which can lead to an acute host-tissue reaction by producing highly corrosive enzymes and chemicals which in return will affect the biomaterial. Thus, it is necessary to develop methods for fatigue evaluation for biomaterials to understand the host-tissue reaction to fragments formation and simulate accurately *in vivo* stress-strain behaviour and environmental conditions. The development of such biomaterials with high resistance to fatigue and wear conditions is still in its early stage [33].

## 1.3 Layered Silicate Nanocomposites for Biomaterials

Nanocomposites are materials with unique properties which have found applications in wide areas of activity: aircraft industry, automotive, packaging, construction, electronics, and especially in medicine and in the pharmaceutical industry. Materials with 2 to 7% inorganic nanofillers (i.e. a layered silicate) exhibit improved properties like composites with 20 to 40% inorganic filler dispersed at macro or microscopic scale. Among these, several polymer nanocomposites have potential to be used as biomaterials in the biomedical field.

### 1.3.1 Layered Silicate Properties

Clay minerals used in nanocomposites belong to the general family of layered silicates whose main representative in terms of “utilization degree” is the montmorillonite. The crystal structure of montmorillonite consists in layers of oxyanions (with thickness of 0.95 nm), formed by fusion of two sheets of  $[\text{SiO}_4]^{4-}$  silica tetrahedral arranged in hexagonal rings with a sheet of  $[\text{AlO}_4(\text{OH})_2]$  alumina or magnesia octahedral, sandwiched between two opposing tetrahedral sheets (Figure 1.1.).

The ratio between the octahedral and tetrahedral sheets is 2:1. A feature of the montmorillonite is that it contains molecular water that is fixed by adsorption between layers. Between the layers of montmorillonite, water molecules associate in according with hexagonal symmetry. Therefore, montmorillonite formula is  $\text{Al}_2\text{O}_3 \cdot 4\text{SiO}_2 \cdot \text{H}_2\text{O} + x\text{H}_2\text{O}$  [35].

Studies of the composition of the natural montmorillonite (bentonite) showed that in the sheet of tetrahedrons,  $\text{Si}^{4+}$  ion might be partially replaced by  $\text{Al}^{3+}$  ion, and in the sheet of octahedral,  $\text{Al}^{3+}$  ion might be replaced by  $\text{Mg}^{2+}$ ,  $\text{Fe}^{2+}$ ,  $\text{Zn}^{2+}$ , etc. ions, such as, by the replacement of  $\text{Si}^{4+}$  and  $\text{Al}^{3+}$  ions with lower valence ions, resulted an excess of negative charges. To obtain the electric neutrality between layers hydrated cations  $\text{Na}^+$ ,  $\text{K}^+$ ,  $\text{Ca}^{2+}$ , etc. are adsorbed [36].

By arranging of oxyanions layers, spaces (galleries) are formed, connected by weak Van der Waals links [37]. These galleries are occupied by mobile hydrated cations that compensate the charge deficit generated by isomorphic substitution between the layers. The water from the space between the layers tends to be associated with mobile cations and forms around them “hydrated coatings”, whose number depends on the relative humidity and of cations nature between the layers [38].



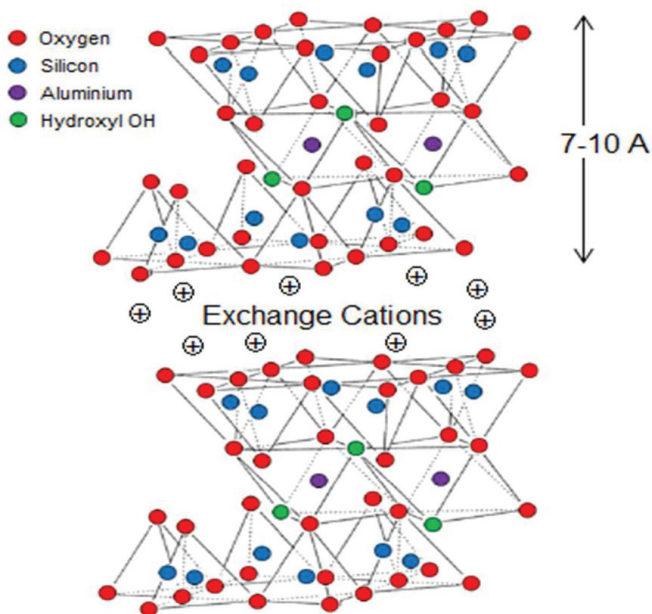


**Figure 1.1** Montmorillonite structure (Modified form [34])

Montmorillonite can absorb water increasing the volume of 20–30 times. Each layered sheet is smaller than 1 nm thick, with surface of about 1  $\mu\text{m}$  (1000 nm). For an aspect ratio (length to thickness ratio of silicate layers) of about 1000, clays specific surface area is about 750  $\text{m}^2/\text{g}$ , resulting in high reinforcement efficiency at lower clay concentrations (2–5%) [39]. However, natural layered silicates are not suitable for obtaining nanocomposites because they are too hydrophilic and layers are compacted too tightly by inorganic cations to interact with the hydrophobic molecules of polymer and to be able to disperse among them. To ensure compatibility between the clay and the polymer matrix, modification of the layered silicate surface (organophilisation) is necessary. This technology implies two steps:

- layered silicate purification to a sufficiently high level requested by the field of application;
- modification of the layered silicate surface (organophilisation).

The large specific surface area, layer charge, swelling capacity and adsorption properties of different organic/ inorganic substances make clay minerals (hydrated layered silicates) to be useful as materials for pollution control [40],

carriers of pesticides [41], liners in waste disposal [42], barriers in nuclear waste management [43] and last but not least as materials beneficial to human health.

The intelligent properties of clays are known from antiquity in all part of the world: antiseptic, bactericides, scar action, antitoxic properties, sans microbial germs. Since prehistoric times, a large variety of clays and clay minerals (i.e. bentonite, kaolinite, montmorillonite, smectite) have been used for therapeutic purposes, including the treatment of wounds, inhibition of haemorrhages and as a preservative in mummification (in ancient Egypt), used as antiseptic cataplasms to cure skin diseases, as scars, or as an anti-inflammatory agent for snake bites [44]. Based on the capacity to adsorb and retain harmful and toxic substances, the mineral clays have beneficial effects in the treatment of gastrointestinal disorders. Clays can adsorb a variety of toxic substances, such as toxins, pesticides, viruses, bacteria, and other digestive irritant [45]. However, clay minerals can be harmful to human health when they are inhaled over a very long period. The toxicity of these minerals is generally related to the presence of very fine-grained quartz and cristobalite in the range from 0 to 24% [46], which inhaled in the lung, can cause cancer. For this reason, the purification process of clay minerals is very important especially for uses in biomedicine.

### 1.3.2 Layered Silicate Purification

Usually, the natural layered silicates are mixtures or associations of minerals and/or amorphous materials. In order to enrich one clay mineral and/or to remove other unwanted clay mineral, a purification step is necessary. Purification is also required for identification and for characterization of clay minerals. Very important is the chemical composition of layered silicates when they are used as reinforcing agent for preparing nanocomposites. The final properties of nanocomposites depend on stable compositions. The montmorillonite (MMT) is the most important layered silicate used for preparation of nanocomposites. Different minerals such as quartz, zeolite, calcite, feldspar and pyrite have a great effect on the composition and influence the purification technology [47].

The purification procedure involves two main steps: one of them consists in removal of carbonates, hydroxides, and organic materials and the other one consists in fractionation by sedimentation. However, not all the purification steps are always necessary. The purification of layered silicates from identified

geological deposits consists in replacing the exchangeable cations with  $\text{Na}^+$  followed by washing with water.

The natural layered silicates (bentonites) may contain different percentages (5–40%) of quartz and other impurities, which act as a sterile, hindering the surface modification process, in order to ensure the compatibility between the silicate and a polymer matrix [48]. Purification is made by dispersing the layered silicate in distilled water at 60–90 °C. Quartz and other hydrophobic impurities are separated by decantation [49]. Often is required additional purification to ensure a high degree of purity, imposed in the biomedical field. By additional purification, the concentration of MMT increases with 7–10% [49].

### **1.3.3 Layered Silicate in Drug Release Systems**

Layered silicates are widely used ingredients in pharmaceutical products as both excipients and active substances. Based on their adsorption capacities, swelling and colloidal properties, clay minerals can be used in drug delivery systems to achieve technological (taste masking), chemical (increasing stability), biopharmaceutical (decreasing or increasing dissolution rate, delaying and/or targeting drug release) and pharmacological (prevention or reduction of side effects) benefits [50].

Layered silicates, especially montmorillonite and saponite, because of their high cation exchange capacity, were used and studied in controlled-release drug delivery systems. The interaction between clay minerals and active substances depends on the type of mineral involved and on the functional groups and the properties of the organic compounds.

There are some mechanisms of interaction or complexation between montmorillonite and drug [51–67]:

- Cation exchange with cationic drugs. This produces a strong interaction bonds between montmorillonite and basic molecules;
- Anion exchange of anionic drugs at slightly positive-charged platelet edges. This produces weak interaction bonds with anionic drugs;
- Hydrogen bonding at platelet faces;
- Intercalation of non-ionic drugs via ion-dipole interactions;
- Adsorption by solvent deposition onto the high surface area of the clay to increase the dissolution rate of poorly soluble drugs.

Depending on the degree of interaction between montmorillonite and drug, nanostructured systems with intercalated, partial exfoliated or exfoliated

lamellar structures, able to release faster or slowly the bioactive substance could be obtained [68].

#### 1.3.4 Biopolymers Properties

Biopolymers are materials produced from renewable resources. In recent years, the worldwide interest in biopolymers increased due to their positive environmental impact such as reduced carbon dioxide emissions. Many biopolymers are biodegradable, being degraded and gradually absorbed and/or eliminated by the body. This property is of high interest for biomedical applications (tissue engineering, bone replacement/repair, dental applications and controlled drug delivery).

Many biomedical applications require biomaterials with high performance and mechanical properties. For such materials to be used in biomedicine is not enough to be biocompatible and biodegradable, certain mechanical properties are imposed (i.e., low friction coefficient, wear resistance, thermal stability, modulus, strength and toughness). Not all these properties can be achieved by using the biopolymer alone [69–71]. By dispersion of inorganic/organic fillers at the nanometer scale into a biopolymer matrix, new class of bionanocomposites, with enhanced mechanical properties as compared to conventional microcomposites, was developed.

One of the most researched and used biomaterial in various fields of medicine is collagen, due to its biocompatibility, biodegradability, and weak antigenicity [72]. It is well known the use of collagen as biomaterial, biocompatible and bioresorbable for connective tissue prosthesis in which collagen is the basic protein. To use collagen as a scaffold in bone reconstruction, modifications are necessary in the structure and composition of the matrix to achieve the osteoconductive and osteoinductive effect. This was achieved by preparation of biocomposites with  $\text{SiO}_2$ ,  $\text{TiO}_2$ , clays, hydroxyapatite, etc. [73, 74]. The collagen fibrils have high elasticity while the mechanical properties are relatively limited. Substantial improvement of its properties can be achieved by the nanoscale dispersion of the layered silicate in a collagen matrix. Depending on the collagen morphologies, nanocomposites with intercalated or exfoliated lamellar structures and improved thermal stability were obtained [75].

In order to use a material in biomedicine, both its bulk and surface properties are important to be known, especially interfacial behaviour with aqueous environment. The wettability capacity, the swelling behaviour, the presence of surface roughness, liquid and vapour water absorption are only

a few of the properties required for biomaterials with biomedical purposes. Valuable informations about these properties were achieved by water contact angle and determination of water absorbency [68].

## **1.4 Routes for Obtaining Bio-Nanocomposites**

In literature, there have been described three main processes to prepare polymer layered silicate nanocomposites [76]:

The first process is known as intercalation from solution. The layered silicate is swelled in the same solvent in which the polymer is soluble. Using an adequate solvent and due to the weak forces that are between silicate platelets, the sheets of layered silicate can be dispersed and form a stable suspension. Furthermore, the solvated polymer penetrates into the silicate galleries. In this way the sheets are delaminated and an ordered multi-layered structure is formed when the solvent is evaporated [77, 78].

The second technique also takes place in solution and is called in situ intercalative polymerization. As compared to the previous one, this time the silicate is swelled into liquid monomer or prepolymer followed by polymerization reaction. This reaction takes place between the silicate platelets if the initiator is introduced in the swelling step or in special cases if the sample is subjected to heat or radiation [77, 78].

Melt intercalation technique is the third process in which the already modified clay is mixed with melted polymer [77]. To obtain nanocomposites in which the polymer melt must be intercalated between modified silicates, a temperature with 10–12 °C higher than polymer softening temperature is required when using static or shear stress thermal treatment [79]. In this case, no solvent is involved and thus if the compatibility between polymer and modified silicate is good enough, intercalated or exfoliated nanocomposites can be formed [78].

It has been demonstrated that melt intercalation technique is more effective in terms of dispersion rather than intercalation of a monomer followed by polymerization or by intercalation of a polymer from solution [80]. However, when obtaining nanocomposite biomaterials, other aspects need to be considered, hence all these techniques have some limitations. There are biopolymers like collagen, which cannot be extruded or melted due to low polymer degradation temperature.

Intercalative polymerization technique can be used to obtain nanocomposite biomaterials if the solvent in which the polymer is soluble should not produce toxic or carcinogenic effects, since traces of solvent may still be present in the final material.

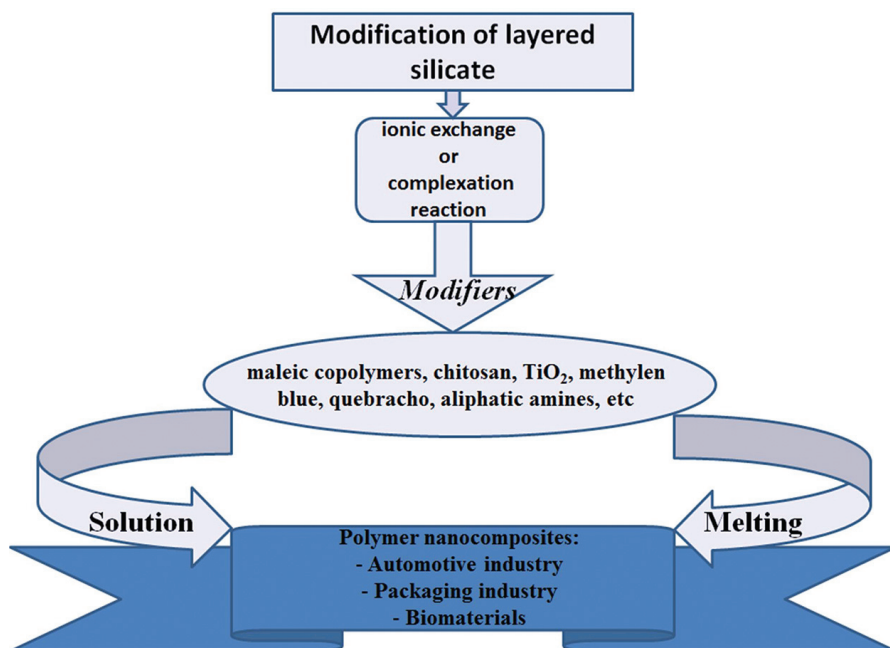
Among all techniques, in situ intercalative polymerization presents most limitations, since traces of monomer, initiator and other impurities, which can produce abnormal reactions inside the body, may still be present in the scaffold.

Figure 1.2 synthesise the main steps for obtaining a nanocomposite, furthermore one must take into consideration all the implications discussed above and the factors that influence the quality of a biomaterial.

Complex polymer bio-nanocomposite materials are being developed as scaffolds, tissue regenerating patches and control drug release systems for the hope of better and faster treatment of diseases. Implants in general must have superior performance and mechanical properties as well as biological function. Thus, facing these challenges, implants properties and design can be tailored so to optimize the functionality and performance [81].

Taking into consideration the final application of the scaffold and the necessity to create biomaterials with complex structures, porous matrices or transparent membranes can be obtained (Figure 1.3.)

Porous scaffolds play an important role in tissue engineering and they were used to construct cartilage, bone, skin, ligaments a.s.o [82–85]. Three



**Figure 1.2** Scheme flow for obtaining layered silicate nanocomposites

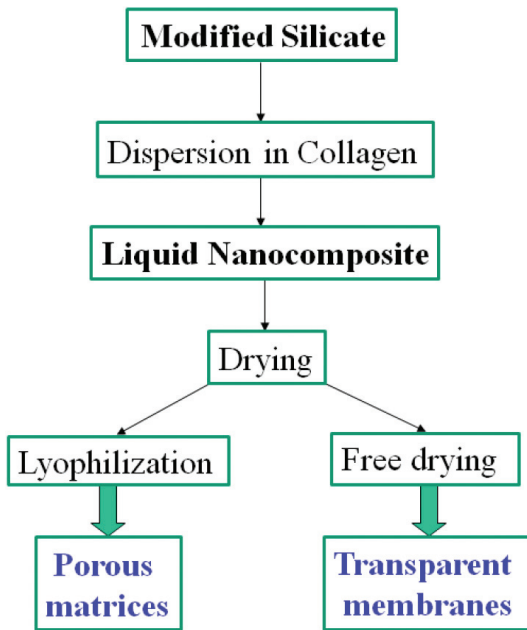


**Figure 1.3** Scheme flow for obtaining collagen based nanocomposites

dimensional porous scaffolds can be obtained from synthetic polymers such as poly(glycolic acid) (PGA), poly(lactic acid) (PLA), and their copolymer poly(DL- lactic-co-glycolic acid) (PLGA), and from naturally derived polymers such as collagen [86–88].

To obtain hybrid collagen microsponges, gaseous glutaraldehyde was used as cross-linking agent to form their pores and to stabilize the collagen in water [22, 89, 90].

## 1.5 Biomaterials Development

The quality of biomaterials is strongly influenced by composition, architecture and three-dimensional design, biocompatibility, but also by mechanical strength of the scaffold that mimics the mechanical strength of the tissue intended to repair or replace. Pore size distribution as well as pore types influences the attachment of specific cells and interaction of biomaterials with the body. Furthermore, it is important also to identify and isolate the appropriate cells from the primary source, when selecting the cells for the engineered scaffold [91].

In the recent years, more and more encouraging results are being obtained. Biomaterials that may find applications in bone tissue engineering were developed which showed impressive results. Such hybrids were synthesised by dispersing of layered silicate modified with maleic anhydride methyl methacrylate copolymer into collagen gel denoted CG/PB/MA-MMA. Nanocomposites in form of microporous matrix (scaffold) having a spongy structure, which contains macro, and micro interconnected nanopores were obtained at different pH's using freeze-drying technique.

The spongy matrix was *in vitro* tested on osteoblast cell cultures and followed after 24 and 72 hours from hatching. Figure 1.4. presented that cells proliferated on the ternary nanocomposite and no cytotoxic response was observed. The cells presented normal phenotype and moreover, the viability was reported to be 97% [49].

Layered silicate/collagen membranes with different amounts of methylene blue and quebracho were also obtained and their biocompatibility was tested

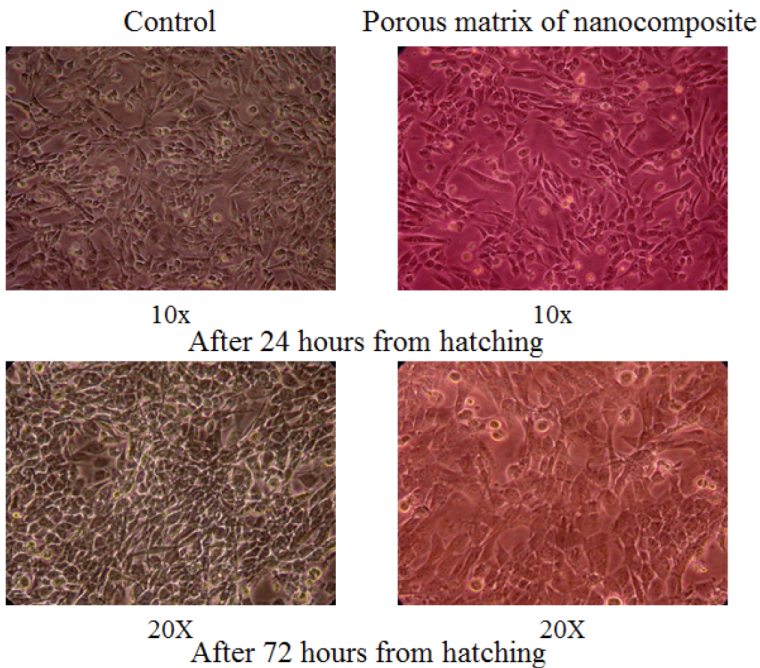


**Figure 1.4** Microscopic analysis of osteoblast culture samples sowed on CG/PB/MA-MMA ternary nanocomposite (Originally published in [49] under CC BY 3.0 license. Available from: <http://dx.doi.org/10.5772/25947>).



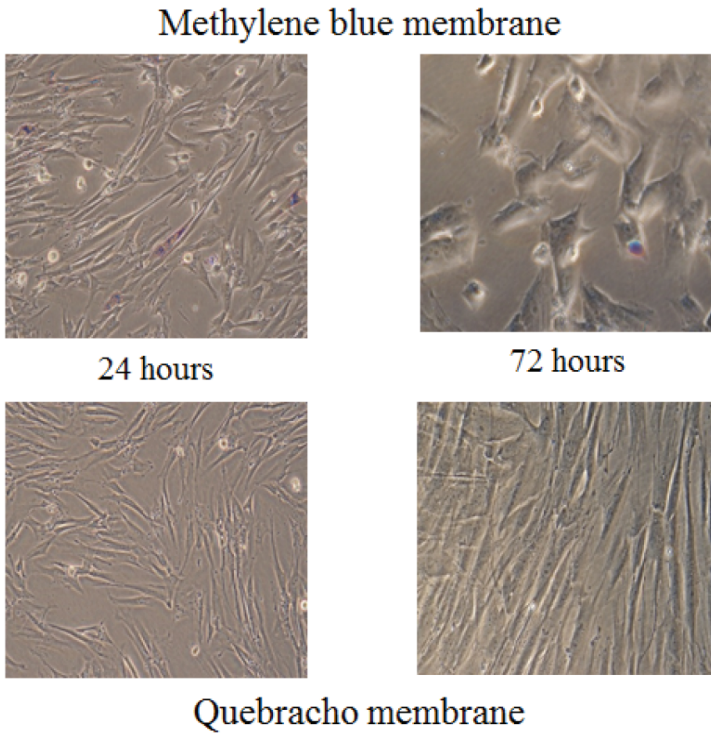


**Figure 1.5** Microscopic analysis of human dermal fibroblast culture samples sowed on collagen/clay/bioactive substance membranes (Reproduced with permission from [92])

on human dermal fibroblast (HDF) cells. Figure 1.5. presents *in vitro* results after 24 and 72 hours, respectively. The cells were uniformly distributed and presented a normal phenotype after 24 h. However, quebracho membrane showed a 99% cell viability as compared to methylene blue membrane which after 72 h presented only 30% viable cells [92].

Water vapour adsorption was also tested for the same type of materials and compared to collagen membrane. Figure 1.6. shows the adsorption curves of the membranes for 48 hours. It was observed that the collagen membrane presented a continuous increasing variation as compared to nanocomposite membranes. The hybrids continuously adsorbed water vapours in the first 24 hours from exposure, then reached a plateau and the adsorption remained constant [92].

These findings showed that such type of materials especially the membrane with quebracho, which presented a biostimulating effect on the growth

and development of fibroblast cells, could be used as antiseptic and good regenerating patches [92].

Other collagen/layered silicate nanocomposites which contained gentamicin as active substance were obtained. *In vitro* biocompatibility test was performed on human dermal fibroblast cells and the results were compared to a collagen membrane as it can be seen in Figure 1.7. The layered silicate increased the biocompatibility of the materials; the cells presented a normal phenotype and proliferated. As compared to the collagen

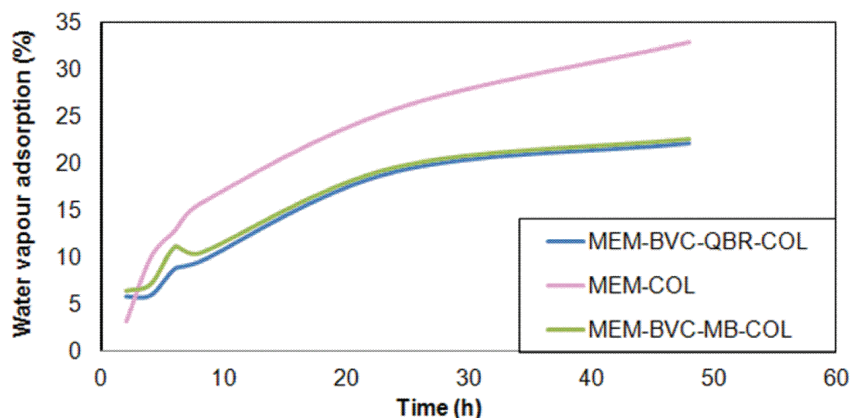
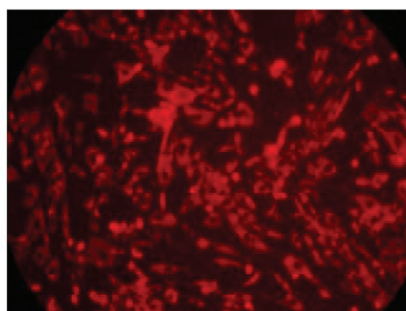


**Figure 1.6** Water vapour adsorption for nanocomposite membranes with quebracho and methylene blue (Reproduced with permission from [92])



Collagen membrane



Collagen/Clay/Gentamicine  
Membrane

**Figure 1.7** Microscopic analysis of human dermal fibroblast culture samples sowed on collagen/clay/gentamicine membrane (Reproduced with permission from [74])

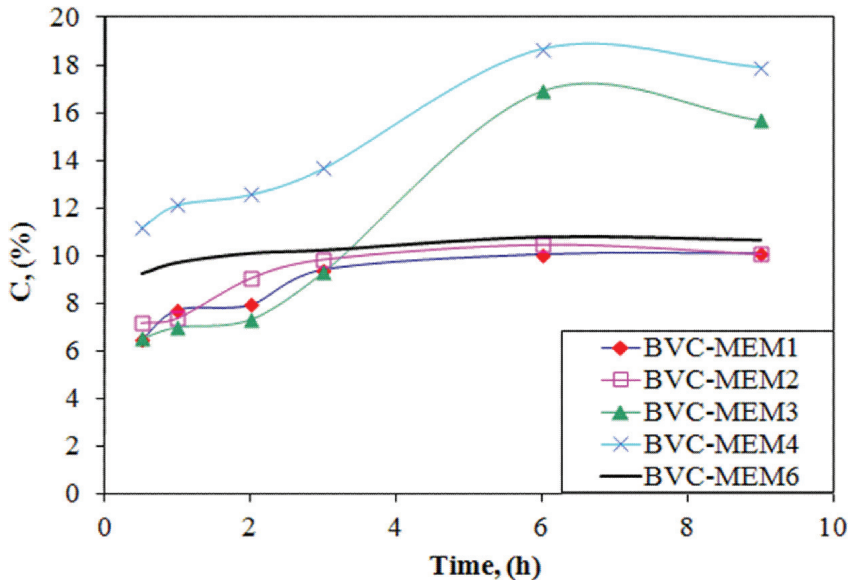


**Figure 1.8** Gentamicin release concentration in time from collagen/layered silicate membranes (Reproduced with permission from [74])

membrane, the viability of the cells increased which showed that gentamicine had a positive effect on cells viability and diminished the cytotoxic effect.

In Figure 1.8. it is presented the drug release capacity of gentamicine from such membranes. This is evidence that these materials can act like drug delivery systems [75], moreover it shows that the drug release can be tailored by changing the order of introducing the components when mixing the materials [74].

## 1.6 Conclusions

Today, advances in tissue engineering are extending the possibility to treat and heal diseases that have put medicine in difficulty. To achieve a successful development in this field, researchers from various disciplines like biology, medicine, material science, mechanical engineering a.s.o. have to cooperate. It has been showed that there is the possibility to tailor biomaterials so to obtain scaffolds with specific properties. Moreover, nanotechnology is accelerating the development of biomaterial-based systems with effective

individual approaches. However, from material science point of view to ensure a successful development of biomaterials, certain aspects need to be considered to realize their maximum potential:

- The raw materials must be selected from natural based resources so they exhibit good compatibility with the human body and must be as pure as possible to avoid inflammatory response.
- While processing the material, contamination with impurities, residual initiator or catalyst, which can affect the biocompatibility and biointegration of implant and additionally cytotoxic and carcinogenic effects, must be avoided.
- Materials must be selected such that cell adhesion and/or proliferation occur so the scaffolds perform as intended.
- Performance of scaffolds must be considered from mechanical point of view, so that the implant should resist to fatigue and cyclic loading as long as possible.
- Last but not least and probably most important, the final application of the scaffold needs to be considered starting from materials selection.

The successful development in this field lies in the complexity and understanding of how to rationally design biomaterials. Even though there is no ideal biomaterial that satisfies all the requirements needed for implants, the possibility to regenerate tissues and organs and even more to grow organs from stem cells should not be neglected. The possibility to modify surfaces and obtain tailored materials constitutes one of the major breakthroughs because it opens new horizons in this young field of study.

## References

- [1] G. Orive, E. Anitua, J. L. Pedraz, D. F. Emerich, 'Biomaterials for promoting brain protection, repair and regeneration', *Nature Reviews*, pp. 682–692, 10, 2009.
- [2] W. Cao, L. L. Hench, 'Bioactive Materials', *Ceramics International*, pp. 493–507, 22, 1996.
- [3] A. Tathe, M. Ghodke, A. P. Nikalje, 'A brief review: biomaterials and their application', *International Journal of Pharmacy and Pharmaceutical Sciences*, pp. 19–23, 2, 2010.
- [4] A. Ovsianikov, B. Chichkov, O. Adunka, H. Pillsbury, A. Doraiswamy, R. J. Narayan, 'Rapid prototyping of ossicular replacement prostheses', *Appl. Surf. Sci.*, pp. 6603–6607, 253, 2007.

- [5] Y. He, M. Ye, C. Wang, 'A method in the design and fabrication of exact-fit customized implant based on sectional medical images and rapid prototyping technology', *Int. J. Adv. Manuf. Technol.*, pp. 504–508, 28, 2006.
- [6] T. Burg, C. A. P. Cass, R. Groff, M. Pepper, K. J. L. Burg, 'Building off-the-shelf tissue engineered composites', *Phil. Trans. R. Soc. A*, pp. 1839–1862, 368, 2010.
- [7] L. E. Murr, S. M. Gaytan, F. Medina, H. Lopez, E. Martinez, B. I. Machado, D. H. Hernandez, L. Martinez, M. I. Lopez, R. B. Wicker, J. Bracke, 'Next-generation biomedical implants using additive manufacturing of complex, cellular and functional mesh arrays', *Phil. Trans. R. Soc. A*, pp. 1999–2032, 368, 2010.
- [8] R. J. Narayan, 'The next generation of biomaterial development', *Phil. Trans. R. Soc. A*, pp. 1831–1837, 368, 2010.
- [9] L. L. Hench, 'Biomaterials', *Science*, pp. 826–831, 208, 1980.
- [10] L. L. Hench, J. Polak, 'Third generation biomedical materials', *Science*, pp. 1014–1017, 295, 2002.
- [11] D. Hutmacher, M. B. Hurzeler, H. Schliephake, 'A review of material properties of biodegradable and bioresorbable polymer for GTR and GBR', *J. Oral Maxillofac. Implants*, pp. 667–678, 11, 2000.
- [12] J. S. Temenoff, A. G. Mikos, 'Tissue engineering for regeneration of articular cartilage', *Biomaterials*, pp. 431–440, 21, 2000.
- [13] C. M. Agrawal, R. B. Ray, 'Biodegradable polymeric scaffolds for musculoskeletal tissue engineering', *J. Biomed. Mater. Res.*, pp. 141–150, 55, 2001.
- [14] J. C. Fernyhough, J. J. Schimandle, M. C. Weigel, C. C. Edwards, A. M. Levine, 'Chronic donor site pain complicating bone graft harvest from the posterior iliac crest for spinal fusion', *Spine*, pp. 1474–1480, 17, 1992.
- [15] J. C. Banwart, M. A. Asher, R. S. Hassanein, 'Iliac crest bone graft harvest donor site morbidity. A statistical evaluation', *Spine*, pp. 1055–1060, 20, 1995.
- [16] J. A. Goulet, L. E. Senunas, G. L. DeSilva, M. L. V. H. Greengield, 'Autogenous iliac crest bone graft. Complications and functional assessment', *Clin. Orthop.*, pp. 76–81, 339, 1997.
- [17] P. Hardouin, K. Anselme, B. Flautre, F. Bianchi, G. Bascouluget, Bouxin, B. 'Tissue engineering and skeletal diseases', *Joint Bone Spine*, pp. 419–424, 67, 2000.

- [18] M. Navarro, A. Michiardi, O. Castano, J. A. Planell, 'Biomaterials in orthopaedics', *J. R. Soc. Interface*, pp. 1137–1158, 5, 2008.
- [19] L. G. Griffith, 'Emerging design principles in biomaterials and scaffolds for tissue engineering', *Ann. NY Acad. Sci.*, pp. 83–95, 961, 2002.
- [20] L. G. Griffith, M. A. Schwartz, 'Capturing complex 3D tissue physiology *in vitro*', *Nat. Rev. Mol. Cell. Biol.*, pp. 211–224, 7, 2006.
- [21] A. D. Metcalfe, M. W. J. Ferguson, 'Tissue engineering of replacement skin: the crossroads of biomaterials, wound healing, embryonic development, stem cells and regeneration', *J. R. Soc. Interface*, pp. 413–437, 4, 2007.
- [22] G. Chen, T. Ushida, T. Tateishi, 'Development of biodegradable porous scaffolds for tissue engineering', *Materials Science and Engineering C*, pp. 63–69, 17, 2001.
- [23] R. Zange, Y. Li, T. Kissel, 'Biocompatibility testing of ABA triblock copolymers consisting of poly(L-lactic-co-glycolic acid) A blocks attached to a central poly(ethylene oxide) B block under *in vitro* conditions using different L929 mouse fibroblasts cell culture models', *Journal of Controlled Release*, pp. 249–258, 56, 1998.
- [24] J. J. Grzesiak, M. D. Pierschbacher, M. F. Amodeo, T. I. Malaney, J. R. Glass, 'Enhancement of cell interactions with collagen/glycosaminoglycan matrices by RGD derivatization', *Biomaterials*, pp. 1625–1632, 18, 1997.
- [25] S. Sofia, B. M. McCarthy, G. Gronowicz, D. L. Kaplan, 'Functionalized silk-based biomaterials for bone formation', *J Biomed Mat Res*, pp. 139–148, 54, 2001.
- [26] P. J. VandeVord, H. W. T. Matthew, S. P. DeSilva, L. Mayton, B. Wu, P. H. Wooley, 'Evaluation of the biocompatibility of a chitosan scaffold in mice', *J Biomed Mater Res*, pp. 585–590, 59, 2002.
- [27] A. G. A. Coombes, E. Verderio, B. Shaw, X. Li, M. Griffin, S. Downes, 'Biomposites of non-crosslinked natural and synthetic polymers', *Biomaterials*, pp. 2113–2118, 23, 2002.
- [28] J. A. Hubbell, 'Biomaterials in tissue engineering', *Biotechnology*, 565–576, 13, 1995.
- [29] F. J. Schoen, R. J. Levy, 'Bioprosthetic heart valve failure: pathology and pathogenesis', *Cardiol Clin*, pp. 717–739, 2, 1984.
- [30] J. Dong, Q. Sun, J.-Y. Wang, 'Basic study of corn protein, zein, as a biomaterial in tissue engineering, surface morphology and biocompatibility', *Biomaterials*, pp. 4691–4697, 25, 2004.

- [31] K. A. Athanasiou, G. G. Niederauer, C. M. Agrawal, 'Sterilization, toxicity, biocompatibility and clinical applications of polylactic acid/ polyglycolic acid copolymers', *Biomaterials*, pp. 93–102, 17, 1996.
- [32] L. G. Griffith, 'Polymeric biomaterials', *Acta mater.*, pp. 263–277, 48, 2000.
- [33] S. H. Teoh, 'Fatigue of biomaterials: a review', *International Journal of Fatigue*, pp. 825–837, 22, 2000.
- [34] K. Magniez, 'Development of novel melt-spun nanocomposite fibers', *Society of Plastics Engineers*, pp. 1–3, 10.1002/spepro.003802, 2011.
- [35] O. Solacolu, 'Physical chemistry of technical silicates', Second Edition, Technical Publishing, Bucharest, 1968.
- [36] J. C. Hutchison, R. Bissessur, D. F. Shriver, 'Enhancement of ion mobility in alumino-silicate-polyphosphazene nanocomposites', *Mat. Res. Soc. Symp. Proc.*, pp. 489–494, 457, 1997.
- [37] R. A. Vaia, E. P. Giannelis, 'Lattice model of polymer melt intercalation in organically-modified layered silicates', *Macromolecules*, pp. 7990–7999, 30, 1997.
- [38] B. K. G. Theng, 'Formation and properties of clay - polymer complexes', Elsevier Scientific Publishing Co., Amsterdam, Oxford, New York, 1979.
- [39] R. L. D'Aquino, 'A little clay goes a long way', *Chem. Eng. Mag.*, pp. 1–2, 106, 1999.
- [40] G. J. Churchman, W. P. Gates, B. K. G. Theng G. Yuan, 'Clays and clay minerals for pollution control', *Handbook of Clay Science*, pp. 625–675, Elsevier, Oxford, UK, 2006.
- [41] S. Nir, Y. El Nahhal, T. Undabeytia, G. Rytwo, T. Polubesova, Y. Mishael, U. Rabinovitz, B. Rubin, 'Clays and pesticides', *Handbook of Clay Science*, pp. 677–691, Elsevier, Oxford, UK, 2006.
- [42] K. Czurda, 'Clay liners and waste disposal', *Handbook of Clay Science*, pp. 693–701, Elsevier, Oxford, UK, 2006.
- [43] R. Pusch, 'Clays and nuclear waste management', *Handbook of Clay Science*, pp. 703–716, Elsevier, Oxford, UK, 2006.
- [44] M. I. Carretero, C. S. F. Gomes, F. Tateo, 'Clays and human health', *Handbook of Clay Science*, pp. 717–741, Elsevier, Oxford, UK, 2006.
- [45] M. T. Droy-Lefaix, F. Tateo, 'Clays and clay minerals as drugs', *Handbook of Clay Science*, pp. 743–752, Elsevier, Oxford, UK, 2006.
- [46] M. Ross, R. P. Nolan, A. M. Langer, W. C. Cooper, 'Health effects of mineral dusts other than asbestos', *Health Effects of Mineral Dusts*.

- Reviews in Mineralogy, pp. 361–409, 28, Mineralogical Society of America, Washington, DC, 1993.
- [47] Y. C. Ke, P. Stroeve ‘Polymer-layered silicate and silica nanocomposites’, Elsevier B. V., 2005.
- [48] K. A. Carrado, ‘Synthetic clay minerals and purification of natural clays’, Handbook of Clay Science, pp. 115–139, Elsevier, Oxford, UK, 2006.
- [49] Z. Vuluga, G. C. Potarniche, M. G. Albu, V. Trandafir, D. Iordachescu, E. Vasile, ‘Collagen - modified layered silicate biomaterials for regenerative medicine of bone tissue’, Materials Science and Technology, pp. 125–148, InTech, 2012.
- [50] C. Aguzzi, P. Cerezo, C. Viseras, C. Caramella, ‘Use of clays as drug delivery systems: Possibilities and limitations’, Applied Clay Science, pp. 22–36, 36 (1–3), 2007.
- [51] Y. Chen, A. Zhou, B. Liu, J. Liang, ‘Tramadol hydrochloride/montmorillonite composite: Preparation and controlled drug release’, Appl. Clay Sci., pp. 108–112, 49 (3), 2010.
- [52] M. S. Lakshmi, M. Sriranjani, H. B. Bakrudeen, A. S. Kannan, A. B. Mandal, B. S. R. Reddy, ‘Carvedilol/montmorillonite: Processing, characterization and release studies’, Appl. Clay Sci., pp. 589–593, 48 (4), 2010.
- [53] G. V. Joshi, B. D. Kevadiyaa, H. A. Patel, H. C. Bajaj, R. V. Jasrab, ‘Montmorillonite as a drug delivery system: Intercalation and *in vitro* release of timolol maleate’, Int. J. Pharm., pp. 53–57, 374, 2009.
- [54] N. Meng, N. Zhou, S. Zhang, J. Shen, ‘Controlled release and antibacterial activity chlorhexidine acetate (CA) intercalated in montmorillonite’, Int. J. Pharm., pp. 45–49, 382 (1–2), 2009.
- [55] J. K. Park, Y. B. Choy, J.-M. Oh, J. Y. Kima, S.-J. Hwanga, J. H. Choy, ‘Controlled release of donepezil intercalated in smectite clays’, Int. J. Pharm., pp. 198–204, 359, 2008.
- [56] J. P. Zheng, L. Luan, H. Y. Wang, L. F. Xi, K. D. Yao, ‘Study on ibuprofen/montmorillonite intercalation composites as drug release system’, Appl. Clay Sci., pp. 297–301, 36, 2007.
- [57] T. Kollár, I. Palinko, Z. Konya, I. Kiricsi, ‘Intercalating amino acid guests into montmorillonite host’, J. Mol. Struct., pp. 335–340, 651–653, 2003.
- [58] F. H. Lin, Y. H. Lee, C. H. Jian, ‘A study of purified montmorillonite intercalated with 5-fluorouracile as drug carrier’, Biomaterials, pp. 1981–1987 23 (9), 2002.



- [59] M. J. Sanchez, M. Sanchez-Camazano, M. T. Vicente, A. Dominguez-Gil, 'Physicochemical study of the adsorption of oxprenolol hydrochloride by montmorillonite', *Drug Dev. Ind. Pharm.*, pp. 1019–1029, 9 (6), 1983.
- [60] M. R. Harris, J. W. McGinity, 'Optimization of slowrelease tablet formulations containing montmorillonite. II. Factors affecting drug release', *Drug Dev. Ind. Pharm.*, pp. 783–793, 8, 1982.
- [61] M. R. Harris, J. W. McGinity, 'Optimization of slowrelease tablet formulations containing montmorillonite. III. Mechanism of release', *Drug Dev. Ind. Pharm.*, pp. 795–809, 8, 1982.
- [62] J. W. McGinity, J. A. Hill, 'Influence of monovalent and divalent electrolytes on sorption of neomycin sulfate to attapulgite and montmorillonite clays', *J. Pharm. Sci.*, pp. 1566–1568, 64 (9), 1975.
- [63] J. W. McGinity, J. L. Lach, 'Sustained-release applications of montmorillonite interaction with amphetamine sulphate', *J. Pharm. Sci.*, pp. 63–66, 66 (1), 1977.
- [64] J. W. McGinity, M. R. Harris, 'Optimization of slow release tablet formulations containing montmorillonite. I. Properties of tablets', *Drug Dev. Ind. Pharm.*, pp. 399–410, 6 (4), 1980.
- [65] M. Sánchez-Camazano, M. J. Sánchez Martín, M. T. Vicente, A. Dominguez-Gil, 'Adsorption of chlorpheniramine maleate by montmorillonite', *Int. J. Pharm.*, pp. 243–251, 6, 1980.
- [66] T. Takahashi, M. Yamaguchi, 'Host-guest interaction between swelling clay minerals and poorly water-soluble drugs: 1. Complex formation between a swelling clay mineral and griseofulvin', *J. Incl. Phenom. Mol. Recognit. Chem.*, pp. 283–297, 10, 1991.
- [67] T. Takahashi, M. Yamaguchi, 'Host-guest interaction between swelling clay minerals and poorly water-soluble drugs: II. Solubilization of griseofulvin by complex formation with a swelling clay mineral', *J. Colloid Interface Sci.*, pp. 556–564, 146, 1991.
- [68] M. Olteanu, D. Achimescu, Z. Vuluga and V. Trandafir, 'Measurement and interpretation of wetting properties of new collagen-silicate biomaterial', *Revue Roumaine de Chimie*, pp. 157–163, 53(2), 2008.
- [69] A. Okada, A. Usuki, 'Twenty years of polymer-clay nanocomposites', *Macromol. Mater. Eng.*, pp. 1449–1476, 291, 2006.
- [70] R. A. Vaia, E. P. Gianellis, 'Polymer Nanocomposites: Status and Applications', *MRS Bull.*, pp. 394–401, 62, 2001.
- [71] H. D. Wagner, 'Nanocomposites-Paving the way to stronger materials', *Nat. Nanotech.*, pp. 742–744, 2, 2007.

- [72] M. G. Albu, I. Titorencu, M. V. Ghica, 'Collagen-based drug delivery systems for tissue engineering', *Biomaterials Applications for Nanomedicine*, pp. 125–148, InTech, 2011.
- [73] Z. Vuluga, V. Danciu, V. Trandafir, C. Radovici, D. M. Vuluga, E. Vasile, S. Serban, C. G. Potarniche, 'Titania modified layered silicate for polymer/ inorganic nanocomposites', *Mol. Cryst. Liq. Cryst.*, pp. 258–265, 483, 2008.
- [74] J. deC. Christiansen, C.-G. Potarniche, Z. Vuluga, A. Drozdov, 'Nanomaterials in biomedical applications', 2nd International Conference on Wireless Communications Vehicular Technology, Information Theory and Aerospace & Electronic Systems Technology". IEEE, Chennai, India, River Publishers, 2011.
- [75] Zina Vuluga, Dan Donescu, Viorica Trandafir, Constantin Radovici et Sever Serban, 'L'influence de la Morphologie des Extraits de Collagene sur les Proprietes des Nanocomposites a Silicates Naturels', *Revue Roumaine de Chimie*, pp. 395–404, 52, 2007.
- [76] C. Oriakhi, 'Nano sandwiches', *Chem. Br.*, pp. 59–62, 34, 1998.
- [77] Q. H. Zeng, A. B. Yu, G. Q. (Max) Lu, D. R. Paul, 'Clay-based polymer nanocomposites: research and commercial development', *Journal of Nanoscience and Nanotechnology*, pp. 1574–1592, 5, 2005.
- [78] M. Alexandre, P. Dubois, 'Polymer-layered silicate nanocomposites: preparation, properties and uses of a new class of materials', *Materials Science and Engineering*, pp. 1–63, 28, 2000.
- [79] Z. Vuluga, H. Paven, D. Donescu, 'Thermoplastic polymer layered silicate nanocomposites. I. Obtaining, properties and applications', *Materiale Plastice*, pp. 19–27, 39, 2002.
- [80] R. A. Vaia, H. Ishii, E. P. Giannelis, 'Synthesis and properties of 2-dimensional nanostructures by direct intercalation of polymer melts in layered silicates', *Chem. Mater.*, pp. 1694–1696, 5, 1993.
- [81] C.-J. Wu, A. K. Gaharwar, P. J. Schexnailder, G. Schmidt, 'Development of Biomedical Polymer-Silicate Nanocomposites: A Materials Science Perspective', *Materials*, pp. 2986–3005, 3, 2010.
- [82] L. E. Freed, J. C. Marquis, A. Nohria, J. Emmanuel, A. C. Mikos, R. Langer, 'Neocartilage formation *in vitro* and *in vivo* using cells cultured on synthetic biodegradable polymers', *J. Biomed. Mater. Res.*, pp. 11–23, 27, 1993.
- [83] S. L. Ishaq, G. M. Crane, M. J. Miller, A. W. Yasko, M. J. Yaszemski, A. G. Mikos, 'Bone formation by three-dimensional stromal osteoblast

- culture in biodegradable polymer scaffolds', *J. Biomed. Mater. Res.*, pp. 17–28, 36, 1997.
- [84] M. G. Dunn, J. B. Liesch, M. L. Tiku, J. P. Zawadsky, 'Development of fibroblast-seeded ligament analogs for ACL reconstruction', *J. Biomed. Mater. Res.*, pp. 1363–1371, 29, 1995.
- [85] G. Nechifor, S. I. Voicu, A. C. Nechifor, S. Garea, 'Nanostructure hybrid membrane polysulfone-carbon nanotubes for hemodialysis', *Desalination*, pp. 342–348, 241, 2009.
- [86] S. J. Peter, M. J. Miller, A. W. Yasko, M. J. Yaszemski, A. G. Mikos, 'Polymer concepts in tissue engineering', *J. Biomed. Mater. Res.*, pp. 422–427, 43, 1998.
- [87] L. E. Freed, G. Vunjak-Novakovic, R. J. Biron, D. B. Eagles, D. C. Lesnoy, S. K. Barlow, R. Langer, 'Biodegradable polymer scaffolds for tissue engineering', *Bio/Technology*, pp. 689–693, 12, 1994.
- [88] B. S. Kim, D. J. Mooney, 'Development of biocompatible synthetic extracellular matrices for tissue engineering', *TIBTECH*, pp. 224–230, 16, 1998.
- [89] L. H. H. Olde Damink, P. J. Dijkstra, M. J. A. van Luyn, P. B. van Wachem, P. Nieuwenhuis, J. Feijen, 'Glutaraldehyde as a crosslinking agent for collagen-based biomaterials', *J. Mater. Sci.*, pp. 460–472, 6, 1995.
- [90] N. Barbani, P. Giusti, L. Lazzeri, G. Polacco, G. Pizzirani, 'Bioartificial materials based on collagen: 1. Collagen cross-linking with gaseous glutaraldehyde', *J. Biomater. Sci.*, pp. 461–469, 7, 1995.
- [91] M. S. Chapekar, 'Tissue Engineering: Challenges and Opportunities', *J Biomed Mater Res (Appl Biomater)*, pp. 617–620, 53, 2000.
- [92] C.-G Potarniche, Z. Vuluga, C. Radovici, S. Serban, D. M. Vuluga, M. Ghiurea, V. Purcar, V. Trandafir, D. Iordachescu, M. G. Albu, 'Nanocomposites based on collagen and Na-montmorillonite modified with bioactive substances', *Materiale Plastice*, pp. 267–273, 47, 2010.

# 2

---

## Cerium Dioxide Nanoparticles Protect Cardiac Progenitor Cells against the Oxidative Stress

---

Francesca Pagliari<sup>1,2</sup>, Giorgia Nardone<sup>3</sup>, Enrico Traversa<sup>1</sup>  
and Paolo Di Nardo<sup>2</sup>

<sup>1</sup>Physical Science and Engineering Division, King Abdullah University of Science and Technology, Jeddah, Saudi Arabia

<sup>2</sup>Laboratory of Cellular and Molecular Cardiology (LCMC), Department of Clinical Sciences and Translational Medicine, University of Rome “Tor Vergata”, Rome, Italy

<sup>3</sup>International Clinical Research Center (ICRC), Integrated Center of Cellular Therapy and Regenerative Medicine, St. Anne’s University Hospital, Brno, Czech Republic

Corresponding author: Paolo Di Nardo <dinardo@uniroma2.it>

### Abstract

In the last decade, the combined applications of nano- and stem cell technology are among the newest approaches in regenerative medicine and Tissue Engineering (TE). In this context, the possibility to fabricate scaffolds with composite materials consisting of a polymer matrix and nanoparticles (NPs) as structural elements could allow to develop a novel generation of bioactive materials, capable of directing and controlling cell behavior. In particular, cerium dioxide (CeO<sub>2</sub>) NPs are promising tools to scavenge reactive oxygen species (ROS) and to confer protection to cells from the oxidative stress owing to cerium ability to switch the oxidation state (Ce<sup>4+</sup>/Ce<sup>3+</sup>). In the present experimental study, 10, 25, or 50 µg/mL CeO<sub>2</sub> powder was administered to murine adult cardiac progenitor cells (CPCs) in complete medium for 24 hours (h) and the effects onto cells evaluated at 1, 3 and 7 days (d) from the ceria powder withdrawal from the culture. After a single 24 h CeO<sub>2</sub>

*Mayuri Prasad and Paolo Di Nardo (Eds.), Innovative Strategies in Tissue Engineering, 25–36.*

© 2014 River Publishers. All rights reserved.

pulse, CPCs were able to take up the NPs and retain them inside the cytosol, while preserving their stemness phenotype and multipotential capability at all time-points considered. Moreover, when challenged with 50  $\mu\text{M}$   $\text{H}_2\text{O}_2$  for 30 min,  $\text{CeO}_2$ -treated CPCs were protected from the oxidative stress. In particular, after 24 h, only the highest concentration was protective; after 7 d, ROS levels were mitigated with all concentrations. This study demonstrated that internalized  $\text{CeO}_2$  NPs can act as a long-term defense against the oxidative insult. NPs were activated only when cells were hit by an external oxidative perturbation, remaining inert in respect to the main CPC characteristics. In conclusion, these results suggest that  $\text{CeO}_2$  nanoparticles hold an enormous potential in TE treatments protecting stem cells against the oxidative damage.

**Keywords:** Cerium dioxide, cardiac precursor cells, tissue engineering, reactive oxygen species.

## 2.1 Interaction of Cerium Oxide Nanoparticles with Biological Systems

Over the last few years, nanotechnology has made significant strides especially in the field of regenerative medicine, thus enabling the development of a new generation of nanostructured biomaterials for medical applications. In particular, nano-composite hybrid scaffolds, made by incorporating nanoparticles into bio-compatible/erodible polymeric matrices, have gained rising attention. The possibility to fine-tune the properties of these materials to meet a broad range of applications makes them attractive systems for tissue engineering. For example, polymeric scaffolds loaded with hydroxyapatite nanoparticles are already used for bone tissue reconstruction [1]. In this respect, deciphering how cells interact with scaffolds and the mechanisms through which nano-components are internalized without exerting direct effects on cell behavior is particularly intriguing in order to obtain novel biomaterials with promising and controllable properties.

Recently, cerium oxide nanoparticles ( $\text{CeO}_2$ , nanoceria) have been demonstrated to favor cardiac precursor cell (CPC) adhesion and growth when embedded into PLGA scaffolds [2]. In particular, cerium oxide nanoparticle filling of PLGA films resulted in enhanced mechanical properties and in a change in scaffold nano-rugosity. On these functionalized supports, cells exhibited better adhesion and growth as compared with PLGA alone. CPCs were able to acquire a typical alignment, due to support rugosity, which, combined with that determined by the presence of ceramic nanoparticles, provided

better anchorage sites for cell engraftment. Nevertheless, cardiac-derived cells displayed better growth performance when cultured onto CeO<sub>2</sub>-PLGA films, as compared with films loaded with titanium oxide (TiO<sub>2</sub>), thus suggesting a potential chemical stimulus can be exerted by ceria nanoparticles on cardiac resident progenitor cells [2].

CeO<sub>2</sub> is a rare earth oxide material of the lanthanide series commonly used in important industrial applications [3, 4], but recent reports highlighted the beneficial effects of cerium oxide in biological systems [5, 6]. In particular, it has been proposed that ceria nanoparticles could exhibit an oxidant scavenging activity reducing the cytotoxic effects of intracellular oxidative stress conditions via changes of the oxidation state: Ce<sup>4+</sup> / Ce<sup>3+</sup> [7–9]. Ceria nanoparticles display their unique property to store and release oxygen because of the great mobility of these atoms inside the lattice; each released oxygen atom causes the formation of a vacancy and electron transfer to Ce<sup>4+</sup> which reduces to Ce<sup>3+</sup>. This mechanism seems to be greatly facilitated in nanoparticles, where the higher surface area is accompanied by more oxygen vacancies and, thus, higher Ce<sup>3+</sup> concentration in the lattice, resulting in enhanced catalytic properties [10, 11]. Indeed, reactive oxygen species (ROS), such as superoxides and peroxides, could react on these active sites and be counteracted; as a consequence, Ce<sup>3+</sup> ions would be oxidized in Ce<sup>4+</sup> ions in a reversible and autocatalytic way. This is because of the cerium ability to switch between the 3+ state under reducing conditions and 4+ state under oxidizing conditions [6, 12]. This ability, combined with multiple active sites that may be generated on a single nanoparticle, could provide an explanation to ceria antioxidant properties with the ability to scavenge ROS and mostly as a catalyst with superoxide dismutase (SOD) and catalase mimetic activities [13–15]. These properties candidate ceria as a novel long-lasting antioxidant compound with the promise to actively participate in mitigating oxidative stress, which is considered a critical actor in the establishment and progression of several diseases, including cardiovascular dysfunctions [16–19], or after treatments such as chemotherapy [20].

## **2.2 Cerium Oxide Nanoparticles Shield Cardiac Precursor Cells against the Oxidative Stress**

In the last decade, evidence has been acquired that an adult stem cell pool is present in almost every organ of the body. These cells are endowed with self-renewal capability and can be committed to a specific cell lineage. The identification of a cardiac progenitor cell (CPC) population in the adult

mammalian heart has definitively broken the dogma that the adult myocardium is a terminally differentiated tissue [21, 22]. CPCs are believed to control the healthy tissue homeostasis and to repair the diseased tissue in pathological conditions [23]. Cardiovascular diseases, such as the Myocardial Infarction (MI), represent the first cause of mortality and morbidity in both industrialized and developing countries, and the oxidative stress is cause and/or consequence leading to a reduced cardiac functionality [24]. Moreover, ROS plays a crucial role in reducing stem cell lifespan and inducing senescence [25] as well as in maintaining self-renewal [26] into special hypoxic microenvironments, named “niches”. Ito K. and co-workers have demonstrated an active role of ROS in inducing loss of Hematopoietic Stem Cell self-renewal capacity via p38 MAPK phosphorylation [27]. In particular, in the post-ischemic myocardium, the release of inflammatory cytokines and ROS production [28–30] generate a hostile microenvironment, which, on one hand, could favour stem cell recruitment, also from other body districts [31], while, on the other hand, might hamper resident progenitor cell proliferation and differentiation [32]. Indeed, recent reports suggested an inductive role for low-levels of oxidant production and cytokines in promoting stem cell differentiation [32–34] and in cardiomyogenesis during the embryonic development [35]. Conversely, the generation of high-ROS levels during pathophysiological conditions contributes to cell damage and remodelling [36]. Thus, the stem cell behavior appears tightly dependent on the microenvironmental niche properties, not only in terms of nutrient and oxygen supply, but also of reactive oxygen species balance [37].

In a recent work, our research group investigated mouse *Lin<sup>neg</sup>/Sca-1<sup>pos</sup>* CPC (CPCs) response following CeO<sub>2</sub> nanoparticle treatment<sup>38</sup>. In particular, the possibility that CeO<sub>2</sub> could confer protection to cells against the oxidative stress was investigated. For this purpose CPCs were grown in the presence of various concentrations of CeO<sub>2</sub> (10 µg/mL, 25 µg/mL and 50 µg/mL) having mean particle size of about 5–8 nm (Figure 2.1).

Ceria antioxidant effects have been already proved in other biological systems, but the interactions between these nanoparticles and cardiac resident progenitor cells has never been analyzed, to the best of our knowledge. In this study, cells were subjected to a single administration for 24 hours; after that, ceria was removed and analyses were conducted. Interestingly, at 7 days after ceria withdrawal, nanoparticles had been internalized and retained as aggregates inside the cell cytoplasm (Figure 2.2).

CPC morphology and undifferentiated phenotype were not affected being Sca-1 expression stable at all time points and preserved at high levels with

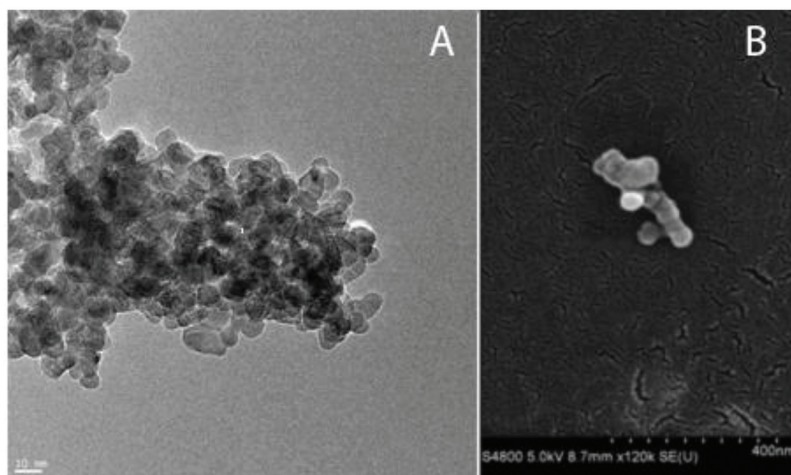


**Figure 2.1** Transmission (A) and Scanning (B) electron micrographs of CeO<sub>2</sub> nanoparticles.

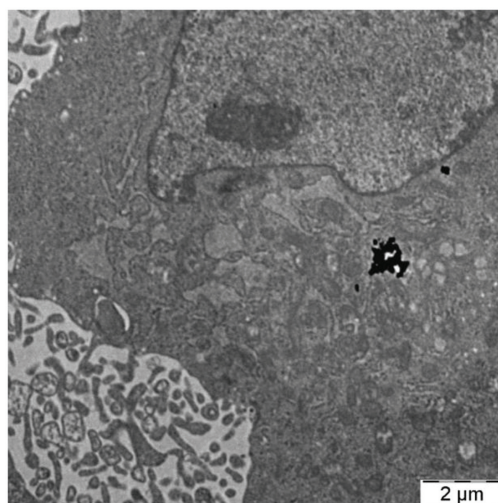
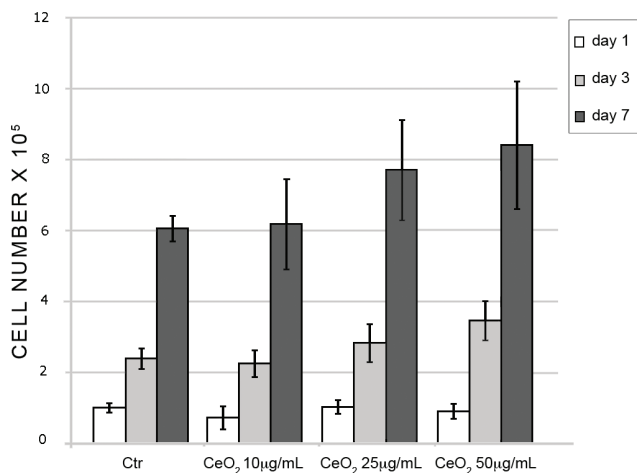


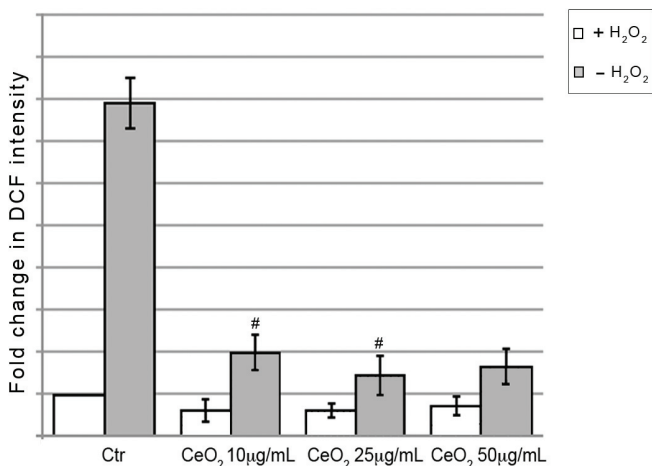
**Figure 2.2** Representative TEM micrograph showing CeO<sub>2</sub> NPs inside the cytoplasm of a CPC at 7 days from the administration of 50 µg/mL CeO<sub>2</sub> *in vitro*.

all ceria concentrations. Also self-renewal and multipotency, two important properties defining stem cells, were maintained when CPC were pre-treated with 10, 25 and 50 µg/mL of CeO<sub>2</sub> nanoparticles. Cell counts at 1 d, 3 d and 7 d demonstrated that cells were viable and proliferating without significant differences in respect to untreated controls (Figure 2.3, A). Appropriate





A



B

**Figure 2.3** A) CPC proliferation assessed at 1 d, 3 d, and 7 d after 24 h CeO<sub>2</sub> exposure. The values are expressed as means  $\pm$  SD of three independent experiments. (#=  $p > 0.05$ ). B) Effect of H<sub>2</sub>O<sub>2</sub> on intracellular ROS levels in Lin<sup>-</sup> Sca-1<sup>pos</sup> CPCs at 7 days after CeO<sub>2</sub> treatment. ROS production, measured using a DCFH probe, decreased with all NPs concentrations tested. (#= H<sub>2</sub>O<sub>2</sub> treated cells vs. CeO<sub>2</sub>-H<sub>2</sub>O<sub>2</sub> treated cells). The values are expressed as means  $\pm$  SD of the fold change in DCF fluorescence intensity with respect to H<sub>2</sub>O<sub>2</sub>-untreated control (ctr-) from three different tests ( $p < 0.05$ ).

differentiating stimuli as well as the presence of neonatal cardiomyocytes in direct co-culture with CeO<sub>2</sub>-treated CPCs were able to induce adipogenic, osteogenic and cardiac commitment as demonstrated by the occurrence of lipid droplets, calcium deposits, the up-regulation of GATA-4, the membrane translocation of connexin 43 and the expression of  $\alpha$ -sarcomeric actinin, respectively. Furthermore, the incubation with 24 h CeO<sub>2</sub> did not promote a pro-oxidant effect in cells, meaning that, in the absence of any stress stimulus, ROS levels remained unmodified as compared to controls (Figure 2.3, B).

Altogether, these results demonstrated that no toxic effects were exerted by CeO<sub>2</sub> nanoparticles on CPCs at the concentrations tested and NPs were activated only when cells were hit by an external oxidative perturbation, remaining inert in respect to CPC homeostasis and differentiation. In fact, H<sub>2</sub>O<sub>2</sub>-induced cell injury and subsequent dichlorofluorescein fluorescence assay revealed a strong capability to reduce the oxidative stress in the long run (7 days) with all concentrations, while only the higher dose (50  $\mu$ g/mL) was protective in the short run (24 hours). In fact, ROS production decreased by an initial 30% with 50  $\mu$ g/mL NPs to approximately 50% and 75% at 3 and 7 d, respectively, with 25 and 10  $\mu$ g/mL as well. In agreement with other reports, our data indicated that intracellular nanoparticles worked as a potent scavenger able to protect cells from the oxidative damage and markedly attenuated ROS production over time. Consistently, Das et al. reported that, after 30 d, CeO<sub>2</sub> was still able to protect spinal cord cells from H<sub>2</sub>O<sub>2</sub>-induced cytotoxicity, showing better survival than their untreated counterpart [12]. Thus, these results suggest that with a single nanoparticle administration, CeO<sub>2</sub> could be able to act over time, limiting the generation of ROS following a tissue damage and, so, favouring the establishment of better conditions for CPC proliferation and differentiation *in vivo*. On the other hand, such findings also indicated that a possible intracellular threshold level could be necessary before the antioxidant effects could appear. It is clear that a number of aspects, such as the synthesis techniques, nanoceria characteristics in terms of size, shape and charge, dosage and exposure time, administration procedures, need to be considered and thoroughly tuned for maximizing the beneficial effects of the nanoceria before these nanoparticles could be effectively used in therapeutic applications [39]. Indeed, differences in each of these parameters could help explaining the conflicting results so far obtained with cerium oxide in biological systems [5, 38–41]. Recently, Park et al. showed that cerium oxide treatment induced oxidative stress with ROS formation and cytotoxicity in some mammalian cells; however, the authors also admitted that these

effects were not detectable in other cell types [41]. Therefore, it could be worth conducting further investigations in order: i) to elucidate the biological mechanisms behind the action of cerium oxide; ii) to understand the interactions between this promising material and tissues (both healthy and damaged) *in vivo*.

## References

- [1] N. T. Ba Linh, Y. K. Min, B. T. Lee, 'Hybrid hydroxyapatite nanoparticles-loaded PCL/GE blend fibers for bone tissue engineering' *J Biomater Sci Polym Ed.*, 24:520–38 doi: 10.1080/09205063.2012.697696, 2013.
- [2] C. Mandoli, F. Pagliari, S. Pagliari, G. Forte, P. Di Nardo, S. Licoccia, E. Traversa, 'Stem Cell Aligned Growth Induced by CeO<sub>2</sub> Nanoparticles in PLGA Scaffolds with Improved Bioactivity for Regenerative Medicine' *Adv. Funct. Mater.*, 20, 1617–1624, 2010.
- [3] A. M. El-Toni, S. Yin, T. Sato, 'Enhancement of Ceria Doped Ceria Nanoparticles Performance as UV Shielding Material' *Adv. Sci. Technol.*, 45, 673–678, 2006.
- [4] V. Esposito, E. Traversa, 'Design of electroceramics for solid oxide fuel cell applications: playing with ceria' *J. Am. Ceram. Soc.*, 91, 1037–1051, 2008.
- [5] J. Chen, S. Patil, S. Seal, J. F. McGinnis, 'Rare Earth Nanoparticles Prevent Retinal Degeneration Induced by Intracellular Peroxides' *Nat. Nanotechnol.*, 1, 142–150, 2006.
- [6] A. S. Karakoti, N. A. Monteiro-Riviere, R. Aggarwal, J. P. Davis, R. J. Narayan, W. T. Self, J. McGinnis, S. Seal, 'Nanoceria as Antioxidant: Synthesis and Biomedical Applications' *JOM (1989)* 60, 33–37, 2008.
- [7] R. W. Tarnuzzer, J. Colon, S. Patil, S. Seal, 'Vacancy Engineered Ceria Nanostructures for Protection from Radiation-Induced Cellular Damage' *Nano Lett.*, 5, 2573–2577, 2005.
- [8] F. Esch, S. Fabris, L. Zhou, T. Montini, C. Africh, P. Fornasiero, G. Comelli, R. Rosei, 'Electron Localization Determines Defect Formation on Ceria Substrates' *Science*, 309, 752–755, 2005.
- [9] I. Celardo, J. Z. Pedersen, E. Traversa, L. Ghibelli, 'Pharmacological potential of cerium oxide nanoparticles' *Nanoscale*, 3:1411–20. doi: 10.1039/c0nr00875c, 2011.

- [10] A. Migani, G. N. Vayssilov, S. T. Bromley, F. Illas, K. M. Neyman, 'Greatly Facilitated Oxygen Vacancy Formation in Ceria Nanocrystallites' *Chem. Comm.*, 46, 5936–5938, 2010.
- [11] T. C. Campbell, C. H. Peden, 'Chemistry. Oxygen Vacancies and Catalysis on Ceria Surfaces' *Science*, 309, 713–714, 2005.
- [12] M. Das, S. Patil, N. Bhargava, J. F. Kang, L. M. Riedel, S. Seal, J. J. Hickman, 'Auto-Catalytic Ceria Nanoparticles Offer Neuroprotection to Adult Rat Spinal Cord Neurons' *Biomater.*, 28, 918–1925, 2007.
- [13] E. G. Heckert, A. S. Karakoti, S. Seal, W. T. Self, 'The Role of Cerium Redox State in the SOD Mimetic Activity of Nanoceria' *Biomater.*, 29, 2705–2709, 2008.
- [14] C. Korsvik, S. Patil, S. Seal, W. T. Self, 'Superoxide Dismutase Mimetic Properties Exhibited by Vacancy Engineered Ceria Nanoparticles' *Chem. Comm.*, 14, 1056–1058, 2007.
- [15] T. Pirmohamed, J. M. Dowding, S. Singh, B. Wasserman, E. Heckert, A. S. Karakoti, J. E. King, S. Seal, W. T. Self, 'Nanoceria Exhibit Redox State-Dependent Catalase Mimetic Activity' *Chem. Comm.*, 46, 2736–2738, 2010.
- [16] R. Kohen, A. Nyska, 'Oxidation of Biological Systems: Oxidative Stress Phenomena, Antioxidants, Redox Reactions, and Methods for Their Quantification' *Toxicol. Pathol.*, 30, 620–650, 2002.
- [17] B. Kumar, S. Koul, L. Khandrika, R. B. Meacham, H. K. Koul, 'Oxidative Stress Is Inherent in Prostate Cancer Cells and Is Required for Aggressive Phenotype' *Cancer Res.*, 68, 1777–1785, 2008.
- [18] M. K. Misra, M. Sarwat, P. Bhakuni, R. Tuteja, N. Tuteja, 'Oxidative Stress and Ischemic Myocardial Syndromes' *Med. Sci. Monit.*, 15, 209–219, 2009.
- [19] G. S. Gaki, A. G. Papavassiliou, 'Oxidative Stress-Induced Signaling Pathways Implicated in the Pathogenesis of Parkinson's Disease' *Neuromolecular Med.*, 2014.
- [20] K. A. Conklin, 'Chemotherapy-associated oxidative stress: impact on chemotherapeutic effectiveness' *Integr Cancer Ther.*, 3:294–300, 2004.
- [21] K. Urbanek, D. Torella, F. Sheikh, A. De Angelis, D. Nurzynska, F. Silvestri, C. A. Beltrami, R. Bussani, A. P. Beltrami, F. Quaini, R. Bolli, A. Leri, J. Kajstura, P. Anversa, 'Myocardial Regeneration by Activation of Multipotent Cardiac Stem Cells in Ischemic Heart Failure' *Proc. Natl. Acad. Sci. USA.*, 102, 8692–8697, 2005.
- [22] O. Bergmann, R. D. Bhardwaj, S. Bernard, S. Zdunek, F. Barnabé-Heider, S. Walsh, J. Zupicich, K. Alkass, B. A. Buchholz, H. Druid, S. Jovinge,

- J. Frisén, 'Evidence for Cardiomyocyte Renewal in Humans' *Science*, 324, 98–102, 2009.
- [23] A. P. Beltrami, D. Cesselli, N. Bergamin, P. Marcon, S. Rigo, E. Puppato, F. D'Aurizio, R. Verardo, S. Piazza, A. Pignatelli, A. Poz, A.; U. Baccarani, D. Damiani, R. Fanin, L. Mariuzzi, N. Finato, P. Masolini, S. Burelli, O. Belluzzi, C. Schneider, C. A. Beltrami, 'Multipotent Cells Can Be Generated *in Vitro* from Several Adult Human Organs (Heart, Liver, and Bone Marrow)' *Blood*, 110, 3438–3446, 2007.
- [24] G. F. Tomaselli, A. S. Barth, 'Sudden cardio arrest: oxidative stress irritates the heart' *Nat Med*, 16:648–9. doi: 10.1038/nm0610–648, 2010.
- [25] L. Shao, H. Li, S. K. Pazhanisamy, A. Meng, Y. Wang, D. Zhou, 'Reactive oxygen species and hematopoietic stem cell senescence' *Int J Hematol.*, 94:24–32. doi: 10.1007/s12185-011-0872-1, 2011.
- [26] A. Mohyeldin, T. Garzón-Muvdi, A. Quiñones-Hinojosa, 'Oxygen in stem cell biology: a critical component of the stem cell niche. *Cell Stem Cell* 7, 150– 161, 2010.
- [27] K. Ito, A. Hirao, F. Arai, K. Takubo, S. Matsuoka, K. Miyamoto, M. Ohmura, K. Naka, K. Hosokawa, Y. Ikeda, T. Suda, 'Reactive oxygen species act through p38 MAPK to limit the lifespan of hematopoietic stem cells', *Nat Med.*, 12:446-51, 2006.
- [28] N. G. Frangogiannis, C. W. Smith, M. L. Entman, 'The inflammatory response in myocardial infarction' *Cardiovasc Res.*, 53:31–47, 2002.
- [29] D. Sorescu, K. K. Griendling, 'Reactive oxygen species, mitochondria, and NAD(P)H oxidases in the development and progression of heart failure' *Congest. Heart Fail.*, 8:132 – 40, 2008.
- [30] M. Hori, K. Nishida, 'Oxidative stress and left ventricular remodelling after myocardial infarction' *Cardiovasc Res.*, 15; 81:457–64, 2009.
- [31] A. Aicher, A. M. Zeiher, S. Dimmeler, 'Mobilizing endothelial progenitor cells' *Hypertension*, 45, 321–325, 2005.
- [32] H. Sauer, M. Wartenberg, J. Hescheler, 'Reactive Oxygen Species as Intracellular Messengers During Cell Growth and Differentiation' *Cell. Physiol. Biochem.*, 11, 173–186, 2011.
- [33] Y. Kanda, T. Hinata, S. W. Kang, Y. Watanabe, 'Reactive oxygen species mediate adipocyte differentiation in mesenchymal stem cells' *Life Sci.*, 89, 250–258, 2011.
- [34] A. Behfar, L. V. Zingman, D. M. Hodgson, J. M. Rauzier, G. C. Kane, A. Terzic, M. Pucéat, 'Stem cell differentiation requires a paracrine pathway in the heart' *FASEB J.*, 16:1558–66, 2002.

- [35] S. Kanno, P. K. Kim, K. Sallam, J. Lei, T. R. Billiar, L. L. 2nd Shears LL, 'Nitric oxide facilitates cardiomyogenesis in mouse embryonic stem cells' *Proc. Natl. Acad. Sci. U S A*, 101:12277–81, 2004.
- [36] E. Takimoto, D. A. Kass, 'Role of oxidative stress in cardiac hypertrophy and remodeling' *Hypertension*, 49:241–8, 2007.
- [37] H. Sauer H, M. Wartenberg, 'Impact of Reactive Oxygen and Reactive Nitrogen Species for Stem Cell Mobilization, Function and Cardiovascular Differentiation, Embryonic Stem Cells: The Hormonal Regulation of Pluripotency and Embryogenesis' Prof. Craig Atwood (Ed.), ISBN: 978-953-307-196-1, InTech, DOI: 10.5772/15329. Available from: <http://www.intechopen.com/books/embryonic-stem-cells-the-hormonal-regulation-of-pluripotency-and-embryogenesis/impact-of-reactive-oxygen-and-reactive-nitrogen-species-for-stem-cell-mobilization-function-and-card> DOI: 10.5772/15329, 2011.
- [38] F. Pagliari, C. Mandoli, G. Forte, E. Magnani, S. Pagliari, G. Nardone, S. Licocchia, M. Minieri, P. Di Nardo, E. Traversa, 'Cerium oxide nanoparticles protect cardiac progenitor cells from oxidative stress' *ACS Nano*, 6:3767–75, 2012.
- [39] L. K. Limbach, Y. Li, R. N. Grass, T. J. Brunner, M. A. Hintermann, M. Muller, D. Gunther, W. J. Stark, 'Oxide Nanoparticle Uptake in Human Lung Fibroblasts: Effects of Particle Size, Agglomeration, and Diffusion at Low Concentrations' *Environ. Sci. Technol.*, 39, 9370–9376, 2005.
- [40] S. M. Hirst, A. S. Karakoti, R. D. Tyler, N. Sriranganathan, S. Seal, C. M. Reilly, 'Anti-Inflammatory Properties of Cerium Oxide Nanoparticles' *Small*, 5:2848–2856, 2009.
- [41] E. J. Park, J. Choi, Y. K. Park, K. Park, 'Oxidative Stress Induced by Cerium Oxide Nanoparticles in Cultured BEAS-2B Cells' *Toxicology*, 245:90–100, 2008.



**Taylor & Francis**

Taylor & Francis Group

<http://taylorandfrancis.com>

# 3

---

## **Animals Models and *In Vitro* Alternatives in Regenerative Medicine: Focus on Biomaterials Development**

---

**Monika Kozak Ljunggren, DVM, PhD  
and May Griffith, PhD**

Integrative Regenerative Medicine Centre, and Department of Clinical and Experimental Medicine, Linköping University, Sweden

Corresponding author: Monika Kozak Ljunggren

<Monika.Kozak.Ljunggren@liu.se>; May Griffith <May.Griffith@liu.se>

### **3.1 Introduction**

#### **3.1.1 Animals in Medical Research**

The use of animals has been considered an essential part of biomedical research. Researchers have studied and experimented on animals in order to better understand the functioning of the healthy, living body, and what goes wrong in disease or injury. Animals are also used in the safety and efficacy testing of drugs and other means of preventing or treating those diseases or traumatic insults to the body. Indeed, to date, the use of animals has enabled the various advances that have been made to both human and veterinary medicine.

#### **3.1.2 Ethical Considerations of Animal Use**

The welfare of animals used for scientific experiments is in most countries protected by strict laws and regulations dictating the extent of research that can be performed. These laws usually incorporate the three R's principals introduced by Russel and Burch (1959) [1] encouraging the reduction, refinement and replacement of animal research. Any animal experiment requires obtaining an ethical permit, which is granted based on appropriate justification of the experimental design and the potential benefits of the experiment are weighed against the suffering of the animals. The selection of the animal

*Mayuri Prasad and Paolo Di Nardo (Eds.), Innovative Strategies  
in Tissue Engineering, 37–52.*

© 2014 River Publishers. All rights reserved.



model of the lowest possible phylogenic scale and the lowest possible animal numbers is encouraged [1]. On the other hand the researcher must consider the translational relevance of the animal species and use an appropriate number of animals to ensure significance. It is also important to conduct pilot experiments where variation can be tested and this data can be used for power calculations. Experiments with too low animal numbers do not save animals as the ones used go to waste and in the end a higher number of animals will be sacrificed to obtain reliable results. Pilot studies are also very valuable for optimizing methods, e.g. surgical skills. It is important to achieve a certain level of reproducibility in an animal model because a high variation or mortality will require higher animal numbers. All these efforts are qualified as refinements. Finally, before starting an animal experiment, it is important to fully explore all *in vitro* test methods to fulfil the replacement demand. A large number of biocompatibility and *in vitro* characterisation studies can be done using cell culture or organotypic cultures.

In this chapter, we will briefly review animal testing in general and show how we complement animal testing with *in vitro* organ equivalent models for testing of biomaterials, using the development of biosynthetic corneal implants as an example.

## **3.2 Designing Animal Experiments**

### **3.2.1 Randomization and Blinding**

The lack of a proper randomization protocol is an important source of bias. Many animal studies do not report the randomization method or even whether it was used. Picking animals randomly from a cage does not qualify as randomization. The physiological status of the animal can affect the ease at which it is caught thus producing bias [2]. One must develop a system where the animal selection is totally at chance, e.g. using sealed envelopes or throwing dice. Both complete randomization and randomized blocking can be used [3]. Another important factor is blinding the experimental groups, so that the person analysing the data and evaluating outcomes does not know which animals received the treatment and which the controls are. This ensures that the researchers do not tend to see results that they expect or hope for. This is especially important when using subjective criteria or scoring systems for outcomes. Generally, these should be avoided if possible and substituted by more objective ones, e.g. instead of mild to severe redness, a number for the area affected or intensity of colour change [4].

### **3.2.2 Control Groups**

Designing the appropriate control groups is crucial for obtaining reliable results. They should include positive, negative, sham and comparative controls at the least. When performing any invasive, traumatic procedure it is important to have sham-operated animals to test whether the procedure itself could affect the outcome. In the case of developing new treatments as an alternative to established ones, it is desirable to include a group receiving the standard treatment as a comparative control [5].

### **3.2.3 Statistical Analysis**

The selection of the appropriate statistical test is extremely important for the outcome of the study. It should be selected already at the planning stage based on the type of data obtained, expected distribution and variation. It is not acceptable to analyse the experimental data with a series of tests until one of them generates the desired p-value. The statistical analysis method should be decided upon after a pilot study or based on data obtained from published studies along with the power calculations and estimation of the minimum number of animals needed.

### **3.2.4 Design Stages**

Any animal experiment should be carefully planned and preceded by a thorough literature search to obtain as much information as possible about the available animal models and their limitations as well as to avoid repeating experiments that have already been done. Performing pilot studies is very beneficial, especially for new experimental systems, as they can lead to refinement of the methodology and help calculate the group sizes. As mentioned above, selection of the statistical method should be done at this stage [6].

## **3.3 Limitations of Animal Models**

There have been many concerns raised about the usefulness of animal experimentation to predict the outcome of human responses to treatments or assess their safety.

### **3.3.1 Animal Species**

As mentioned above the demand to choose the animal species on the lowest phylogenetic level has to be balanced with selecting the one closest to humans with regard to the process or organ to be studied. There have been some

publications analysing the relevance of animal models to clinical outcome in patients which have raised concerns about the predictive value of animal experimentation in general. The conclusions drawn by the different authors vary, with some even claiming that animal models have no predictive value whatsoever [7]. Others conclude that this poor outcome may be the result of poor experimental design and incorrect statistics for both the animal and clinical trials and not only differences in the anatomy, physiology and biochemistry [2]. It is very important that the best animal model or models are chosen for every interaction, pathway or process. The costs of experimental models are a limiting factor in the study design and small laboratory animals are favoured due to this. In general animal models can be divided into large outbred models (e.g. pigs, dogs, sheep) and small inbred models (e.g. mice, rats). They offer a different level of uniformity, with inbred animals being more genetically similar while outbred animals will exhibit a higher degree of variation. The larger species can be especially helpful when anatomical similarity is important whereas the inbred species might be more useful when studying pathways, processes on a lower, molecular level, where greater genetic variation could conceal small differences [8].

### **3.3.2 Health and Age Status**

An important difference between the test animal and the patient is the health background and age. The experimental model is usually young and healthy whereas the patient is often older and with an underlying disease condition. Furthermore, patients usually receive a battery of medication for their condition whereas the animal is exposed only to anaesthetics if the tested therapy requires invasive procedures. All these differences can affect the outcome of the tested treatment.

### **3.3.3 Reproducibility**

The reproducibility of the model is important for the outcome as it affects variation, power and significance. It is affected by factors originating from both the scientist and the animal. The scientist's skills in performing a surgical procedure will determine the reproducibility and this can lead to bias or the necessity to use large numbers of animals. On the other hand the differences in the animal's anatomy or physiology can also determine how reproducible a model is. It is therefore important to conduct pilot studies to gain the necessary skills and estimate the natural variation occurring within each species and strain [5].

## **3.4 Examples of Animal Models for Cardiac and Corneal Regenerative Medicine Testing**

### **3.4.1 Myocardial Infarct and Other Ischemic Models**

Ischemia of the myocardium due to a blockage in a coronal artery leads to myocardial infarction (MI). Depending on the size of the vessel obstructed and duration of blood flow the degree of tissue damage and its consequences will vary [9]. Thanks to advances in reperfusion therapy, the mortality of acute MI has decreased greatly [10]. However, this has led to an increase in patients with chronic heart failure as a result of the infarction. The patients develop a progressive heart disease, mainly as a result of ventricular remodelling occurring post-MI [11]. In humans the size of the infarct is approximately 10% of the left ventricle but with quite high variation (7–28%). If reperfusion therapy is introduced quickly, the infarct size is decreased to 7% [12]. During the ischemic event the amount of tissue without blood flow is the area at risk. Depending on the location of this area, development of collateral circulation or applied reperfusion therapy the actual infarcted area will be smaller to a certain extent. Cell death occurs in the MI region, followed by infiltration of immune cells and finally scar formation [13].

Different animal species ranging from rodents (mice, rats) to large animals (e.g. pigs) have been used. A range of different methods have also been used to create the infarcts. Examples of these are given below.

#### **3.4.1.1 Myocardial coronary artery ligation**

The most commonly used method for induction of a myocardial infarct in animals is ligation of the left anterior descending (LAD) artery [14–16]. This is one of the arteries providing blood supply to the left ventricle and septum in some species. This model is technically challenging as it requires open chest surgery and therefore intubation and ventilation of the animal. Two different types of LAD occlusion are used – permanent and temporary [17]. Temporary ligation of the artery is an ischemia-reperfusion model, which in fact better resembles the clinical reality. It has been shown that damage to the myocardium occurs not only during the ischemic phase but also during reintroduction of blood circulation [18]. This however requires the animal's chest remains open for up to an additional 30 minutes before the occluded artery can be released and the operation completed. This affects the mortality of the model and the requirement for better surgical skills and equipment [19]. Figure 3.1 shows an example of a LAD occluded rat heart.

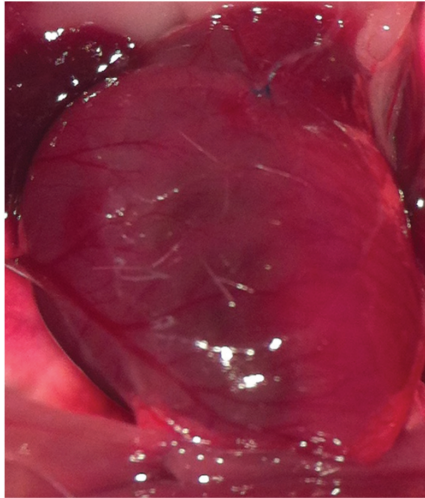


**Figure 3.1** Ischemia resulting from ligation of the LAD in a rat model.

An overview of human and animal trials using stem cell therapies for heart regeneration showed that large animal myocardial infarct models do exhibit clinical relevance [10]. The results from rodent models are unfortunately not as comparable, yet they remain the most commonly used, probably due to the much lower cost of small animal experimentation. One of the limitations of rodent models is the very large infarct size after LAD binding (60–80%). This is not representative of the clinical situation where infarcts tend to be smaller, usually about 10% of the left ventricle [12]. The rodent models do not allow for fine tuning the infarct size, due to anatomical and technical reasons. Very small changes in the location of the LAD binding site in the mouse model can lead to a shift from an extensive infarct to no infarct [20].

### **3.4.1.2 Cryoinjury**

A model for myocardial damage as a result of very low temperatures has been proposed as an alternative to the LAD ligation, where infarct size can be controlled in a better fashion. A probe of varying size that is chilled down with liquid nitrogen and then applied to the exposed myocardium for a fixed amount of time resulting in cell death and focal necrosis [21, 22]. This method is technically easier than LAD ligation but from a physiological point of view does not reflect the pathological processes that occur during an ischemic event. Another limitation is that the heart failure that results from this damage is usually not overt and therefore the evaluation

of the tested therapies success or failure in clinical terms is not as easy. However, this can be considered as an initial model for testing various therapies [21].

### 3.4.1.3 Hind-limb ischemia

An alternative to a MI model for testing therapies aimed at restoring circulation is the ligation of the femoral artery in the inguinal canal leading to ischemia of the hind leg. It is a much less technically demanding model and the success rate, as well as animal survival rate is much higher. It has been widely used for testing cell and material based therapies in which the goal is to stimulate in-growth of vessels into the damaged tissue. We have previously used the rat hind-limb ischaemia model in the development of injectable collagen-based hydrogels used to deliver angiogenic progenitor cells and growth factors for promoting re-vascularization [23, 24].

## 3.4.2 Corneal Transplantation Models

The use of animal models for corneal transplantation dates as far back as 1853, when a corneal transplant was performed in a gazelle. Animal experiments made it possible to develop the techniques and instruments that lead to successful corneal transplantations in people [8].

### 3.4.2.1 Animal species

A variety of animals are used for modelling corneal transplantation, ranging from mice, through rabbits to pigs and sheep. The choice of model depends on the particular question that is to be answered.

The larger models are more useful for investigations of clinical changes and the host responses to the graft, as they respond more similarly since their eye anatomy is closer to that of humans [8]. In this case, similar equipment used for non-invasive examination of human patients are applicable to these animal models. Examples of these examinations include slit lamp biomicroscopy, *in vivo* confocal microscopy (Figure 3.2), and measurements of ocular pressure, sensitivity as we have previously reported [25, 26].

However, the rodent models, as mentioned earlier are valuable for their genetic uniformity and therefore are very useful in studies on the immunology of graft rejection. Especially mice offer the possibility of detailed investigations of immunological responses due to the availability of knock-out



**Figure 3.2** *In vivo* confocal microscopy is used after transplantation as a non-invasive means to track in-growth or overgrowth of cells and nerves into the implant, and also to detect any undesired issues, e.g. neovascularisation, inflammatory cell invasion.

models. Knock-out animals allow for the removal of any element of a response pathway and how this potentially affects the immunological outcome can be determined [8].

### **3.4.2.2 Lamellar and penetrating keratoplasty**

Full-thickness replacement of the cornea is referred to as penetrating keratoplasty (PK). Lamellar keratoplasty (LK) refers to partial-thickness corneal transplantation, which can reach all the way to Descemet's membrane, the layer just before the corneal endothelium. The preservation of the endothelial layer is significant for the outcome of grafting,

The larger animal models are appropriate for both lamellar and penetrating keratoplasty, however the rabbit reacts very strongly to any entry into the anterior chamber, leading to extensive clotting. This is a limiting factor in the case of PK [8].

### **3.4.2.3 Infectious models**

In both humans and animals, there are a range of pathogens that infect the cornea and where the infection leads to severe immunopathological reactions, the cornea is scarred and requires transplantation with a donor graft. However, there is a severe shortage of human donor corneas worldwide and also in a number of conditions, donor grafting is contraindicated. An example is in the

case of Herpes Simplex Virus-1 (HSV-1) keratitis, where the virus remains latent within the host and can reactivate to cause active disease and rejection of the donor graft. Animal models of viral and bacterial infection have been established, most of them in rodents [27–29].

### **3.5 *In Vitro* Systems as Alternatives to Animal Testing**

The demand to replace research on live animals when possible makes it necessary to explore alternative methods before commencing *in vivo* experiments. *In vitro* methods are faster and more cost effective compared to animal experimentation. Initial screening of new materials or compounds using cell lines to assess biocompatibility and to detect possible cytotoxicity is a standard. Organotypic culture is another alternative to animal trials, giving the benefit of a maintained tissue structure and sometimes functions.

An example of this is the beating heart slice culture system. Heart slices obtained from newborn rats sustain spontaneous beating for weeks to months if cultivated in the air-liquid interface [30]. This model has been used for testing cell engraftment when developing stem cell therapies for heart regeneration. The rhythmic beating of the heart slices is important to evaluate how the contractions of the heart tissue could affect materials or cells being introduced, as engraftment is less challenging in a static tissue. Whole organ cultures have also been developed, e.g. the isolated heart [31]

Within our group, we have developed 3-dimensional organotypic equivalents to the human cornea, which we have used in pre-screening all our biomaterials prior to testing within animals. This is detailed below.

Apart from being simply cost effective alternative to animal trials, organotypic cultures allow for studies of specific cell interactions with bioactive factors that would be possible in whole animals due to the presence of often confounding systemic effects.

#### **3.5.1 *In Vitro* Corneal Equivalents for Screening Biomaterials as Potential Implants**

In 1999, Griffith et al. reported the development of the first 3-dimensional human corneal equivalent made using human corneal cell lines that reproduced the key morphology and functional characteristics of the human cornea [32]. This was followed up by innervation of the whole system that allowed for



discrimination of potentially neurotoxic substances [33]. The same models have been used to evaluate the potential safety and efficacy of biomaterials that we have been developing as potential replacements for human donor corneas [25]. Figure 3.3 shows an example of our innervated human corneal equivalent.

To test a potential biomaterial as a corneal implant, the construct under investigation is “implanted” into the *in vitro* corneal model by embedding into the 3D *in vitro* models during the fabrication process. For example, in Figure 3.4, a hydrogel implant was evaluated for its ability to support the proliferation and differentiation of corneal epithelial cells. A hydrogel formulation that does not support epithelialization is discarded while a formulation that supports epithelial differentiation and stratification is retained for further investigation, e.g. in an animal model. Similarly, the model can be used to determine the capacity for promoting nerve in-growth (Figure 3.5).

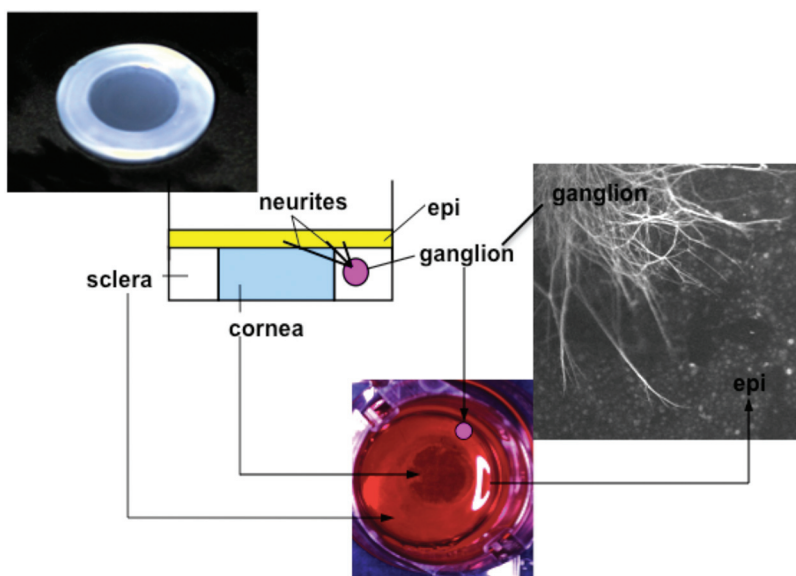


**Figure 3.3** *In vitro* model of “cornea” with surrounding “sclera” with a nerve source embedded within the “sclera”. This allows for in-growth of neuritis into the cornea, mimicking albeit in a highly simplistic manner, the *in vivo* situation where the nerves enter the cornea from the limbal area just beyond the cornea.

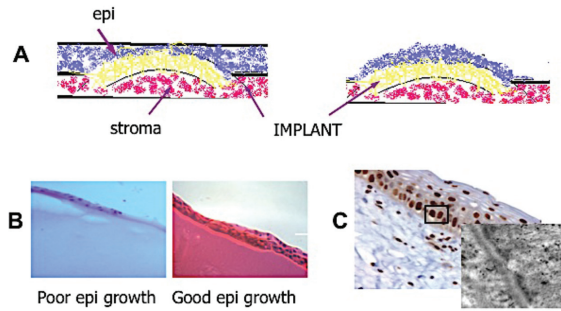


**Figure 3.4** A) A potential hydrogel constructed is “implanted” into a 3D human corneal equivalent model to evaluate the potential for that biomaterial formulation to support growth, differentiation and stratification of corneal epithelial cells. B) Examples of poor and good epithelial growth on two different hydrogel formulations. C) After implantation of the hydrogels that supported good epithelial development into a mini-pig model, the hydrogel did indeed support epithelial re-growth with the formation of a basement membrane complex including anchoring fibrils.

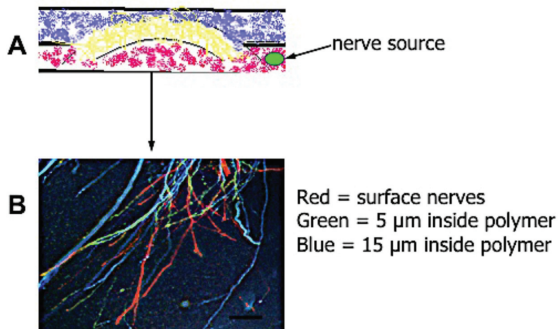


**Figure 3.5** A) A corneal construct is “implanted” into a 3D human corneal equivalent that is supplied with a nerve source, e.g. from a ganglion. B) Nerve growth patterns within the a collagen-polyamide hydrogel as viewed by confocal microscopy. The pseudo-coloured image shows surface located neurites that are coloured red, and neurites inside the polymer, coloured green and blue are at depths of 5  $\mu\text{m}$  and 15  $\mu\text{m}$ , respectively. Bar, 20  $\mu\text{m}$ .

### 3.5.2 In Vitro Angiogenesis Models

A number of *in vitro* angiogenesis and vasculogenesis models have been developed and various kits have been made commercially available [34, 35]. A simple system is illustrated in Figure 3.6, where different collagen-chitosan formulations were screened for their ability to support angiogenesis prior to selection of the best formulations for *in vivo* evaluation.

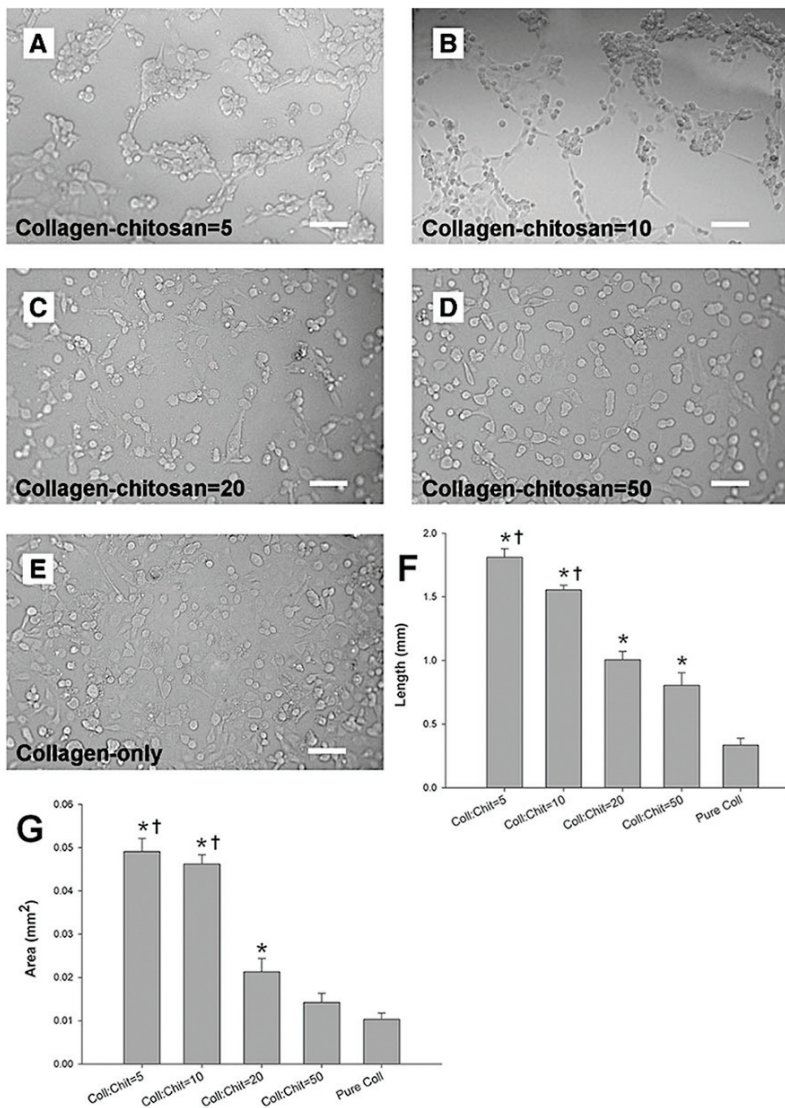


**Figure 3.6** (A–E) Images of human umbilical vein endothelial cells cultured on various hydrogels after 2 days. Capillary-like networks were formed on (A) 5:1 and (B) 10:1 ratio collagen–chitosan hydrogels. (F) The average complete tube length on the different hydrogels. \* $p < 0.003$  versus collagen; { $p < 0.04$  versus all other groups. Scale bar  $\frac{1}{4}75$  mm. (G) The average complete area of tubule structure formation on the different hydrogels. \* $p < 0.005$  versus collagen; { $p < 0.0004$  versus all other groups. Reproduced from Deng C et al. (2010) [36].

### 3.6 Conclusion

We have shown some examples of how animal models are still the mainstay for testing the safety and efficacy of many bioactives, and here in particular, for testing biomaterials as potential implants and injectable delivery systems. However, 3-dimensional, mechanistically accurate *in vitro* models can be developed as alternatives to animal use, particularly for the initial screening of biomaterials implants.

### References

- [1] Russell WMS, Burch RL. The principles of humane experimental technique. London: Methuen & Co. Ltd.; 1959.
- [2] Couzin-Frankel J. When mice mislead. *Science* 2013; 342:922–5.
- [3] Festing MFW. Principles: The need for better experimental design. *Trends in pharmacological sciences* 2003; 24:341–5.
- [4] Festing MFW, Altman DG. Guidelines for the design and statistical analysis of experiments using laboratory animals. *Ilar J* 2002; 43:244–58.
- [5] Johnson PD, D.G. B. Practical aspects of experimental design in animal research. *Ilar J* 2002; 43:202–6.
- [6] Aguilar-Nascimento JE. Fundamental steps in experimental design for animal studies. *Acta Cir Bras* 2005; 20.
- [7] Shanks N, Greek R, Greek J. Are animal models predictive for humans? Philosophy, ethics, and humanities in medicine: PEHM 2009; 4:2.
- [8] Forrester JV, Kuffova L. Corneal transplantation. London: Imperial College Press; 2004.
- [9] Ertl G, Frantz S. Healing after myocardial infarction. *Cardiovascular research* 2005; 66:22–32.
- [10] van der Spoel TI, Jansen of Lorkeers SJ, Agostoni P, van Belle E, Gyongyosi M, Sluijter JP, et al. Human relevance of pre-clinical studies in stem cell therapy: Systematic review and meta-analysis of large animal models of ischaemic heart disease. *Cardiovascular research* 2011; 91:649–58.
- [11] Minicucci MF, Azevedo PS, Polegato BF, Paiva SA, Zornoff LA. Heart failure after myocardial infarction: Clinical implications and treatment. *Clinical cardiology* 2011; 34:410–4.
- [12] Miura T, Miki T. Limitation of myocardial infarct size in the clinical setting: Current status and challenges in translating animal experiments into clinical therapy. *Basic research in cardiology* 2008; 103: 501–13.

- [13] Sun Y. Myocardial repair/remodelling following infarction: Roles of local factors. *Cardiovascular research* 2009; 81:482–90.
- [14] Hasenfuss G. Animal models of human cardiovascular disease, heart failure and hypertrophy. *Cardiovascular research* 1998; 39:60–76.
- [15] Ytrehus K. The ischemic heart—experimental models. *Pharmacological research: the official journal of the Italian Pharmacological Society* 2000; 42:193–203.
- [16] Arvola L, Bertelsen E, Lochner A, Ytrehus K. Sustained anti-beta-adrenergic effect of melatonin in guinea pig heart papillary muscle. *Scandinavian cardiovascular journal: SCJ* 2006; 40:37–42.
- [17] Abarbanell AM, Herrmann JL, Weil BR, Wang Y, Tan J, Moberly SP, et al. Animal models of myocardial and vascular injury. *The Journal of surgical research* 2010; 162:239–49.
- [18] Fröhlich GM, Meier P, White SK, Yellon DM, Hausenloy DJ. Myocardial reperfusion injury: Looking beyond primary pci. *Eur Heart J* 2013; 34:1714–22.
- [19] Michael LH, Entman ML, Hartley CJ, Youker KA, Zhu J, Hall SR, et al. Myocardial ischemia and reperfusion: A murine model. *The American journal of physiology* 1995; 269:H2147–54.
- [20] Degabriele NM, Griesenbach U, Sato K, Post MJ, Zhu J, Williams J, et al. Critical appraisal of the mouse model of myocardial infarction. *Experimental physiology* 2004; 89:497–505.
- [21] van den Bos EJ, Mees BM, de Waard MC, de Crom R, Duncker DJ. A novel model of cryoinjury-induced myocardial infarction in the mouse: A comparison with coronary artery ligation. *American journal of physiology Heart and circulatory physiology* 2005; 289:H1291–300.
- [22] van Amerongen MJ, Harmsen MC, Petersen AH, Popa ER, van Luyn MJ. Cryoinjury: A model of myocardial regeneration. *Cardiovascular pathology: the official journal of the Society for Cardiovascular Pathology* 2008; 17:23–31.
- [23] Kuraitis D, Zhang P, Zhang Y, Padavan DT, McEwan K, Sofrenovic T, et al. A stromal cell-derived factor-1 releasing matrix enhances the progenitor cell response and blood vessel growth in ischaemic skeletal muscle. *European cells & materials* 2011; 22:109–23.
- [24] Kuraitis D, Zhang P, McEwan K, Zhang J, McKee D, Sofrenovic T, et al. Controlled release of stromal cell-derived factor-1 for enhanced progenitor response in ischemia. *Journal of controlled release: official journal of the Controlled Release Society* 2011; 152 Suppl 1: e216–8.

- [25] Li F, Carlsson D, Lohmann C, Suuronen E, Vascotto S, Kobuch K, et al. Cellular and nerve regeneration within a biosynthetic extracellular matrix for corneal transplantation. *Proceedings of the National Academy of Sciences of the United States of America* 2003; 100:15346–51.
- [26] Liu W, Deng C, McLaughlin CR, Fagerholm P, Lagali NS, Heyne B, et al. Collagen-phosphorylcholine interpenetrating network hydrogels as corneal substitutes. *Biomaterials* 2009; 30:1551–9.
- [27] Cowell BA, Wu C, Fleiszig SMA. Use of an animal model in studies of bacterial corneal infection. *Inst Lab Animal Res J* 1999; 40:43–50.
- [28] Webre JM, Hill JM, Nolan NM, Clement C, McFerrin HE, Bhattacharjee PS, et al. Rabbit and mouse models of hsv-1 latency, reactivation, and recurrent eye diseases. *Journal of biomedicine & biotechnology* 2012; 2012:612316.
- [29] Stuart PM, Keadle TL. Recurrent herpetic stromal keratitis in mice: A model for studying human hsk. *Clinical & developmental immunology* 2012; 2012:728480.
- [30] Habeler W, Pouillot S, Plancheron A, Puceat M, Peschanski M, Monville C. An *in vitro* beating heart model for long-term assessment of experimental therapeutics. *Cardiovascular research* 2009; 81:253–9.
- [31] Asimakis GK, Inners-McBride K, Medellin G, Conti VR. Ischemic preconditioning attenuates acidosis and postischemic dysfunction in isolated rat heart. *The American journal of physiology* 1992; 263:H887–94.
- [32] Griffith M, Osborne R, Munger R, Xiong X, Doillon CJ, Laycock NL, et al. Functional human corneal equivalents constructed from cell lines. *Science* 1999; 286:2169–72.
- [33] Suuronen EJ, McLaughlin CR, Stys PK, Nakamura M, Munger R, Griffith M. Functional innervation in tissue engineered models for *in vitro* study and testing purposes. *Toxicological sciences: an official journal of the Society of Toxicology* 2004; 82:525–33.
- [34] Vailhe B, Vittet D, Feige JJ. *In vitro* models of vasculogenesis and angiogenesis. *Laboratory investigation; a journal of technical methods and pathology* 2001; 81:439–52.
- [35] Nakatsu MN, Hughes CC. An optimized three-dimensional *in vitro* model for the analysis of angiogenesis. *Methods in enzymology* 2008; 443: 65–82.
- [36] Deng C, Zhang P, Vulesevic B, Kuraitis D, Li F, Yang AF, et al. A collagen-chitosan hydrogel for endothelial differentiation and angiogenesis. *Tissue engineering Part A* 2010; 16:3099–109.



**Taylor & Francis**

Taylor & Francis Group

<http://taylorandfrancis.com>

# 4

---

## Differentiation Plasticity of Germline Cell-Derived Pluripotent Stem Cells and Their Potential Application in Regenerative Medicine

---

Sharmila Fagoonee, Letizia De Chiara, Lorenzo Silengo  
and Fiorella Altruda

Molecular Biotechnology Center, Department of Molecular Biotechnology and Health Science, University of Torino, Italy  
Corresponding author: Fiorella Altruda <fiorella.altruda@unito.it>

### Abstract

Pluripotent stem cells hold the key to replacing cells in several degenerative and intractable diseases as well as offer the possibility of modeling human diseases and developing new drugs. Stem cells can be differentiated into specialized cell types and can be a useful source of healthy cells in genetic disease, especially those which can be corrected by only a small amount of functional protein. In the last years impressive efforts have been made in understanding the potential application of pluripotent stem cells in the field of regenerative medicine.

In these review, we will discuss the differentiation plasticity of mouse Germline Cell-derived Pluripotent Stem Cells (GPSCs) into different cell types with the aim to translating these potentialities to human organ regeneration.

**Keywords:** Embryonic stem cells, Spermatogonial stem cells, iPS, differentiation, regenerative medicine.



## 4.1 Introduction

Most of the evidence that pluripotent stem cells can be directed to differentiate into specific types of cells suitable for transplantation comes from experiments with mouse cells, and offers the cues for translational research. The application of stem cells in human regenerative medicine could be an alternative to organ transplantation, avoiding the problem of donor shortage and rejection [1]. One important question that has to be answered before stem cells can be effectively translated into significant medical treatments is what type of pluripotent stem cells are the most suitable for human clinical application.

Embryonic stem cells (ESC) are the most versatile cells among pluripotent stem cells. These cells, derived from the inner cells mass of blastocysts, are able to give rise to all type of adult differentiated cells. The development of human embryonic stem cells (hESC) gave an incredible acceleration to stem cell research [2, 3]. Human ESC, like murine ESC, can be differentiated into tissue derived from all three germ layers and have a limitless reproductive capacity. Despite their huge potentiality, the use of human ESC in cell therapy is impeded by moral and ethical concern of destroying human embryos for derivation of ESCs [4]. The recent discovery of the ability to reprogram adult cells into pluripotent embryonic-like stem cells (known as induced pluripotent stem cells; iPS) has profound implications for stem cell therapy [5–8]. The first generation of iPS was generated by introduction of transcription factors, including c-Myc, by retroviral vectors, this probably lead to the generation of neoplastic cells from some induced cells. This problem was solved by using alternative vectors that do not comprise c-Myc [9]. Rapid progress has been made in finding alternative ways to reprogram cells. Now virus-free iPS are available from adult somatic cells [10, 11], this could have important implication in terms of clinical application. iPS have shown remarkable promises in many ways, including the generation of patient-specific iPS [12]. However, the drawback of iPS-based therapy is the need of transducing cells with reprogramming factors to achieve an efficient generation of iPS. Moreover, the existence of inherent epigenetic differences between iPS and ESC can affect iPS functionality [13, 14]. Adult stem cells have been identified in several human tissues, such as liver [15], blood [16], skin [17] and testis [18]. Adult stem cells could be an autologous, free-from-ethical concern, source of pluripotent stem cells. A particular type of adult stem cells that have attracted the interest of the scientific community in the last years are spermatogonial stem cells. Spermatogonial stem cells (SSCs) reside in the basal membrane of testis, these cells are the only stem

cells that undergo self-renewal during all life and generate male gametes. Spermatogonial stem cells derive from primordial germ cells (PGCs) which migrate from proximal epiblast to the gonocytes. Around 7 days post-partum in mice, the gonocytes turn into SSCs that then provide the basis for the first and the following rounds of spermatogenesis [19, 20]. This rare population of cells (0.03%) can give rise to spermatozoa through subsequent division and it is able to restore spermatogenesis once injected in the testis of infertile mice [21]. The capacity to generate spermatozoa seems to be strictly related to the microenvironment, that probably inhibits the potentiality of SSCs and maintains their unipotent state [22, 23]. When transferred *in vitro*, SSCs get free from the inhibitory action of niche, show a broad developmental potential. SSCs are highly specialized cells but several lines of evidence highlight the multipotency of these cells. In fact, teratomas, that are particular types of benign tumors containing derivatives of the three germ layers, occur almost exclusively in the gonads [24]. Moreover, PGCs have the unique feature to give rise to pluripotent ESCs once cultured *in vitro* [25, 26]. In the last ten years, the research demonstrated that SSCs can undergo a spontaneous process to re-acquire pluripotency when cultured *in vitro* for a long period of time [27–33]. In 2004, the first report about SSCs conversion of Kanatsu-Shinoara proved that murine neonatal SSCs could be converted to a ESC-like feature. Since 2004, a large number of groups demonstrate that not only murine neonatal SSCs can form ES-like colony but adult murine SSCs as well. The ES-like colonies derived from SSCs (called Germline Cell-derived Pluripotent Stem Cells, GPSCs) share many hallmarks with ES cells. GPSCs are able to self-renew and differentiate into derivatives of all three germ layers [32]. GPSCs also display a broad potential in that they can be differentiated *in vitro* into functional cardiomyocytes, neurons, glia and hepatocytes [34–36]. Furthermore, GPSCs are capable of forming teratomas once injected subcutaneously in immunocompromized mice and to generate chimeras when injected into blastocytes [27]. Taken together, these data show a huge potential of GPSCs in regenerative medicine. In 2008, Conrad et al. for the first time, claimed to be able to obtain ES-like cells starting from human SSCs [29]. Initially, the pluripotency of these ES-like cells has been demonstrated [30, 31, 33], but more recently, some researchers challenged the concept of pluripotency of human SSCs (hSSC). Despite the murine counterpart, hSSC seems to have less developmental potential in that they are not able to give rise to teratomas or to form all three germ layers after EBs induction [37]. The debate is currently open and more investigation is needed.

## 4.2 Hepatocytes Derived from GPSCs

Hepatic disorders affect hundreds of millions of people worldwide. The mild conditions, if not cured properly, may lead to progressive liver injury, liver fibrosis and ultimately cirrhosis, portal hypertension, liver failure, and, in some instances, cancer [38]. Orthotopic liver transplantation (OLT) has become the standard of care for the treatment of patients with end-stage liver disease resulting in elevated request for OLT. However, the ongoing organ shortage has impeded the treatment of all recurrent-incurable hepatic diseases. Importantly, adult hepatocytes are capable of replicating under particular conditions, for e.g. after a partial hepatectomy [39]. The human liver also contains resident stem cells and the bipotential oval cells that can differentiate into hepatocytes when necessary [15, 40]. However, in a severely compromised liver, the regenerative capacity of hepatocytes and liver stem cells is impaired and can no longer restore functionality. Thus, cell therapy may be the only way out. Hepatocytes transplant have been reported in several cases. For e.g., repeated hepatocyte transplantation in a patient with acute liver failure due to mushroom poisoning has been shown to improve patient's condition and liver functionality [41]. The reported viability of the thawed primary hepatocytes was 62%. This loss in cell viability upon thawing may be a problem, especially when billions of cells are needed for transplant in patients. Hence, alternative sources of hepatocytes are being looked for. Human bone marrow-derived stem cells have been shown to differentiate to hepatocytes *in vitro* and reverse liver failure *in vivo*, but these cells are present in minute fractions and thus are tedious to isolate and difficult to expand [42]. ESCs are considered a very promising source of hepatocytes for cell therapy due to their limitless capacity for self-renewal and proliferation, and their ability to differentiate into all major cell lineages [42]. However, the allogenic nature of these cells as well as the ethical burden, has impeded their use in the clinical setting. GPSCs are an interesting alternative. The differentiative potential of GPSCs are being extensively studied in the mouse with the aim of extending the results to human. EBs generated from mouse GPSCs express the early hepatic marker, alpha fetoprotein. We and others have reported on the directed differentiation of GPSCs into hepatocyte-like cells [36, 43]. Metabolically active hepatocytes, capable of albumin and haptoglobin secretion, urea synthesis, glycogen storage, and indocyanine green uptake can be derived from GPSCs *in vitro* [36]. Our large scale microarray analysis comparing GPSCs to ESCs during hepatocyte differentiation revealed that there was a marked similarity in gene expression profile between these two

cell lines. The GPSC-derived hepatocytes, at Day 28 of *in vitro* differentiation, were closer to fetal hepatocytes (embryonic day 16) than adult hepatocytes (post natal day 1) [36]. *In vivo* studies in mouse models of liver diseases will reveal if these GPSC-derived hepatocytes can home to liver and restore functionality.

GPSCs are thus a promising tool for the treatment of liver diseases. Hepatocytes derived from GPSCs may provide the minimal amount of functional protein that is required to correct certain metabolic diseases. These cells may also be useful in the period awaiting transplant as in the case of newborns with genetic defects [44]. As liver transplant requires mainly blood group compatibility, there is the possibility of transplanting GPSC-derived hepatocytes in both male and female patients [45].

### 4.3 Cardiac Cells Derived from GPSCs

Heart transplantation is one the most effective treatment for severe cardiomyopathies. However, the insufficient number of matching donor hearts has elicited search for other sources of cardiomyocytes including extracardiac ones. Transplantable cell sources identified hitherto comprise cardiac progenitor cells [46], mesenchymal stem cells [47], fetal cardiomyocytes [48], bone marrow cells [49], ES cells [50] and iPS cells [51]. Due to the advantages described above, GPSCs may also offer a substitute to ES cells or iPS cells in cardiomyocytes generation. EBs formed from mouse GPSCs form contracting areas which show cardiomyocyte phenotype characterized by sarcomeric striations when stained for  $\alpha$ -sarcomeric actinin, sarcomeric MHC and cardiac troponin T, organized in bundles [32]. Functional cardiomyocytes could also be generated from these GPSC-derived EBs [34]. Through molecular, cellular, and physiological assays, Guan et al. demonstrated that GPSC-derived cardiomyocytes engrafted into the left ventricular free wall of mice one month post-injection. These cells proliferated in the normal heart without giving rise to teratoma. However, no spontaneous *in vivo* differentiation into cardiomyocytes were observed in the normal heart. The GPSCs differentiated *in loco* into vascular endothelial and smooth muscle cells probably related to the fact that these cells were not induced to differentiate into cardiomyocytes prior to transplantation [52]. Interestingly, Flk1+ cells from differentiating GPSCs could give rise to mature cardiomyocytes and endothelial cells as efficiently as ES cells [53]. Transplantation of these Flk1+ GPSCs directly into the heart of ischemic mice improved cardiac function [54]. Four weeks after treatment,

there was a small number of cardiomyocytes derived from Flk1+ GPSCs in these mice. Enhanced angiogenesis and decreased senescence around the ischemic area was noted the early phase of ischemia [54]. These results are quite promising and indicate GPSCs as potential cardiomyocyte-generating cells for cardiac repair.

#### **4.4 Neuronal Cells Derived from GPSCs**

Stem cells that have the propensity to form neural precursors, mature neurons and glia upon induction *in vitro* are good candidates for cell therapy of neurodegenerative diseases. These include fetal neuroprogenitor cells, bone marrow stem cells [55, 56], ES cells [57] and iPS cells [58]. Recently, the direct conversion of adult human bone marrow stromal cells or skin fibroblasts to neurons have been reported [56, 59, 60]. GPSCs are also capable to differentiating into different neural cell types when given the right cues *in vitro* [35]. Electrophysiological analyses showed maturation of these progenitors into functional neurons (GABAergic, glutamatergic, serotonergic, and dopaminergic neurons) and glial cells (astrocytes and oligodendrocytes) was achieved in the mouse. It was also shown that GPSC-derived neurons can give rise to functional networks which use both GABAergic synaptic transmission and engage in synchronised oscillatory activity [52, 61]. Another important point is that GPSC-derived oligodendrocytes are capable of undergoing complete maturation and ensheathing host axons in myelin-deficient tissue in organotypic slice cultures of the myelin-deficient rat cerebellum [61]. Neural cells can thus be derived from mouse GPSCs and assuming translation to the human system, these cells represent a great potential for the treatment of neurodegenerative diseases.

#### **4.5 Hematopoietic Cells from GPSCs**

GPSCs are also promising candidate for the generation of hematopoietic stem cells for transplantation in patients suffering from hematological malignancies and inherited disorders. GPSCs have been shown to generate CD45+ hematopoietic cells, including Gr-1+Mac1+ myeloid cells and Ter119+ erythroid cells [27]. In a recent report, Yoshimoto *et al.* reported the generation of multipotent hematopoietic progenitor cells with myeloid and lymphoid potential emerging from Flk1+ differentiating GPSCs and described the localisation of GPSC-derived hematopoietic cells in the bone marrow cavity

after intra-bone marrow injection in immunodeficient mice [52, 62]. These GPSC-derived hematopoietic cells, however, failed to expand and showed stem cell repopulating ability *in vivo*. Improved *in vitro* differentiation conditions may be needed to generate a more efficient multipotent hematopoietic progenitor that is capable of proliferating *in vivo*. But there may be also no need to leave the SSCs to acquire pluripotency for so long *in vitro* prior to the transplantation experiments. Ning et al. have shown that GFP<sup>+</sup> Sca-1<sup>+</sup> H-2K<sup>b+</sup> cells isolated from mouse testis and transplanted directly into the bone marrow of GFP<sup>-</sup> male busulfan-treated recipient mice acquired the functional properties of hematopoietic stem cells. Donor derived-GFP<sup>+</sup> cells were present in the bone marrow, peripheral blood and spleen 12 weeks after transplantation. These observations indicate the transdifferentiation potential of mouse SSCs to hematopoietic stem cells *in vivo* [63]. This concurs with a previous observation, in another system, that mouse SSCs, when transplanted into the renal parenchyma of whole body irradiated adult mice, could directly differentiate into mature renal parenchyma cells [64].

#### 4.6 Vascular Cells Derived from GPSCs

Most recently, Im et al. demonstrated that GPSCs can be induced to differentiate into vascular endothelial cells and smooth muscle cells *in vitro* [65]. The vascular differentiation process of GPSCs displayed a developmentally appropriate sequence of transcription factor expression, similar to ES cells, indicating again that GPSCs and ES cells have similar differentiation properties [36]. The GPSC-induced vascular endothelial cells expressed VE-cadherin or CD31 proteins at their cell-cell junctions as observed in primary endothelial cells and these VE-cadherin- or CD31-positive cells formed sprouted branch-like structures. The efficiency of conversion of GPSCs to vascular endothelial cells was 7% compared to 18% of ES cells. The authors also demonstrated that GPSCs could be differentiated into vascular smooth muscle cells. Some differentiated cells from GPSCs were co-stained with anti-SM22- $\alpha$  and anti- $\alpha$ -SMA IgGs, typical markers of adult vascular smooth muscle cells, and exhibited the intracellular fibril structure seen in the control vascular smooth muscle cells. These findings indicate that GPSCs may be considered as a source of vascular smooth muscle cells and endothelial cells for potential therapeutic applications like for the treatment of ischemic vascular diseases.

## References

- [1] Chistiakov DA. Liver Regenerative Medicine: Advances and Challenges. *Cells Tissues Organs*. 2012.
- [2] Thomson JA, Itskovitz-Eldor J, Shapiro SS, Waknitz MA, Swiergiel JJ, Marshall VS, Jones JM. Embryonic stem cell lines derived from human blastocysts. *Science*. 1998; 282(5391): 1145–1147.
- [3] Guhr A, Kurtz A, Friedgen K, Loser P. Current state of human embryonic stem cell research: an overview of cell lines and their use in experimental work. *Stem Cells*. 2006; 24(10): 2187–2191.
- [4] de Wert G, Mummery C. Human embryonic stem cells: research, ethics and policy. *Hum Reprod*. 2003; 18(4): 672–682.
- [5] Takahashi K, Yamanaka S. Induction of pluripotent stem cells from mouse embryonic and adult fibroblast cultures by defined factors. *Cell*. 2006; 126(4): 663–676
- [6] Gibson SA, Gao GD, McDonagh K, Shen S. Progress on stem cell research towards the treatment of Parkinson’s disease. *Stem Cell Res Ther*. 2012; 3(2): 11
- [7] Takahashi K, Tanabe K, Ohnuki M, Narita M, Ichisaka T, Tomoda K, Yamanaka S. Induction of pluripotent stem cells from adult human fibroblasts by defined factors. *Cell*. 2007; 131(5): 861–872.
- [8] Yu J, Vodyanik MA, Smuga-Otto K, Antosiewicz-Bourget J, Frane JL, Tian S, Nie J, Jonsdottir GA, Ruotti V, Stewart R, Slukvin, II, Thomson JA. Induced pluripotent stem cell lines derived from human somatic cells. *Science*. 2007; 318(5858): 1917–1920.
- [9] Nakagawa M, Koyanagi M, Tanabe K, Takahashi K, Ichisaka T, Aoi T, Okita K, Mochizuki Y, Takizawa N, Yamanaka S. Generation of induced pluripotent stem cells without Myc from mouse and human fibroblasts. *Nat Biotechnol*. 2008; 26(1): 101–106.
- [10] Kaji K, Norrby K, Paca A, Mileikovsky M, Mohseni P, Woltjen K. Virus-free induction of pluripotency and subsequent excision of reprogramming factors. *Nature*. 2009; 458(7239): 771–775.
- [11] Lengner CJ. iPS cell technology in regenerative medicine. *Ann NY Acad Sci*. 2010; 1192: 38–44.
- [12] Dimos JT, Rodolfa KT, Niakan KK, Weisenthal LM, Mitsumoto H, Chung W, Croft GF, Saphier G, Leibel R, Golland R, Wichterle H, Henderson CE, Eggan K. Induced pluripotent stem cells generated from patients with ALS can be differentiated into motor neurons. *Science*. 2008; 321(5893): 1218–1221.

- [13] Stadtfeld M, Apostolou E, Akutsu H, Fukuda A, Follett P, Natesan S, Kono T, Shioda T, Hochedlinger K. Aberrant silencing of imprinted genes on chromosome 12qF1 in mouse induced pluripotent stem cells. *Nature*. 2010; 465(7295): 175–181.
- [14] Lister R, Pelizzola M, Kida YS, Hawkins RD, Nery JR, Hon G, Antosiewicz-Bourget J, O'Malley R, Castanon R, Klugman S, Downes M, Yu R, Stewart R, Ren B, Thomson JA, Evans RM, Ecker JR. Hotspots of aberrant epigenomic reprogramming in human induced pluripotent stem cells. *Nature*. 2011; 471(7336): 68–73.
- [15] Herrera MB, Bruno S, Buttiglieri S, Tetta C, Gatti S, Deregibus MC, Bussolati B, Camussi G. Isolation and characterization of a stem cell population from adult human liver. *Stem Cells*. 2006; 24(12): 2840–2850.
- [16] Notta F, Doulatov S, Laurenti E, Poeppl A, Jurisica I, Dick JE. Isolation of single human hematopoietic stem cells capable of long-term multilineage engraftment. *Science*. 2011; 333(6039): 218–221.
- [17] Boehnke K, Falkowska-Hansen B, Stark HJ, Boukamp P. Stem cells of the human epidermis and their niche: composition and function in epidermal regeneration and carcinogenesis. *Carcinogenesis*. 2012.
- [18] Liu S, Tang Z, Xiong T, Tang W. Isolation and characterization of human spermatogonial stem cells. *Reprod Biol Endocrinol*. 2011; 9: 141.
- [19] de Rooij DG, Russell LD. All you wanted to know about spermatogonia but were afraid to ask. *J Androl*. 2000; 21(6): 776–798.
- [20] Hayashi K, de Sousa Lopes SM, Surani MA. Germ cell specification in mice. *Science*. 2007; 316(5823): 394–396.
- [21] Lo KC, Domes T. Can we grow sperm? A translational perspective on the current animal and human spermatogenesis models. *Asian J Androl*. 2011; 13(5): 677–682
- [22] de Rooij DG. The spermatogonial stem cell niche. *Microsc Res Tech*. 2009; 72(8): 580–585.
- [23] Kostereva N, Hofmann MC. Regulation of the spermatogonial stem cell niche. *Reprod Domest Anim*. 2008; 43 Suppl 2: 386–392.
- [24] Stevens LC. Spontaneous and experimentally induced testicular teratomas in mice. *Cell Differ*. 1984; 15(2-4): 69–74.
- [25] Matsui Y, Zsebo K, Hogan BL. Derivation of pluripotential embryonic stem cells from murine primordial germ cells in culture. *Cell*. 1992; 70(5): 841–847.
- [26] Shambloott MJ, Axelman J, Wang S, Bugg EM, Littlefield JW, Donovan PJ, Blumenthal PD, Huggins GR, Gearhart JD. Derivation of pluripotent



- stem cells from cultured human primordial germ cells. *Proc Natl Acad Sci U S A*. 1998; 95(23): 13726–13731.
- [27] Kanatsu-Shinohara M, Inoue K, Lee J, Yoshimoto M, Ogonuki N, Miki H, Baba S, Kato T, Kazuki Y, Toyokuni S, Toyoshima M, Niwa O, Oshimura M, Heike T, Nakahata T, Ishino F, Ogura A, Shinohara T. Generation of pluripotent stem cells from neonatal mouse testis. *Cell*. 2004; 119(7): 1001–1012.
- [28] Seandel M, James D, Shmelkov SV, Falcatori I, Kim J, Chavala S, Scherr DS, Zhang F, Torres R, Gale NW, Yancopoulos GD, Murphy A, Valenzuela DM, Hobbs RM, Pandolfi PP, Rafii S. Generation of functional multipotent adult stem cells from GPR125+ germline progenitors. *Nature*. 2007; 449(7160): 346–350.
- [29] Conrad S, Renninger M, Hennenlotter J, Wiesner T, Just L, Bonin M, Aicher W, Buhring HJ, Mattheus U, Mack A, Wagner HJ, Minger S, Matzkies M, Reppel M, Hescheler J, Sievert KD, Stenzl A, Skutella T. Generation of pluripotent stem cells from adult human testis. *Nature*. 2008; 456(7220): 344–349.
- [30] Golestaneh N, Kokkinaki M, Pant D, Jiang J, DeStefano D, Fernandez-Bueno C, Rone JD, Haddad BR, Gallicano GI, Dym M. Pluripotent stem cells derived from adult human testes. *Stem Cells Dev*. 2009; 18(8): 1115–1126.
- [31] Kossack N, Meneses J, Shefi S, Nguyen HN, Chavez S, Nicholas C, Gromoll J, Turek PJ, Reijo-Pera RA. Isolation and characterization of pluripotent human spermatogonial stem cell-derived cells. *Stem Cells*. 2009; 27(1): 138–149.
- [32] Guan K, Nayernia K, Maier LS, Wagner S, Dressel R, Lee JH, Nolte J, Wolf F, Li M, Engel W, Hasenfuss G. Pluripotency of spermatogonial stem cells from adult mouse testis. *Nature*. 2006; 440(7088): 1199–1203.
- [33] Mizrak SC, Chikhovskaya JV, Sadri-Ardekani H, van Daalen S, Korver CM, Hovingh SE, Roepers-Gajadien HL, Raya A, Fluiter K, de Reijke TM, de la Rosette JJ, Knegt AC, Belmonte JC, van der Veen F, de Rooij DG, Repping S, van Pelt AM. Embryonic stem cell-like cells derived from adult human testis. *Hum Reprod*. 2010; 25(1): 158–167.
- [34] Guan K, Wagner S, Unsold B, Maier LS, Kaiser D, Hemmerlein B, Nayernia K, Engel W, Hasenfuss G. Generation of functional cardiomyocytes from adult mouse spermatogonial stem cells. *Circ Res*. 2007; 100(11): 1615–1625.

- [35] Streckfuss-Bomeke K, Vlasov A, Hulsmann S, Yin D, Nayernia K, Engel W, Hasenfuss G, Guan K. Generation of functional neurons and glia from multipotent adult mouse germ-line stem cells. *Stem Cell Res.* 2009; 2(2): 139–154.
- [36] Fagoonee S, Hobbs RM, De Chiara L, Cantarella D, Piro RM, Tolosano E, Medico E, Provero P, Pandolfi PP, Silengo L, Altruda F. Generation of functional hepatocytes from mouse germ line cell-derived pluripotent stem cells *in vitro*. *Stem Cells Dev.* 2010; 19(8): 1183–1194.
- [37] Chikhovskaya JV, Jonker MJ, Meissner A, Breit TM, Repping S, van Pelt AM. Human testis-derived embryonic stem cell-like cells are not pluripotent, but possess potential of mesenchymal progenitors. *Hum Reprod.* 2012; 27(1): 210–221.
- [38] Piscaglia AC, Campanale M, Gasbarrini A, Gasbarrini G. Stem cell-based therapies for liver diseases: state of the art and new perspectives. *Stem Cells Int.* 2010; 2010: 259–461.
- [39] Brezillon N, Kremsdorf D, Weiss MC. Cell therapy for the diseased liver: from stem cell biology to novel models for hepatotropic human pathogens. *Dis Model Mech.* 2008; 1(2–3): 113–130.
- [40] Oh SH, Hatch HM, Petersen BE. Hepatic oval ‘stem’ cell in liver regeneration. *Semin Cell Dev Biol.* 2002; 13(6): 405–409.
- [41] Schneider A, Attaran M, Meier PN, Strassburg C, Manns MP, Ott M, Barthold M, Arseniev L, Becker T, Panning B. Hepatocyte transplantation in an acute liver failure due to mushroom poisoning. *Transplantation.* 2006; 82(8): 1115–1116.
- [42] Cho CH, Parashurama N, Park EY, Suganuma K, Nahmias Y, Park J, Tilles AW, Berthiaume F, Yarmush ML. Homogeneous differentiation of hepatocyte-like cells from embryonic stem cells: applications for the treatment of liver failure. *FASEB J.* 2008; 22(3): 898–909.
- [43] Loya K, Eggenschwiler R, Ko K, Sgodda M, Andre F, Bleidissel M, Scholer HR, Cantz T. Hepatic differentiation of pluripotent stem cells. *Biol Chem.* 2009; 390(10): 1047–1055.
- [44] Cowles RA, Lobritto SJ, Ventura KA, Harren PA, Gelbard R, Emond JC, Altman RP, Jan DM. Timing of liver transplantation in biliary atresia—results in 71 children managed by a multidisciplinary team. *J Pediatr Surg.* 2008; 43(9): 1605–1609.
- [45] Navarro V, Herrine S, Katopes C, Colombe B, Spain CV. The effect of HLA class I (A and B) and class II (DR) compatibility on liver transplantation outcomes: an analysis of the OPTN database. *Liver Transpl.* 2006; 12(4): 652–658.

- [46] Rosenblatt-Velin N, Lepore MG, Cartoni C, Beermann F, Pedrazzini T. FGF-2 controls the differentiation of resident cardiac precursors into functional cardiomyocytes. *J Clin Invest.* 2005; 115(7): 1724–1733.
- [47] Psaltis PJ, Zannettino AC, Worthley SG, Gronthos S. Concise review: mesenchymal stromal cells: potential for cardiovascular repair. *Stem Cells.* 2008; 26(9): 2201–2210.
- [48] Skobel E, Schuh A, Schwarz ER, Liehn EA, Franke A, Breuer S, Gunther K, Reffelmann T, Hanrath P, Weber C. Transplantation of fetal cardiomyocytes into infarcted rat hearts results in long-term functional improvement. *Tissue Eng.* 2004; 10(5–6): 849–864.
- [49] Loffredo FS, Steinhauser ML, Gannon J, Lee RT. Bone marrow-derived cell therapy stimulates endogenous cardiomyocyte progenitors and promotes cardiac repair. *Cell Stem Cell.* 2011; 8(4): 389–398.
- [50] Kolossov E, Bostani T, Roell W, Breitbach M, Pillekamp F, Nygren JM, Sasse P, Rubenchik O, Fries JW, Wenzel D, Geisen C, Xia Y, Lu Z, Duan Y, Kettenhofen R, Jovinge S, Bloch W, Bohlen H, Welz A, Hescheler J, Jacobsen SE, Fleischmann BK. Engraftment of engineered ES cell-derived cardiomyocytes but not BM cells restores contractile function to the infarcted myocardium. *J Exp Med.* 2006; 203(10): 2315–2327.
- [51] Zhang J, Wilson GF, Soerens AG, Koonce CH, Yu J, Palecek SP, Thomson JA, Kamp TJ. Functional cardiomyocytes derived from human induced pluripotent stem cells. *Circ Res.* 2009; 104(4):e30–41.
- [52] Fagoonee S, Pellicano R, Silengo L, Altruda F. Potential applications of germline cell-derived pluripotent stem cells in organ regeneration. *Organogenesis.* 2011; 7(2): 116–122.
- [53] Baba S, Heike T, Umeda K, Iwasa T, Kaichi S, Hiraumi Y, Doi H, Yoshimoto M, Kanatsu-Shinohara M, Shinohara T, Nakahata T. Generation of cardiac and endothelial cells from neonatal mouse testis-derived multipotent germline stem cells. *Stem Cells.* 2007; 25(6): 1375–1383.
- [54] Iwasa T, Baba S, Doi H, Kaichi S, Yokoo N, Mima T, Kanatsu-Shinohara M, Shinohara T, Nakahata T, Heike T. Neonatal mouse testis-derived multipotent germline stem cells improve the cardiac function of acute ischemic heart mouse model. *Biochem Biophys Res Commun.* 2010; 400(1): 27–33.
- [55] Zhang XM, Du F, Yang D, Yu CJ, Huang XN, Liu W, Fu J. Transplanted bone marrow stem cells relocate to infarct penumbra and co-express endogenous proliferative and immature neuronal markers in a mouse model of ischemic cerebral stroke. *BMC Neurosci.* 2010; 11: 138.

- [56] Woodbury D, Schwarz EJ, Prockop DJ, Black IB. Adult rat and human bone marrow stromal cells differentiate into neurons. *J Neurosci Res*. 2000; 61(4): 364–370.
- [57] Kriks S, Shim JW, Piao J, Ganat YM, Wakeman DR, Xie Z, Carrillo-Reid L, Auyeung G, Antonacci C, Buch A, Yang L, Beal MF, Surmeier DJ, Kordower JH, Tabar V, Studer L. Dopamine neurons derived from human ES cells efficiently engraft in animal models of Parkinson's disease. *Nature*. 2011; 480(7378): 547–551.
- [58] Karumbayaram S, Novitsch BG, Patterson M, Umbach JA, Richter L, Lindgren A, Conway AE, Clark AT, Goldman SA, Plath K, Wiedau-Pazos M, Kornblum HI, Lowry WE. Directed differentiation of human-induced pluripotent stem cells generates active motor neurons. *Stem Cells*. 2009; 27(4): 806–811.
- [59] Vierbuchen T, Ostermeier A, Pang ZP, Kokubu Y, Sudhof TC, Wernig M. Direct conversion of fibroblasts to functional neurons by defined factors. *Nature*. 2010; 463(7284): 1035–1041.
- [60] Qi X, Shao M, Peng H, Bi Z, Su Z, Li H. *In vitro* differentiation of bone marrow stromal cells into neurons and glial cells and differential protein expression in a two-compartment bone marrow stromal cell/neuron co-culture system. *J Clin Neurosci*. 2010; 17(7): 908–913.
- [61] Glaser T, Opitz T, Kischlat T, Konang R, Sasse P, Fleischmann BK, Engel W, Nayernia K, Brustle O. Adult germ line stem cells as a source of functional neurons and glia. *Stem Cells*. 2008; 26(9): 2434–2443.
- [62] Yoshimoto M, Heike T, Chang H, Kanatsu-Shinohara M, Baba S, Varnau JT, Shinohara T, Yoder MC, Nakahata T. Bone marrow engraftment but limited expansion of hematopoietic cells from multipotent germline stem cells derived from neonatal mouse testis. *Exp Hematol*. 2009; 37(12): 1400–1410.
- [63] Ning L, Goossens E, Geens M, Van Saen D, Van Riet I, He D, Tournaye H. Mouse spermatogonial stem cells obtain morphologic and functional characteristics of hematopoietic cells *in vivo*. *Hum Reprod*. 2010; 25(12): 3101–3109.
- [64] Wu DP, He DL, Li X, Liu ZH. Differentiations of transplanted mouse spermatogonial stem cells in the adult mouse renal parenchyma *in vivo*. *Acta Pharmacol Sin*. 2008; 29(9): 1029–1034
- [65] Im JE, Song SH, Kim JY, Kim KL, Baek SH, Lee DR, Suh W. Vascular differentiation of multipotent spermatogonial stem cells derived from neonatal mouse testis. *Exp Mol Med*. 2012; 44(4): 303–309.



**Taylor & Francis**

Taylor & Francis Group

<http://taylorandfrancis.com>

# 5

---

## Mechanical Stimulation in Tissue Engineering

---

**John Rasmussen, Cristian Pablo Pennisi, Tea Rasmussen, Marcelo Ferreira, Christian Gammelgaard Olesen and Vladimir Zachar**

Aalborg University, Denmark

Corresponding author: John Rasmussen <jr@m-tech.aau.dk>

### 5.1 Background and Introduction

It is well accepted that mechanical stimulation influences cell differentiation and growth. In the related field of pressure ulcers, investigations have revealed that mechanical deformations can lead to tissue necrosis. For a comprehensive review of theories explaining tissue necrosis under mechanical loads, please refer to Olesen, de Zee, & Rasmussen (2010) [1]. In other words, mechanics plays an important role for the entire lifecycle of cells and tissue in general. Methods for the consistent investigation of the related phenomena are therefore important.

This chapter reports on development of methods to impart controlled states of deformation to tissue samples *in vitro*. These methods are generally applicable for tissue growth but we shall focus on experimental investigation of cell necrosis in response to different loading conditions. This can possibly contribute to development of an injury criterion for tissue, which can have direct impact on healthcare practices.

#### 5.1.1 Mechanical Theories of Material Damage

Mechanics of materials is a well-developed area considering both macroscopic and microscopic behavior of materials. In this field, the concept of strength refers to the ability of a material or a structure to withstand loads without breaking or collapsing. The applied loads may be static, such as the self-weight of a bridge, or dynamic, such as the vibrations affecting the wing of an aircraft in turbulent air or the cyclic bending and torsion of a bicycle

*Mayuri Prasad and Paolo Di Nardo (Eds.), Innovative Strategies in Tissue Engineering, 67–78.*

© 2014 River Publishers. All rights reserved.

crankshaft. Common to these cases is the idea that the material is inert, i.e. does not change its properties except from the damage caused by the applied loads.

Stress and strain are central concepts in strength of materials, and the concept of strength is coupled to an idea of the local stresses or strains causing immediate or cumulative damage at each material point. For materials with linear behavior (which is usually the case for sufficiently small deformations) stresses are coupled to strains through Hooke's law, stating that

$$\boldsymbol{\sigma} = \mathbf{E}\boldsymbol{\varepsilon} \quad (5.1)$$

where  $\boldsymbol{\sigma}$  is the stress tensor,  $\boldsymbol{\varepsilon}$  is the strain tensor, and  $\mathbf{E}$  is the elasticity tensor. Two points are important for later application of this idea to living tissues. Firstly, stress cannot be measured but only calculated, whereas strain is derived directly from deformation, which can be experimentally observed. It may not be immediately obvious to the casual student of mechanics that force (and stress) are imaginary physical quantities, but it becomes obvious if we look at methods for measuring force: they are all based on some form of observation of deformation.

Secondly, all terms of Equation (5.1) are tensors, i.e. multidimensional properties. In its most general form,  $\mathbf{E}$  contains 81 components, which by means of symmetry conditions and thermodynamic considerations can be drastically reduced. All properties, however, remain multidimensional to some extent depending on the properties of the material in question. It therefore rarely makes sense to discuss "the strain" or "the stress" as though the property is one-dimensional.

It is therefore also impossible, except in much idealized cases, to appoint a single stress or strain level that breaks a given material. However, many technically important materials can with good approximation be assumed ductile, homogeneous and isotropic and, for such materials, the yield criterion of von Mises is well-established. This criterion is based on a scalar combination of components of the stress tensor. We shall call this scalar combination the von Mises stress. For a certain class of materials, it is well accepted that yield, i.e. permanent deformation, occurs when the von Mises stress exceeds a magnitude that is characteristic for the given material. It is important to notice that many different combinations of stress components can result in the same value of the von Mises stress and therefore lead to yield. Similar yield or failure criteria have been developed with varying success for more complex materials, for instance the Tsai-Hill [2] and Tsai-Wu [3] criteria for

composites or statistical failure prediction based on Weibull statistics [4] for ceramics.

Let us review the definition of the von Mises stress. A material has six stress components in its tensor. These components depend on the coordinate system, so the stress tensor changes when the reference frame is rotated, although the material remains in the same state. In other words, the same stress state in the same material point can be expressed by many different stress tensors. In its general form, a stress tensor contains the following components:

$$\boldsymbol{\sigma} = \begin{bmatrix} \sigma_{xx} & \sigma_{xy} & \sigma_{xz} \\ \sigma_{xy} & \sigma_{yy} & \sigma_{yz} \\ \sigma_{xz} & \sigma_{yz} & \sigma_{zz} \end{bmatrix} \quad (5.2)$$

where indices  $x$ ,  $y$  and  $z$  refer to directions in the chosen coordinate system. The diagonal elements,  $\sigma_{ii}$ , are normal stresses and designate pure compression or tension of the material, and the off-diagonal elements are shear stresses. The tensor is always symmetrical and positive definite for any physical material.

It turns out that stress tensors have the interesting property that it is always possible to rotate the coordinate system such that the tensor takes the simplified form:

$$\boldsymbol{\sigma} = \begin{bmatrix} \sigma_1 & 0 & 0 \\ 0 & \sigma_2 & 0 \\ 0 & 0 & \sigma_3 \end{bmatrix} \quad (5.3)$$

In this particular rotation of the coordinate system, the material experiences no shear stress. The normal stresses in this state,  $\sigma_1$ ,  $\sigma_2$  and  $\sigma_3$ , are called principal stresses, and  $\sigma_1 \geq \sigma_2 \geq \sigma_3$  by definition. Most people have an immediate physical comprehension of the difference between shear and normal deformation and are able to recognize these states when they see them applied to a soft material with sufficiently large deformations. It is mind-boggling that viewing the same material point in the same state of deformation from a different vantage point would reveal no shear. That is, however, a mathematical fact.

There exists another rotation of the coordinate system where the shear stresses are at their maximum, and it furthermore turns out that these shear stresses are equivalent to the so-called deviations of the principal stresses:  $\sigma_1 - \sigma_3$ ,  $\sigma_1 - \sigma_2$ , and  $\sigma_2 - \sigma_3$ . We can therefore conclude that there exists only a single state of stress that has no shear, namely the case where  $\sigma_1 = \sigma_2 = \sigma_3$ . This case of similar stress in all directions is called a hydrostatic



stress state because it is equivalent to the state of a material subjected to constant pressure from all sides as if it were submersed into water.

We can now look at the definition of von Mises stress in terms of principal stresses:

$$\sigma_{vM} = \sqrt{\frac{1}{2} \left( (\sigma_1 - \sigma_2)^2 + (\sigma_1 - \sigma_3)^2 + (\sigma_2 - \sigma_3)^2 \right)} \quad (5.4)$$

Notice that Equation (5.4) contains only the principal stress deviations. This means that

1. Hydrostatic pressure, according to this criterion, does not contribute in any way to the yield of a material.
2. Shear stress, measured in the direction where it is at its maximum, is actually the sole contributor to damage of a material.

### 5.1.2 Damage of Living Tissue

There is good experimental evidence [5] that deformation alone, as with engineering materials, can cause injury in the form of cell necrosis to living tissue, but a criterion for material damage similar to the von Mises yield criterion does not exist for living tissues.

It is also fair to state that living tissues from a material science point-of-view are very different from the underlying assumptions of ductility, homogeneity and isotropy necessary for the von Mises criterion. Furthermore, living tissues in a state of homeostasis have the ability to repair themselves, whereas a partial damage of an engineering material is permanent.

It would appear that there is no reason to presume that living tissue composed of cells and protein structures would be damaged by similar mechanisms as engineering materials. However, similarly to living tissue, engineering materials are only homogeneous on a macroscopic scale. Metals are composed of crystals, many alloys even of patterns of different crystals and, on a smaller scale, materials are made of discrete molecules and atoms. Any material is in fact a structure on a sufficiently small scale.

Living tissues also share a high resistance towards hydrostatic pressure with engineering materials. Marine animals can transition without tissue injury between the sea surface and great depth where the water pressure is significant.

On the other hand, it is also known from clinical practice that a deformation of sufficient size sustained for sufficient time will lead to tissue necrosis. This is the case for pressure ulcers, a serious tissue injury affecting individuals with reduced sensibility and/or inability to relieve pressure on the tissues,

such as paraplegics, diabetics and bedridden patients in general. The etiology of pressure ulcers is poorly understood [1], and this lack of understanding is an obstacle to prevention and treatment of pressure ulcers.

It is obvious that a closer investigation of the matter requires experiments in which living tissue can be subjected to controlled states of deformation. We shall base the following on strains rather than stress because strain is an experimentally measurable quantity and the strain tensor shares the aforementioned properties of the stress tensor, i.e. we can discuss normal strains, shear strains and principal strains.

## 5.2 Mechanical Loading in Two Dimensions

Mechanical stimulation of growing tissue in two dimensions can conveniently take place on elastic membranes, such as the Flexcell well system. This system comprises a circular silicone membrane on which tissue samples can be grown. The membrane can be subjected to deformation to impart strain on the attached tissue sample. The deformation is obtained by draping the membrane over a post by means of vacuum on one side of the membrane as illustrated in Figure 5.1.

Deformation experiments with the Flexcell system have traditionally taken place using circular posts. However, with non-circular posts, non-hydrostatic strain states can be obtained. It is possible by finite element analysis to obtain accurate predictions of the resulting strain states as illustrated in Figure 5.2.

Figure 5.2 shows the resulting maximum shear strains when draping a membrane over differently shaped posts ranging from circular (left) to elliptical with an axis ratio of 1.23 (right). Please notice that the circular post results in zero shear strain on the membrane over the post while non-circular posts impart shear strain to the membrane and thereby to the tissue sample.

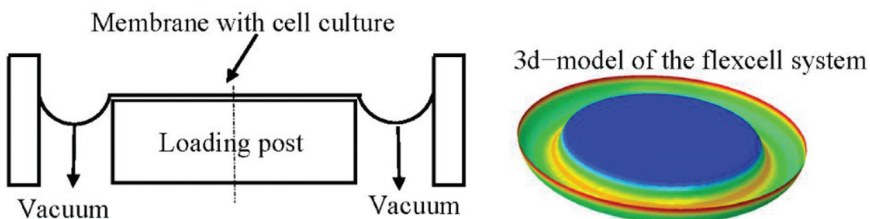


**Figure 5.1** Draping the membrane over a post by means of vacuum. The colors on the right-hand picture are membrane shear strains simulated by a 3-D model. Notice that the strain field is uniform over the post.

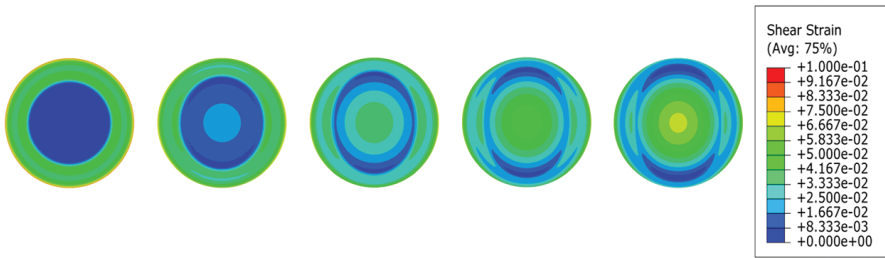


**Figure 5.2** Finite element simulation of maximum shear strains on a membrane draped over posts with varying degrees of ovality.

While it is theoretically possible to control the amount of shear strain imposed on a tissue sample by means of non-circular posts, it unfortunately turns out that the adhesion between the silicon membrane and the tissue sample is insufficient to cause tissue injury. When imposing strain levels similar to those experienced by, for instance, muscle tissue in the buttocks in the seated posture, the cells come loose from the membrane and cease to follow the membrane's deformation. Thus, this method is not suitable for investigations of tissue injury, but it does allow for mechanical stimulation of tissue samples for other purposes [6].

### 5.2.1 Hertz-inspired Tissue Deformation

An alternative loading mechanism, inspired by Hertz contact mechanics [7], was invented to enable imposition of sufficient strain to cause necrosis. Mechanical problems of contact are in general highly nonlinear and very challenging, but a famous analytical solution attributed to Heinrich Hertz covers the special case of two linearly elastic spheres in contact. Given the material properties, the radii of the two spheres and the compression force, the analytical solution predicts the deformation state including strain and stress fields in the two parts. This is one of the truly classical problems of mechanics and it is an important part of the basis of the field of tribology and the ability to develop many important machine parts such as bearings and gears. An important special case of Hertz' solution is when one of the spheres has an infinite radius, i.e. is flat.

The case of a sphere pressed into a planar surface is axisymmetric and so is the resulting strain state. If we focus on the planar part, this means that the strain tensor in a given point depends only on the force (or relative displacement of the two parts), the point's depth under the planar surface

and the point's radial distance from the center of pressure as illustrated in Figure 5.3.

Thus, a cell embedded in the material under the flat surface will be subjected to a predictable strain state depending only on its location in the material. Furthermore, the strain state created by surface pressure is non-hydrostatic and three-dimensional, such that the strain ingredients that would be decisive to material yield or failure would be present in various amounts at different locations.

The feasibility of this idea depends on the material into which the cell is embedded being an order of magnitude stiffer than the cell, such that the deformation of the cell is commanded completely by the surrounding material. Furthermore, the material must sustain the life of the cell, i.e. be permeable to oxygen and provide nutrition. It was experimentally verified that specific compositions of alginate gels have these properties and can be exploited in the experimental setup illustrated in Figure 5.4.

In this setup, tissue in a culture dish is covered with a layer of gel and a spherical indenter controlled by means of precision motors can be pressed into the gel causing axisymmetric strain as described above.

Hertz' surface pressure model requires linear elasticity of the involved materials, and this is not the case for a gel undergoing large deformations. The actual prediction of the strain field therefore cannot be based on Hertz' equations but must be computed numerically by a nonlinear finite element analysis as illustrated in Figure 5.5.

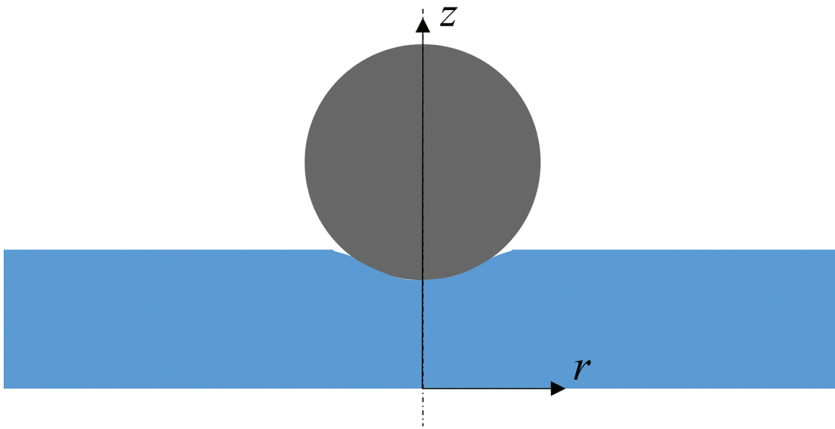


**Figure 5.3** Indentation of a sphere into a planar surface. The strain state will be symmetrical about the  $z$  axis, and the strain tensor at a given  $(r, z)$  position can be predicted.

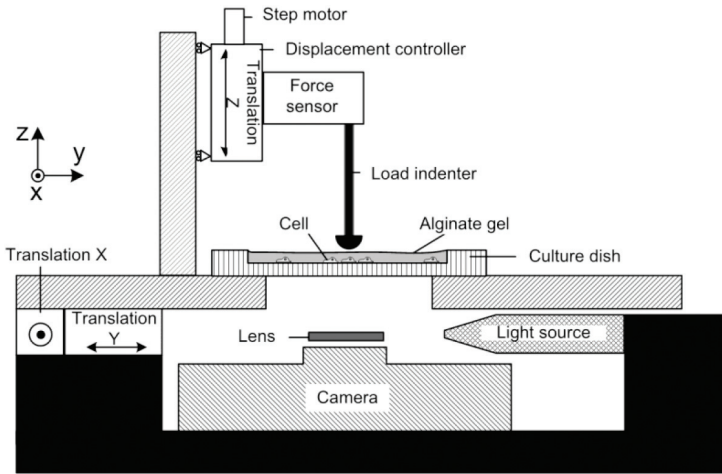


**Figure 5.4** Experimental setup.

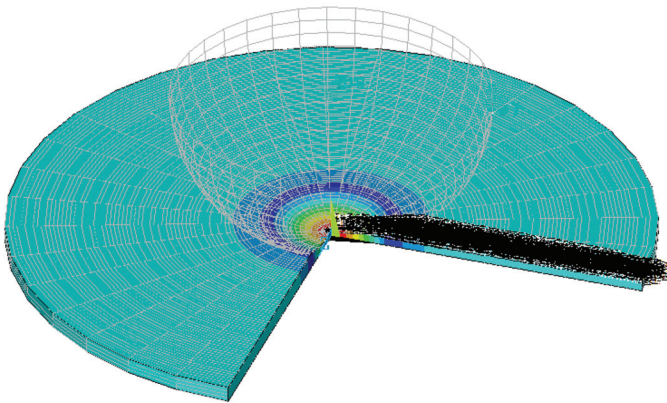


**Figure 5.5** Axisymmetric, nonlinear finite element model of sphere indentation into an alginate gel.

The finite element model predicts the strain field under the indenter and consequently also the strain state felt by a cell located at a given point in the gel. It is possible to visualize the strain field in terms of maximum shear strain to obtain the strain map of Figure 5.6.

The fact that the strain field decreases systematically (albeit nonlinearly) from the center of pressure to zero at about 8 mm distance means that the viability of cells under varying shear strain can be studied systematically using this setup.

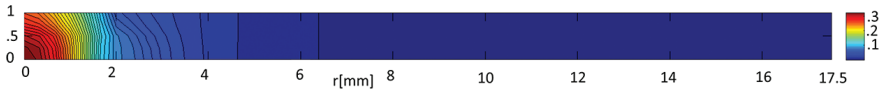


**Figure 5.6** Maximum shear strain as a function of radius ( $r$ ) and height ( $z$ ) in a gel under compression of a circular indenter. The strain is at its maximum at  $(r, z) = (0, 0)$  i.e. directly below the center of pressure and decreases radially.

The viability of the cells is observed under microscope by means of Lentiviral transfection of emerald green fluorescent protein (GFP). This staining technique allows the simultaneous study of cell morphology and viability by combination of the red and green channels of the microscope image. Necrotic cells appear as bright spots in the image.

### 5.2.2 Preliminary Results of Cell Straining

Figure 5.7 shows the viability of cells under the indenter, where the yellow dots designate dead cells. In this test, the indentation was increased over time to compensate for a significant stress relaxation of the gel.

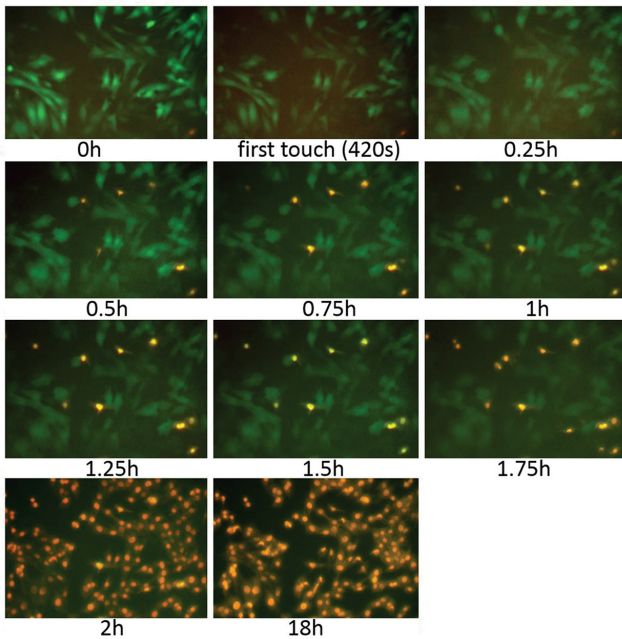


**Figure 5.7** Necrosis of cells over time with different compression forces applied.

It is obvious that cell necrosis increases significantly over time until all cells are dead after about two hours. Please notice that it was verified prior to this experiment that no significant necrosis occurred under similar circumstances in the absence of the indenter load. Thus, the experiment corroborates the theory that imposed and sustained deformation causes cell necrosis.

This experiment simply observed cells directly under the indenter, while an attempt to determine the correlation between location, and thereby strain state, and the risk of necrosis is left to future studies.

### **5.3 Conclusions and Outlook**

A theoretical foundation addressing strain state and cell necrosis has been developed, and an experimental procedure capable of imposing controlled amounts of strain to cells imbedded into gel is established and tested. The tests show that the imposed strain has a clear influence on the necrosis of the cells, and it is possible that such experiments, when conducted systematically, can lead to development of an actual cell necrosis theory.

Such a theory, in turn, is of fundamental as well as practical interest. The clinical uses include prevention and treatment of pressure ulcers and tissue engineering in a broader sense.

### **References**

- [1] Olesen, C. G., de Zee, M., Rasmussen, J., 2010. Missing Links in Pressure Ulcer Research - An Interdisciplinary Overview. *J. Appl. Physiol.*
- [2] Hill, R., 1948. A Theory of the Yielding and Plastic Flow of Anisotropic Metals. *Proceedings of the Royal Society of London. Series A. Mathematical and Physical Sciences.* 193, 281–297.
- [3] Tsai, S. W., Wu, E. M., 1971. A General Theory of Strength for Anisotropic Materials. *Journal of Composite Materials.* 5, 58–80.
- [4] Klein, C. A., 2009. Characteristic strength, Weibull modulus, and failure probability of fused silica glass. *OPTICA.* 48, 113401-1-113401-10.
- [5] Breuls, R. G., Bouten, C. V., Oomens, C. W., Bader, D. L., Baaijens, F. P., 2003. Compression induced cell damage in engineered muscle tissue: an in vitro model to study pressure ulcer aetiology. *Ann. Biomed. Eng.* 31, 1357–1364.

- [6] Pennisi, C. P., Olesen, C. G., de Zee, M., Rasmussen, J., Zachar, V., 2011. Uniaxial Cyclic Strain Drives Assembly and Differentiation of Skeletal Myocytes. *Tissue Engineering Part A*. 17, 2543–2550.
- [7] Hertz, H., 1882. Über die Berührung fester elastischer Körper. *Journal für die reine und angewandte Mathematik*. 92, 156–171.





**Taylor & Francis**

Taylor & Francis Group

<http://taylorandfrancis.com>

# 6

---

## Immune Properties of Mesenchymal Stem Cells in the Translation of Neural Disorders

---

Garima Sinha<sup>1,2</sup>, Sarah A. Bliss<sup>1,2</sup>, Vipul Nagula<sup>1,2</sup>, Lauren S. Sherman<sup>1,2</sup>, Pranela Rameshwar<sup>1,2,3</sup>

<sup>1</sup>Graduate School of Biomedical Science, Rutgers University, Newark, NJ, USA

<sup>2</sup>Dept of Medicine, Hematology/Oncology, New Jersey Medicine School, Rutgers University, Newark, NJ, USA

<sup>3</sup>Department of Medicine – Division of Hematology/Oncology, New Jersey Medical School, Rutgers School of Biomedical Health Science, Newark, NJ 07103 USA

Corresponding author: Pranela Rameshwar <rameshwa@njms.rutgers.edu>

### Abstract

Mesenchymal Stem cells (MSCs) are in clinical trials for a variety of disorders and thus far, there is no report of deleterious effect. Early studies suggested that MSCs were mesodermal in origin. However, more recent studies indicate that MSCs could be neuroectodermal in origin. This origin might explain why MSCs can efficiently form functional neurons. MSCs are proposed for several medical indications, mostly due to reduced ethical concerns, ease in expansion, ability to be transplanted across allogeneic barrier (off the shelf) and plasticity. Indications include, but are not limited to therapy for inflammation, tissue repair, protection of tissue damage and neuronal disorder. Despite the therapeutic promise for MSCs, there are variations in the data among and within labs. The hindrance appears to be mostly due to the lack of consensus to expand MSCs. We discuss the potential treatment of spinal cord and traumatic brain injury with MSCs and, the utilization of zebrafish as a model system for regenerative medicine. We also discuss the importance of a molecular balance to prevent transformation of MSCs during differentiation to

neural cells. We explain the over-arching chapter role of the immune properties of MSCs in the translation of MSCs as well as safety issues for clinical application.

**Keywords:** mesenchymal stem cells, immunosuppression, bone marrow, cytokine, cancer, stem cells.

## 6.1 Introduction

Stem cells have the potential to self-renew and differentiate into all cell types, making stem cells as the future therapy for tissue regeneration and organogenesis. Embryonic stem cells are linked to ethical concerns and scientifically, in tumor formation. These issues dampen the regenerative potential of embryonic stem cells. Similar arguments can be also made for induced pluripotent stem cells. Thus, clinical application is narrowed to adult stem cells such as those in the brain and in bone marrow, such as mesenchymal stem cells (MSCs). The clinical and experimental data indicated that MSCs can have regenerative/repair potential for several clinical disorders ([www.clinicaltrials.gov](http://www.clinicaltrials.gov)).

The multipotent mesenchymal stem cells are primordial in origin and can be isolated from fetal and adult tissues such as the placenta, bone marrow and adipose tissues [1–4]. Several membrane proteins have been identified to select and to phenotype MSCs. These include, but not limited to CD73, CD90, CD105. MSCs do not express markers like CD45, CD34, CD14, CD19. In addition to phenotype, other molecules have been proposed as methods to identify MSCs. These include vimentin and fibronectin. In all studies, the function of MSCs need to be validated for multipotency. In general, it is acceptable to induce MSCs to differentiate into osteoblast, adipocyte and chondrocyte [5].

MSCs are attractive for stem cell treatment, mostly due to reduced ethical concerns and ease of *in vitro* expansion. Furthermore, there is no need for a match at the major histocompatibility complex; thus making MSCs available as ‘off the shelf’ sources in cell therapy. The microenvironment plays an important role in the functional response of MSCs. The immune function of MSCs is particularly relevant. MSCs can be immune enhancer and suppressor cells. The immune function of MSCs depends on the milieu of the microenvironment. Specific cytokines and chemokines can be chemoattractant to facilitate the migration and homing of MSCs and other immune cells to the site of tissue injury.

## 6.2 MSC Immunology

MSCs show functional plasticity with regards to their immune properties by exerting both immune suppressor and enhancer functions [6], producing various cytokines that can stimulate the cells through autocrine and/or paracrine manner [7]. It has been suggested that major histocompatibility complex-II (MHC-II) expression be included among the minimum requirements for designating a cell as MSC [5]. However, there are several reports of MHC-II-negative cells with a phenotype and multi-lineage capacity similar to MSCs [8], suggesting that a population of MSCs do not express (detectable amounts of) MHC-II.

MHC-II allows cells to act as antigen presenting cells (APCs), with the cell mounting the antigen within the MHC-II groove to activate CD4+ T cells. The MSCs expressing MHC-II may then be able to act as APCs. However, unlike most APCs, MSCs express MHC-II in a bimodal fashion, with high MHC-II densities at low levels of interferon gamma ( $\text{IFN}\gamma$ ), and low MHC-II density at high  $\text{IFN}\gamma$  levels [9]. This is highly significant when considering MSCs as a therapeutic tool, as the MSCs would be in an inflammatory microenvironment, in the presence of a milieu of inflammatory cytokines – including  $\text{IFN}\gamma$ . This bimodal activity has been observed *in vitro* in MSC-derived neurons, whereby the neurons expressed low levels of MHC-II, but MHC-II level could be restored by stimulation with  $\text{IFN}\gamma$  [10]. Thus MHC-II expression has the potential to be problematic in case the MHC-II is re-expressed. If so, this could result in rejection of the transplanted MSCs.

Since the majority of MSCs show low to undetectable expression of MHC-II molecules on their cell surface they fail to activate T-cell response [5, 8]. In the absence of an allogeneic response, MSCs are suitable candidates for allogeneic transplant [6]. In the absence of pro- and anti-inflammatory cytokines, MSCs are further immunoprivileged in that they interfere with other immune cell functions, such as inhibiting B-cell proliferation and chemotaxis [11], suppressing the activity of dendritic and natural killer cells [12], and triggering the proliferation of regulatory T-cells to suppress an immune response [13]. It has been suggested that these immunosuppressive properties may play a role in tissue repair, modulating the other immune cells to prevent immune inflicted tissue injury and promote healing [14]. An equilibrium of these two properties must be understood and balanced for normal MSC function, as well as for MSC function in regeneration and repair [6, 15].

## 6.3 MSCs and Cancer

As a consideration to the translational potential of MSCs, one must examine the long-term effects of their presence in patients. We have discussed the immunomodulatory properties of MSCs and now must consider what may happen when the cellular signals go awry. This brings us to the role of MSCs in cancer; the current research has found them to be both tumor suppressive and enhancing, depending on the microenvironment. This section reviews the supportive and inhibitory properties of MSC in cancer and then takes a closer look at MSCs and cancer of the brain. In this special case we will consider how MSCs can be used for treatment of this deadly disease.

The association of MSCs with respect to tumors is of great interest from the past decade. MSCs have a contradictory role in cancer, in some studies it is found that MSCs can promote tumor progression through immune modulation, increase in metastasis, or increasing tumor cells, while in others a tumor suppressive role of MSCs was described. This contradicting behavior may be due to difference in the source of tissue, method of cell administration, individual donor variability, and injection timing of MSCs.

### 6.3.1 Role in Tumor Growth

MSCs, irrespective of their origin, were shown to have a role in tumor progression by initiation, growth and metastasis of the cancer or tumor cells [16–20]. Function and properties of MSCs can also vary depending on the origin of MSCs. Although MSCs are ubiquitous, there are two major organs of MSC. In the adult, the bone marrow and adipose tissues are the major sources of MSCs. Other sources of MSCs include the skin, muscle, lung, tendons and periodontal ligament. MSCs from peripheral origin exhibit greater tumor tropism than the MSCs from bone marrow. The immune suppressive function of MSCs is relevant for tumor initiation and growth. This was observed in an experimental transplantation model of B16 melanoma cells, which formed tumors only when co-injected with MSCs into allogeneic mice [16]. MSCs role in metastasis of cancer was demonstrated by co-injecting human breast cancer cells with human MSCs derived from bone marrow into immune compromised mice [18].

Growth-promoting effect of MSCs was shown in an *in vivo* model of colon cancer with co-injecting of adult and fetal MSCs [21]. The role of MSCs in tumor survival was shown *in vitro* with human B-cell lymphoma. [22]. Tumor promoting properties of MSCs were also shown with MSCs derived from peripheral tissues like adipose tissue [23]. These MSCs were also responsible

for the increase in the tumor size and the viable tumor cells count when co-injected with lung cancer or glioma cells [24].

The research studies that showed MSCs aiding tumor growth needs careful evaluation as MSCs have the tendency to proliferate in the presence of tumor cells. Hence, the increase in tumor mass could be due to the ability of MSCs forming carcinoma associated fibroblasts to support tumor growth.

### 6.3.2 MSCs in Tumor Suppression

MSCs can be used as tumor suppressors by secreting anti-tumor molecules like TNF, IFN- $\beta$  and Dickkopf-related protein-1 (DKK-1) [25–27]. These molecules will modify pathways that include Akt signaling,  $\beta$ -catenin and c-Myc, which are linked to tumor progression [25, 26, 28, 29].

The tumor suppressive effect of MSCs was shown when they were co-administered with glioma cells, resulting in modified Akt signaling [26]. Glioma cells secrete VEGF and other soluble factors to facilitate the invasion and migration of the transplanted MSCs to the site of the tumor. Human fetal skin-derived MSCs inhibited human liver cancer cell lines, with reduced proliferation, colony formation, and oncogene expression both *in vitro* and *in vivo* [30]. When these cell lines were co-injected with equal ratio of MSCs, tumor development was delayed and tumor size decreased. MSCs were shown to inhibit the growth of rat colon cancer when equal number of MSCs and tumor cells were co-injected [31]. The pro-inflammatory role of MSCs was suggested by the infiltration by Macrophages and granulocytes when co-injected with tumors. The anti-tumor effect of MSCs was noted when  $\beta$ -catenin signaling was inhibited through DKK-1 with solid and hematological tumors [25, 32].

### 6.3.3 MSC and Brain Cancer

The most common type of primary brain tumor is glioblastoma multiforme (GBM). GBM is a very aggressive and invasive cancer with an extremely poor prognosis. Current therapy involves tumor resection followed by both radio- and chemotherapy and these results in a median survival of less than 15 months [33]. Due to an urgent need for new treatments, scientists have begun to look at MSCs as tumor targeting drug delivery vehicles. This is partly due to the many characteristics that make MSCs a great transplant option. This topic is discussed above, describing the ease of access, production, and the donor of MSCs as universal. In addition to these benefits, MSCs also showed tumor tropism.

An increase in the interest of the mechanisms of homing and migration of MSCs to tumors, has led to a better understanding of this process. There are several different molecules that have been found to be involved. Although the candidate molecules vary with the cancer type, they include growth factors, chemokines, and cytokines that are released from the tumor or surrounding stroma. One example is stromal cell derived factor 1 $\alpha$  (SDF-1 $\alpha$ ) and its receptor chemokine (C-X-C motif) receptor 4 (CXCR4) commonly expressed on cancer cells. MSCs have been found to use SDF-1 $\alpha$ -CXCR4 signaling for migration to areas of inflammation, which is often common in the tumor microenvironment [34].

Other factors, such as VEGF, can enhance tumor tropism of MSCs to tumors. Breast cancer and gliomas have been reported to express high levels of VEGF, which induces the migration and invasion of MSCs to tumors [35]. MSC migration may be also increased in response to irradiation and hypoxia. Radiation may lead to increased expression of inflammatory mediators to enhance the migration of MSC to the tumor [35]. Hypoxia is often associated with tumor progression and can lead to the production of IL-6 which acts in a paracrine fashion on MSCs, causing increased migration to the tumor [36]. The mechanism of MSC homing and migration to the tumor site continues to be elucidated. However, the clinical and experimental evidence provided information on the tropism of MSC to brain tumors.

One of the earlier reports showing MSCs migrating to the region of gliomas was indicated with an experimental model using rats [37]. Autologous MSCs were intracranially implanted into rats that developed gliomas. The MSCs migrated and dispersed within the tumor mass [37]. Subsequent studies with immunocompromised mice showed human MSCs migrating to the region of human gliomas [38]. The MSCs were injected into the ipsilateral and contralateral carotid arteries of the mice [38]. In other studies, rat MSCs were injected intratumorally and this resulted in the migration to the invasive rat glioma and to the distant tumor microsatellites [39]. The investigators also observed that the implanted MSCs avoided the normal brain gray matter [40].

Based on the above findings, MSCs show promise as a delivery system for toxic substances to the tumor while being able to avoid adverse effects of the drug on normal brain tissue. Given the dire need for improved therapy for GBM researchers have also started looking at ways to increase the efficacy of current treatments by sensitizing the cells. Our group has recently published on the chemosensitization of GBM cells through the transfer of functional anti-miR-9 within MSCs, by packaging it within the exosomes [41]. As a cellular vehicle, MSCs could deliver chemosensitizing reagents as adjuvant to other treatments.

As an example, TRAIL-secreting MSCs in combination with lipoxygenase inhibitor, MK886, enhanced apoptosis of the resistant cancer *in vitro* and, also increased tumor regression in an orthotopic mouse model of glioma [42].

The reports are not consistent with regards to favoring the use of MSCs as cellular targets for brain cancer. Rather, there is some evidence of a supportive role for MSCs in brain tumors [43, 44]. In a murine model of GBM, MSCs were shown to infiltrate the tumor and this correlated with tumor progression [43]. Similarly, *in vitro* studies with the tumor-associated MSCs led to increased proliferation of the GBM cells [43]. One must also consider the source of the MSCs that will be used for cellular based therapy. Akimoto *et al* examined the effect of MSCs from different sources on primary GBM cells and found that umbilical cord blood-derived MSCs inhibited the proliferation of the GBM cells while the adipose tissue-derived MSCs supported proliferation of the cells' proliferation [44]. Although there is substantial data to support the use of MSCs as cellular vehicle of drugs to brain cancers there are still some reports that should not be ignored.

A major concern with using MSCs in the treatment of cancer is their potential to become immunosuppressive, which could become a survival advantage for the very GBM cells that are being targeted. One must also consider the long-term fate of the transplanted MSCs in patients after the treatment has been completed. There are two major reasons for this, first would be to avoid continuous exposure of normal tissue to anti-tumor agents delivered by the MSCs. Second, MSCs respond strongly to their microenvironment, which may change dramatically once the cancer is eliminated and could lead to malignant transformation. To avoid these issues, scientists have developed suicide gene therapy. This method involves the transfer of a gene encoding a suicide protein into the MSCs for selective elimination. Herpes simplex virus thymidine kinase (HSV-TK) is the most commonly used. Expression of HSV-TK in the cells sensitizes it to the prodrug ganciclovir (GCV) by phosphorylating GCV into its toxic form. This will allow targeting of only the cells producing thymidine kinase. The activated form of GCV inhibits DNA synthesis, which leads to cells death of the MSCs but also has a significant bystander effect that will cause the death of neighboring cells [40]. There is continued research to increase the efficacy of the suicide gene engineered MSCs, by co-expressing other proteins known to target cancer cells. One example is a group that co-expressed a potent and secretable variant of tumor necrosis factor apoptosis-inducing ligand (S-TRAIL) in addition to HSV-TK. This caused caspase-mediated GBM cell death and selective sensitization of the MSCs to the prodrug GCV [45].



## 6.4 Regenerative Potential

MSC was discovered by Friedenstein *et al.* and was referred as CFU-F (colony forming unit-fibroblasts). Similar cells were isolated from the bone marrow and with similar formation of colonies [46, 47]. MSCs have several functions, including support of hematopoiesis during transplantation with simultaneous decrease of graft versus host through veto property [48].

MSCs have been shown to restore heart function [49, 50]. At a high dose of MSC when injected into the intracoronary region of left ventricle showed significant improvement in the normal function of the heart [49, 50]. This is a highly significant property of MSCs because cardiac failure is the leading cause of death in USA. The use of MSCs for neurological disorder has not yet reached the patients. However, the use of MSCs for neural disorder is widely accepted. Several animal models have shown full recovery of the damaged neurons. There are three possible explanations why MSCs might be important for neural repair. MSCs can differentiate into neurons, undergo cell fusion, release neurotropic factors to maintain the survival of the neurons and/or the release of non-neurotropic factors to promote the tissue repair [51]. Despite MSC is able to introduce repair and regeneration in the brain, it is still unclear if it is able to cross the blood brain barrier [52].

Human MSCs injected at the site of brain injury release neurotropic factors to induce endogenous recovery of damaged neurons [53]. This occurred by reduced inflammation, inhibition of apoptosis and increased proliferation and differentiation of neural stem cells. An early set of studies [54, 55] used a co-culture technique to shown that brain derived neurotropic factor (BDNF), glial derived neurotropic factor secreted by MSCs, induced neurite formation in neuroblastoma cell line. The role of BDNF was demonstrated with neutralizing antibodies, which prevented the regenerative potential of MSCs [54, 55]. In a spinal cord injury model with zebrafish, *TAC1* expression in MSCs improved the sensory and locomotors recovery by releasing some neurotropic factor [56]. Other examples of neurotropic factors can be nerve growth factor, neurotrophin-3, ciliary neurotropic factor and vascular endothelial factor. In addition to neurotropic factors, *in vitro* studies showed that the extracellular matrix from MSCs can have a positive effect on the adhesion of neuronal cells by inducing neurite growth and astrocyte proliferation [57].

Both *in vitro* and *in vivo* studies suggest that MSCs can transdifferentiate into neurons, thereby providing these cells with the potential to promote neuronal repair. MSCs can be induced with defined condition and with cytokines to differentiate into neurons [56]. There are occasions if transdifferentiation of

MSC to neural cells can occur within a few hours and, whether the formation of neurons can be solely dependant on morphology [58, 59]. Subsequent studies indicated that transdifferentiation could happen only under stress and not under normal conditions [58–61]. In 2001, noggin, which can induce neural formation by inhibiting BMP2/4, TGF- $\beta$ , was used to induce neuron formation by transfecting MSCs. The noggin-transfectants expressed neuronal and astrocyte markers [62]. Retinoic acid (RA) was identified as an inducer of MSCs to form neurons with the expression of the neurotransmitter gene, *TAC1* with synaptic transmission [63]. There are several induction factors that can up regulate transdiffentiation of MSCs into neural cells such as matrigel [64]. The logic behind transdifferentiation of MSCs is not based solely on *in vitro* studies, as the conditions provided are totally artificial. When MSCs were injected to rat it migrated to the brain in the way neural stem cell (astrocyte engraft) migrated further losing MSC marker [65]. This showed the engrafted MSCs was well supported by the microenvironment of the rodents. The gradual increase in the neural marker in these MSCs showed its ability to transdifferentiate.

In Parkinson's disease (PD) rat model when hMSCs were injected it improved the motor function [66]. This was followed by clinical trial of using hMSCs in PD patient and it eventually lead to improvement in motor function with no significant side effect [67]. Amyotrophic Lateral Sclerosis (ALS) is a neurodegenerative disease caused by the death of motor neurons in cerebral cortex, brain stem and spinal cord. Human MSCs when transplanted in transgenic ALS mouse model with spinal cord injury improved the motor activity [68].

Patients with stroke who were injected with autologous MSCs showed transient improvement [69]. A subsequent repeat of the trial indicated that the transdifferentiated MSCs were able to retain their function for a prolonged period [69]. A recent *in vitro* study generated neurosphere-like aggregates from MSCs and then when injected them into a rat model of ischemic stroke to show that this method induced neuroprotection [70].

Other than neurotropic factor and transdifferentiaton, it is possible for the injected MSCs might fuse with the neural cells at the site of injury to cause functional improvement. Although evidence for this mechanism is limited there was a report in which MSCs were introduced into the rodent model [71, 72]. There was fusion with the neural cells and epigenetic changes with complete recovery of neuronal function [71, 72].

MSCs can be obtained and expanded easily without any ethical issues. These cells can differentiate into both mesenchymal and non-mesenchymal

types of cell depending on the microenvironment. There are several successful clinical trials with MSCs. There are concerns associated with these successes. Long-term follow up are needed with the MSC transplantation since MSCs can also exert immune regulation. Also, as discussed above, MSC therapy has to cautiously examined for patients who have survived cancer since this could reactive the tumor. Hence, long-term follow up is necessary for any patient receiving MSC or regeneration of the damaged tissue.

## 6.5 Safety

The safety of MSCs has been addressed throughout the text above. However, this section discusses that issue of care for tumor formation by the MSC itself. Here we discuss the differentiation of MSCs to neurons. *REST*, which is a tumor suppressor gene, is expressed in MSCs [73]. During differentiation to dopamine neurons, *REST* is decreased [74]. Thus, there is point where the balance between neuronal formation and the decrease of a tumor suppressor gene in stem cells could become tumorigenic (Figure 6.1). Similarly, the

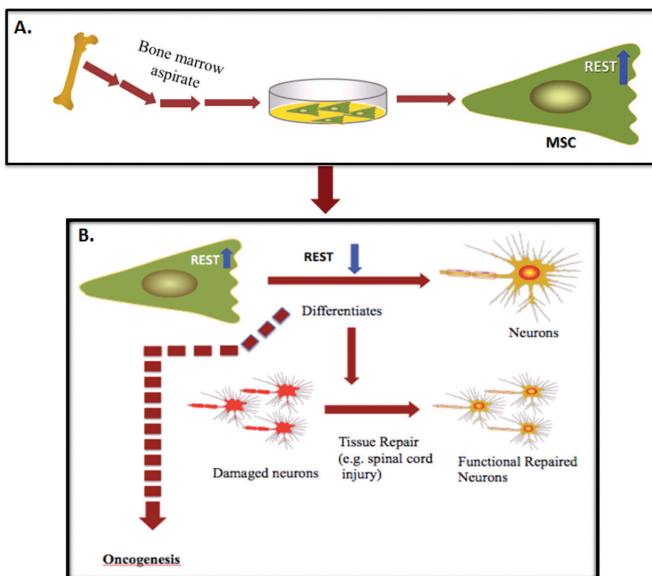


**Figure 6.1** Shown is the differentiation of MSCs into neurons. **A.** MSCs are cultured from bone marrow aspirates and then subjected to differentiation to neurons. **B.** As the MSCs differentiate, *REST* expression is decreased. If *REST* protein is rapidly decreased this could cause cell transformation.

decrease in REST during neuronal differentiation can cause the oncogenic *TAC1* gene to be expressed [75]. This shows a scenario in which a tumor suppressor gene (*REST*) is decreased with concomitant increase in the oncogenic *TAC1*. Going forward, studies are needed to carefully determine how the balance occurs and the rate of differentiation for safe trials.

## 6.6 Conclusion

MSCs have a dual role in regulating the immune response, depending on the microenvironment where the MSCs are placed. MSCs have the potential to introduce tissue repair and regeneration in brain and other organs. The differentiation of MSCs to neurons is mostly regulated by transcriptional repressor RE1-silencing transcription factor (REST; also known as neuron restrictive silencer factor-NRSF). REST regulates neurogenesis negatively and is degraded during normal neural differentiation. Its reduction induces MSCs to differentiate into neuron and repopulate the damaged neurons. (Figure 6.1), which under normal condition is highly expressed MSC, as it is tumor suppressor protein. Thus, the level of REST protein needs to be downregulated for efficient differentiation to neurons. A rapid decrease in REST protein in MSCs can also be oncogenic. Therefore, before using MSCs as a clinical therapeutic in neuronal damaged tissue for its repair, there is a need to figure out ways to balance REST protein.

Translation of this exciting research to the clinic will take time but the supportive results seen thus far have promise. MSCs are an ideal candidate for cellular therapy, their ease of isolation and lack of ethical concerns, along with tumor targeting properties make them a model transplant cell. Development of MSCs that release more potent tumor destroying molecules, addressing safety concerns of MSC transformation with improved therapeutic transgenes, and identifying the best route of administration are areas of continued research. However, a scenario where MSCs can be genetically modified and implanted into inoperable or partially resected invasive tumors, giving patients much needed treatment options is definitely on the horizon.

## References

- [1] Campagnoli, C., et al., Identification of mesenchymal stem/progenitor cells in human first-trimester fetal blood, liver, and bone marrow. *Blood*, 2001. **98**(8): pp. 2396–402.

- [2] He, Q., C. Wan, and G. Li, Concise review: multipotent mesenchymal stromal cells in blood. *Stem Cells*, 2007. **25**(1): pp. 69–77.
- [3] Lee, O. K., et al., Isolation of multipotent mesenchymal stem cells from umbilical cord blood. *Blood*, 2004. **103**(5): pp. 1669–75.
- [4] Tsuda, H., et al., Allogenic fetal membrane-derived mesenchymal stem cells contribute to renal repair in experimental glomerulonephritis. *Am J Physiol Renal Physiol*, 2010. **299**(5): pp. F1004–13.
- [5] Dominici, M., et al., Minimal criteria for defining multipotent mesenchymal stromal cells. The International Society for Cellular Therapy position statement. *Cytotherapy*, 2006. **8**(4): pp. 315–7.
- [6] Sherman, L. S., et al., Moving from the laboratory bench to patients' bedside: considerations for effective therapy with stem cells. *Clin Transl Sci*, 2011. **4**(5): pp. 380–6.
- [7] Castillo, M., et al., The immune properties of mesenchymal stem cells. *Int J Biomed Sci*, 2007. **3**(2): pp. 76–80.
- [8] Jacobs, S. A., et al., Immunological characteristics of human mesenchymal stem cells and multipotent adult progenitor cells. *Immunol Cell Biol*, 2013. **91**(1): pp. 32–9.
- [9] Tang, K. C., et al., Down-regulation of MHC II in mesenchymal stem cells at high IFN-gamma can be partly explained by cytoplasmic retention of CIITA. *J Immunol*, 2008. **180**(3): pp. 1826–33.
- [10] Cheng, Z., et al., Targeted migration of mesenchymal stem cells modified with CXCR4 gene to infarcted myocardium improves cardiac performance. *Mol Ther*, 2008. **16**(3): pp. 571–9.
- [11] Corcione, A., et al., Human mesenchymal stem cells modulate B-cell functions. *Blood*, 2006. **107**(1): pp. 367–72.
- [12] De Miguel, M. P., et al., Immunosuppressive properties of mesenchymal stem cells: advances and applications. *Curr Mol Med*, 2012. **12**(5): pp. 574–91.
- [13] Maccario, R., et al., Interaction of human mesenchymal stem cells with cells involved in alloantigen-specific immune response favors the differentiation of CD4+ T-cell subsets expressing a regulatory/suppressive phenotype. *Haematologica*, 2005. **90**(4): pp. 516–25.
- [14] Hoogduijn, M. J., et al., The immunomodulatory properties of mesenchymal stem cells and their use for immunotherapy. *Int Immunopharmacol*, 2010. **10**(12): pp. 1496–500.
- [15] Lotfinegad, P., et al., Immunomodulatory Nature and Site Specific Affinity of Mesenchymal Stem Cells: a Hope in Cell Therapy. *Adv Pharm Bull*, 2014. **4**(1): pp. 5–13.

- [16] Djouad, F., et al., Immunosuppressive effect of mesenchymal stem cells favors tumor growth in allogeneic animals. *Blood*, 2003. **102**(10): pp. 3837–44.
- [17] Goldstein, R. H., et al., Human bone marrow-derived MSCs can home to orthotopic breast cancer tumors and promote bone metastasis. *Cancer Res*, 2010. **70**(24): pp. 10044–50.
- [18] Karnoub, A. E., et al., Mesenchymal stem cells within tumour stroma promote breast cancer metastasis. *Nature*, 2007. **449**(7162): pp. 557–63.
- [19] Shinagawa, K., et al., Mesenchymal stem cells enhance growth and metastasis of colon cancer. *Int J Cancer*, 2010. **127**(10): pp. 2323–33.
- [20] Yu, J. M., et al., Mesenchymal stem cells derived from human adipose tissues favor tumor cell growth in vivo. *Stem Cells Dev*, 2008. **17**(3): pp. 463–73.
- [21] Zhu, W., et al., Mesenchymal stem cells derived from bone marrow favor tumor cell growth in vivo. *Exp Mol Pathol*, 2006. **80**(3): pp. 267–74.
- [22] Ame-Thomas, P., et al., Human mesenchymal stem cells isolated from bone marrow and lymphoid organs support tumor B-cell growth: role of stromal cells in follicular lymphoma pathogenesis. *Blood*, 2007. **109**(2): pp. 693–702.
- [23] Dubois, S. G., et al., Isolation of human adipose-derived stem cells from biopsies and liposuction specimens. *Methods Mol Biol*, 2008. **449**: pp. 69–79.
- [24] Gottschling, S., et al., Mesenchymal stem cells in non-small cell lung cancer—different from others? Insights from comparative molecular and functional analyses. *Lung Cancer*, 2013. **80** (1): pp. 19–29.
- [25] Qiao, L., et al., Dkk-1 secreted by mesenchymal stem cells inhibits growth of breast cancer cells via depression of Wnt signalling. *Cancer Lett*, 2008. **269**(1): pp. 67–77.
- [26] Ho, I. A., et al., Human bone marrow-derived mesenchymal stem cells suppress human glioma growth through inhibition of angiogenesis. *Stem Cells*, 2013. **31**(1): pp. 146–55.
- [27] Loebinger, M. R., et al., Mesenchymal stem cell delivery of TRAIL can eliminate metastatic cancer. *Cancer Res*, 2009. **69**(10): pp. 4134–42.
- [28] Khakoo, A. Y., et al., Human mesenchymal stem cells exert potent antitumorigenic effects in a model of Kaposi's sarcoma. *J Exp Med*, 2006. **203**(5): pp. 1235–47.
- [29] Dasari, V. R., et al., Upregulation of PTEN in glioma cells by cord blood mesenchymal stem cells inhibits migration via downregulation of the PI3K/Akt pathway. *PLoS One*, 2010. **5**(4): p. e10350.

- [30] Qiao, L., et al., Suppression of tumorigenesis by human mesenchymal stem cells in a hepatoma model. *Cell Res*, 2008. **18**(4): pp. 500–7.
- [31] Ohlsson, L. B., et al., Mesenchymal progenitor cell-mediated inhibition of tumor growth in vivo and *in vitro* in gelatin matrix. *Exp Mol Pathol*, 2003. **75**(3): pp. 248–55.
- [32] Zhu, Y., et al., Human mesenchymal stem cells inhibit cancer cell proliferation by secreting DKK-1. *Leukemia*, 2009. **23**(5): pp. 925–33.
- [33] Stupp, R., et al., Radiotherapy plus concomitant and adjuvant temozolomide for glioblastoma. *N Engl J Med*, 2005. **352**(10): pp. 987–96.
- [34] Stoicov, C., et al., Mesenchymal stem cells utilize CXCR4-SDF-1 signaling for acute, but not chronic, trafficking to gastric mucosal inflammation. *Dig Dis Sci*, 2013. **58**(9): pp. 2466–77.
- [35] Yagi, H. and Y. Kitagawa, The role of mesenchymal stem cells in cancer development. *Front Genet*, 2013. **4**: pp. 261.
- [36] Rattigan, Y., et al., Interleukin 6 mediated recruitment of mesenchymal stem cells to the hypoxic tumor milieu. *Exp Cell Res*, 2010. **316**(20): pp. 3417–24.
- [37] Nakamura, K., et al., Antitumor effect of genetically engineered mesenchymal stem cells in a rat glioma model. *Gene Ther*, 2004. **11** (14): pp. 1155–64.
- [38] Nakamizo, A., et al., Human bone marrow-derived mesenchymal stem cells in the treatment of gliomas. *Cancer Res*, 2005. **65**(8): pp. 3307–18.
- [39] Bexell, D., et al., Bone marrow multipotent mesenchymal stroma cells act as pericyte-like migratory vehicles in experimental gliomas. *Mol Ther*, 2009. **17**(1): pp. 183–90.
- [40] Bexell, D., S. Scheduling, and J. Bengzon, Toward brain tumor gene therapy using multipotent mesenchymal stromal cell vectors. *Mol Ther*, 2010. **18**(6): pp. 1067–75.
- [41] Munoz, J. L., et al., Delivery of Functional Anti-miR-9 by Mesenchymal Stem Cell-derived Exosomes to Glioblastoma Multiforme Cells Conferred Chemosensitivity. *Mol Ther Nucleic Acids*, 2013. **2**: p. e126.
- [42] Kim, S. M., et al., Effective combination therapy for malignant glioma with TRAIL-secreting mesenchymal stem cells and lipoxigenase inhibitor MK886. *Cancer Res*, 2012. **72**(18): pp. 4807–17.
- [43] Behnan, J., et al., Recruited brain tumor-derived mesenchymal stem cells contribute to brain tumor progression. *Stem Cells*, 2013.
- [44] Akimoto, K., et al., Umbilical cord blood-derived mesenchymal stem cells inhibit, but adipose tissue-derived mesenchymal stem cells promote,

- glioblastoma multiforme proliferation. *Stem Cells Dev*, 2013. **22**(9): pp. 1370–86.
- [45] Martinez-Quintanilla, J., et al., Therapeutic efficacy and fate of bimodal engineered stem cells in malignant brain tumors. *Stem Cells*, 2013. **31**(8): pp. 1706–14.
- [46] Friedenstein, A. J., R. K. Chailakhjan, and K. S. Lalykina, The development of fibroblast colonies in monolayer cultures of guinea-pig bone marrow and spleen cells. *Cell Tissue Kinet*, 1970. **3**(4): pp. 393–403.
- [47] Friedenstein, A. J., J. F. Gorskaja, and N. N. Kulagina, Fibroblast precursors in normal and irradiated mouse hematopoietic organs. *Exp Hematol*, 1976. **4**(5): pp. 267–74.
- [48] Angelopoulou, M., et al., Cotransplantation of human mesenchymal stem cells enhances human myelopoiesis and megakaryocytopoiesis in NOD/SCID mice. *Exp Hematol*, 2003. **31** (5): pp. 413–20.
- [49] Chen, S., et al., Intracoronary transplantation of autologous bone marrow mesenchymal stem cells for ischemic cardiomyopathy due to isolated chronic occluded left anterior descending artery. *J Invasive Cardiol*, 2006. **18**(11): pp. 552–6.
- [50] Chen, S. L., et al., Effect on left ventricular function of intracoronary transplantation of autologous bone marrow mesenchymal stem cell in patients with acute myocardial infarction. *Am J Cardiol*, 2004. **94**(1): pp. 92–5.
- [51] Maltman, D. J., S. A. Hardy, and S. A. Przyborski, Role of mesenchymal stem cells in neurogenesis and nervous system repair. *Neurochem Int*, 2011. **59**(3): pp. 347–56.
- [52] Liu, L., et al., From blood to the brain: can systemically transplanted mesenchymal stem cells cross the blood-brain barrier? *Stem Cells Int*, 2013. 2013: p. 435093.
- [53] Uccelli, A., et al., Neuroprotective features of mesenchymal stem cells. *Best Pract Res Clin Haematol*, 2011. **24**(1): pp. 59–64.
- [54] Crigler, L., et al., Human mesenchymal stem cell subpopulations express a variety of neuro-regulatory molecules and promote neuronal cell survival and neuritogenesis. *Exp Neurol*, 2006. **198**(1): pp. 54–64.
- [55] Wilkins, A., et al., Human bone marrow-derived mesenchymal stem cells secrete brain-derived neurotrophic factor which promotes neuronal survival *in vitro*. *Stem Cell Res*, 2009. **3**(1): pp. 63–70.
- [56] Patel, N., et al., Developmental regulation of TAC1 in peptidergic-induced human mesenchymal stem cells: implication for spinal cord injury in zebrafish. *Stem Cells Dev*, 2012. **21**(2): pp. 308–20.



- [57] Aizman, I., et al., Extracellular matrix produced by bone marrow stromal cells and by their derivative, SB623 cells, supports neural cell growth. *J Neurosci Res*, 2009. **87**(14): pp. 3198–206.
- [58] Woodbury, D., et al., Adult rat and human bone marrow stromal cells differentiate into neurons. *J Neurosci Res*, 2000. **61**(4): pp. 364–70.
- [59] Lu, P., A. Blesch, and M. H. Tuszynski, Induction of bone marrow stromal cells to neurons: differentiation, transdifferentiation, or artifact? *J Neurosci Res*, 2004. **77**(2): pp. 174–91.
- [60] Bertani, N., et al., Neurogenic potential of human mesenchymal stem cells revisited: analysis by immunostaining, time-lapse video and microarray. *J Cell Sci*, 2005. **118**(Pt 17): pp. 3925–36.
- [61] Neuhuber, B., et al., Reevaluation of *in vitro* differentiation protocols for bone marrow stromal cells: disruption of actin cytoskeleton induces rapid morphological changes and mimics neuronal phenotype. *J Neurosci Res*, 2004. **77**(2): pp. 192–204.
- [62] Kohyama, J., et al., Brain from bone: efficient “meta-differentiation” of marrow stroma-derived mature osteoblasts to neurons with Noggin or a demethylating agent. *Differentiation*, 2001. **68**(4–5): pp. 235–44.
- [63] Cho, K. J., et al., Neurons derived from human mesenchymal stem cells show synaptic transmission and can be induced to produce the neurotransmitter substance P by interleukin-1 alpha. *Stem Cells*, 2005. **23**(3): pp. 383–91.
- [64] Krabbe, C., J. Zimmer, and M. Meyer, Neural transdifferentiation of mesenchymal stem cells—a critical review. *APMIS*, 2005. **113**(11–12): pp. 831–44.
- [65] Azizi, S. A., et al., Engraftment and migration of human bone marrow stromal cells implanted in the brains of albino rats—similarities to astrocyte grafts. *Proc Natl Acad Sci U S A*, 1998. **95**(7): pp. 3908–13.
- [66] Dezawa, M., et al., Specific induction of neuronal cells from bone marrow stromal cells and application for autologous transplantation. *J Clin Invest*, 2004. **113**(12): pp. 1701–10.
- [67] Venkataramana, N. K., et al., Open-labeled study of unilateral autologous bone-marrow-derived mesenchymal stem cell transplantation in Parkinson’s disease. *Transl Res*, 2010. **155**(2): pp. 62–70.
- [68] Vercelli, A., et al., Human mesenchymal stem cell transplantation extends survival, improves motor performance and decreases neuroinflammation in mouse model of amyotrophic lateral sclerosis. *Neurobiol Dis*, 2008. **31**(3): pp. 395–405.

- [69] Lee, J. S., et al., A long-term follow-up study of intravenous autologous mesenchymal stem cell transplantation in patients with ischemic stroke. *Stem Cells*, 2010. **28**(6): pp. 1099–106.
- [70] Heo, J. S., et al., Neural transdifferentiation of human bone marrow mesenchymal stem cells on hydrophobic polymer-modified surface and therapeutic effects in an animal model of ischemic stroke. *Neuroscience*, 2013. **238**: pp. 305–18.
- [71] Terada, N., et al., Bone marrow cells adopt the phenotype of other cells by spontaneous cell fusion. *Nature*, 2002. **416**(6880): pp. 542–5.
- [72] Ying, Q. L., et al., Changing potency by spontaneous fusion. *Nature*, 2002. **416**(6880): pp. 545–8.
- [73] Reddy, B. Y., et al., RE-1-silencing transcription factor shows tumor-suppressor functions and negatively regulates the oncogenic TAC1 in breast cancer cells. *Proc Natl Acad Sci U S A*, 2009. **106**(11): pp. 4408–13.
- [74] Trzaska, K. A., et al., Loss of RE-1 silencing factor in mesenchymal stem cell-derived dopamine progenitors induces functional maturity. *Mol Cell Neurosci*, 2008. **39**(2): pp. 285–90.
- [75] Greco, S. J., et al., Synergy between the RE-1 silencer of transcription and NFkappaB in the repression of the neurotransmitter gene TAC1 in human mesenchymal stem cells. *J Biol Chem*, 2007. **282**(41): pp. 30039–50.



**Taylor & Francis**

Taylor & Francis Group

<http://taylorandfrancis.com>

---

# Novel Design of Manufacturing Bioreactor and Facility of Cell-Based Health Care Products for Regenerative Medicine

---

Masahiro Kino-oka

Department of Biotechnology, Osaka University, Osaka, Japan  
Corresponding author: Masahiro Kino-oka  
<kino-oka@bio.eng.osaka-u.ac.jp>

## Abstract

The processing systems for cell and tissue cultures suitable for therapeutic application are promising devices to save labor tasks, space, and contamination risk. Similar to the isolator system in the aseptic processing of healthcare products based on pharmaceutical regulation, the installation of a decontamination apparatus into the processing system will realize a further reduction in manufacturing costs based on the proposed siting criterion in an ISO Class 8 clean area without any increment of contamination risk. Furthermore, flexible modular platform (fMP) technology will realize the flexible combination of isolator modules, the practical design for cell sheet assembling was successfully performed. These proposals of the siting criterion and manufacturing system for the isolator and fMP technologies are expected to enhance process versatility accompanied by safety, security and cost-saving.

**Keywords:** bioreactor, manufacturing facility, flexible modular platform, automation, cell processing facility, cell sheet.

## 7.1 Introduction

In the last decade, cell and tissue therapies have encompassed a broad, rapidly growing field of medicine that involves the manipulation and administration of cells for the treatment of disease. Especially, the advances in tissue engineering

have offered promising strategies for reconstructing and repairing defective tissues *in vivo* (1-2), enabling damaged tissue to be replaced with cultured tissues that meet the needs of the individual patients. A number of companies manufacturing cultured tissues have been established. The manufacture of cultured tissues is still burdened by instability owing to the qualitative fluctuation of cell sources as raw materials and the risk of biological contamination.

Innovative techniques of cell and tissue processing have been developed for therapeutic applications. The subculturing for cell expansion is a core process. In manufacturing, strict management against contamination and human error are compelled due to un-sterilable products and the complexity of culture techniques, respectively. In addition, the development of a processing system is considered to lead to safety, security and cost-saving for cell and tissue cultures. However, the criterion of facility design to date has not been clear. This article describes a novel strategy for bioreactor and facility designs.

## **7.2 Bioreactor Design for Cell Processing**

Bioreactors are a core element to produce high-value materials in biological processes using mammary cells which can be employed for many purposes on various scales of operation in pharmaceutical production, cell therapies and tissue engineering (3). These range from simple, small-scale systems for basic research to sophisticated production-scale systems, which are in use for commercial manufacture. The development of industrial-scale bioreactors was initiated in the mid-1950s to meet the demand for mass production of vaccines. The cell culture bioreactors employed stirred tanks containing micro-carriers with adherent cells, which were, in principle, an adaptation of homogeneous culture systems used for microbial culture to meet the requirements of mechanically sensitive animal cells. The fundamental idea was to overcome the major limitations of cell cultivations that caused slow cell growth and low attainable cell densities by providing an environment that allowed the cells to continuously produce the products of interest at high levels.

In recent years, a new trend has emerged, that of tissue engineering. In contrast to traditional approaches of bioreactor design for mass production, the manufacturing features inherent for cell-based health care products leads to the requirement for small-scale design of patient-oriented bioreactors for clinical use. The automation platform becomes the core technology to realize the 3S (safety, security and cost-saving of manufacturing). Especially, the installation of a processing system for cell and tissue cultures leads

to: 1) process automation of machinery operations, 2) maintenance of the closed aseptic environment to reduce contamination risks, 3) mimicry of the biological environment with chemical and mechanical stimuli, and 4) information utilization of culture monitoring. These functional progresses provide some solutions to the features inherent to cell and tissue processing, being contributable not only to the process control including the saving of labor and process stability, but also to the quality control including the evaluation of cell and tissue potentials.

In our previous study, the automation for expansion process including the operations of seeding, medium change, passage as well as observation were developed (4, 5), and proposed the intelligent culture system accompanied by automated operations (liquid transfer and cell passage) to perform serial cultures of human skeletal muscle myoblasts, as shown in Figure 7.1(6). An automated culture system that could manage two serial cultures by monitoring the confluence degree was constructed. The automated operation with the intelligent determination of the time for passage was successfully performed without serious loss of growth activity, compared with manual operation using conventional flasks. This intelligent culture system can be applied to cultures of other adherent cells and will lead to the qualitative stability of products in the practical manufacturing of cells available for transplantation.

Recently, this technique applied to the development of chip culture system for maturation of retina pigment epithelial cells derived from human iPS cells (Figure 7.2). The chip bioreactor system for long-term culture of human retina pigment epithelial (RPE) cells consists of incubation unit and medium supplier unit. In the incubation unit, the chip as closed vessel (2.5 mm in diameter, working volume 25 ml) was set to be 37°C and 5% CO<sub>2</sub>, where gas permeable resin (PDMS) was used for the vessel wall. Whole bottom surface of chip was observed through the culture to detect the immature

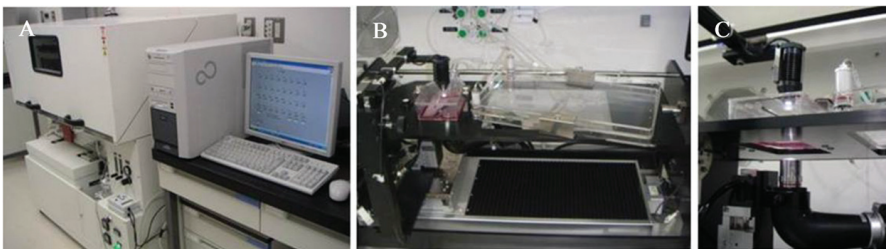


**Figure 7.1** Intelligent bioreactor system for passage automation. A; overview of the system, B; culture vessel, and C; monitoring system.

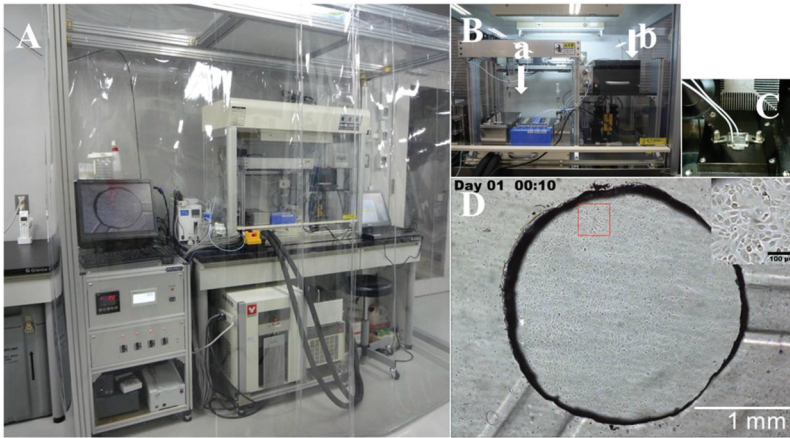


**Figure 7.2** Chip bioreactor system for maturation of retina pigment epithelial cells. A; overview of the system, B; medium supplement (arrow a) unit and incubation unit (arrow b), C; chip culture vessel, and D; culture image in chip.

RPE cells. The medium was changed with fresh one every day by introducing from the medium supplier unit by syringe pump. Here, the storage solutions were stocked in the refrigerator and freezer parts, and the fresh medium was prepared on time for the medium change by warming up to 37°C and mixing. The seeding were conducted at  $5.0 \times 10^4$  cells/cm<sup>2</sup> to be confluent state at initial, and long-term culture for 36 days is initiated for the maturing of RPE cells. The culture system will contribute to the process control as well as the quality control by detecting morphology of whole cells in their chip.

### 7.3 Facility Design for Cell Processing

Efforts to commercialize cell-based therapies are driving the need for capable, scalable, manufacturing technologies (7–10). It should be certificated that these therapies meet regulatory requirements and are economically valuable at the industrial scale production. In a commercial aspect, a major challenge is to translate lab-scale designs into production-scale designs of biologically functioned products that are reproducible, safe and clinically effective, as well as being economically acceptable and competitive, so that the engineering knowledge for the strategies of cell and tissue processing can be realized on the production scale (11).

On the basis of the guidelines for aseptic processing for healthcare products, the siting criterion of the processing systems for cell and tissue cultures is discussed in perspective of manufacturing therapeutic products (12, 13). The practical managements of processing systems for cell and tissue cultures have referred to the guidance for aseptic processing of healthcare products. The guidance describe that aseptic processes are designed to minimize exposure of sterile articles to the potential contamination hazards of the manufacturing operation. Limiting the duration of exposure of sterile product elements, providing the highest possible environmental control, optimizing process flow, and designing equipment to prevent entrainment of lower quality air into the clean room are essential to achieving aseptic process for product sterility. In addition, the International Organization for Standardization (ISO) guideline for the aseptic processing of healthcare products (Part 1: General requirements, ISO 13408-1) states the set-up of an aseptic processing area (APA). To site the highly controlled area, the influx prevention of chemical and biological contamination sources is one of the critical issues. The critical processing zone in the APA is defined to be an ISO Class 5 clean area using the biological safety cabinet (or laminar flow hood) where the sterilized drug products, containers, and closures are exposed to environmental conditions that must be designed to maintain product sterility. Moreover, the critical processing zone must be set in the direct support zone (ISO Class 7 clean area) where the indirect support zone (ISO Class 8 clean area) is surrounded.

In terms of autologous cell processing for therapeutic application, the fundamental criterion of the APA has been applied to the siting of the cell processing facility (CPF) for therapeutic purpose. In this respect, the bioreactor system should be installed in the direct support zone (ISO Class 7) of CPF because some culture operations including the cell seeding and harvesting are conducted in the critical processing zone of a laminar flow hood. The costs for operation and facility maintenance for the processing in CPF are known to be very high. Therefore, it is difficult to turn a profit for the small scale production with the autologous cell processing. For the cost saving, the aseptic processing has required a promising device: 1) to minimize the space where the closed and regulated environments are maintained rather than minimizing the critical processing zone within the aseptic processing area, 2) to minimize operator's entrance to reduce contamination risk, and 3) to minimize cross-contaminations leading to catastrophic events such as the expansion of serious contaminations which is transmitted from one batch operation to another by the aerosolized route.



In the pharmaceutical manufacturing of healthcare products, the minimization of space, operator's entrance and cross-contamination raise the development of the isolator as useful alternatives to full-scale clean rooms, being described as: "A device creating a small, enclosed, controlled or clean-classified environment in which a process or activity can be placed with a high degree of assurance that effective segregation will be maintained between the closed environment, its surroundings and any personnel involved with the process or manipulation" (14). According to the ISO guideline for the aseptic processing of healthcare products (Part 6: Isolator systems, ISO 13408-6), the isolator is placed in a clean room in which the environment is controlled to give the same conditions as an ISO Class 8 clean area equivalent to an indirect supporting zone in the aseptic processing of healthcare products. An economic analysis using the parameter of lifecycle cost indicated that the total cost per lot in the infrastructures for aseptic cell processing was based on: (i) the critical processing zone with manual operations, (ii) the isolator with manual operations, and (iii) the isolator with automated operations using the robot arm. Aseptic cell processing based on the isolator system with manual operations could reduce the lifecycle cost by 43%, compared with that based on the critical processing zone (15). The installation of a robotic system to realize automated processing in the isolator was suggested to achieve a 38% reduction in cost in the production scale, although the expenses related to facility costs increased by 2% compared with that based on the critical processing zone. Even though a further estimation will be required for practical management of the aseptic processing of cells and tissues for therapeutic use, these estimations are considered to promote the broad utility of the isolator for the aseptic cell processing for not only healthcare products but also for therapeutic cells and tissues.

The installation of isolator technology applied to the cell and tissue processing for therapeutic application would be a similar layout to that for aseptic processing of healthcare products as mentioned above. The critical issue of the isolator is to equip the pass box with a decontamination apparatus, so that the aseptic environment can be prepared by exposing it to decontamination reagents such as vaporized hydrogen peroxide using the decontamination apparatus, enabling materials such as culture vessels and containers for cells and medium to pass through the border from the ISO Class 8 clean area (equivalent to indirect supporting zone) to the ISO Class 5 clean area (equivalent to critical processing zone) without any additional buffer spaces (equivalent to the ISO Class 7 clean area of direct support zones), enabling the saving of costs for the operation and maintenance as well as space in the manufacturing of cell and tissues. As the siting criteria depend on the

respective processing, further discussion on the availability of these proposed manufacturing systems with the decontamination apparatus will be required in terms of the GMP regulatory issue, accompanied by validation data for the aseptic environment and biohazard level. The expectation shows that culture systems equipped with a decontamination apparatus takes countermeasures against biohazards and can be met for the autologous cell and tissue cultures because of specific requirements including: (i) the small-scale production for each patient, (ii) the utilization of non-sterilable materials derived from patient's cells, and (iii) independent biohazard spaces for healthy and virus-carrying (infected) patients. These specific requirements provide reasonable basis for the installation of manufacturing systems equipped with a decontamination apparatus for autologous cell processing. On the basis of the siting criterion mentioned above, the comparison of management between CPF and cell aseptic processing system (CAPS) employing isolator technology revealed that CAPS leads to reductions of the running cost as well as operational laboriousness in the small production.

## 7.4 Flexible Modular Platform Technology

Recently, as shown in Figure 7.3, a novel design of manufacturing facility based on a flexible Modular Platform (fMP) has been proposed to realize that the individual aseptic modules can connect and disconnect flexibly with keeping the aseptic environment in each module, leading to the compactness of aseptic processing area and quick change-over for multi-purposes and patients. This technology will make cost-saving with safety and security. To effectively implement this fMP technology an interface that can be aseptically detached and attached from one device to another is required and such a device must be able to handle diverse aseptic processing requirements. A common approach utilized in isolator based manufacturing of sterile pharmaceuticals is a transfer system using rapid transfer ports (RTP) or Double Porte de Transfert Etanche (DPTE). However, its interface limited to a circular configuration, and a more versatile aseptic transfer mechanism is sought for handling the connection between devices.

As shown in Figure 7.4, in the collaboration with Profs. Okano and Shimizu in Tokyo Women's Medical University and several companies in Japan, the isolator module system based on fMP for the cell sheet assembly has been developed, which will make automated formation of multilayered sheets and their incubation. The machinery operations were successfully performed. And this system can realize some procedures by having flexible connections

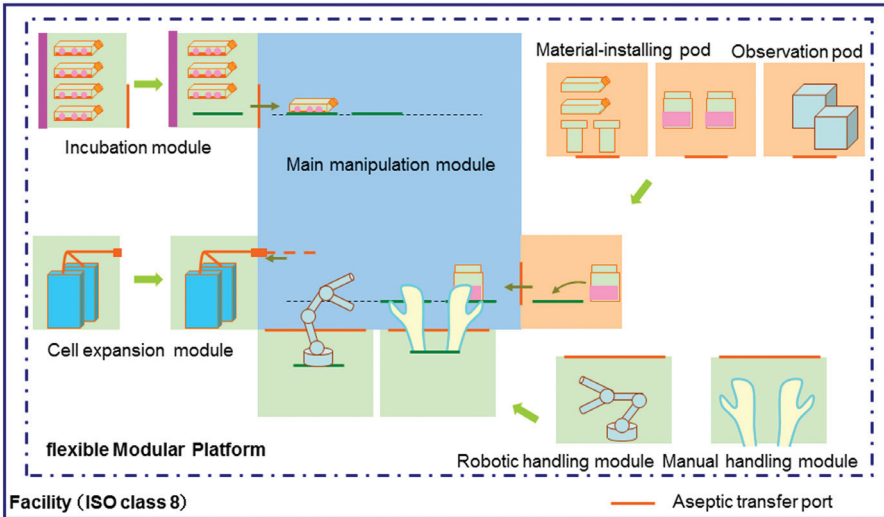


**Figure 7.3** Proposal of manufacturing system based on flexible Modular Platform (fmp)



**Figure 7.4** Automation system of sheet assembly based on the fmp technology

between modules under aseptic conditions by developing the interface of double door system for modules, suggesting the broad versatility for the production in other types of multilayered cell sheets.

## 7.5 Acknowledgments

This study was supported by the Japan Society for the Promotion of Science (JSPS) through the “Funding Program for World-Leading Innovative R&D on Science and Technology (FIRST Program),” initiated by the Council for

Science and Technology Policy (CSTP) and by the Strategic Promotion of Innovative Research and Development (S-Innovation) program of the Japan Science and Technology Agency (JST), and by the project of “Development of cell manufacturing and processing system for industrialization of regenerative medicine” (No.P14006) commissioned by the New Energy and Industrial Technology Development Organization (NEDO).

## References

- [1] Mason, C. and Hoare, M.: Regenerative medicine bioprocessing: building a conceptual framework based on early studies. *Tissue Eng.*, 13, 301–311 (2007).
- [2] Hesse, F. and Wagner, R.: Developments and improvements in the manufacturing of human therapeutics with mammalian cell cultures. *Trends Biotechnol.*, 18, 173–180 (2000).
- [3] Taya, M. and Kino-oka, M.: Bioreactors for animal cell cultures, *Comprehensive Biotechnology*, 2nd edition (eds. by M. Butler, C. Webb, A. Moreira, B. Grodzinski, Z. F. Cui, S. Agathos, M. Moo-Young), Vol.2, pp. 373–382, Elsevier (2011)
- [4] Kino-oka, M. and Prenosil, J. E.: Development of an on-line monitoring system of human keratinocyte growth by image analysis and its application to bioreactor culture, *Biotechnol. Bioeng.*, 67, 234–239 (2000).
- [5] Kino-oka, M., Ogawa, N, Umegaki, R., and Taya, M.: Bioreactor design for successive culture of anchorage-dependent cells operated in an automated manner. *Tissue Eng.*, 11, 535–545 (2005).
- [6] Kino-oka, M., Chowdhury, S. R., Muneyuki, Y., Manabe, M., Saito, A., Sawa, Y., and Taya, M.: Automating the expansion process of human skeletal muscle myoblasts with suppression of myotube formation, *Tissue Eng.*, 15, 717–728 (2009).
- [7] Thomas, R. J. Hourd, P. C., and Williams, D. J.: Application of process quality engineering techniques to improve the understanding of the *in vitro* processing of stem cells for therapeutic use. *J. Biotechnol.*, 136, 148–155 (2008).
- [8] Portner, R., Nagel-Heyer, S., Goepfert, C., Adamiez, P., and Meenen, N. M.: Bioreactor design for tissue engineering. *J. Biosci. Bioeng.*, 100, 235–245 (2005).

- [9] Wendt, D., Jakob, M., and Martin, I.: Bioreactor-based engineering of osteochondral grafts: from model systems to tissue manufacturing. *J. Biosci. Bioeng.*, 100, 489–494 (2005).
- [10] Williams, D. J. and Sebastine, I. M.: Tissue engineering and regenerative medicine: manufacturing challenges. *IEE Proc.-Nanobiotechnol.*, 152, 207–210 (2005).
- [11] Ratcliffe, A. and Niklason, A. E.: Bioreactor and bioprocessing for tissue engineering. *Ann. N. Y. Acad. Sci.*, 961, 210–215 (2002).
- [12] Weber D. J.: Manufacturing considerations for clinical uses of therapies derived from stem cells. *Methods Enzymol*, 420, 410–430 (2006).
- [13] Kino-oka, M. and Taya, M.: “Recent developments in processing systems for cell and tissue cultures toward therapeutic application”, *J. Biosci. Bioeng.*, 108, 267–276 (2009).
- [14] Farquharson, G.: Isolator applications in aseptic processing. *Innov. Pharm. Technol.*, 1, 148–152 (2000).
- [15] Dutton, R. L. and Fox, J. S.: Robotic processing in barrier-isolator environments: life cycle cost approach. *Pharm. Eng.*, 26, 1–8 (2006).

---

# Insight into Melanoma Stem Cells: The Role of the Hedgehog Signaling in Regulating Self-Renewal and Tumorigenicity

---

**Barbara Stecca and Roberta Santini**

Tumor Cell Biology Unit, Core Research Laboratory - Istituto Toscano Tumori (CRL-ITT), Florence, Italy.

Corresponding author: Barbara Stecca <barbara.stecca@ittumori.it>

## 8.1 Introduction

Cutaneous melanoma is among the most aggressive types of human cancer, and if untreated, has the potential to metastasize. While patients with low tumor thickness can be cured in 90% of cases by surgery, the majority of patients with metastatic disease die because of the inefficiency of current systemic treatments to produce long-term effects.

Cutaneous melanoma is defined as a malignant tumor derived from the transformation and proliferation of epidermal melanocytes, enabling a stepwise progression from common melanocytic nevus to radial growth phase melanoma, vertical growth phase melanoma and, finally, metastatic disease [1]. However, recent data suggest that a considerable number – around 60% to 75% – of melanomas develop *de novo*, without any precursor lesions. On the basis of these observations and according to repeated findings on melanoma heterogeneity, an alternative hypothesis has been proposed in light of the emerging cancer stem cell (CSC) concept. Mounting evidence suggests that melanoma may arise from a multipotent CSC that is able to self-renew, differentiate into diverse progenies and drive continuous growth [2]. In this context, the term *melanoma stem cell* represents an operational definition, indicating a multipotent tumor-initiating cell subset that – although monoclonal in origin – can give rise to a heterogeneous progeny that recapitulates the tissue of origin.

## 8.2 Evidence for the Existence of Melanoma Stem Cells with Self-Renewing and Tumorigenic Properties

During the past decades, indirect evidence has supported the presence of melanoma stem cells. First, melanomas show phenotypic heterogeneity both *in vitro* and *in vivo*, suggesting an origin from a cell with multilineage differentiation abilities. Melanomas retain their morphologic and biological plasticity, despite repeated cloning. Second, melanoma cells often express developmental genes such as Sox10, Pax3, Mitf and Nodal. Melanomas also express the intermediate filament Nestin, which is associated with multiple stem cell populations. Third, melanoma cells can differentiate into a wide range of cell lineages, including neural, mesenchymal and endothelial cells.

Next to these indirect findings, recent studies have provided direct evidence for the existence of melanoma stem cells [reviewed in 2]. Applying growth conditions suitable to human embryonic stem cells, Fang and colleagues [3] found a subpopulation of melanoma cells propagating as non-adherent spheres in approximately 20% of metastatic melanomas, whereas in standard media only adherent monolayer cultures developed. Sphere formation *in vitro* has been proposed by different groups as a common growth feature of stem cells, including neural crest-derived stem cells. The authors showed that melanoma spheres can differentiate under appropriate culture conditions into multiple lineages, such as melanocytes, adipocytes, osteocytes, and chondrocytes, recapitulating the plasticity of neural crest stem cells [3]. Multipotent melanoma spheroid cells persisted over several months after serial cloning *in vitro* and transplantation *in vivo*, indicating a stable capacity to self-renew. Interestingly, sphere cells were more tumorigenic than their adherent counterparts when grafted into mice. Finally, the authors found that the stemness criteria were significantly enriched in a small CD20-positive subpopulation, indicating that CD20 might be a suitable surface marker for the identification of melanoma stem cells [3].

Additional support for the existence of melanoma stem cells came from the finding that the surface marker CD133, a stem cell marker previously applied to neural stem cells, could be employed to isolate a subset of stem-like melanoma cells from patient biopsies [4]. Using fluorescence-activated cell sorting (FACS) from freshly isolated melanoma cells, the authors demonstrated that the CD133-positive subpopulation represents less than 1% of the total tumor mass of melanoma, a finding consistent with designated stem cell subpopulations from other tissues. Like the CD20-positive population defined by Fang and colleagues [3], CD133-positive melanoma cells revealed an

increased tumorigenicity when injected into non-obese diabetic/severe combined immunodeficiency disease (NOD/SCID) mice [4]. However, because of stringent experiments on self-renewal and transdifferentiation capacity of CD133-positive melanoma cells were not performed, the role of CD133 as a potential melanoma stem cell marker remains elusive. Of interest however, the marker CD133 was highly co-expressed with ABCG2, a member of the ATP-binding cassette (ABC) transporter family [4].

Another common characteristic of stem cells is the ability to efflux Hoechst 33342 dye and thus to exhibit low fluorescence in FACS analysis. Using flow sorting of three melanoma cell lines isolated from lymph node metastases, Grichnik and colleagues detected a tiny subpopulation (also called the side population) of small-sized cells with Hoechst 33342 efflux and with the ability to give rise to cells of different morphology when cultured *in vitro* [5]. Cells from this sub-population additionally showed a low proliferation rate but a high ability to self-renew.

Later, an important study showed that ABCB5 is a functional biomarker of melanoma stem cells [6]. In contrast to previous reports, this study examined *i*) serial xenotransplantation of prospectively isolated subpopulations of melanoma cells, *ii*) *in vivo* genetic lineage tracking and *iii*) targeting of melanoma cells using a monoclonal antibody to ABCB5, to demonstrate the existence of ABCB5-expressing cells. ABCB5+ melanoma cells, but not their ABCB5- counterpart, not only proved capable of tumorigenesis, but also of self-renewal and differentiation into a heterogeneous population. Interestingly, the authors established also a clinical correlation between ABCB5 expression and disease progression, suggesting that ABCB5 may be a biomarker of melanoma progression [6]. Most importantly for therapeutic purposes, administration of anti-ABCB5 monoclonal antibodies impaired growth of melanoma xenografts in nude mice [6].

However, soon after the identification of ABCB5 as a melanoma stem cell marker, the existence of cancer stem cells in human melanoma was questioned. In fact, two studies using a severely immunocompromised mouse model (interleukin-2 receptor  $\gamma$  chain-null NOD/SCID) suggested high frequency of tumor-initiating cells in melanoma [7, 8]. These studies failed to find any correlation between a specific phenotype and tumor-initiating ability and led to questioning the existence of melanoma stem cells [7, 8]. Much of the controversy might be found on the use of dissimilar methodologies to study melanoma stem cells and on differences in the definition of cancer stem cells and their abundance.



Additional evidence that melanoma follows a cancer stem cell model came from recent studies. Melanoma cells from primary and metastatic tumors that expressed CD271 (nerve growth factor receptor), a surface marker of neural crest stem cells, displayed a marked capacity for self-renewal and differentiation plasticity when compared with CD271- melanoma cells. Furthermore, when tumorigenesis was examined CD271+ melanoma cells, but not CD271-, formed tumors and metastases [9, 10]. Interestingly, CD271 and ABCB5 were recently found to be co-expressed in clinical human melanoma samples.

In another study, a sub-population of melanoma cells identified by higher aldehyde dehydrogenase (ALDH) activity displayed enhanced tumorigenicity and capacity to self-renewal when compared to ALDH-negative cells [11]. Melanoma cells that express the receptor activator of NK- $\kappa$ B (RANK) demonstrated increased tumorigenicity compared with RANK-negative melanoma cells. Moreover, RANK was coexpressed with ABCB5 and CD133 in melanoma cells, and preferentially expressed by peripheral circulating melanoma cells [12]. Recently, a temporary distinct subpopulation of slow-cycling cells characterized by the expression of the H3K4 demethylase JARID1B has been shown to be required for continuous melanoma growth [13].

### **8.3 The Hedgehog Signaling Pathway**

A handful of morphogenetic signaling pathways regulating developmental processes, organ homeostasis and self-renewal in normal stem cells, plays also a critical role in tumorigenesis. Among them, Hedgehog (Hh) is crucial for determining proper embryonic patterning and controlling growth and cell fate during animal development. Similarly, in the adult, is involved in tissue maintenance and repair, regulating stem cell behaviour.

Activation of the Hh signaling is initiated by the binding of Hh ligands (Sonic, Indian and Desert) to the trans-membrane protein Patched (Ptch), which, in absence of the ligands, represses the pathway by preventing the activation of the essential trans-membrane protein Smoothed (Smo). Binding of Hh to Ptch allows activation of Smo, leading to the formation of activating forms of the Gli zinc finger transcription factors Gli1, Gli2 and Gli3 [14, 15] (Figure 8.1). Direct transcriptional activation of Gli1 by Gli2/3 enhances the level of Gli activators and high level expression of Gli1 is considered a reliable indicator of Hh pathway activity. Gli1 and Gli2 act as main mediators of Hh signaling in cancer by controlling the expression of target genes involved in proliferation, metastasis, survival and

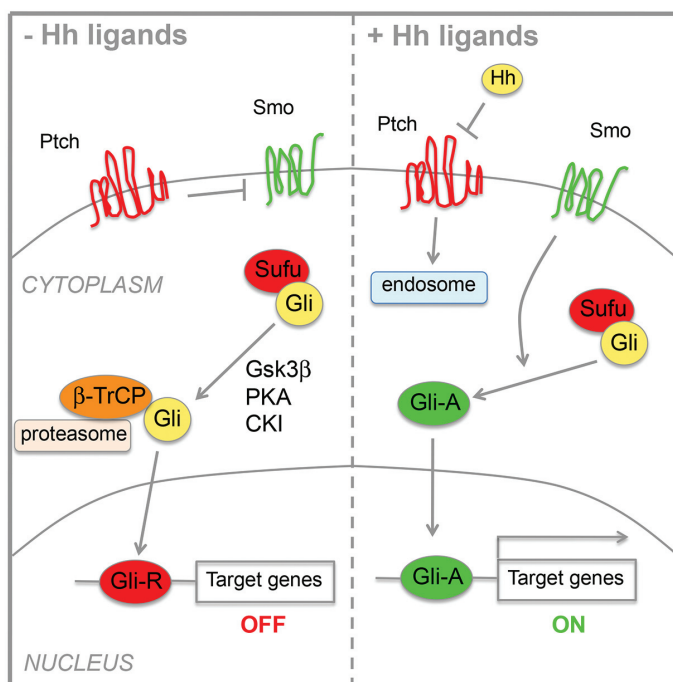


**Figure 8.1** Schematic diagram of the Hh signaling pathway. In the absence of the ligand (left), the Ptch receptor suppresses the function of Smo. Full-length Gli proteins (Gli, yellow) are converted to a C-terminally truncated repressor form (Gli-R, red). Formation of the Gli-R is promoted by sequential phosphorylation of full-length Gli by GSK3  $\beta$ , PKA and CKI, which creates binding sites for the adapter protein  $\beta$ -TrCP, becoming subject of ubiquitination. The Gli-R mediates transcriptional repression of target genes. In presence of the ligands (right), binding inhibits Ptch's function, which results in activation of Smo. Active Smo promotes the activation of full-length Gli proteins (Gli, green), which enters the nucleus and promotes transcription of target genes.

stemness [14, 15]. The activity of the three Gli proteins is tightly controlled. First, nuclear-cytoplasmic shuttling is tightly regulated by protein kinase A (PKA) and by Suppressor of Fused (Sufu), which not only prevents their nuclear translocation, but also inhibits Gli1-mediated transcriptional activity. Second, ubiquitination and protein degradation of Gli proteins are regulated by several distinct mechanisms, including  $\beta$ -TrCP-, cul3/BTB-, Numb/Itch- and acetylation-mediated ubiquitination. Third, Gli3 and, to a lesser extent, Gli2, can be processed into transcriptional repressors [reviewed in 16] (Figure 8.1).

## 8.4 Role of the Hedgehog Signaling in Regulating Self-Renewal and Tumorigenicity of Melanoma Stem Cells

In physiological conditions, Sonic Hh promotes the development of multipotent neural crest progenitors [17], from which melanocytes derive, and regulates proliferation of human melanocytes [18]. Similarly, it regulates brain stem cell lineages [e.g. 19] and skin stem cells [e.g. 20]. Aberrant activation of the HH-GLI signaling has been demonstrated in several types of human cancers [16]. The HH pathway is active and required for melanoma proliferation and growth *in vivo* of human melanoma xenografts [18] and GLI2 has been shown to drive melanoma invasion and metastasis [21]. In particular, our group has showed that HH signaling is active in the matrix of human hair follicles and that it is required for the normal proliferation of human melanocytes in culture. HH signaling additionally regulated the proliferation and survival of human melanomas. The growth, recurrence, and metastasis of melanoma xenografts in mice were prevented by local or systemic interference of HH function. Moreover, we presented evidence that oncogenic RAS-induced melanomas in transgenic mice express Gli1 and require Hh signaling *in vitro* and *in vivo* [18].

HH signaling has been shown to regulate CSC survival and expansion in several types of cancer, such as glioma, colon and gastric cancer, multiple myeloma and myeloid leukemia [22–26].

In a recent work, we have used the sphere assay to enrich for melanoma stem cells in a collection of primary and metastatic human melanoma samples obtained from a broad spectrum of sites and stages [27]. We have found that spheres display extensive *in vitro* self-renewal ability and that as few as 10 melanoma cells can sustain tumor growth *in vivo*, generating human melanoma xenografts that recapitulate the phenotypic composition of the parental tumor. We have shown that spheres express high levels of HH pathway components and embryonic pluripotent stem cell factors, such as *SOX2*, *NANOG*, *OCT4* and *KLF4*. In addition, we have demonstrated by FACS and immunocytochemistry that human melanomas contain a subset of cells expressing high ALDH activity (ALDH<sup>high</sup>), which is endowed with higher self-renewal and tumorigenic abilities than the ALDH<sup>low</sup> population. Moreover, we found a good correlation between the number of ALDH<sup>high</sup> cells and sphere formation efficiency *in vitro* [27]. In addition, we discovered a potential clinical correlation between ALDH expression and melanoma progression. In fact, primary and metastatic melanomas contained more cells expressing

ALDH than normal and dysplastic melanocytic nevi. We also detected more ALDH-positive cells in thick primary melanomas and melanoma metastases than in thin primary melanomas. Interestingly, in most of the thick melanomas ALDH was highly expressed in tumor cells at the tumor-host interface, suggesting that the ALDH-positive melanoma stem cells might be mainly localized at the invading tumor front. These results led us to hypothesize that ALDH-positive cells might therefore be involved in the formation of metastatic melanoma, whereas less aggressive tumors might originate from other types of melanoma-initiating cells. Notably, the aggressive biological behaviour demonstrated in mice by isolated ALDH<sup>high</sup> cells and the high percentages of these cells detected in some rapidly lethal melanomas of our collection suggested that ALDH might be a melanoma stem cell marker that correlates with a poor prognosis [27].

To demonstrate the role of the HH signaling pathway in regulating self-renewal and tumorigenicity of human melanoma stem cells, we knocked-down the transmembrane protein SMO and the transcription factor GLI1 by using specific short hairpin RNA (shRNA). Silencing of SMO and GLI1 drastically reduced self-renewal of melanoma spheres and the number and self-renewal of putative ALDH<sup>high</sup> melanoma stem cells. Similar results in terms of decrease in self-renewal were obtained by pharmacological inhibition of SMO with the antagonist cyclopamine and of GLI with GANT61, a novel GLI inhibitor [27].

To test the role of the HH signaling in ALDH<sup>high</sup> melanoma stem cells *in vivo*, we engrafted subcutaneously into athymic nude mice ALDH<sup>high</sup> melanoma cells transduced with shRNA specific for SMO and GLI1. Cells transduced with the control yielded rapidly growing tumors, whereas silencing of SMO and GLI1 greatly reduced tumor growth. These results strongly suggest that the HH signaling is required for growth *in vivo* of ALDH<sup>high</sup> melanoma stem cells [27].

## 8.5 Conclusions

During the past decades, numerous reports have portrayed melanoma as an aggressive cancer with an exceptionally high degree of heterogeneity and plasticity. Today, a growing body of experimental data provides direct evidence that many characteristics of melanoma might be found on the existence of a cell population with stem cell-like properties. Recent data support the existence within human melanomas of a subpopulation of highly tumorigenic cells with features similar to embryonic stem cells, including the potential to self-renew and differentiate into a variety of tissue types. Our

study highlights the role of the HH signaling pathway in driving self-renewal and tumorigenicity of melanoma stem cells and points to SMO and GLI1 as novel and effective therapeutic targets for the treatment of human melanoma.

Although most reported findings seem to be highly promising, many unanswered questions still exist. We do not yet know how many subpopulations of melanoma cells with stem cell properties exist. First, is there a definite number of clearly distinguishable subpopulations, or is there a continuous spectrum of cells, that is passing through a state of trans-amplifying cells that gradually lose their stemness, to differentiated tumor cells? Second, although many cancers contain cells that display stem cell-like features, the identity of the normal cell that acquires the first genetic hit leading to the tumor-initiating cell remains elusive in melanoma. Normal cells that already have stem cell properties represent likely targets, but other mechanisms are conceivable. Third, almost nothing is known so far about the niche of melanoma stem cells. What is the impact of the niche on melanoma development, maintenance and metastasis? As a long-term perspective, melanoma stem cell research will certainly influence and improve the diagnosis, prognosis, and therapy of melanoma. Traditional treatments might be recalibrated and novel therapies need to be developed focusing on the ability to target the melanoma stem cell population and its specific signaling pathways.

## 8.6 Acknowledgement

Work in the authors laboratory has been supported by Associazione Italiana per la Ricerca sul Cancro (AIRC, 9566), Regional Health Research Program 2009 and Fondazione Cassa di Risparmio di Firenze.

## References

- [1] Ko J. M., Fisher D. E. A new era: melanoma genetics and therapeutics. *J Pathol.* 223:241–250, 2011.
- [2] Girouard S. D., Murphy G. F. Melanoma stem cells: not rare, but well done. *Lab Invest.* 91:647–664, 2011.
- [3] Fang D., Nguyen T. K., Leishear K. et al. A tumorigenic subpopulation with stem cell properties in melanomas. *Cancer Res.* 65:9328–9337, 2005.
- [4] Monzani E., Facchetti F., Galmozzi E. et al. Melanoma contains CD133 and ABCG2 positive cells with enhanced tumorigenic potential. *Eur J. Cancer* 43:935–946, 2007.

- [5] Grichnik J. M., Burch J. A., Schulteis R. D., et al. Melanoma, a tumor based on a mutant stem cell? *J. Invest Dermatol.* 126:142–53, 2006.
- [6] Schatton T., Murphy G. F., Frank N. Y. et al. Identification of cells initiating human melanomas. *Nature* 451:345–349, 2008.
- [7] Quintana E., Shackleton M., Sabel M. S. et al. Efficient tumor formation by single human melanoma cells. *Nature* 456:593–598, 2008.
- [8] Quintana E., Shackleton M., Foster H. R. et al. Phenotypic heterogeneity among tumorigenic melanoma cells from patients that is reversible and not hierarchically organized. *Cancer Cell* 18:510–523, 2010.
- [9] Boiko A. D., Razorenova O. V., van de Rijn M. et al. Human melanoma-initiating cells express neural crest nerve growth factor receptor CD271. *Nature* 466:133–137, 2010.
- [10] Civenni G., Walter A., Kobert N. et al. Human CD271-Positive Melanoma Stem Cells Associated with Metastasis Establish Tumor Heterogeneity and Long-Term Growth. *Cancer Res.* 71:3098–3109, 2011.
- [11] Boonyaratanakornkit J. B., Yue L., Strachan L. R. et al. Selection of tumorigenic melanoma cells using ALDH. *J. Invest. Dermatol.* 130:2799–2808, 2010.
- [12] Kupas V., Weishaupt C., Siepmann D., et al. RANK is expressed in metastatic melanoma and highly upregulated on melanoma-initiating cells. *J Invest Dermatol.* 131:944–55, 2011.
- [13] Roesch A., Fukunaga-Kalabis M., Schmidt E. C. et al. A temporary distinct subpopulation of slow-cycling melanoma cells is required for continuous tumor growth. *Cell* 141:583–594, 2010.
- [14] Jiang J., Hui C. C. Hedgehog signaling in development and cancer. *Dev Cell* 15:801–812, 2008.
- [15] Stecca B., Ruiz i Altaba A. Context-dependent regulation of the GLI code in cancer by HEDGEHOG and non-HEDGEHOG signals. *J Mol Cell Biol* 2:84–95, 2010.
- [16] Teglund S., Toftgård R. Hedgehog beyond medulloblastoma and basal cell carcinoma. *Biochim Biophys Acta* 1805:181–208, 2010.
- [17] Calloni G. W., Glavieux-Pardanaud C., Le Douarin N. M. et al. Sonic Hedgehog promotes the development of multipotent neural crest progenitors endowed with both mesenchymal and neural potentials. *Proc Natl Acad Sci USA* 104:19879–19884, 2007.
- [18] Stecca B., Mas C., Clement V. et al. Melanomas require HEDGEHOG-GLI signaling regulated by interactions between GLI1 and the RAS-MEK/AKT pathways. *Proc Natl Acad Sci USA* 104:5895–5900, 2007.

- [19] Lai K., Kaspar B. K., Gage F. H. et al. Sonic hedgehog regulates adult neural progenitor proliferation *in vitro* and *in vivo*. *Nat Neurosci.* 6: 21–27, 2003.
- [20] Hutchin M. E., Kariapper M. S., Grachtchouk M. et al. Sustained Hedgehog signaling is required for basal cell carcinoma proliferation and survival: conditional skin tumorigenesis recapitulates the hair growth cycle. *Genes Dev* 19:214–233, 2005.
- [21] Alexaki V. I., Javelaud D., Van Kempen L. C. et al. GLI2-mediated melanoma invasion and metastasis. *J Natl Cancer Inst* 102:1148–1159, 2010.
- [22] Clement V., Sanchez P., de Tribolet N. et al. HEDGEHOG-GLI1 signaling regulates human glioma growth, cancer stem cell self-renewal and tumorigenicity. *Curr Biol* 17:165–172, 2007.
- [23] Varnat F., Duquet A., Malerba M. et al. Human colon cancer epithelial cells harbour active HEDGEHOG-GLI signaling that is essential for tumor growth, recurrence, metastasis and stem cell survival and expansion. *EMBO Mol Med* 1:338–351, 2009.
- [24] Song Z., Yue W., Wei B. et al. Sonic hedgehog pathway is essential for maintenance of cancer stem-like cells in human gastric cancer. *PLoS One* 6:e17687, 2011.
- [25] Peacock C. D., Wang Q., Gesell G. S. et al. Hedgehog signaling maintains a tumor stem cell compartment in multiple myeloma. *Proc Natl Acad Sci USA* 104:4048–4053, 2007.
- [26] Dierks C., Beigi R., Guo G. R. et al. Expansion of Bcr-Abl-positive leukemic stem cells is dependent on Hedgehog pathway activation. *Cancer Cell* 4:238–249, 2008.
- [27] Santini R., Vinci M. C., Pandolfi S. et al. HEDGEHOG-GLI Signaling Drives Self-Renewal and Tumorigenicity of Human Melanoma-Initiating Cells. *Stem Cells* 30:1808–18, 2012.

## **A Quest for Refocussing Stem Cell Induction Strategies: How to Deal with Ethical Objections and Patenting Problems**

---

**Hans-Werner Denker**

Lehrstuhl für Anatomie und Entwicklungsbiologie,  
Universität Duisburg-Essen, Germany\*  
Corresponding author: Hans-Werner Denker  
<hans-werner.denker@uni-due.de>

### **Abstract**

A recent ruling of the European Court of Justice (EU-CJ) in Luxembourg (18 October 2011) on ES cell patenting has renewed the interest in addressing so-far unsolved ethical problems of stem cell research. In this contribution I will outline ethical and patenting problems that arise when working with pluripotent stem cells, specifically in the modern field of induced pluripotent stem cell (iPSC) technology. The focus will be on stem cell potentiality, and I will argue that potentiality rather than the act of sacrificing embryos will have to be a central point of concern in stem cell ethics and patenting in the future. Possible solutions will be discussed.

When somatic cells are reprogrammed to gain “full” pluripotency, they acquire (so to say as a by-product) the capability to form viable embryos if tetraploid complementation (TC) is performed (termed “gold standard” by some authors). I argue that any human cells possessing this capability cannot be patented. In analogy to the arguments used by the EU-CJ, this must apply not only to patenting cell lines themselves but also to patenting technologies using these cells. The patenting problem is more than an obstacle for researchers and

---

This contribution reflects a lecture given at the Symposium ‘3rd Disputations on Native and Induced Pluripotent Stem Cell Standardization’, March 19-21, 2012, Florence, Italy.  
\*web: <http://www.uni-due.de/denker/>



companies: It points to an ethical problem behind. The fact that the problem is being created by the process of iPSC induction asks for alternative strategies of stem cell derivation as well as for stringent criteria how to define and to test pluripotency vs. lower levels of potentiality. It will have to be discussed which genes should be seen here as crucial (e.g. genes involved in early embryonic pattern formation / self-organization processes). For ethical reasons it cannot be defended to use TC as a test for “full” pluripotency with human cells. It is thus necessary to discuss alternative test criteria.

Recent reports suggest that it may indeed be possible to directly induce lower degrees of potentiality (e.g. multipotency) while bypassing a pluripotent state, thus avoiding the addressed problems. It appears timely and prudent, therefore, to redefine goals and to refocus strategies for stem cell derivation, in addition to stem cell quality testing criteria, in order to avoid the ethical and patenting dilemma.

**Keywords:** iPSC, potentiality, pluripotency, multipotency, derivation strategies, bypassing pluripotency, direct reprogramming, tetraploid complementation, patenting, ethics.

## 9.1 Introduction

A recent ruling (of October 18, 2011) of the European Court of Justice in Luxembourg (EU-CJ) has renewed the interest of researchers as well as of the broader public in addressing so-far unsolved ethical problems of stem cell research [1, 2]. The Court ruled that human embryonic stem cells (hESCs) are to be excluded from patentability due to the fact that their derivation involves sacrificing embryos, an act that is considered contrary to *ordre public* and morality. Remarkably, the Court, by addressing definitions of the term “embryo”, specifies that its rulings include products of artificial activation of eggs, i.e. parthenotes, and products of nuclear transfer to oocytes. This is in contrast to arguments that had been put forward by some authors before, i.e. that such artificially created embryos would not deserve the same moral status. Thus the EU-CJ puts emphasis on potentiality as an ethical argument, which is indeed a new focus and is in contrast to the circumstantial arguments used before by others (e.g. putting weight on the question where and how an embryo had been created, *in vivo* or in the lab, by sperm penetration or by nuclear transfer, etc.) which had led them to different conclusions.

I will argue in this contribution that considering the potentiality of cells is very timely and needs to be pursued seriously in stem cell ethics, in the

future. This argument is based not only on the ruling of the EU-CJ but even more so on the fact that most stem cell laboratories now focus on actively changing cell potentiality, specifically when deriving induced pluripotent stem cells (iPSCs). By endowing cells with properties they did not have before researchers unintentionally create at the same time an ethical problem: When cells reach pluripotency they acquire the ability to enable direct cloning by tetraploid complementation (TC). Acquisition of this new property, I will argue, must indeed preclude patentability, a consideration that illuminates the ethical ambiguity of inducing pluripotency.

For many researchers this warning may come as a surprise. Indeed, human iPSCs (hiPSCs) are so far most often addressed as ethically non-problematical since, in contrast to ESCs, iPSC derivation does not involve sacrificing embryos. Examples for such statements can be found often in the literature, e.g.: “*Direct reprogramming through the ectopic expression of defined transcription factors. . . represents a simple way to obtain pluripotent stem-cell lines from almost any somatic tissue and mammalian species. The use of such cells also circumvents the ethical issues associated with human cells*” [3]. However, there are also contrasting statements but they are so far found more rarely in the literature, e.g.: “*There would be severe ethical problems associated with using tetraploid complementation technology [with iPSCs] in humans, even without the intention of implanting the resulting artificially created embryos into a uterus (see, for example [4]). The issues are similar to those that have arisen over embryonic stem cells and include aspects of patentability.*” [5]. Likewise: “*The use of iPSCs and tetraploid complementation for human reproductive cloning would raise profound ethical objections. Professional standards and laws that ban human reproductive cloning by somatic cell nuclear transfer should be revised to also forbid it by other methods, such as iPSCs via tetraploid complementation.*” [6].

In the present contribution I will discuss in some detail what reasons are behind such warnings, focussing on the potentiality of ESCs and iPSCs. I will specifically address a peculiar property that pluripotent stem cells (ESCs and iPSCs) have, i.e. early embryonic pattern formation potential, which becomes particularly obvious when tetraploid complementation (TC) is performed. I will argue that this precludes patentability. Finally, I will put emphasis on alternative strategies for stem cell derivation, circumventing pluripotency, and I will argue that these strategies indeed appear successful and practical, which leads to the conclusion that their use is clearly preferable under ethical and patenting aspects.

## 9.2 Potential for Autonomous Pattern Formation: Embryoid Bodies

One of the remarkable biological properties of pluripotent cells is their ability to form, in suspension cultures, “**embryoid bodies**” (EBs). What is most widely known about EBs is that formation of these embryo-like structures promotes the formation of germ layers. Much less intensely studied is the degree of order that the germ layers and their derivatives can attain in EBs, and how close their organisation can really come to the basic body plan of viable embryos. Surprisingly, this aspect appears to receive increased attention only recently.

A particularly remarkable observation on early embryonic pattern formation in EBs was published already in one of the pioneering papers on ESCs [7]. In this case the spontaneous formation of astonishingly embryo-like structures was observed in dense cultures of common marmoset ESCs (*Callithrix jacchus*, a South American primate): These structures were described to consist of a flat embryonic disc as typical for primates, with primitive ectoderm, primitive endoderm, an amnion with amniotic cavity, a yolk sac. Most remarkably, those authors also depicted and described, within this embryonic disc, an area of ordered ingression of cells, which they addressed as a primitive streak (PS). The PS is of utmost importance in vertebrate embryology, because it is the site where not only the formation of the definitive germ layers (in particular mesoderm and definitive endoderm) takes place but is also instrumental in individuation: The anterior part of the PS is the equivalent of Spemann’s organizer which plays a central role in laying down the basic body plan, i.e. the ordered arrangement of germ layers and their derivatives according to the main body axes (dorso-ventral, anterior-posterior = cranio-caudal). The development of single or double organizers is decisive for the formation of a singlet vs. monozygotic twins (discussed in [8]).

While the structures formed spontaneously in the marmoset ESC cultures according to Thomson et al. [7] were remarkably embryo-like, and even appeared to show signs of incipient individuation (discussed in [8]) a comparable degree of order has never since been described to occur in ESC cultures in any other species, including the rhesus monkey and the mouse. Locally restricted gastrulation-like events have, however, been observed [9–12]. The degree of order attained appears to depend very much on physical conditions of culturing [9, 12], as was to be expected on the basis of what we know from developmental biology [8]. It is strongly influenced by other (non-stem) cells or matrix simultaneously present in the cultures. On the other

hand, such an early embryonic pattern-formation process has never been observed in comparable cultures of non-pluripotent cell types (e.g. fibroblasts) and thus obviously primarily depends on **intrinsic properties of pluripotent cells**. It was observed to occur either in suspension cultures, i.e. without the addition of other cell types and without attachment, or in dense flat cultures on feeder cells (fibroblasts) which likewise cannot be expected to provide specific pattern information, so that it is reasonable to assume that this pattern formation process is primarily **autonomous** and can be correctly addressed as a process of **self-organization** [9, 11]. The biological basis for these self-organization phenomena has been discussed earlier [8]. With respect to the question how close the observed *in-vitro* events may come to embryogenesis, ten Berge et al. [11] were astonished to observe a much higher degree of spatiotemporal order in gene activation cascades than they had expected to see in ESC cultures, specifically concerning *wnt* pathway-associated events, and that this was comparable to what is observed in mouse gastrulation *in vivo*.

What can EBs teach us with respect to ethical considerations? According to the described observations, pluripotent stem cells (PSCs) possess **gastrulation** potential and can show impressive early embryonic pattern formation (**self-organization**) potential *in vitro*. These processes are central elements of **basic body plan** formation and **individuation** during embryogenesis (for a review see [8]). Formation of EBs *in vitro* obviously can (depending on culturing conditions) come much closer to *in vivo* embryogenesis than originally thought by many. However, *in praxi* EBs rarely reach the high degree of order of a harmonious basic body plan. Therefore, depending on the degree of stringency one likes to use with respect to ethical norms, it could be argued that EB formation does or does not offer arguments with respect to ethical aspects of PSC use. With the recent focus of PSC research in mind we should not leave this discussion, however, without noticing that all these considerations do not only apply to ESCs but also to iPSCs because the latter cells basically show the same biological properties, including EB formation capacity, although the latter has so far been studied much less in detail with iPSCs than with ESCs.

### 9.3 Potential for Assisted Development: Tetraploid Complementation

**Tetraploid complementation (TC)** is a method for **cloning viable individuals from PSCs** (ESCs, but also iPSCs). We are discussing it here as a topic concerning stem cell quality testing strategies, ethics, legislation, and patenting regulations that is just beginning to be recognized.

TC was developed as a variant of chimera formation in the mouse. It provides a method to produce viable embryos and even offspring derived entirely from PSCs that had been propagated before *in vitro* [13–15]. The method relies on the combination of the pluripotent cells with tetraploidized blastomeres or, alternatively, on the injection into tetraploidized blastocysts. Remarkably, this method of cloning viable individuals is successful not only with ESCs but also with iPSCs. In the latter case the term “**all-iPSC mice**” has become popular for the products of this type of cloning [16–20].

Cloning by TC is widely used in experimental research as some type of quality control for PSCs (ESCs and iPSCs) in the mouse. Testing cells for TC capability is being addressed by some authors as the “gold standard” of pluripotency and its use is being advocated in a way that might suggest using it also with human cells [16, 18].

Why would anyone possibly be interested in applying TC with **human** cells? It may appear improbable that TC will be used in the near future for **reproductive cloning** in the human since so far there is widespread consensus to consider this unethical. However, there appears to be reason to question whether this consensus can be expected to hold for long and worldwide. In the Western world, it has already been proposed to consider using TC technology in order to increase success rates in *in-vitro* fertilization/embryo transfer (IVF-ET) clinics [21]. The idea is to derive ESCs from human IVF embryos, expand them *in vitro*, and (re-)construct from them a (larger) number of embryos by TC which can then be used for embryo transfer (while aliquots of the ESCs as well as some of the numerous identical embryos produced could of course be stored in liquid nitrogen to be available for later use in repeated attempts) [21]. Since this means cloning, and since reproductive cloning in the human is considered illegal at least in a number of countries, one may be skeptical whether this technique will ever be applied in Western world countries. However, it cannot be excluded that legislation may develop in a different direction in other cultural environments. As an example, Buddhist authorities have expressed that they would consider embryo destruction in the course of “therapeutic cloning” (for the production of ESCs) unethical, but not so the (re-)construction of embryos in the course of reproductive cloning (for literature see [4]).

While any application of TC for reproductive cloning in the human may appear improbable at the moment its use for **research** and **quality testing** purposes has indeed been proposed frequently, in the mouse, and with respect to human cells at least indirectly. This notion is found in the literature particularly often since the advent of iPSC research. First of all TC is

recommended as the most rigorous pluripotency test (“gold standard”) for iPSC cells in the mouse (“*We therefore consider the tetraploid complementation as the state-of-the-art technique to assess the pluripotency of a given cell line*” [22]; “*This study underscores the intrinsic qualitative differences between iPSC cells generated by different methods and highlights the need to rigorously characterize iPSC cells beyond in vitro studies.*” [23]). Likewise in the first reports on the generation of viable mice from iPSCs it had already been suggested indirectly to apply TC technology for iPSC quality testing also in the human, for the reason that this is considered the most rigorous pluripotency test [16, 18]. Remarkably, it was felt necessary, therefore, to publish a comment on these papers (in the same journal) clarifying that for ethical reasons it cannot be defended to follow this (implicit) recommendation, i.e. to use the technique for iPSC quality testing in the human [5].

Temptations may indeed be high to consider applying TC technology with human pluripotent cells, in spite of these warnings. Why? Recent literature is full of data asking for stringent quality testing in iPSC research. Individual iPSC lines are observed, in the mouse as well as in the human, to vary with respect to differentiation capacities, gene expression patterns and epigenetic marks/memory [24–28]. Stadtfeldt et al. [20] provided a typical and interesting example. They observed that transcripts encoded within the imprinted *Dlk1-Dio3* gene cluster were aberrantly silenced in most of the iPSC clones, and that these clones failed to support the development of entirely iPSC-derived animals (“all-iPSC mice”) when TC was performed thus revealing a lack of “complete pluripotency”. This failure could, however, be corrected by a treatment with a histone deacetylation inhibitor which reactivated the locus. It is clear that investigators wish to have a test available to monitor the success of this type of cell quality improvement. In addition to epigenetic peculiarities of PSC lines (as compared to early embryonic cells) even chromosomal aberrations and gene deletions have been observed in some cases [29, 30].

Such observations obviously could be seen as a strong argument for using the most stringent pluripotency test (TC) also with human iPSCs in order to select “optimal” cell lines and/or stem cell derivation protocols. This logic may be particularly obvious if cells are to be used for **therapeutic purposes** (cell and tissue replacement) in the human, and likewise whenever iPSCs are used for **disease modelling**. In cell and tissue replacement, the concern is that transplanted cells should be genetically and epigenetically as “normal” as possible in order to minimize risks e.g. with respect to tumor formation. In disease modelling with genetic/epigenetic focus, experiments are usually done in the first place in the mouse model, sometimes including TC technology

(which of course poses no ethical problem in the mouse) (as an example, see [22]: “*Genetic manipulation of iPSC cells in combination with tetraploid embryo aggregation provides a practical and rapid approach to evaluate the efficacy of gene correction of human diseases in mouse models.*”). But: How then could that be translated to human therapy without testing human iPSCs with comparable stringency, as it is being done with the mouse cells within the same experimental project? Would such considerations be a valid argument for the application of TC with human cells in order to use again the most stringent test? A simple and strict logic might suggest studying differentiation and gene expression in human TC embryos so produced *in vitro*. It should be seen, however, that even without transferring such human embryos created from iPSCs (“artificial“ or “test” embryos) to a uterus such a procedure would (re-)create the problem of embryo destruction which the original idea of iPSC technology intends to eliminate. It would clearly be in conflict with e.g. the German embryo protection law (Embryonenschutzgesetz). Furthermore, any use or possible use of such a quality testing strategy involving cloning by TC would definitely need to be included in the catalogue of information to be given to cell donors when **informed consent** is obtained; so far cell donors are not informed about the possibility of cloning embryos from PSCs by TC at all. Indeed, the catalogue of information that is so far routinely given to cell donors must urgently be updated, in particular with regard to hiPSC derivation: It cannot be defended anymore to omit information that the gain of pluripotency implies the gain of cloning capability by TC. I will not expand on this important topic here because it has been addressed before [31] but it should be seen that appropriate regulations are still missing so that the ethical problem remains unsolved.

## 9.4 Pluripotency, an Obstacle for Patenting

The recent ruling of the European Court of Justice (EU-CJ) mentioned in the Introduction is of interest not only with respect to embryo use for stem cell derivation, i.e. the point that received most of the attention of the broader public. This decision is also of interest with respect to consequences to be drawn from the developmental potential of pluripotent cells just discussed, in particular the TC capability. The court emphasized, in the definitions which it had been asked to provide of the term “embryo” in the context of the legal/patenting regulations in question, the aspect of **potentiality**. It was ruled that “*any human ovum after fertilisation, any non-fertilised human ovum into which the cell nucleus from a mature human cell has been transplanted,*

*and any non-fertilised human ovum whose division and further development have been stimulated by parthenogenesis constitute a 'human embryo'; - it is for the referring court to ascertain, in the light of scientific developments, whether a stem cell obtained from a human embryo at the blastocyst stage constitutes a 'human embryo' within the meaning of Article 6(2)(c) of Directive 98/44.” [1].*

Previously a number of authors had argued that the degree of respect to be paid to human embryos (and the degree of legal protection given to them) should depend on the way how they had been created (natural fertilization vs. intracytoplasmic sperm injection or nuclear transfer technologies, artificial egg activation/parthenogenesis), on the actual location of the early embryo in question (within the female genital tract or *in vitro*) or whether the embryo is already implanted in the uterus or not yet. So for example Vrtovec and Vrtovec have argued with respect to ethical aspects of patenting of PSCs that “*the exclusion from patentability is probably not justifiable for human totipotent cells that are produced outside the human body by (...) 'techniques which human beings alone are capable of putting into practice and which nature is incapable of accomplishing by itself'*” ([32], p. 3028). This argument has immediately been rejected [33] but can still be heard. A logical consequence of the recent ruling of the EU-CJ, however, is that the potentiality of the cells (original embryonic cells or cells possessing equivalent potential, i.e. hESCs or hiPSCs) need to be seen as a major argument for ethical considerations and patenting. My prediction is, therefore, that future court decisions and legislative actions will have to use potentiality as a new focus, and that this will necessarily play a major role in future decisions specifically with respect to iPSCs, since the main point in the derivation of iPSCs is to endow originally ethically non-problematic cells with new potentiality. In case of PSCs these peculiar new properties include, as discussed above, early embryonic pattern formation (individuation) and TC capability, the main biological characteristics of early embryonic cells.

## 9.5 Alternative Approaches

Are there alternative strategies available for deriving stem and/or precursor cells while avoiding the ethical and patenting problems just discussed?

Recent literature suggests that it is indeed possible to choose alternative strategies for stem and precursor cell derivation bypassing pluripotency. Until recently it was assumed by most authors that somatic/adult stem cells are not sufficiently expandable *in vitro*, and that only pluripotent stem cells



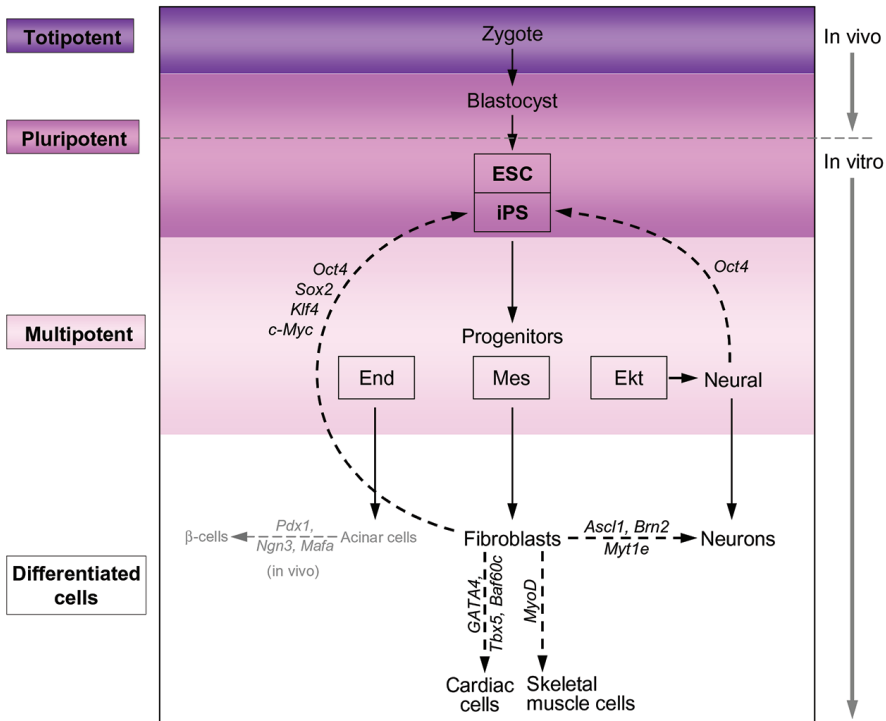


**Figure 9.1** Strategies for stem and progenitor cell derivation and cell reprogramming. The “traditional” strategy includes a pluripotent state of cells (ESC, iPSC; above); from these pluripotent stem cells multipotent lineage-specific progenitors and finally the various differentiated cell types are derived. In case of iPSC, the cells of origin are differentiated cells (e.g. fibroblasts) which are reprogrammed by activation of the four pluripotency-associated genes Oct4, Sox2, Klf4 and c-Myc (Yamanaka factors; left part of diagram). The *alternative strategy* (lower part of the diagram) avoids the induction of the ethically problematic pluripotent state (*direct reprogramming, bypassing pluripotency*): In this strategy, transcription factor-induced lineage reprogramming results either in cells remaining within the same cell lineage (i.e. mesoderm), or may produce functional cells of other lineages (converting mesodermal fibroblasts into ectodermal neurons). This transcription factor-induced lineage reprogramming not only avoids the ethical problem posed by a self-organizing and cloning capability gained (e.g. TC capability) but possibly also reduces tumor-formation risks (from [48] with permission).

(ESCs and iPSCs) offer the advantage of growing well and of being able, in addition, to differentiate as desired for regenerative medicine. In the “classical” approach, iPSCs are created by transduction and overexpression or at least temporal activation of the “Yamanaka factor” genes Oct4, Sox2,

Klf4, c-Myc; for transplantation or for disease modelling experiments the pluripotent cells so created are subsequently converted into multipotent progenitor cells, and these to the various differentiated cell types of interest (Figure 9.1). This strategy has been more or less the same in all investigations involving the creation of PSCs, irrespective of the cell type of origin chosen (fibroblasts, epithelial cells, etc.), and also irrespective of the mode of derivation (transient or permanent genetic, or epigenetic modification). Since with this “classical” strategy the induction of pluripotency is the first goal (in case of iPSCs; in case of ESCs it is not the induction but the maintenance of it), this strategy unfortunately creates exactly the ethical problem discussed above.

According to recent literature it appears possible, however, to use **alternative strategies bypassing pluripotency**. This opens a chance to avoid the ethical (and patenting) problems posed by an early embryonic pattern formation/self-organization potential of cells. Direct reprogramming, not including a (transient) state of pluripotency, has now been described for the derivation of e.g. cardiomyocytes, blood progenitors and neuronal cells, and in some of these cases the derived cells were efficiently expandable *in vitro*, a property that many authors previously considered to be a specific characteristic and major advantage of PSCs only. Literature on this new line of research is very rapidly expanding at present. These alternative strategies are depicted graphically in the lower part of Figure 9.1. The cells of origin (e.g. fibroblasts) are in these cases directly reprogrammed to form stem and progenitor cells possessing a lower level potentiality (without passing through a pluripotent state), using combinations of transcription factors that are specific for the desired differentiation pathway (direct transduction or indirect epigenetic modification). Examples are given in the lower part of Figure 9.1 (for more examples see [34–44]).

## 9.6 Conclusions

That the developmental potential of pluripotent stem cells must be considered as an eminent aspect of the ethics of stem cell use (including aspects of patenting) has been pointed out and discussed already since many years [4, 45, 46]. In particular after the advent and widespread use of cell reprogramming technologies it must be seen as a logical necessity to discuss which avenues could be taken to develop strategies for stem cell derivation which avoid the ethical problem of pluripotency [4, 47]. While this argumentation had originally been based predominantly on theory and only on few experimental findings, the numerous recent publications on direct

reprogramming/bypassing pluripotency mentioned in the previous paragraph suggest that we have now arrived at a point at which such avenues become indeed a most attractive option. One may ask why such a redirection of focus (direct reprogramming) has not been searched for more actively already during previous years, although the ethical arguments why such efforts should appear necessary had already been published since years.

The new strategies of inducing direct conversion of somatic cells to a stem/progenitor state, bypassing pluripotency, appear highly promising and recommendable. They are obviously preferable for ethical reasons because they avoid the problem created by inducing an embryo formation/cloning potential which fully pluripotent cells have. An additional advantage of these new strategies may be to reduce the risk of tumor formation after transplanting such cells because the tumor formation potential may be connected with the embryonic pattern formation/self-organization potential. A word of caution appears to be in place, nevertheless: In order for any such alternative strategy to be ethically acceptable, it must be made sure that it does not involve a transitory state of pluripotency that could remain undetected. Many of the induction protocols require very long culturing time periods, and we are far from understanding exactly what cascade of events takes place during this time period. Some of the protocols include while some omit Oct4, some use combinations of certain (but not all) of the Yamanaka factors while others do not. Which of the possible protocols will be safest in order to exclude TC capability as well as tumor formation risks? It will have to be discussed which genes should be seen here as crucial (e.g. genes involved in early embryonic pattern formation / self-organization processes) [4, 47]. This will be an important topic for future research. Strategies for testing this will need to be developed and discussed: For ethical reasons it cannot be defended to test human cells by cloning via TC [5]. It will thus be necessary to define appropriate combinations of *in vitro* gene expression profiling that may be useful instead in a first approximation, combined with *in vitro* culturing conditions that avoid the initiation of individuation processes. In any case it will be necessary to improve the catalogue of informations routinely given to cell donors: This information needs to include all aspects of the potentiality that the donated cells will or may acquire as a result of reprogramming, including TC capability, because this touches upon personal interests donors have (genetic identity and uniqueness). Implications of cell banking need to be included keeping in mind that ethical and legal standards may change and already differ in the various cultural environments. These aspects are

particularly relevant when long term storage and widespread use of the cells are envisaged.

Obviously this complex field of ethical problems can be avoided by circumventing any gain of pluripotency at all. A general recommendation for strategies of stem cell derivation would thus be to deviate from the widespread practice of activating the pluripotency program (creating iPSCs) and rather to rely on the alternative strategies bypassing pluripotency, i.e. to convert cells directly to multipotent stem/progenitor cells as in the examples given above.

## 9.7 Acknowledgments

I like to thank Anna M. Wobus and John Wiley & Sons for granting me permission to re-publish Figure 9.1 (Figure 2 in [48]).

## References

- [1] EU-CJ, Judgment of the Court (Grand Chamber) of 18 October 2011 (reference for a preliminary ruling from the Bundesgerichtshof - Germany) - Oliver Brüstle v Greenpeace e.V. (Case C-34/10) 1. EUGH Curia Europa (<http://curia.europa.eu/juris/document/document.jsf?docid=115334&mode=lst&pageIndex=1&dir=&occ=first&part=1&text=&doclang=EN&cid=114275>), 2011.
- [2] Callaway E. European court bans patents based on embryonic stem cells. Final decision could stifle investments in developing therapies. *Nature News* (Published online 18 October 2011, doi:10.1038/news.2011.597), 2011
- [3] González F., Boué S., Belmonte J. C. Methods for making induced pluripotent stem cells: reprogramming a la carte. *Nat. Rev. Genet.*, 12: 231–242, 2011.
- [4] Denker H.-W. Induced pluripotent stem cells: how to deal with the developmental potential. *Reprod. Biomed. Online*, 19 Suppl 1: 34–37, 2009.
- [5] Denker H.-W. Ethical concerns over use of new cloning technique in humans. *Nature*, 461 (7262): 341, 2009.
- [6] Lo B., Parham L., Alvarez-Buylla A., Cedars M., Conklin B., Fisher S., Gates E., Giudice L., Halme D. G., Hershon W., Kriegstein A., Kwok P. Y., Wagner R. Cloning mice and men: prohibiting the use of iPS cells for human reproductive cloning. *Cell Stem Cell*, 6 (1): 16–20, 2010.

- [7] Thomson J. A., Kalishman J., Golos T. G., Durning M., Harris C. P., Hearn J. P. Pluripotent Cell Lines Derived from Common Marmoset (*Callithrix jacchus*) Blastocysts. *Biol. Reprod.*, 55(2): 254–259, 1996.
- [8] Denker H.-W. Early human development: new data raise important embryological and ethical questions relevant for stem cell research. *Naturwissenschaften*, 91 (1): 1–21, 2004.
- [9] Fuchs C., Scheinast M., Pasterner, W., Lagger S., Hofner, M., Hoellrigl A., Schultheis M., Weitzer, G. Self-Organization Phenomena in Embryonic Stem Cell-Derived Embryoid Bodies: Axis Formation and Breaking of Symmetry during Cardiomyogenesis. *Cells Tissues Organs*, 195(5): 377–391, 2012.
- [10] Behr R., Heneweer C., Viebahn C., Denker H.-W., Thie M. Epithelial-mesenchymal transition in colonies of rhesus monkey embryonic stem cells: a model for processes involved in gastrulation. *Stem Cells*, 23 (6): 805–816, 2005.
- [11] ten Berge D., Koole W., Fuerer C., Fish M., Eroglu E., Nusse R. Wnt signaling mediates self-organization and axis formation in embryoid bodies. *Cell Stem Cell*, 3 (5): 508–518, 2008.
- [12] Maranca-Hüwel B., Denker H.-W. Epithelial-mesenchymal transition in rhesus monkey embryonic stem cell colonies: the role of culturing conditions. *In Vitro Cell. Dev. Biol. Anim.*, 46 (6): 516–528, 2010.
- [13] Nagy A., Gocza, E., Diaz E. M., Prideaux V. R., Ivanyi E., Markkula M., Rossant J. Embryonic stem cells alone are able to support fetal development in the mouse. *Development*, 110 (3): 815–821, 1990.
- [14] Nagy A., Rossant J., Nagy R., Abramow-Newerly W., Roder J. C. Derivation of completely cell culture-derived mice from early-passage embryonic stem cells. *Proc. Natl. Acad. Sci. USA*, 90 (18): 8424–8428, 1993.
- [15] Tam P. P. L., Rossant J. Mouse embryonic chimeras: tools for studying mammalian development. *Development*, 130 (25): 6155–6163, 2003.
- [16] Boland M. J., Hazen J. L., Nazor K. L., Rodriguez A. R., Gifford W., Martin G., Kupriyanov S., Baldwin K. K. Adult mice generated from induced pluripotent stem cells. *Nature*, 461 (7260): 91–94, 2009.
- [17] Kang L., Wang J., Zhang Y., Kou Z., Gao S. iPS cells can support full-term development of tetraploid blastocyst-complemented embryos. *Cell Stem Cell*, 5 (2): 135–138, 2009.
- [18] Zhao X.-y., Li W., Lv Z., Liu L., Tong M., Hai T., Hao J., Gou C.-l., Ma Q.-w., Wang L., Zeng F., Zhou Q. iPS cells produce viable mice through tetraploid complementation. *Nature*, 461: 86–90, 2009.

- [19] Zhao X.-Y., Lv Z., Li W., Zeng F., Zhou Q. Production of mice using iPS cells and tetraploid complementation. *Nat Protoc*, 5 (5): 963–971, 2010.
- [20] Stadtfeld M., Apostolou E., Akutsu H., Fukuda A., Follett P., Natesan, S., Kono T., Shioda T., Hochedlinger, K. Aberrant silencing of imprinted genes on chromosome 12qF1 in mouse induced pluripotent stem cells. *Nature*, 465 (7295): 175–181, 2010.
- [21] Devolder K., Ward C. M., Rescuing human embryonic stem cell research: The possibility of embryo reconstruction after stem cell derivation. *Metaphilosophy*, 38 (2): 245–263, 2007.
- [22] Wu G., Liu N., Rittelmeyer I., Sharma A. D., Sgodda M., Zaehres H., Bleidissel M., Greber B., Gentile L., Han D. W., Rudolph C., Steinemann D., Schambach A., Ott M., Schöler H. R., Cantz T. Generation of Healthy Mice from Gene-Corrected Disease-Specific Induced Pluripotent Stem Cells. *PLoS Biol.*, 9 (7): e1001099, 2011.
- [23] Han J., Yuan P., Yang H., Zhang J., Soh B. S., Li P., Lim S. L., Cao S., Tay J., Orlov Y. L., Lufkin T., Ng H. H., Tam W. L., Lim B. Tbx3 improves the germ-line competency of induced pluripotent stem cells. *Nature*, 463: 1096–1100, 2010.
- [24] Liu L., Luo G. Z., Yang W., Zhao X., Zheng Q., Lv Z., Li W., Wu H. J., Wang L., Wang X. J., Zhou Q. Activation of the imprinted Dlk1-Dio3 region correlates with pluripotency levels of mouse stem cells. *J. Biol. Chem.*, 285 (25): 19483–19490, 2010.
- [25] Kim K., Doi A., Wen B., Ng K., Zhao R., Cahan P., Kim J., Aryee M. J., Ji H., Ehrlich L. I., Yabuuchi A., Takeuchi A., Cunniff K. C., Hongguang H., McKinney-Freeman S., Naveiras O., Yoon T. J., Irizarry R. A., Jung N., Seita J., Hanna J., Murakami P., Jaenisch R., Weissleder R., Orkin S. H., Weissman I. L., Feinberg A. P., Daley G. Q. Epigenetic memory in induced pluripotent stem cells. *Nature*, 467 (7313): 285–290, 2010.
- [26] Bar-Nur O., Russ H. A., Efrat S., Benvenisty N. Epigenetic memory and preferential lineage-specific differentiation in induced pluripotent stem cells derived from human pancreatic islet beta cells. *Cell Stem Cell*, 9 (1): 17–23, 2011.
- [27] Lister R., Pelizzola M., Kida Y. S., Hawkins R. D., Nery J. R., Hon G., Antosiewicz-Bourget J., O'Malley R., Castanon R., Klugman S., Downes M., Yu R., Stewart R., Ren B., Thomson J. A., Evans R. M., Ecker J. R. Hotspots of aberrant epigenomic reprogramming in human induced pluripotent stem cells. *Nature*, 471 (7336): 68–73, 2011.

- [28] Nazor K. L., Altun G., Lynch C., Tran H., Harness J. V., Slavin I., Garitaonandia I., Muller F. J., Wang Y. C., Boscolo F. S., Fakunle E., Dumevska B., Lee S., Park H. S., Olee T., D’Lima D. D., Semechkin R., Parast M. M., Galat V., Laslett A. L., Schmidt U., Keirstead H. S., Loring J. F., Laurent L. C. Recurrent variations in DNA methylation in human pluripotent stem cells and their differentiated derivatives. *Cell Stem Cell*, 10 (5): 620–634, 2012.
- [29] Mayshar Y., Ben-David U., Lavon N., Biancotti J. C., Yakir B., Clark A. T., Plath K., Lowry W. E., Benvenisty N. Identification and classification of chromosomal aberrations in human induced pluripotent stem cells. *Cell Stem Cell*, 7 (4): 521–531, 2010.
- [30] Laurent L. C., Ulitsky I., Slavin I., Tran H., Schork A., Morey R., Lynch C., Harness J. V., Lee S., Barrero M. J., Ku S., Martynova M., Semechkin R., Galat V., Gottesfeld J., Izpisua Belmonte J. C., Murry C., Keirstead H. S., Park H. S., Schmidt U., Laslett A. L., Muller F. J., Nievergelt C. M., Shamir R., Loring J. F. Dynamic Changes in the Copy Number of Pluripotency and Cell Proliferation Genes in Human ESCs and iPSCs during Reprogramming and Time in Culture. *Cell Stem Cell*, 8 (1): 106–118, 2011.
- [31] Denker U., Denker H.-W. Embryonale Stammzellforschung: Aufklärung notwendig. Problematik der informierten Zustimmung der Spender. *Deutsches Ärzteblatt*, 102 (13): A892–A893, 2005.
- [32] Vrtovec K. T., Vrtovec B. Is Totipotency of a Human Cell a Sufficient Reason to Exclude its Patentability under the European Law? *Stem Cells*, 25 (12): 3026–3028, 2007.
- [33] Denker H.-W. Totipotency/pluripotency and patentability. *Stem Cells*, 26 (6): 1656–1657, 2008.
- [34] Ieda M., Fu J. D., Delgado-Olguin P., Vedantham V., Hayashi Y., Bruneau B. G., Srivastava D. Direct Reprogramming of Fibroblasts into Functional Cardiomyocytes by Defined Factors. *Cell*, 142 (3): 375–386, 2010.
- [35] Szabo E., Rampalli S., Risueno R. M., Schnerch A., Mitchell R., Fiebig-Comyn A., Levadoux-Martin M., Bhatia M. Direct conversion of human fibroblasts to multilineage blood progenitors. *Nature*, 468 (7323): 521–526, 2010.
- [36] Vierbuchen T., Ostermeier A., Pang Z. P., Kokubu Y., Sudhof T. C., Wernig M. Direct conversion of fibroblasts to functional neurons by defined factors. *Nature*, 463 (7284): 1035–1041, 2010.
- [37] Caiazzo M., Dell’anno M. T., Dvoretzkova E., Lazarevic D., Taverna S., Leo D., Sotnikova T. D., Menegon A., Roncaglia P., Colciago G,

- Russo G., Carninci P., Pezzoli G., Gainetdinov, R. R., Gustincich S., Dityatev A., Broccoli V. Direct generation of functional dopaminergic neurons from mouse and human fibroblasts. *Nature*, 476 (7359): 224–227, 2011.
- [38] Pfisterer U., Kirkeby A., Torper O., Wood J., Nelander J., Dufour A., Bjorklund A., Lindvall O., Jakobsson J., Parmar M. Direct conversion of human fibroblasts to dopaminergic neurons. *Proc. Natl. Acad. Sci. USA*, 108 (25): 10343–10348, 2011.
- [39] Son E. Y., Ichida J. K., Wainger B. J., Toma J. S., Rafuse V. F., Woolf C. J., Eggan K. Conversion of Mouse and Human Fibroblasts into Functional Spinal Motor Neurons. *Cell Stem Cell*, 9 (3): 205–218, 2011.
- [40] Qiang L., Fujita R., Yamashita T., Angulo S., Rhinn H., Rhee D., Doege C., Chau L., Aubry L., Vanti W. B., Moreno H., Abeliovich A. Directed conversion of Alzheimer’s disease patient skin fibroblasts into functional neurons. *Cell*, 146 (3): 359–371, 2011.
- [41] Yoo A. S., Sun A. X., Li L., Shcheglovitov A., Portmann T., Li Y., Lee-Messer C., Dolmetsch R. E., Tsien R. W., Crabtree G. R. MicroRNA-mediated conversion of human fibroblasts to neurons. *Nature*, 476 (7359): 228–231, 2011.
- [42] Jayawardena T. M., Egemnazarov B., Finch E. A., Zhang L., Payne J. A., Pandya K., Zhang Z., Rosenberg P., Mirotsov M., Dzau V. J. MicroRNA-Mediated *In Vitro* and *In Vivo* Direct Reprogramming of Cardiac Fibroblasts to Cardiomyocytes. *Circ. Res.*, 110 (11): 1465–1473, 2012.
- [43] Thier M., Worsdorfer P., Lakes, Y. B., Gorris R., Herms S., Opitz T., Seiferling D., Quandt T., Hoffmann P., Nothen, M. M., Brüstle O., Edenhofer F. Direct Conversion of Fibroblasts into Stably Expandable Neural Stem Cells. *Cell Stem Cell*, 10 (4): 473–479, 2012.
- [44] Han D. W., Tapia N., Hermann, A., Hemmer K., Hoing S., Arauzo-Bravo M. J., Zaehres H., Wu G., Frank S., Moritz S., Greber B., Yang J. H., Lee H. T., Schwamborn J. C., Storch A., Schöler H. R. Direct Reprogramming of Fibroblasts into Neural Stem Cells by Defined Factors. *Cell Stem Cell*, 10 (4): 465–472, 2012.
- [45] Denker H.-W. Embryonic stem cells: An exciting field for basic research and tissue engineering, but also an ethical dilemma? *Cells Tissues Organs*, 165: 246–249, 1999.
- [46] Denker, H.-W. Potentiality of embryonic stem cells: an ethical problem even with alternative stem cell sources. *J. Med. Ethics*, 32 (11): 665–671, 2006.



- [47] Denker, H.-W. Human embryonic stem cells: the real challenge for research as well as for bioethics is still ahead of us. *Cells Tissues Organs*, 187 (4): 250–256, 2008.
- [48] Wobus, A. M. The Janus face of pluripotent stem cells—connection between pluripotency and tumourigenicity. *Bioessays*, 32 (11): 993–1002, 2010.

## Constitutive Equations in Finite Viscoplasticity of Nanocomposite Hydrogels

---

A.D. Drozdov<sup>1,2</sup>, and J. deClaville Christiansen<sup>2</sup>

<sup>1</sup>Department of Plastics Technology, Danish Technological Institute, Taastrup, Denmark

<sup>2</sup>Department of Mechanical and Manufacturing Engineering, Aalborg University, Aalborg, Denmark

Corresponding author: A.D. Drozdov <add@teknologisk.dk>

### 10.1 Introduction

This paper deals with constitutive modeling of the viscoplastic response of nanocomposite hydrogels under an arbitrary deformation with finite strains.

Hydrogels are three-dimensional networks of polymer chains connected by physical and chemical cross-links. When a hydrogel is brought in contact with water, it swells retaining its structural integrity and ability to withstand large (up to 3000%) deformations. A shortcoming of conventional (chemically cross-linked) gels that restrains their applicability is that these materials become relatively weak and not sufficiently tough in the swollen state. To enhance mechanical properties of hydrogels without sacrifice of their swellability and extensibility, concentration of reversible physical crosslinks is to be increased [1] either by changes of molecular architecture (double-network hydrogels, gels with hydrophilic and hydrophobic chains [2]) or by reinforcement with nanoparticles that serve as effective multi-functional cross-linkers [3, 4].

Mechanical properties of hydrogels have been a focus of attention in the past decade as these materials demonstrate potential for a wide range of applications including biomedical devices, drug delivery carriers, superabsorbent materials, filters and membranes for selective diffusion, sensors for on-line process monitoring, smart optical systems, and soft actuators [5–8].

As mechanical properties of nanocomposite hydrogels are close to those of extracellular matrix (ECM), our interest to their analysis is driven by potential use of these materials for manufacturing synthetic multi-functional scaffolds for *in vitro* support of stem cell culture. The present study focuses on the viscoplastic response of nanocomposite hydrogels in uniaxial tensile cyclic tests. This choice of experimental program is explained by the fact that to ensure survival, proliferation, and differentiation of stem cells imbedded into a hydrogel-based matrix, the latter should be subjected to biophysical cues [9], among which mechanical stimuli play the key role [10, 11]. The standard protocol for mechanical stimulation of stem cells involves periodic deformations with relatively large amplitudes (cyclic loading) followed by periods of rest when thermodynamic equilibrium is established between the hydrogel and its environment [12, 13].

In the past five years, advanced constitutive models for the elastic behavior of hydrogels subjected to swelling have been developed in [14–22], to mention a few. Experimental and theoretical studies of relaxation mechanisms in hydrogels have been performed in [23–26]. Fracture, crack propagation, and self-healing of hydrogels have been investigated in [27–31].

Substantially less attention has been paid to the analysis of irreversible (associated with plastic flow and damage accumulation) phenomena in hydrogels. Stress–strain relations in finite viscoplasticity of hydrogels were developed in [32]. Constitutive equations for the elastic response and damage accumulation in double-network hydrogels were derived in [33, 34]. Time-dependent recovery of residual strains was investigated experimentally in [2, 35, 36].

The objective of this study is threefold: (i) to develop constitutive equations in finite viscoplasticity of nanocomposite hydrogels, (ii) to find adjustable parameters in the stress–strain relations by fitting observations in uniaxial tensile tests with various strain rates and tensile cyclic tests, and (iii) to reveal peculiarities of the mechanical behavior of hydrogels reinforced with various types of nanofiller (silica particles versus clay platelets).

As this work concentrates on the mechanical response of nanocomposite hydrogels swollen in salt-free water, and our aim is to derive relatively simple constitutive equations for their viscoplastic behavior, it seems natural to treat these composite materials as neutral gels and disregard the effects of co- and counter-ions. The novelty of the present approach consists in the following: (i) the initial configuration of a dry undeformed hydrogel is presumed to differ from the reference configuration of an equivalent polymer network (in which stresses in chains vanish), (ii) transformation of the initial

configuration into the reference configuration involves solvent-induced isotropic inflation of the polymer network and its traceless deformation driven by sliding of junctions between chains with respect to their reference positions, (iii) the specific free energy of the polymer network equals the sum of the mechanical energy stored in polymer chains (which depends on the Cauchy–Green tensor for elastic deformation) and the energy of interaction between chains and nanoparticles (which is treated as a function of the Cauchy–Green tensor for plastic deformation).

The exposition is organized as follows. Constitutive equations in finite viscoplasticity of nanocomposite hydrogels under an arbitrary three-dimensional deformation accompanied by swelling are developed in Section 10.2. The governing equations are simplified for uniaxial tension in Section 10.3. Adjustable parameters in the stress–strain relations are determined in Section 10.4 by fitting observations under cyclic deformation. Concluding remarks are formulated in Section 10.5.

## 10.2 Constitutive Model

To develop constitutive equations for the viscoplastic behavior of a nanocomposite hydrogel that involve a relatively small number of adjustable parameters, a homogenization concept is applied. The solid phase of a nanocomposite hydrogel (formed by a permanent network of flexible chains and a secondary network of clay platelets) is replaced with an equivalent viscoplastic medium whose behavior captures characteristic features of its mechanical response. The presence of nanoparticles within the polymer matrix is accounted for by assuming adjustable parameters in the stress–strain relations to depend on filler content.

### 10.2.1 Kinematic Relations

Macro-deformation of a nanocomposite hydrogel coincides with that of the equivalent medium. For definiteness, the initial configuration of a hydrogel is chosen to coincide with that of an undeformed dry specimen. Transformation of the initial configuration into the actual configuration is determined by the deformation gradient  $\mathbf{F}$ . The Cauchy–Green tensors for transition from the initial to actual configuration read

$$\mathbf{B} = \mathbf{F} \cdot \mathbf{F}^{\top}, \quad \mathbf{C} = \mathbf{F}^{\top} \cdot \mathbf{F}, \quad (10.1)$$

where the dot stands for inner product, and  $\top$  denotes transpose. The principal invariants of the Cauchy–Green tensors are denoted as  $J_1, J_2, J_3$ .

The reference configuration of the equivalent network (the configuration in which stresses in chain vanish) differs from the initial configuration. Denote by  $\mathbf{F}_*$  and  $\mathbf{F}_e$  deformation gradients for transition from the initial configuration into the reference configuration and from the reference configuration into the actual configuration, respectively (the subscript index “e” designates elastic deformation). These tensors are connected with deformation gradient for macro-deformation  $\mathbf{F}$  by the multiplicative decomposition formula

$$\mathbf{F} = \mathbf{F}_e \cdot \mathbf{F}_*. \quad (10.2)$$

Transition from the initial configuration into the reference configuration reflects two processes: (i) changes in specific volume (swelling and shrinkage) induced by solvent transport, and (ii) viscoplastic deformation (sliding of junctions between strands in the equivalent polymer network and slippage of nanoparticles with respect to their positions in the initial configuration).

Local transformation of the initial configuration into the reference configuration due to solvent diffusion is described by the deformation gradient  $\mathbf{f}$ . For an isotropic equivalent medium,

$$\mathbf{f} = f^{\frac{1}{3}} \mathbf{I}, \quad (10.3)$$

where  $f$  stands for the coefficient of inflation induced by solvent uptake, and  $\mathbf{I}$  is the unit tensor. Local transformation reflecting irreversible sliding is described by the deformation gradient  $\mathbf{F}_p$  where the subscript index “p” refers to plastic flow. The plastic deformation is presumed to be volume-preserving,

$$\det \mathbf{F}_p = 1. \quad (10.4)$$

It follows from the multiplicative decomposition formula that [21]

$$\mathbf{F}_* = \mathbf{F}_p \cdot \mathbf{f}. \quad (10.5)$$

Equations (10.2), (10.3), (10.5) imply that

$$\mathbf{F} = f^{\frac{1}{3}} \mathbf{F}_e \cdot \mathbf{F}_p. \quad (10.6)$$

The Cauchy–Green tensors for elastic deformation read

$$\mathbf{B}_e = \mathbf{F}_e \cdot \mathbf{F}_e^\top, \quad \mathbf{C}_e = \mathbf{F}_e^\top \cdot \mathbf{F}_e. \quad (10.7)$$

To develop differential equations for principal invariants  $J_{e1}$ ,  $J_{e2}$ ,  $J_{e3}$  of these tensors, we differentiate Equation (10.6) with respect to time  $t$ , introduce velocity gradients

$$\mathbf{L} = \dot{\mathbf{F}} \cdot \mathbf{F}^{-1}, \quad \mathbf{L}_e = \dot{\mathbf{F}}_e \cdot \mathbf{F}_e^{-1}, \quad \mathbf{l}_p = \dot{\mathbf{F}}_p \cdot \mathbf{F}_p^{-1}, \quad (10.8)$$

and obtain

$$\mathbf{L} = \mathbf{L}_e + \mathbf{L}_p + \frac{\dot{f}}{3f} \mathbf{I} \quad (10.9)$$

with

$$\mathbf{L}_p = \mathbf{F}_e \cdot \mathbf{l}_p \cdot \mathbf{F}_e^{-1}. \quad (10.10)$$

Equation (10.9) implies that that

$$\mathbf{D} = \mathbf{D}_e + \mathbf{D}_p + \frac{\dot{f}}{3f} \mathbf{I}, \quad (10.11)$$

where

$$\mathbf{D} = \frac{1}{2}(\mathbf{L} + \mathbf{L}^\top), \quad \mathbf{D}_e = \frac{1}{2}(\mathbf{L}_e + \mathbf{L}_e^\top), \quad \mathbf{D}_p = \frac{1}{2}(\mathbf{L}_p + \mathbf{L}_p^\top) \quad (10.12)$$

denote rate-of-strain tensors. Under the conventional hypothesis that the plastic spin vanishes,

$$\mathbf{l}_p = \mathbf{l}_p^\top = \mathbf{d}_p, \quad (10.13)$$

where  $\mathbf{d}_p$  is the rate-of-strain tensor for plastic deformation in the reference configuration, Equations (10.10)–(10.12) imply that

$$2\mathbf{D}_p = \mathbf{F}_e \cdot \mathbf{d}_p \cdot \mathbf{F}_e^{-1} + \mathbf{F}_e^{-\top} \cdot \mathbf{d}_p \cdot \mathbf{F}_e^\top. \quad (10.14)$$

Derivatives of the principal invariants of the Cauchy–Green tensors for elastic deformation with respect to time are given by

$$\dot{J}_{e1} = 2\mathbf{B}_e : \mathbf{D}_e, \quad \dot{J}_{e2} = 2(J_{e2}\mathbf{I} - J_{e3}\mathbf{B}_e^{-1}) : \mathbf{D}_e, \quad \dot{J}_{e3} = 2J_{e3}\mathbf{I} : \mathbf{D}_e, \quad (10.15)$$

where the colon stands for convolution of tensors. Combination of Equations (10.11) and (10.15) implies that

$$\begin{aligned} \dot{J}_{e1} &= 2\mathbf{B}_e : (\mathbf{D} - \mathbf{D}_p) - \frac{2\dot{f}}{3f} J_{e1}, \\ \dot{J}_{e2} &= 2(J_{e2}\mathbf{I} - J_{e3}\mathbf{B}_e^{-1}) : (\mathbf{D} - \mathbf{D}_p) - \frac{4\dot{f}}{3f} J_{e2}, \\ \dot{J}_{e3} &= 2J_{e3} \left[ \mathbf{I} : (\mathbf{D} - \mathbf{D}_p) - \frac{\dot{f}}{f} \right]. \end{aligned} \quad (10.16)$$

It follows from Equations (10.7) and (10.14) that

$$\mathbf{B}_e : \mathbf{D}_p = \mathbf{C}_e : \mathbf{d}_p, \quad \mathbf{I} : \mathbf{D}_p = 0, \quad \mathbf{B}_e^{-1} : \mathbf{D}_p = \mathbf{C}_e^{-1} : \mathbf{d}_p.$$

Insertion of these expressions into Equation (10.16) results in

$$\begin{aligned} \dot{J}_{e1} &= 2\mathbf{B}_e : \mathbf{D} - 2\mathbf{C}_e : \mathbf{d}_p - \frac{2\dot{f}}{3f}J_{e1}, \\ \dot{J}_{e2} &= -2(\mathbf{B}_e^{-1} : \mathbf{D} - \mathbf{C}_e^{-1} : \mathbf{d}_p)J_{e3} + 2\left(\mathbf{I} : \mathbf{D} - \frac{2\dot{f}}{3f}\right)J_{e2}, \\ \dot{J}_{e3} &= 2\left(\mathbf{I} : \mathbf{D} - \frac{\dot{f}}{f}\right)J_{e3}. \end{aligned} \quad (10.17)$$

Denote by

$$\mathbf{B}_p = \mathbf{F}_p \cdot \mathbf{F}_p^\top, \quad \mathbf{C}_p = \mathbf{F}_p^\top \cdot \mathbf{F}_p \quad (10.18)$$

the Cauchy–Green tensors for plastic deformation, and by  $J_{p1}$ ,  $J_{p2}$ , and  $J_{p3} = 1$  their principal invariants. Keeping in mind that  $\mathbf{d}_p$  is a traceless tensors, we write, by analogy with Equation (10.17),

$$\dot{J}_{p1} = 2\mathbf{B}_p : \mathbf{d}_p, \quad \dot{J}_{p2} = -2\mathbf{B}_p^{-1} : \mathbf{d}_p. \quad (10.19)$$

### 10.2.2 Free Energy Density of a Hydrogel

Denote by  $\Psi$  the specific free energy of a nanocomposite hydrogel (per unit volume in the initial configuration). For a hydrogel with an isotropic polymer network,  $\Psi$  is treated as a function of seven arguments

$$\Psi = \Psi(J_{e1}, J_{e2}, J_{e3}, J_{p1}, J_{p2}, n, t), \quad (10.20)$$

where  $n$  stands for numbers of water molecules per unit volume of a hydrogel in its initial state. An explicit dependence of  $\Psi$  on time  $t$  is introduced to account for evolution of the equivalent polymer network driven by swelling–shrinkage of a nanocomposite hydrogel. The following equation is adopted for the specific free energy

$$\Psi = \mu_0 n + \Psi_{\text{solid}} + \Psi_{\text{mix}}, \quad (10.21)$$

where  $\mu_0$  is chemical potential per solvent molecule in the bath (which, in general, differs from chemical potential  $\mu$  per solvent molecule in a gel),

$\Psi_{\text{solid}}$  denotes strain energy density of the solid phase,  $\Psi_{\text{mix}}$  stands for the energy of mixing of solvent molecules with chains and nanoparticles in the equivalent network.

The strain energy density of an isotropic equivalent medium reads

$$\Psi_{\text{solid}} = \Psi_{\text{solid}}(J_{e1}, J_{e2}, J_{e3}, J_{p1}, J_{p2}, t). \quad (10.22)$$

Within the Flory–Huggins theory of mixing, the specific energy of mixing is given by

$$\phi_s \Psi_{\text{mix}} = \frac{k_B T}{v} (\phi_f \ln \phi_f + \chi \phi_s \phi_f), \quad (10.23)$$

where  $k_B$  is Boltzmann's constant,  $T$  stands for absolute temperature,  $v$  is the characteristic volume of a solvent molecule,  $\chi$  denotes the Flory–Huggins interaction parameter, and

$$\phi_f = \frac{nv}{1 + nv}, \quad \phi_s = \frac{1}{1 + nv} \quad (10.24)$$

are volume fractions of the fluid and solid phases, respectively. Insertion of Equations (10.22) and (10.23) into Equation (10.21) implies that

$$\Psi = \Psi_{\text{solid}} + \mu_0 n + \frac{k_B T}{v} \left( nv \ln \frac{nv}{1 + nv} + \chi \frac{nv}{1 + nv} \right). \quad (10.25)$$

### 10.2.3 Derivation of Constitutive Equations

To develop constitutive equations, we apply the method of [14]: the problem of mechanical deformation of a hydrogel subjected to swelling is immersed in a larger class of problems with volume and surface mass uptake (in terminology of [14], pumps injecting solvent are ascribed to each elementary volume of a specimen).

Under quasi-static deformation of a hydrogel, the first Piola–Kirchhoff stress tensor  $\mathbf{P}$  satisfies the equilibrium equations

$$\nabla_0 \cdot \mathbf{P} + \mathbf{b} = \mathbf{0} \quad (\text{in } \Omega) \quad \mathbf{n}_0 \cdot \mathbf{P} = \mathbf{t} \quad (\text{at } \partial\Omega), \quad (10.26)$$

where  $\Omega$  is an arbitrary domain occupied by the hydrogel in the initial configuration,  $\partial\Omega$  is its boundary,  $\nabla_0$  is the gradient operator in the initial configuration,  $\mathbf{n}_0$  is unit outward normal vector at  $\partial\Omega$ ,  $\mathbf{b}$  denotes volume force, and  $\mathbf{t}$  is surface traction.



Changes in number of solvent molecules  $n$  with time are governed by the equations

$$\frac{\partial n}{\partial t} + \nabla_0 \cdot \mathbf{j}_0 = R \quad (\text{in } \Omega), \quad \mathbf{n}_0 \cdot \mathbf{j}_0 = -r \quad (\text{at } \partial\Omega). \quad (10.27)$$

Here  $R$  is the rate of injection of solvent molecules per unit volume,  $r$  is the rate of injection of solvent molecules through unit boundary surface, and  $\mathbf{j}_0$  stands for flux of solvent in the initial configuration (number of solvent molecules moving through unit surface per unit time).

Transport of solvent through an isotropic network is described by the diffusion equation

$$\mathbf{j} = -\frac{DN}{k_B T} \nabla \mu, \quad (10.28)$$

where  $D$  stands for diffusivity,  $N = n / \det \mathbf{F}$  denotes concentration of solvent molecules per unit volume in the actual configuration, and  $\mathbf{j}$ ,  $\nabla$  are flux vector and the gradient operator in the actual configuration. Keeping in mind that

$$\mathbf{j}_0 = (\det \mathbf{F}) \mathbf{F}^{-1} \cdot \mathbf{j}, \quad \nabla_0 \mu = \nabla \mu \cdot \mathbf{F},$$

we present Equation (10.28) in the form

$$\mathbf{j}_0 = -\frac{Dn}{k_B T} \mathbf{F}^{-1} \cdot \nabla_0 \mu \cdot \mathbf{F}^{-1}. \quad (10.29)$$

Deformation gradient  $\mathbf{F}$  and number of solvent molecules  $n$  are connected by the molecular incompressibility condition

$$1 + nv = \det \mathbf{F}, \quad (10.30)$$

which means that volumetric macro-deformation is driven by changes in concentration of solvent molecules.

The free energy imbalance equation is written in the form [14]

$$\frac{d}{dt} \int_{\Omega} \Psi dV - \left( \int_{\Omega} \mathbf{b} \cdot \mathbf{v} dV + \int_{\partial\Omega} \mathbf{t} \cdot \mathbf{v} dA \right) - \left( \int_{\Omega} \mu R dV + \int_{\partial\Omega} \mu r dA \right) \leq 0, \quad (10.31)$$

where the term in the first parentheses denotes work of external forces (per unit time), and that in the other parentheses stands for rate of changes in the free energy driven by mass flux. Here  $\mathbf{v}$  stands for the velocity vector,  $dV$  is volume element, and  $dA$  is surface element (the volume and surface elements are determined in the initial configuration).

Standard transformations of the expression in the first parentheses in Equation (10.31) (integration by parts with application of Equation (10.26)) result in the formula

$$\int_{\Omega} \mathbf{b} \cdot \mathbf{v} dV + \int_{\partial\Omega} \mathbf{t} \cdot \mathbf{v} dA = \int_{\Omega} (\det \mathbf{F}) \mathbf{T} : \mathbf{D} dV, \quad (10.32)$$

where  $\mathbf{T}$  is the Cauchy stress tensor connected with the Piola–Kirchhoff tensor  $\mathbf{P}$  by the equation

$$\mathbf{P} = (\det \mathbf{F}) \mathbf{F}^{-1} \cdot \mathbf{T},$$

and  $\mathbf{D}$  is given by Equation (10.11).

Calculation of the derivative of free energy density (10.20) with the help of Equations (10.17) and (10.19) implies that

$$\begin{aligned} \frac{d}{dt} \int_{\Omega} \Psi dV = & \int_{\Omega} \left\{ \frac{\partial \Psi}{\partial t} + \frac{\partial \Psi}{\partial n} \frac{\partial n}{\partial t} - \frac{2f}{3f} \left( J_{e1} \Psi_{,e1} + 2J_{e2} \Psi_{,e2} + 3J_{e3} \Psi_{,e3} \right) + \right. \\ & 2 \left[ (\Psi_{,e1} \mathbf{B}_e - J_{e3} \Psi_{,e2} \mathbf{B}_e^{-1}) + (J_{e2} \Psi_{,e2} + J_{e3} \Psi_{,e3}) \mathbf{I} \right] : \mathbf{D} + \\ & \left. 2 \left[ (\Psi_{,p1} \mathbf{B}_p - \Psi_{,p2} \mathbf{B}_p^{-1}) - (\Psi_{,e1} \mathbf{C}_e - J_{e3} \Psi_{,e2} \mathbf{C}_e^{-1}) \right] : \mathbf{d}_p \right\} dV, \end{aligned} \quad (10.33)$$

where

$$\Psi_{,em} = \frac{\partial \Psi}{\partial J_{em}} \quad \Psi_{,pm} = \frac{\partial \Psi}{\partial J_{pm}}.$$

The second term in Equation (10.33) is transformed by integration by parts with the help of Equation (10.27),

$$\int_{\Omega} \frac{\partial \Psi}{\partial n} \frac{\partial n}{\partial t} dV = \int_{\Omega} \left[ \frac{\partial \Psi}{\partial n} R + \mathbf{j}_0 \cdot \nabla_0 \left( \frac{\partial \Psi}{\partial n} \right) \right] dV + \int_{\partial\Omega} r \frac{\partial \Psi}{\partial n} dA. \quad (10.34)$$

Combination of Equations (10.33) and (10.34) yields

$$\begin{aligned} \frac{d}{dt} \int_{\Omega} \Psi dV = & \int_{\Omega} \left\{ \Theta + 2 \left[ (\Psi_{,e1} \mathbf{B}_e - J_{e3} \Psi_{,e2} \mathbf{B}_e^{-1}) + (J_{e2} \Psi_{,e2} + J_{e3} \Psi_{,e3}) \mathbf{I} \right] : \mathbf{D} + \right. \\ & 2 \left[ (\Psi_{,p1} \mathbf{B}_p - \Psi_{,p2} \mathbf{B}_p^{-1}) - (\Psi_{,e1} \mathbf{C}_e - J_{e3} \Psi_{,e2} \mathbf{C}_e^{-1}) \right] : \mathbf{d}_p + \\ & \left. \left[ \frac{\partial \Psi}{\partial n} R + \mathbf{j}_0 \cdot \nabla_0 \left( \frac{\partial \Psi}{\partial n} \right) \right] \right\} dV + \int_{\partial\Omega} r \frac{\partial \Psi}{\partial n} dA, \end{aligned} \quad (10.35)$$

where

$$\Theta = \frac{\partial \Psi}{\partial t} - \frac{2\dot{f}}{3f} \left( J_{e1} \Psi_{,e1} + 2J_{e2} \Psi_{,e2} + 3J_{e3} \Psi_{,e3} \right). \quad (10.36)$$

The molecular incompressibility condition (10.30) establishes a connection between the deformation gradient  $\mathbf{F}$  and the rate of injection of solvent  $R$ . To account for this dependence, we differentiate Equation (10.30) with respect to time. Keeping in mind that

$$\frac{d}{dt} \det \mathbf{F} = (\det \mathbf{F}) \mathbf{I} : \mathbf{D},$$

and replacing the derivative of  $n$  by means of Equation (10.27), we obtain

$$v(R - \nabla_0 \cdot \mathbf{j}_0) - (\det \mathbf{F}) \mathbf{I} : \mathbf{D} = 0. \quad (10.37)$$

Multiplying Equation (10.37) by an arbitrary function  $\Pi$ , integrating over  $\Omega$ , and performing integration by parts with the help of Equation (10.28), we arrive at

$$\int_{\Omega} \left[ \Pi \left( vR - (\det \mathbf{F}) \mathbf{I} : \mathbf{D} \right) + \mathbf{j}_0 \cdot \nabla_0 (\Pi v) \right] dV + \int_{\partial \Omega} \Pi v r dA = 0. \quad (10.38)$$

Inserting Equations (10.32), (10.35) into Equation (10.31) and adding Equation (10.38), we find that

$$\begin{aligned} & \int_{\Omega} \left\{ 2 \left[ (\Psi_{,e1} \mathbf{B}_e - J_{e3} \Psi_{,e2} \mathbf{B}_e^{-1}) + (J_{e2} \Psi_{,e2} + J_{e3} \Psi_{,e3}) \mathbf{I} - \right. \right. \\ & \qquad \qquad \qquad \left. \left. (\det \mathbf{F})(\mathbf{T} + \Pi \mathbf{I}) \right\} : \mathbf{D} dV + \\ & 2 \int_{\Omega} \left[ (\Psi_{,p1} \mathbf{B}_p - \Psi_{,p2} \mathbf{B}_p^{-1}) - (\Psi_{,e1} \mathbf{C}_e - J_{e3} \Psi_{,e2} \mathbf{C}_e^{-1}) \right] : \mathbf{d}_p dV + \\ & \int_{\Omega} \left( \frac{\partial \Psi}{\partial n} + \Pi v - \mu \right) R dV + \int_{\partial \Omega} \left( \frac{\partial \Psi}{\partial n} + \Pi v - \mu \right) r dA + \\ & \int_{\Omega} \mathbf{j}_0 \cdot \nabla_0 \left( \frac{\partial \Psi}{\partial n} + \Pi v \right) dV + \int_{\Omega} \Theta dV \leq 0. \end{aligned} \quad (10.39)$$

Keeping in mind that  $\mathbf{D}$ ,  $R$ ,  $r$  are now arbitrary functions (the only connection between them (10.30) is accounted for by means of the function  $\Pi$ ), we conclude that the thermodynamic inequality (10.39) is satisfied, provided that (i) the Cauchy stress tensor is given by

$$\mathbf{T} = -\Pi \mathbf{I} + \frac{2}{\det \mathbf{F}} \left[ (\Psi_{,e1} \mathbf{B}_e - J_{e3} \Psi_{,e2} \mathbf{B}_e^{-1}) + (J_{e2} \Psi_{,e2} + J_{e3} \Psi_{,e3}) \mathbf{I} \right], \quad (10.40)$$

and (ii) chemical potential reads

$$\mu = \frac{\partial \Psi}{\partial n} + \Pi v. \quad (10.41)$$

It follows from Equations (10.25) and (10.41) that

$$\mu = \mu_0 + \Pi v + k_B T \left[ \ln \frac{nv}{1+nv} + \frac{\chi}{(1+nv)^2} \right]. \quad (10.42)$$

Substitution of Equations (10.29), (10.40), and (10.41) into Equation (10.39) implies that

$$\begin{aligned} \int_{\Omega} \Theta dV + 2 \int_{\Omega} \left[ (\Psi_{,p1} \mathbf{B}_p - \Psi_{,p2} \mathbf{B}_p^{-1}) - (\Psi_{,e1} \mathbf{C}_e - J_{e3} \Psi_{,e2} \mathbf{C}_e^{-1}) \right] : \\ \mathbf{d}_p dV - \\ \int_{\Omega} \frac{Dn}{k_B T} (\mathbf{F}^{-1} \cdot \nabla_0 \mu) \cdot (\mathbf{F}^{-1} \cdot \nabla_0 \mu) dV \leq 0. \end{aligned} \quad (10.43)$$

Keeping in mind that the last term in Equation (10.43) is non-negative, and using Equations (10.4) and (10.36), we conclude that in order to satisfy the free energy imbalance condition, it suffices to require that (iii) the rate-of-strain tensor for plastic deformation  $\mathbf{d}_p$  is governed by the equation

$$\mathbf{d}_p = P \left[ (\Psi_{,e1} \mathbf{C}_e - J_{e3} \Psi_{,e2} \mathbf{C}_e^{-1}) - (\Psi_{,p1} \mathbf{B}_p - \Psi_{,p2} \mathbf{B}_p^{-1}) \right]', \quad (10.44)$$

where  $P$  is an arbitrary non-negative function, and the prime stands for the deviatoric component of a tensor, and (iv) the coefficient of inflation of the network  $f$  obeys the inequality

$$\frac{\partial \Psi}{\partial t} - \frac{2f}{3f} \left( J_{e1} \Psi_{,e1} + 2J_{e2} \Psi_{,e2} + 3J_{e3} \Psi_{,e3} \right) \leq 0. \quad (10.45)$$

It is convenient to present Equation (10.44) in the form

$$\begin{aligned} \mathbf{d}_p = P \left\{ \left[ \Psi_{,e1} \left( \mathbf{C}_e - \frac{1}{3} J_{1e} \mathbf{I} \right) - J_{e3} \Psi_{,e2} \left( \mathbf{C}_e^{-1} - \frac{1}{3} (\mathbf{C}_e^{-1} : \mathbf{I}) \mathbf{I} \right) \right] - \right. \\ \left. \left[ \Psi_{,p1} \left( \mathbf{B}_p - \frac{1}{3} J_{1p} \mathbf{I} \right) - \Psi_{,p2} \left( \mathbf{B}_p^{-1} - \frac{1}{3} (\mathbf{B}_p^{-1} : \mathbf{I}) \mathbf{I} \right) \right] \right\}. \end{aligned}$$

Taking into account that

$$J_{e3} (\mathbf{C}_e^{-1} : \mathbf{I}) = J_{e2}, \quad \mathbf{B}_p^{-1} : \mathbf{I} = J_{p2},$$

we arrive at the formula

$$\mathbf{d}_p = P \left\{ \left[ \Psi_{,e1} \left( \mathbf{C}_e - \frac{1}{3} J_{1e} \mathbf{I} \right) - \Psi_{,e2} \left( J_{e3} \mathbf{C}_e^{-1} - \frac{1}{3} J_{e2} \mathbf{I} \right) \right] - \left[ \Psi_{,p1} \left( \mathbf{B}_p - \frac{1}{3} J_{1p} \mathbf{I} \right) - \Psi_{,p2} \left( \mathbf{B}_p^{-1} - \frac{1}{3} J_{p2} \mathbf{I} \right) \right] \right\}. \quad (10.46)$$

It follows from Equations (10.8), (10.13), (10.18) that

$$\dot{\mathbf{B}}_p = \mathbf{d}_p \cdot \mathbf{B}_p + \mathbf{B}_p \cdot \mathbf{d}_p.$$

Substitution of Equation (10.46) into this equation yields

$$\begin{aligned} \dot{\mathbf{B}}_p = 2P \left[ \frac{1}{2} \Psi_{,e1} (\mathbf{C}_e \cdot \mathbf{B}_p + \mathbf{B}_p \cdot \mathbf{C}_e) - \frac{1}{2} J_{e3} \Psi_{,e2} (\mathbf{C}_e^{-1} \cdot \mathbf{B}_p + \mathbf{B}_p \cdot \mathbf{C}_e^{-1}) \right. \\ \left. - \frac{1}{3} \left( (J_{e1} \Psi_{,e1} - J_{e2} \Psi_{,e2}) - (J_{p1} \Psi_{,p1} - J_{p2} \Psi_{,p2}) \right) \right. \\ \left. \mathbf{B}_p + \Psi_{,p2} \mathbf{I} - \Psi_{,p1} \mathbf{B}_p^2 \right]. \quad (10.47) \end{aligned}$$

Equations (10.8)–(10.10) and (10.13) imply that

$$\dot{\mathbf{F}}_e = \left( \mathbf{L} - \frac{\dot{f}}{3f} \mathbf{I} \right) \cdot \mathbf{F}_e - \mathbf{F}_e \cdot \mathbf{d}_p.$$

Combination of this equation with Equation (10.37) results in

$$\begin{aligned} \dot{\mathbf{F}}_e = \left( \mathbf{L} - \frac{\dot{f}}{3f} \mathbf{I} \right) \cdot \mathbf{F}_e - P \mathbf{F}_e \cdot \left\{ \left[ \Psi_{,e1} \left( \mathbf{C}_e - \frac{1}{3} J_{e1} \mathbf{I} \right) \right. \right. \\ \left. \left. - \Psi_{,e2} \left( J_{e3} \mathbf{C}_e^{-1} - \frac{1}{3} J_{e2} \mathbf{I} \right) \right] - \right. \\ \left. \left[ \Psi_{,p1} \left( \mathbf{B}_p - \frac{1}{3} J_{p1} \mathbf{I} \right) - \Psi_{,p2} \left( \mathbf{B}_p^{-1} - \frac{1}{3} J_{p2} \mathbf{I} \right) \right] \right\}. \quad (10.48) \end{aligned}$$

Given a free energy density (10.20), Equations (10.40), (10.41), (10.47), (10.48) provide stress–strain relations in finite viscoplasticity of hydrogels.

### 10.3 Simplification of the Constitutive Equations

Our aim now is to perform quantitative investigation of the viscoplastic response of nanocomposite hydrogels in short-term tests whose duration is noticeably lower than the characteristic time for diffusion of solvent. For

this purpose, we simplify the constitutive equations in order (i) to make them suitable for fitting experimental data and (ii) to reduce the number of adjustable parameters.

First, we suppose that the strain energy density  $\Psi_{\text{solid}}$  depends on principal invariants  $J_{e1}$ ,  $J_{e3}$ , and  $J_{p1}$  only, and present this function in the form

$$\Psi_{\text{solid}} = W_1(J_{e1}, J_{e3}, t) + W_2(J_{p1}, t), \quad (10.49)$$

where  $W_1$  denotes mechanical energy stored in individual chains of the equivalent polymer network (this quantity depends on principal invariants of the Cauchy–Green tensor for elastic deformation) and  $W_2$  stands for the energy of interaction between chains and nanoparticles (treated as a function of principal invariants of the Cauchy–Green tensor for plastic deformation). The influence of second principal invariants of the corresponding Cauchy–Green tensors on the mechanical response is disregarded in Equation (10.49).

Substitution of Equations (10.21), (10.24), (10.30), (10.49) into Equation (10.40) implies that

$$\mathbf{T} = -\Pi \mathbf{I} + 2\phi_s(w_1 \mathbf{B}_e + J_{e3} w'_1 \mathbf{I}), \quad (10.50)$$

where

$$w_1 = \frac{\partial W_1}{\partial J_{e1}}, \quad w'_1 = \frac{\partial W_1}{\partial J_{e3}}. \quad (10.51)$$

Combination of Equations (10.47–10.49) results in

$$\begin{aligned} \dot{\mathbf{B}}_p &= 2P \left[ \frac{1}{2} w_1 (\mathbf{C}_e \cdot \mathbf{B}_p + \mathbf{B}_p \cdot \mathbf{C}_e) - \frac{1}{3} (w_1 J_{e1} - w_2 J_{p1}) \mathbf{B}_p - w_2 \mathbf{B}_p^2 \right], \\ \dot{\mathbf{F}}_e &= \left( \mathbf{L} - \frac{\dot{f}}{3f} \mathbf{I} \right) \cdot \mathbf{F}_e - P \mathbf{F}_e \cdot \left[ w_1 \left( \mathbf{C}_e - \frac{1}{3} J_{e1} \mathbf{I} \right) - \right. \\ &\quad \left. w_2 \left( \mathbf{B}_p - \frac{1}{3} J_{p1} \mathbf{I} \right) \right] \end{aligned} \quad (10.52)$$

with

$$w_2 = \frac{\partial W_2}{\partial J_{p1}}. \quad (10.53)$$

Under an arbitrary deformation of a nanocomposite hydrogel subjected to swelling, Equations (10.50)–(10.52) together with Equation (10.42) for chemical potential should be accompanied by the equilibrium equations for the Cauchy stress tensor  $\mathbf{T}$  and diffusion Equation (10.27) with  $R = 0$ ,

$$\dot{n} = \nabla_0 \cdot \left( \frac{Dn}{k_B T} \mathbf{F}^{-1} \cdot \nabla_0 \mu \cdot \mathbf{F}^{-1} \right).$$

In conventional mechanical tests, a hydrogel specimen is, first, swollen in water (to reach a fixed degree of swelling), then annealed without contact with water bath (to reach an homogeneous distribution of solvent across the sample), and, afterwards, loaded with a relatively high strain rate (to avoid evaporation of solvent from the surface). After annealing, concentration of solvent molecules becomes independent of spatial coordinates, but its value differs from that in a fully swollen sample (chemical potential  $\mu$  does not coincide with  $\mu_0$ ). When the characteristic time for diffusion of solvent exceeds substantially duration of a test, changes in  $n$  under deformation can be neglected, and this quantity may be treated as an experimental parameter. Keeping in mind that  $n$  remains constant, we disregard dependencies of  $W_1$ ,  $W_2$  and  $f$  on time. Adjustable parameters in expressions for  $W_1$ ,  $W_2$ ,  $f$  adopt, however, different values for different concentrations of solvent  $n$ .

Introducing the notation  $p = \Pi - 2\phi_s J_e 3w_1'$  and setting  $\dot{f} = 0$  in Equation (10.52), we present Equations (10.50) and (10.52) in the form

$$\begin{aligned}\mathbf{T} &= -p\mathbf{I} + 2\phi_s w_1 \mathbf{B}_e, \\ \dot{\mathbf{B}}_p &= 2P \left[ \frac{1}{2} w_1 (\mathbf{C}_e \cdot \mathbf{B}_p + \mathbf{B}_p \cdot \mathbf{C}_e) - \frac{1}{3} (w_1 J_{e1} - w_2 J_{p1}) \mathbf{B}_p - w_2 \mathbf{B}_p^2 \right], \\ \dot{\mathbf{F}}_e &= \mathbf{L} \cdot \mathbf{F}_e - P \mathbf{F}_e \cdot \left[ w_1 \left( \mathbf{C}_e - \frac{1}{3} J_{e1} \mathbf{I} \right) - w_2 \left( \mathbf{B}_p - \frac{1}{3} J_{p1} \mathbf{I} \right) \right].\end{aligned}\quad (10.54)$$

The deformation gradient  $\mathbf{F}$  is split into the product of the deformation gradient driven by swelling from the dry state into the undeformed swollen state  $(1 + nv)^{\frac{1}{3}} \mathbf{I}$  and the loading-induced deformation gradient  $\tilde{\mathbf{F}}$ ,

$$\mathbf{F} = \tilde{\mathbf{F}} (1 + nv)^{\frac{1}{3}}. \quad (10.55)$$

Combination of Equations (10.6) and (10.55) implies that

$$\mathbf{F}_e = \left( \frac{1 + nv}{f} \right)^{\frac{1}{3}} \tilde{\mathbf{F}} \cdot \mathbf{F}_p^{-1}. \quad (10.56)$$

Under uniaxial deformation of an incompressible medium, tensor  $\tilde{\mathbf{F}}$  reads

$$\tilde{\mathbf{F}} = k \mathbf{e}_1 \mathbf{e}_1 + k^{-\frac{1}{2}} (\mathbf{e}_2 \mathbf{e}_2 + \mathbf{e}_3 \mathbf{e}_3), \quad (10.57)$$

where  $\mathbf{e}_m$  ( $m = 1, 2, 3$ ) are base vectors of a Cartesian frame in the initial state, and  $k$  stands for elongation ratio. Assuming tensor  $\mathbf{F}_p$  to be determined by Equation (10.57) with a coefficient  $k_p$ , we find from Equation (10.56) that

$$\mathbf{F}_e = \left( \frac{1 + nv}{f} \right)^{\frac{1}{3}} \left[ \frac{k}{k_p} \mathbf{e}_1 \mathbf{e}_1 + \left( \frac{k_p}{k} \right)^{\frac{1}{2}} (\mathbf{e}_2 \mathbf{e}_2 + \mathbf{e}_3 \mathbf{e}_3) \right]. \quad (10.58)$$

Insertion of Equations (10.57) and (10.58) into Equation (10.54) results in

$$\dot{k}_p = \frac{2}{3}P \left[ w_1 X \frac{k^3 - k_p^3}{kk_p} - w_2 (k_p^3 - 1) \right] \quad (10.59)$$

with

$$X = \left( \frac{1 + nv}{f} \right)^{\frac{2}{3}}. \quad (10.60)$$

Keeping in mind that under uniaxial tension, the stress tensor is given by

$$\mathbf{T} = \sigma k \mathbf{e}_1 \mathbf{e}_1,$$

where  $\sigma$  stands for engineering tensile stress, we find from Equation (10.54) that

$$\sigma = 2\phi_s w_1 X \frac{k^3 - k_p^3}{k^2 k_p^2}. \quad (10.61)$$

Constitutive equations for uniaxial tension of hydrogels (10.59), (10.61) involve two functions,  $w_1$  and  $w_2$ , that characterize the energy stored in polymer chains and the energy of inter-chain interactions.

The following expression is adopted for the strain energy density of the equivalent polymer network [37]

$$W_1 = -\frac{1}{2}G \left[ J \ln \left( 1 - \frac{J_{e1} - 3}{J} \right) + \frac{1}{2} \ln J_{e3} \right], \quad (10.62)$$

where  $G$  stands for an elastic modulus, and  $J > 0$  characterizes extensibility of chains. When  $J \rightarrow \infty$ , Equation (10.62) is transformed into the specific strain energy of a network of flexible chains [38]

$$\Psi_{\text{solid}} = \frac{1}{2}G \left[ (J_{e1} - 3) - \frac{1}{2} \ln J_{e3} \right].$$

Differentiation of Equation (10.62) with respect to  $J_{e1}$  implies that

$$w_1 = \frac{1}{2}G \left( 1 - \frac{J_{e1} - 3}{J} \right)^{-1}. \quad (10.63)$$

The energy of inter-chain interaction  $W_2$  is determined by integration of Equation (10.53) with

$$w_2 = \frac{1}{2}\tilde{G} \left[ 1 + K(J_{p1} - 3)^\alpha \right], \quad (10.64)$$



where  $\tilde{G}$  stands for an analog of elastic modulus, and  $K > 0$ ,  $\alpha$  are material constants. To reduce the number of adjustable parameters, we presume that

$$K = 1, \quad \alpha = 2$$

under tension, and

$$\alpha = -\frac{1}{2}$$

under retraction.

Insertion of Equations (10.63) and (10.64) into Equations (10.59) and (10.61) results in the stress–strain relation

$$\sigma = GX\phi_s \left[ 1 - \frac{1}{J} \left( X \left( \frac{k^2}{k_p^2} + 2 \frac{k_p}{k} \right) - 3 \right) \right]^{-1} \frac{k^3 - k_p^3}{k^2 k_p^2} \quad (10.65)$$

and the kinetic equation for plastic flow

$$\dot{k}_p = S \left\{ X \left[ 1 - \frac{1}{J} \left( X \left( \frac{k^2}{k_p^2} + 2 \frac{k_p}{k} \right) - 3 \right) \right]^{-1} \frac{k^3 - k_p^3}{k k_p} - R \left[ 1 + K \left( \frac{k^2}{k_p^2} + \frac{2}{k_p} - 3 \right)^\alpha \right] (k_p^3 - 1) \right\} \frac{|\dot{k}|}{k} \quad (10.66)$$

with

$$S = \frac{PG}{3D}, \quad R = \frac{\tilde{G}}{G}, \quad (10.67)$$

where  $D = |\dot{k}|/k$  stands for strain-rate intensity.

Constitutive Equations (10.65) and (10.66) involve six adjustable parameters: (i)  $G$  stands for elastic modulus of an equivalent polymer network, (ii)  $X$  characterizes swelling-induced inflation of the network, (iii)  $J$  is a measure of extensibility of chains, (iv)  $S$  denotes rate of plastic flow, (v)  $R$  stands for strength of inter-chain interactions, (vi)  $K$  characterizes energy of inter-chain interactions under retraction. These quantities may be affected by composition of a hydrogel, strain rate  $\dot{k}$  (due to the neglect of viscoelastic properties associated with rearrangement of polymer network), and deformation program (the energy of interaction  $W_2$  adopts different values under tension and retraction).

Although the number of material constants in the constitutive equations appears to be reasonable compared with conventional models in finite viscoplasticity of polymers, this number can be reduced further for special loading

programs. In particular, when observations are analyzed on as-prepared hydrogels, one can set

$$X = 1, \quad (10.68)$$

which means that the reference state of the equivalent polymer network coincides with the as-prepared state.

In the analysis of active (without unloading) deformations of as-prepared hydrogels, the dimensionless parameter  $K$  is not needed, which implies that the total number of parameters to be found by matching observations is reduced to four.

## 10.4 Fitting of Observations

We intend now to determine adjustable parameters in the stress–strain relations by fitting experimental data on nanocomposite hydrogels under uniaxial tension with finite strains and to assess the effects of type and content of nanofiller on the kinetics of plastic flow. Approximation of experimental stress–strain diagrams is performed for hydrogels with poly(dimethylacrylamide) and polyacrylamide matrices. Hydrogel specimens are characterized by polymer content  $\phi_p = m_{\text{polymer}}/m_{\text{water}}$ , nanofiller content  $\phi_f = m_{\text{filler}}/m_{\text{water}}$ , concentration of solid phase  $\phi_s = (m_{\text{polymer}} + m_{\text{filler}})/(m_{\text{polymer}} + m_{\text{filler}} + m_{\text{water}})$ , where  $m_{\text{polymer}}$ ,  $m_{\text{filler}}$ ,  $m_{\text{water}}$  are masses of monomers, filler particles, and water in the as-prepared state, and degree of swelling  $Q = M_{\text{water}}/(m_{\text{polymer}} + m_{\text{filler}})$ , where  $M_{\text{water}}$  stands for mass of solvent in the actual state.

### 10.4.1 Nanocomposite Hydrogels Subjected to Drying and Swelling

To demonstrate the role of coefficient of inflation  $f$  in constitutive modeling, we focus on the analysis of mechanical response of nanocomposite hydrogels subjected to drying and subsequent swelling.

We begin with observations on poly (N,N-dimethylacrylamide) (DMAA) physical gels reinforced with Laponite XLG nanoclay (NC). Samples are prepared by free-radical polymerization of N,N-dimethylacrylamide (DMAA) in an aqueous dispersion of nanoclay by using potassium peroxydisulfate  $\text{K}_2\text{S}_2\text{O}_8$  (KPS) as an initiator and tetramethylethylenediamine (TEMED) as a catalyst [39].

The experimental procedure involved: (i) drying of as-prepared samples (with  $\phi_p = 99$  g/L,  $\phi_f = 25.4$  g/L, and  $Q = 7.2$ ) down to various degrees of swelling  $Q_{\text{dry}}$  (in the range between 0.06 and 3.0), (ii) re-swelling of

dried samples to the initial degree of swelling  $Q$ , (iii) uniaxial tensile tests on dried–reswollen specimens. Mechanical tests were performed at room temperature with strain rate  $\dot{\epsilon} = 0.02 \text{ s}^{-1}$  ( $\epsilon = k - 1$  stands for engineering tensile strain) up to breakage of samples.

Experimental stress–strain diagrams are depicted in Figure 10.1 where engineering stress  $\sigma$  is plotted versus elongation ratio  $k$ . To reduce the number of material constants to be found by matching observations, we presume the response of the nanocomposite hydrogels to be merely elastic. By setting  $S = 0$  in Equation (10.66), we conclude that  $k_p = 1$  and each stress–strain curve is determined by three parameters  $G, J, X$ .

We begin with fitting observations on the as-prepared specimen for which Equation (10.68) is fulfilled. To find adjustable parameters  $G$  and  $J$ , we fix some interval  $[0, J^\circ]$ , where  $J$  is located, and divide this interval into  $I = 10$  sub-intervals by the points  $J^{(i)} = i\Delta J$  with  $\Delta J = J^\circ/I$  ( $i = 0, 1, \dots, I-1$ ). For each  $J^{(i)}$ , Equations (10.65), (10.66) are integrated numerically by the Runge–Kutta method with step  $\Delta t = 0.01$ . The modulus  $G$  is calculated by the least-squares technique from the condition of minimum of the function

$$F = \sum_n \left[ \sigma^{\text{exp}}(k_n) - \sigma^{\text{num}}(k_n) \right]^2,$$

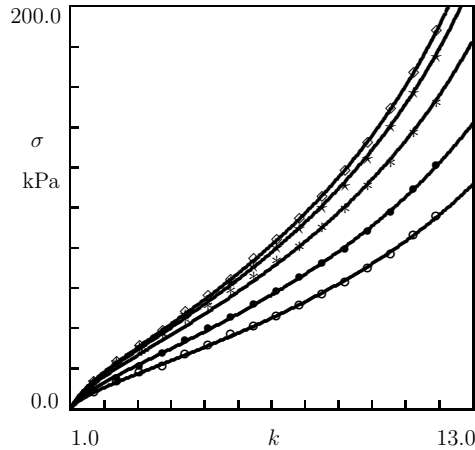


**Figure 10.1** Stress  $\sigma$  versus elongation ratio  $k$ . Symbols: experimental data in tensile tests on DMAA-NC hydrogel subjected to drying down to various  $Q_{\text{dry}}$  and subsequent re-swelling up to  $Q = 7.2$  ( $\circ$  – as-prepared;  $\bullet$  –  $Q_{\text{dry}} = 3.0$ ;  $*$  –  $Q_{\text{dry}} = 1.7$ ;  $\star$  –  $Q_{\text{dry}} = 0.8$ ;  $\diamond$  –  $Q_{\text{dry}} = 0.06$ ). Solid lines: results of simulation.

where summation is performed over all elongation ratios  $k_n$  at which the observations are reported,  $\sigma^{\text{exp}}$  stands for engineering stress measured in the test, and  $\sigma^{\text{num}}$  is given by Equation (10.65). The best-fit value of  $J$  is found from the condition of minimum of  $F$ . Afterwards, the initial interval is replaced with new interval  $[J - \Delta J, J + \Delta J]$ , and the calculations are repeated.

After finding the best-fit value  $G = 48.2$  kPa, we fix this quantity, and match observations on samples subjected to drying-reswelling by means of the above algorithm with adjustable parameters  $X$  and  $J$ . Given  $X$ , we calculate  $f$  from Equation (10.60) and plot  $f$  and  $J$  versus  $Q_{\text{dry}}$  in Figure 10.2. The data are approximated by the linear equations

$$f = f_0 + f_1 Q_{\text{dry}}, \quad J = J_0 + J_1 Q_{\text{dry}} \quad (10.69)$$

with coefficients calculated by the least-squares technique. Following [39], the strong (by twice) reduction in  $f$  induced by drying and re-swelling is attributed to rearrangement of the secondary network (a house-of-cards structure formed by clay platelets).

#### 10.4.2 As-Prepared Poly(Dimethylacrylamide)–Silica Hydrogels

We proceed with the analysis of observations on polydimethylacrylamide–silica (DMAA-Si) hydrogels manufactured by free-radical polymerization of N,N-dimethylacrylamide in aqueous suspensions of silica nanoparticles

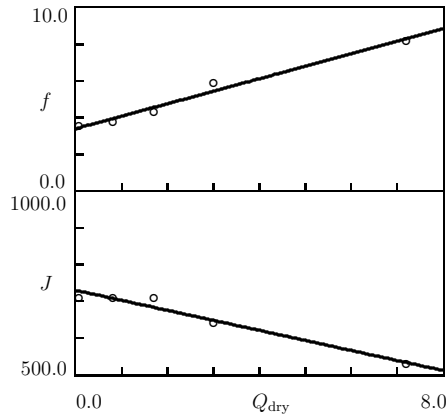


**Figure 10.2** Parameters  $f$  and  $J$  versus solvent content after drying  $Q_{\text{dry}}$ . Circles: treatment of observations on DMAA-NC hydrogels. Solid lines: approximation of the data by Equation (10.69).

(Si) by using KPS and TEMED as initiator and catalyst, respectively [40].

First, experimental data are matched in tensile tests with strain rate  $\dot{\epsilon} = 0.06 \text{ s}^{-1}$  at room temperature on as-prepared specimens with a fixed concentration of polymer network  $\phi_p = 142.2 \text{ g/L}$  and concentrations of nanoparticles  $\phi_f$  ranging from 71.4 to 710.5 g/L (Figure 10.3). According to Equation (10.68), their viscoplastic response is determined by four adjustable parameters  $G, J, R, S$ .

To find these quantities, we start with fitting observations on a specimen with  $\phi_f = 710.5 \text{ g/L}$  by using the above algorithm. After finding the best-fit values  $J = 28.0$  and  $S = 1.7$ , we fix these quantities and approximate experimental data on samples with  $\phi_f = 71.4, 142.7,$  and  $284.4 \text{ g/L}$  with the help of two parameters  $G, R$ .

The influence of concentration of solid phase on elastic moduli  $G$  and  $\tilde{G}$  (given  $R$ , the latter is determined from Equation (10.67)) is illustrated in Figure 10.4 where these quantities are plotted versus  $\phi_s$ . The data are approximated by the equations

$$G = G_0 + G_1\phi_s, \quad \tilde{G} = \tilde{G}_0 \tag{10.70}$$

with coefficients calculated by the least-squares technique. Figure 10.4 shows that  $G$  grows with concentration of silica particles, in agreement with

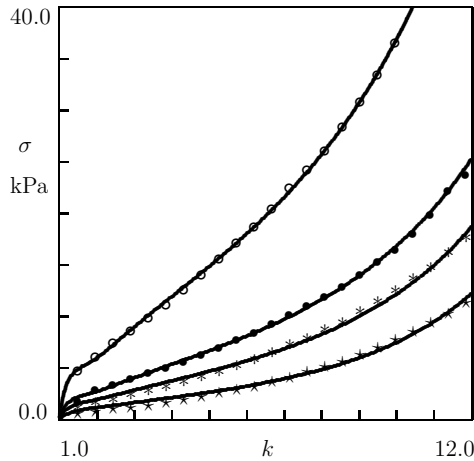


**Figure 10.3** Stress  $\sigma$  versus elongation ratio  $k$ . Symbols: experimental data in tensile tests on DMAA-Si hydrogels with  $\phi_p = 142 \text{ g/L}$  and various  $\phi_f \text{ g/L}$  ( $\circ$  – 710.5;  $\bullet$  – 284.4;  $*$  – 142.7;  $\times$  – 71.4). Solid lines: results of simulation.

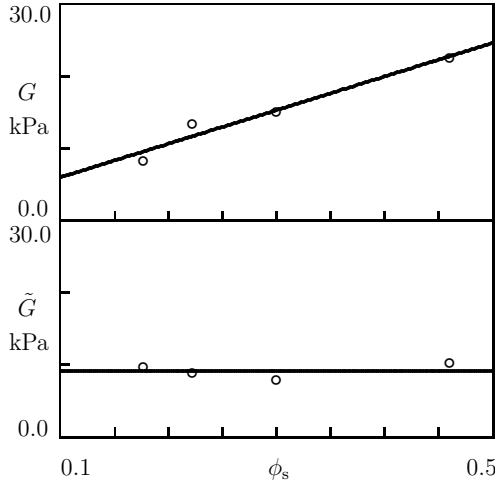


**Figure 10.4** Parameters  $G$  and  $\tilde{G}$  versus concentration of solid phase  $\phi_s$ . Circles: treatment of observations in tensile tests on DMAA-Si hydrogels with  $\phi_p = 142$  g/L and various  $\phi_f$  g/L. Solid lines: approximation of the data by Equation (10.70).

observations on other nanocomposite hydrogels [35], whereas  $\tilde{G}$  remains constant.

To assess plastic flow in nanocomposite hydrogels under tension, simulation of the stress–strain relations is conducted. Results of numerical analysis are reported in Figure 10.5. According to this figure, (i) nanocomposite hydrogels reveal pronounced plastic deformation (with plastic strains exceeding 100%), and (ii) elongation ratio for plastic deformation  $k_p$  decreases weakly with concentration of nanoparticles.

To evaluate the effect of strain rate on the mechanical response of nanocomposite hydrogels, observations are matched on specimens with a fixed concentration of polymer network  $\phi_p = 142.2$  g/L and concentrations of nanoparticles  $\phi_f = 142.7$  and  $\phi_f = 710.5$  g/L under tension with strain rates  $\dot{\epsilon} = 0.06$  and  $0.6$  s<sup>-1</sup>. Experimental data are depicted in Figure 10.6. Adjustable parameters are found by approximation of the experimental data with the help of the above algorithm. Each set of observations is fitted separately with the help of two parameters  $G$ ,  $R$ . The best-fit value of  $J$  and the values of  $S$  and  $R$  at strain rate  $\dot{\epsilon} = 0.06$  s<sup>-1</sup> are taken from Figure 10.4. The value of  $S$  at  $\dot{\epsilon} = 0.6$  s<sup>-1</sup> is calculated from Equation (10.67), whereas the value of  $R$  at this strain rate is determined by matching the stress–strain diagrams.

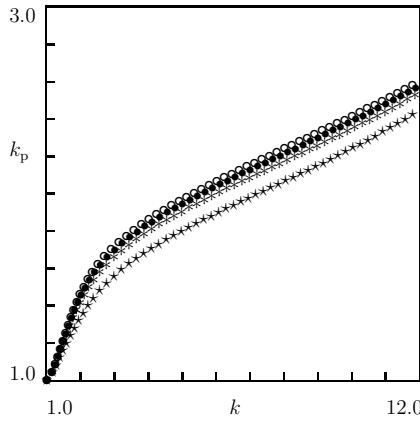


**Figure 10.5** Elongation ratio for plastic deformation  $k_p$  versus elongation ratio  $k$ . Symbols: results of simulation for tensile tests on DMAA-Si hydrogels with  $\phi_p = 142$  g/L and various  $\phi_f$  g/L ( $\circ - 710.5$ ;  $\bullet - 284.4$ ;  $* - 142.7$ ;  $\star - 71.4$ ).

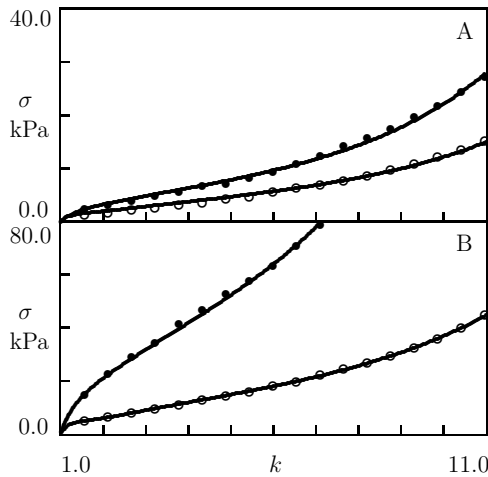


**Figure 10.6** Stress  $\sigma$  versus elongation ratio  $k$ . Symbols: experimental data in tensile tests with various strain rates  $\dot{\epsilon}$  s $^{-1}$  ( $\circ - 0.06$ ;  $\bullet - 0.6$ ) on DMAA-Si hydrogels with  $\phi_p = 142.2$  g/L and  $\phi_f = 142.7$  g/L (A),  $\phi_f = 710.5$  g/L (B). Solid lines: results of simulation.

Evolution of elastic moduli with strain rate  $\dot{\epsilon}$  is illustrated in Figure 10.7 where  $G$  and  $\tilde{G}$  are depicted versus duration of loading  $t' = (k_{\max} - 1)/\dot{\epsilon}$  with  $k_{\max} = 11$ . For comparison, observations in tensile relaxation tests with strain  $\epsilon = 0.5$  are also presented (in semi-logarithmic coordinates with  $\log = \log_{10}$ ). Following [40], relaxation curves are plotted in the form  $\tilde{\sigma}(t')$

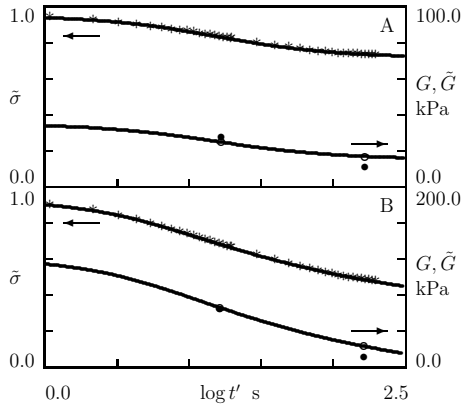


**Figure 10.7** Dimensionless stress  $\tilde{\sigma}$  (\*) versus relaxation time  $t'$  and moduli  $G$  ( $\circ$ ),  $\tilde{G}$  ( $\bullet$ ) versus loading time  $t'$ . Symbols: observations on DMAA-Si hydrogels with  $\phi_n = 142.2$  g/L,  $\phi_f = 142.7$  g/L (A), and  $\phi_f = 710.5$  g/L (B). Asterisks: experimental data in tensile relaxation test with strain  $\epsilon = 0.5$ . Circles: treatment of experimental data in tensile tests with strain rates  $\dot{\epsilon} = 0.06$  and  $0.6$  s $^{-1}$ . Solid lines: results of simulation.

with  $\tilde{\sigma} = \sigma/\sigma_0$  and  $t' = t - t_0$ , where  $t_0$  and  $\sigma_0$  stand for time and stress at the beginning of relaxation. The aim of Figure 10.7 (where observations in relaxation tests are approximated with a model proposed in [41]) is to demonstrate that alteration of elastic modulus  $G$  with strain rate found by fitting observations in tensile tests may be ascribed to the viscoelastic response of nanocomposite hydrogels (treated as rearrangement of chains in a transient network). The latter is disregarded in the constitutive model as its account leads to a substantial increase in the number of adjustable parameters.

To examine the influence of nanofiller on the viscoplastic behavior of DMAA-Si hydrogels under tensile cyclic deformation, we analyze observations reported in Figure 10.8. The experimental stress–strain diagrams are obtained on as-prepared specimens (with a fixed concentration of polymer network  $\phi_p = 142.2$  g/L and various concentrations of nanoparticles  $\phi_f = 142.7, 284.4, 710.5$  g/L) subjected to tension with a constant strain rate  $\dot{\epsilon} = 0.06$  s $^{-1}$  up to maximum elongation ratio  $k_{\max} = 6$  and retraction down to the zero minimum stress  $\sigma_{\min} = 0$ .

As the stress–strain curves under tension reported in Figure 10.8 differ from those depicted in Figure 10.3, we, first, apply the above algorithm (with  $R$  and  $S$  taken from the analysis of observations presented in Figure 10.3) to determine  $G$  and  $J$  under stretching, and afterwards, employ the same technique to find parameters  $K, R, S$  under retraction. The best-fit value  $K = 150.0$



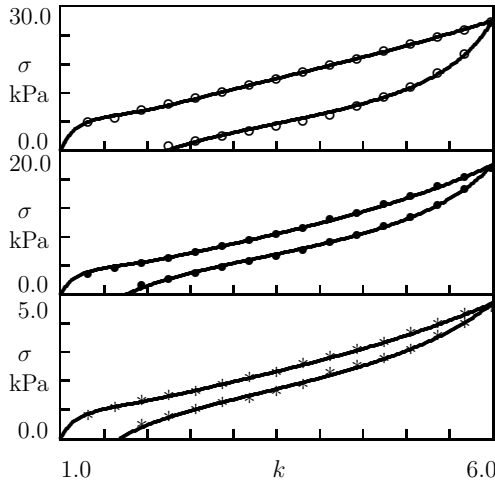


**Figure 10.8** Stress  $\sigma$  versus elongation ratio  $k$ . Symbols: experimental data in cyclic tests on DMAA-Si hydrogels with  $\phi_p = 142$  g/L and various  $\phi_f$  g/L ( $\circ - 710.5$ ;  $\bullet - 284.4$ ;  $* - 142.7$ ). Solid lines: results of simulation.

is found by matching observations on hydrogel with  $\phi_f = 710.5$  g/L and used without changes to approximate observations on other specimens. Numerical analysis shows that the best-fit values of  $J$  are slightly lower and the best-fit values of  $G$  are slightly higher than those found by matching observations in Figure 10.3.

The effect of concentration of solid phase  $\phi_s$  on coefficients  $\tilde{G}$  and  $S$  found by matching observations under retraction is illustrated in Figure 10.9. The data are approximated by the equations

$$\log \tilde{G} = \tilde{G}_0 - \tilde{G}_1 \phi_s, \quad \log S = S_0 + S_1 \phi_s, \quad (10.71)$$

with coefficients calculated by the least-squares method. Figure 10.9 shows that the energy of inter-chain interactions  $\tilde{G}$  decreases and rate of plastic deformation  $S$  increases with concentration of solid phase.

To examine the kinetics of plastic flow under cyclic loading, integration of the stress–strain relations is conducted with the adjustable parameters found by matching observations in Figure 10.8. Results of simulation are presented in Figure 10.10. The following conclusions are drawn: (i) under tension, plastic elongation ratio  $k_p$  increases monotonically with  $k$  and remains practically independent of clay content (in agreement with the data reported in Figure 10.5), (ii) under retraction,  $k_p$  grows pronouncedly at the initial

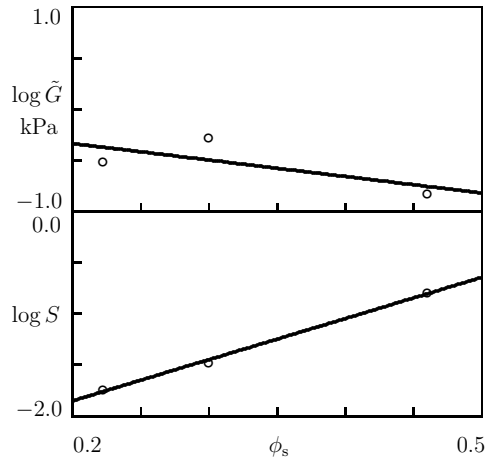


**Figure 10.9** Parameters  $\tilde{G}$  and  $S$  versus concentration of solid phase  $\phi_s$ . Circles: treatment of observations under retraction in cyclic tests on DMAA-Si hydrogels with  $\phi_p = 142$  g/L and various  $\phi_f$  g/L. Solid lines: approximation of the data by Equation (10.71).

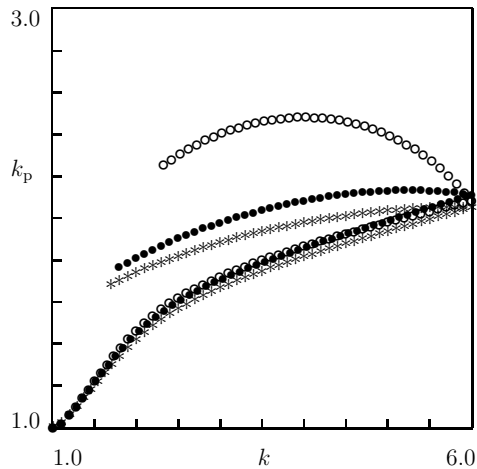


**Figure 10.10** Elongation ratio for plastic deformation  $k_p$  versus elongation ratio  $k$ . Symbols: results of simulation for cyclic tests on DMAA-Si hydrogels with  $\phi_p = 142$  g/L and various  $\phi_f$  g/L ( $\circ$  – 710.5;  $\bullet$  – 284.4;  $*$  – 142.7).

stage of unloading (when  $k$  remains in the vicinity of  $k_{\max}$ ), reaches its maximum (plastic overshoot), and decreases afterwards, (iii) intensity of plastic overshoot ( $k_{p \max}$ ) and residual strain ( $k_p$  at the instant when  $\sigma$  vanishes) increase strongly (by twice) with nanoclay content.

### 10.4.3 As-Prepared Polyacrylamide–Clay Hydrogels

To verify the above conclusions regarding the influence of strain rate and nanofiller content on the viscoplastic response of nanocomposite hydrogels, experimental data are approximated on polyacrylamide–nanoclay (PAM-NC) hydrogels manufactured by free-radical polymerization of acrylamide (AM) monomers in aqueous suspensions of hectorite nanoclay (NC) Laponite RD by using KPS and TEMED as initiator and catalyst, respectively [42].

First, we approximate observations on as-prepared samples with various concentrations of polymer network  $\phi_p$  and filler  $\phi_f$  in tensile tests with strain rates  $\dot{\epsilon} = 0.083, 0.83, \text{ and } 1.67 \text{ s}^{-1}$  at room temperature. Experimental data are presented in Figures 11–13 for nanocomposite hydrogels with  $\phi_p = 200 \text{ g/L}$ ,  $\phi_f = 20 \text{ g/L}$ ,  $\phi_p = 250 \text{ g/L}$ ,  $\phi_f = 20 \text{ g/L}$ , and  $\phi_p = 100 \text{ g/L}$ ,  $\phi_f = 40 \text{ g/L}$ .

For each concentration of polymer and filler, we start with matching observations under tension with the highest strain rate  $\dot{\epsilon} = 1.67 \text{ s}^{-1}$ , and determine parameters  $G, J, R, S$  by means of the above algorithm. Afterwards, we fix the best-fit value of  $J$  and approximate the other stress–strain diagrams with the help of three parameters  $G, S, R$ .

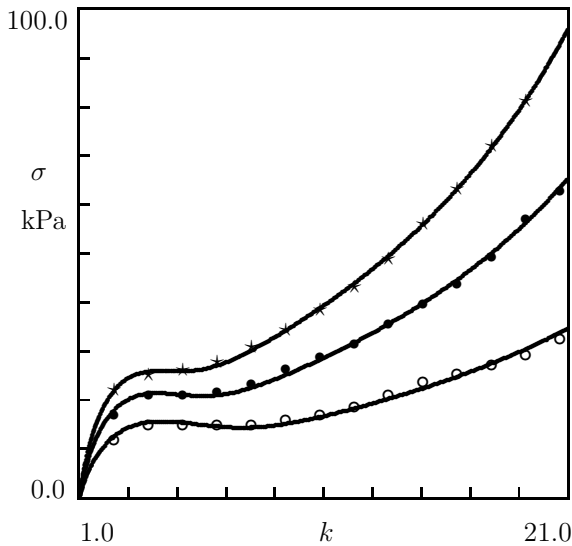


**Figure 10.11** Stress  $\sigma$  versus elongation ratio  $k$ . Symbols: observations in tensile tests with various strain rates  $\dot{\epsilon} \text{ s}^{-1}$  on PAM-NC hydrogels with  $\phi_p = 200 \text{ g/L}$  and  $\phi_f = 20 \text{ g/L}$  ( $\circ - \dot{\epsilon} = 0.083$ ;  $\bullet - \dot{\epsilon} = 0.83$ ;  $\star - \dot{\epsilon} = 1.67$ ). Solid lines: results of simulation.

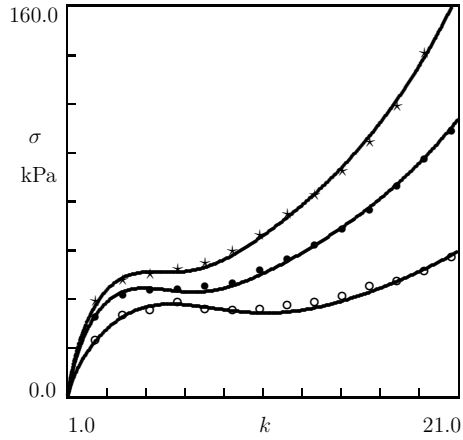


**Figure 10.12** Stress  $\sigma$  versus elongation ratio  $k$ . Symbols: observations in tensile tests with various strain rates  $\dot{\epsilon}$   $\text{s}^{-1}$  on PAM-NC hydrogel with  $\phi_p = 250$  g/L and  $\phi_f = 20$  g/L ( $\circ - \dot{\epsilon} = 0.083$ ;  $\bullet - \dot{\epsilon} = 0.83$ ;  $\star - \dot{\epsilon} = 1.67$ ). Solid lines: results of simulation.

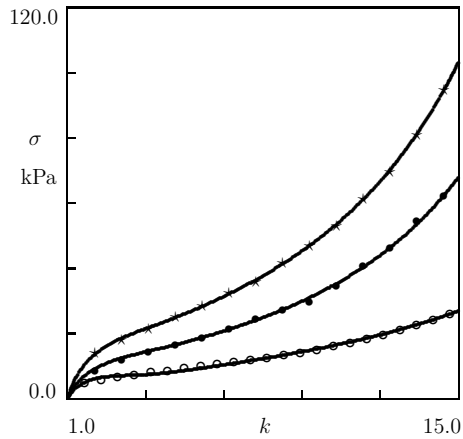


**Figure 10.13** Stress  $\sigma$  versus elongation ratio  $k$ . Symbols: observations in tensile tests with various strain rates  $\dot{\epsilon}$   $\text{s}^{-1}$  on PAM-NC hydrogel with  $\phi_p = 100$  g/L and  $\phi_f = 40$  g/L ( $\circ - \dot{\epsilon} = 0.083$ ;  $\bullet - \dot{\epsilon} = 0.83$ ;  $\star - \dot{\epsilon} = 1.67$ ). Solid lines: results of simulation.

The effect of strain rate  $\dot{\epsilon}$  on elastic modulus  $G$  is illustrated in Figure 10.14 where  $G$  is plotted versus duration of loading  $t' = (k_{\max} - 1)/\dot{\epsilon}$ . For comparison, experimental data in shear relaxation tests with small strain  $\epsilon = 0.005$  are also presented (as observations in relaxation tests on specimens with  $\phi_p = 200$  g/L,  $\phi_f = 20$  g/L were not reported in [42], we replace

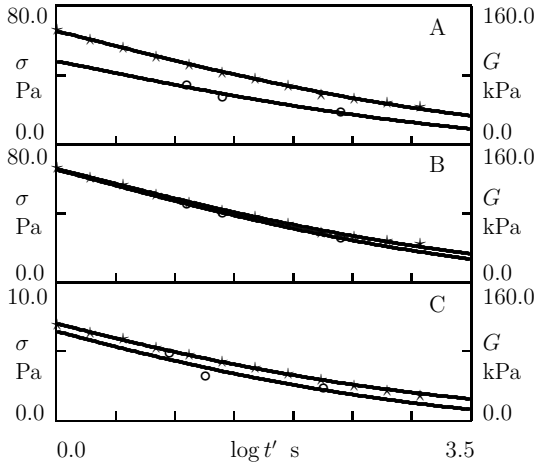


**Figure 10.14** Dimensionless stress  $\tilde{\sigma}$  ( $*$ ) versus relaxation time  $t'$  and modulus  $G$  versus loading time  $t'$ . Symbols: observations on PAM-NC hydrogels with  $\phi_p = 200$  g/L,  $\phi_f = 20$  g/L (A),  $\phi_p = 250$  g/L,  $\phi_f = 20$  g/L (B),  $\phi_p = 100$  g/L,  $\phi_f = 40$  g/L (C). Stars: experimental data in tensile relaxation test with strain  $\epsilon = 0.005$ . Circles: treatment of experimental data in tensile tests with various strain rates. Solid lines: results of simulation.

them with those on samples with  $\phi_p = 250$  g/L,  $\phi_f = 20$  g/L). According to Figure 10.14, an increase in elastic modulus with strain rate revealed by fitting observations in tensile tests may be attributed to the viscoelastic response of hydrogels (in agreement with the conclusion drawn from Figure 10.7).

To assess the influence of strain rate on the viscoplastic flow, parameter  $S$  is plotted versus  $\dot{\epsilon}$  in Figure 10.15. The data are approximated by the equation

$$\log S = S_0 + S_1 \log \dot{\epsilon}, \quad (10.72)$$

where the coefficients are calculated by the least-squares technique. Equation (10.72) demonstrates that  $S$  increases monotonically with  $\dot{\epsilon}$ , but the rate of growth is strongly sub-linear:  $S \sim \dot{\epsilon}^\beta$  with  $\beta \approx 0.2$ .

Given  $G$  and  $R$ , we calculate  $\tilde{G}$  from Equation (10.67) and plot this quantity versus strain rate  $\dot{\epsilon}$  in Figure 10.16. The data are approximated by the equation

$$\log \tilde{G} = \tilde{G}_0 + \tilde{G}_1 \log \dot{\epsilon} \quad (10.73)$$

with coefficients calculated by the least-squares technique. Figure 10.16 demonstrates a pronounced difference between PAM-NC hydrogels (for which  $\tilde{G}$  increases strongly with strain rate) and DMAA-Si hydrogels (for which this parameter is independent of  $\dot{\epsilon}$ ).

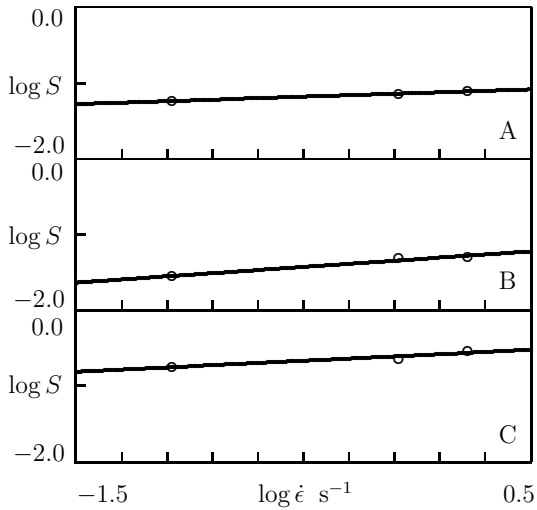


**Figure 10.15** Parameter  $S$  versus strain rate  $\dot{\epsilon}$ . Circles: treatment of observations in tensile tests on PAM-NC hydrogels with  $\phi_p = 200$  g/L,  $\phi_f = 20$  g/L (A),  $\phi_p = 250$  g/L,  $\phi_f = 20$  g/L (B),  $\phi_p = 100$  g/L,  $\phi_f = 40$  g/L (C). Solid lines: approximation of the data by Equation (10.72).

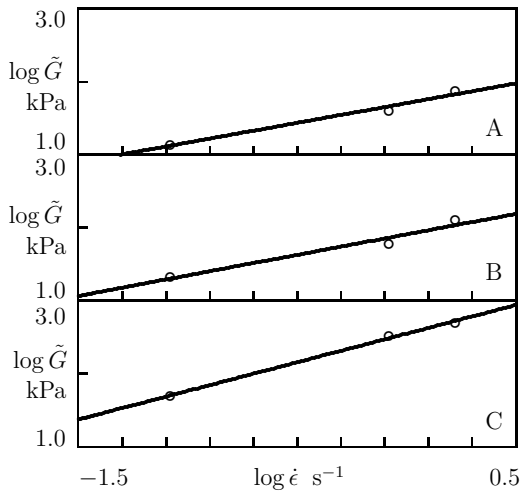


**Figure 10.16** Parameter  $\tilde{G}$  versus strain rate  $\dot{\epsilon}$ . Circles: treatment of observations in tensile tests on PAM-NC hydrogels with  $\phi_p = 200$  g/L,  $\phi_f = 20$  g/L (A),  $\phi_p = 250$  g/L,  $\phi_f = 20$  g/L (B),  $\phi_p = 100$  g/L,  $\phi_f = 40$  g/L (C). Solid lines: approximation of the data by Equation (10.73).

To examine the effect of concentration of solid phase  $\phi_s$  on the mechanical response of nanocomposite hydrogels under cyclic loading, we approximate stress–strain curves under tension with constant strain rate  $\dot{\epsilon} = 0.083 \text{ s}^{-1}$  up to maximum elongation ratio  $k_{\max} = 17$  followed by retraction with the same strain rate down to the zero minimum stress  $\sigma_{\min} = 0$ . Observations on specimens with  $\phi_f = 20 \text{ g/L}$ ,  $\phi_p = 200$  and  $250 \text{ g/L}$  are reported in Figure 10.17, and those on samples with  $\phi_p = 100 \text{ g/L}$ ,  $\phi_f = 30$  and  $40 \text{ g/L}$  are presented in Figure 10.18 together with results of simulation. Adjustable parameters in the stress–strain relations are found by fitting each set of data separately by means of the same algorithm that was employed to match observations in Figure 10.8. As the stress–strain diagrams under tension in Figures 10.17, 10.18 differ from those reported in Figures 10.11–10.13, they are approximated by using four parameters  $G, J, S, R$ . Afterwards, unloading paths of the stress–strain curves are fitted with the help of three coefficients  $K, S, R$ .

Adjustable parameters determined by matching observations under tension and retraction are reported in Figures 10.19, 10.20, where they are plotted versus concentration of solid phase  $\phi_s$ . The data are approximated by the equations

$$\log G = G_0 + G_1 \phi_s, \quad \log \tilde{G} = \tilde{G}_0 + \tilde{G}_1 \phi_s, \quad \log S = S_0 + S_1 \phi_s,$$

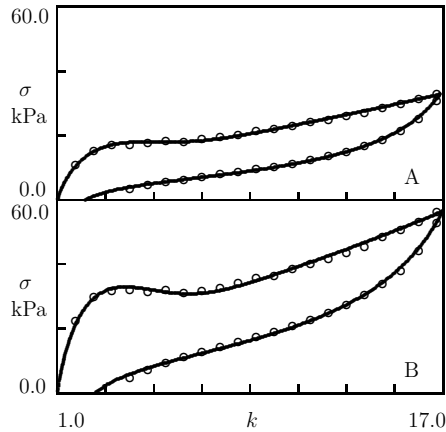


**Figure 10.17** Stress  $\sigma$  versus elongation ratio  $k$ . Circles: experimental data in cyclic tensile tests on PAM-NC hydrogels with  $\phi_f = 20 \text{ g/L}$  and  $\phi_p = 200 \text{ g/L}$  (A),  $\phi_p = 250 \text{ g/L}$  (B). Solid lines: results of simulation.

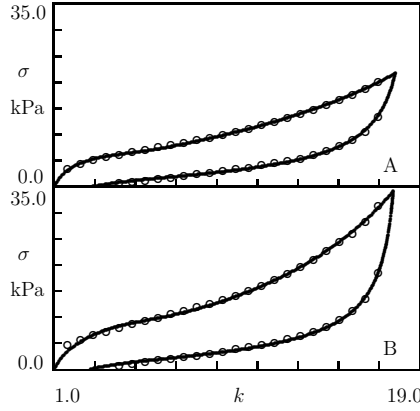


**Figure 10.18** Stress  $\sigma$  versus elongation ratio  $k$ . Circles: experimental data in cyclic tests on PAM-NC hydrogels with  $\phi_n = 100$  g/L and  $\phi_f = 30$  g/L (A),  $\phi_f = 40$  g/L (B). Solid lines: results of simulation.

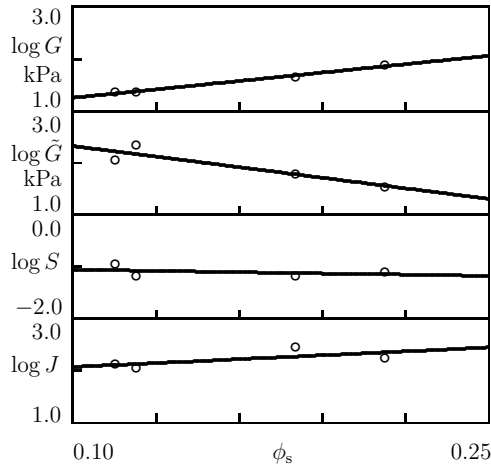


**Figure 10.19** Parameters  $G, \tilde{G}, S, J$  versus concentration of solid phase  $\phi_s$ . Circles: treatment of observations under tension in cyclic tests on PAM-NC hydrogels. Solid lines: approximation of the data by Equation (10.74).

$$\log J = J_0 + J_1\phi_s \quad (10.74)$$

under tension and

$$\log \tilde{G} = \tilde{G}_0 + \tilde{G}_1\phi_s, \quad \log S = S_0 + S_1\phi_s, \quad \log K = K_0 + K_1\phi_s \quad (10.75)$$



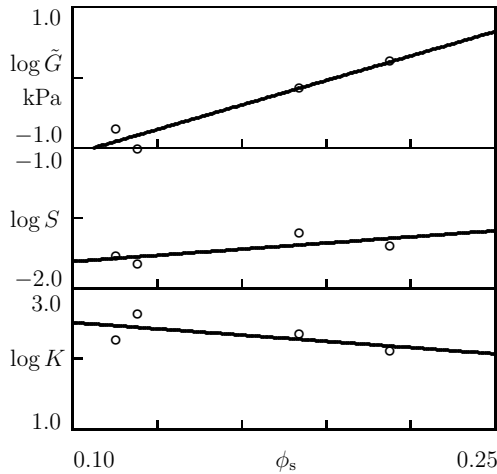


**Figure 10.20** Parameters  $\tilde{G}$ ,  $S$ ,  $K$  versus concentration of solid phase  $\phi_s$ . Circles: treatment of observations under retraction in cyclic tests on PAM-NC hydrogels. Solid lines: approximation of the data by Equation (10.75).

under retraction. The coefficients in Equations (10.74), (10.75) are calculated by the least-squares method.

To examine how concentrations of polymer and filler,  $\phi_p$  and  $\phi_f$ , affect plastic flow in PAM-NC hydrogels under cyclic deformations, numerical integration of the stress–strain relations is performed for cyclic loading with strain rate  $\dot{\epsilon} = 0.083 \text{ s}^{-1}$ , maximum elongation ratio under stretching  $k_{\max} = 17$ , and the zero minimum stress under retraction. Results of simulation are reported in Figure 10.21. The following conclusions are drawn: (i) the dependency  $k_p(k)$  for PAM-NC hydrogels is qualitatively similar to that for DMAA-Si hydrogels (elongation ratio for plastic deformation increases under tension and reveals a pronounced overshoot under retraction), (ii) given  $\phi_f$ , an increase in polymer concentration  $\phi_p$  results in a modest increase in  $k_p$  under tension and retraction, whereas (iii) given  $\phi_p$ , an increase in nanoclay concentration  $\phi_f$  induces a decay in plastic deformation.

#### 10.4.4 Discussion

Figures 10.1, 10.3, 10.6, 10.11–10.13 demonstrate ability of the constitutive model with four adjustable parameters  $G$ ,  $J$ ,  $R$ ,  $S$  to describe stress–strain diagrams under uniaxial tension with finite deformations (elongation ratios up to 20).

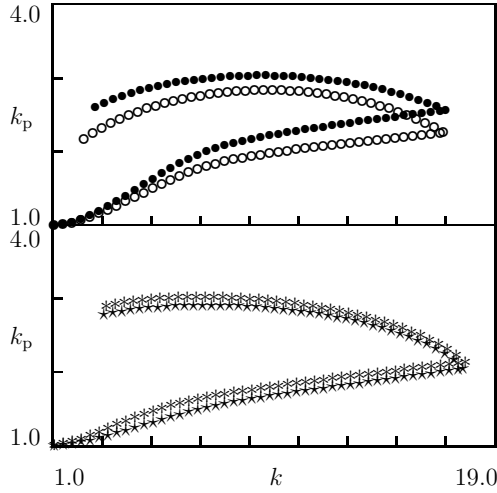


**Figure 10.21** Elongation ratio for plastic deformation  $k_p$  versus elongation ratio  $k$ . Symbols: results of simulation for cyclic tests on PAM-NC hydrogels ( $\circ - \phi_p = 200$  g/L,  $\phi_f = 20$  g/L;  $\bullet - \phi_p = 250$  g/L,  $\phi_f = 20$  g/L;  $* - \phi_p = 100$  g/L,  $\phi_f = 30$  g/L;  $\star - \phi_p = 100$  g/L,  $\phi_f = 40$  g/L).

Figures 10.8, 10.17, 10.18 show good agreement between observations in cyclic (loading–unloading) tests and results of simulation based on the constitutive equations that involve three additional parameters for retraction  $R$ ,  $S$ , and  $K$ .

According to Figures 10.4, 10.9, 10.19, 10.20, phenomenological Equations (10.70), (10.71), (10.74), (10.75) describe correctly evolution of adjustable parameters with concentration of solid phase (which means that  $\phi_s$  may serve as the only parameter characterizing mechanical properties of nanocomposite hydrogels).

Figures 10.15, 10.16 reveal that Equations (10.72), (10.73) predict adequately the effect of strain rate  $\dot{\epsilon}$  on parameters  $\tilde{G}$  and  $S$ .

An advantage of the constitutive equations is that they involve a relatively small number of material constants, on the one hand, and describe correctly experimental data in cyclic tensile tests, on the other. A shortcoming of the model is that it disregards viscoelastic properties of nanocomposite hydrogels. As a result, the elastic modulus is allowed to alter with strain rate in the fitting procedure. Although these changes are confirmed by comparison with observations in relaxation tests (Figures 10.7 and 10.14), they restrict applicability of the model to deformation processes with constant strain rates. To describe

time-dependent phenomena in nanocomposite hydrogels, rearrangement of the networks of flexible chains and nanoparticles should be modeled explicitly (the latter leads, however, to a noticeable increase in the number of material constants).

Comparison of experimental data under cyclic deformation with results of numerical simulation demonstrates that elongation ratio for plastic deformation  $k_p$  grows monotonically under tension and reveals a non-monotonic behavior under retraction:  $k_p$  increases, reaches its maximum value (plastic overshoot), and decreases afterwards (Figures 10.10 and 10.21). Intensity of the overshoot increases with concentration of solid phase, but the rate of its growth depends strongly on type of nanofiller.

## 10.5 Concluding Remarks

A constitutive model is developed in finite viscoplasticity of nanocomposite hydrogels under an arbitrary deformation with finite strains. A hydrogel is treated as a two-phase medium composed of a solid phase (polymer network reinforced with nanoparticles) and a fluid phase (solvent). Transport of solvent through a hydrogel is treated as its diffusion governed by the gradient of chemical potential.

Constitutive equations are derived by means of the free-energy imbalance equation. The free energy of a nanocomposite hydrogel equals the sum of strain energy density of the solid phase and the energy of mixing of the solid phase with solvent.

The solid phase is modeled as an isotropic compressible viscoplastic medium, whose deformation gradient is split into the product of deformation gradients for elastic deformation, plastic deformation, and deformation induced by swelling (characterized by the coefficient of inflation of the polymer network). Strain energy density of the solid phase equals the sum of the stored mechanical energy and the energy of interaction between chains and nanoparticles.

The constitutive equations involve (i) stress–strain relation, (ii) flow rule for plastic deformation, and (iii) diffusion equation for solvent. These relations are accompanied by equations for mechanical equilibrium and appropriate boundary conditions.

The model is applied to the analysis of rapid deformation (the rate of loading exceeds strongly the rate of solvent diffusion) of (i) nanocomposite hydrogels subjected to drying and subsequent re-swelling, and (ii) as-prepared nanocomposite hydrogels.

Analysis of observations in uniaxial tensile tests on nanocomposite hydrogels subjected to drying and reswelling demonstrates that the constitutive equations describe adequately the effect of rearrangement of the secondary network of clay platelets under drying on the mechanical response of reswollen gels (Figure 10.1). The effect of drying–reswelling can be accounted for with the help of the only parameter that changes consistently with solvent content (Figure 10.2).

Approximation of observations in uniaxial tensile tests and tensile cyclic tests on as-prepared nanocomposite hydrogels reinforced with Si particles and clay platelets shows that the constitutive equations with four adjustable parameters under stretching and three more parameters under retraction describe correctly the experimental stress–strain diagrams and predict characteristic features of plastic flow (in particular, plastic overshoot under retraction).

## 10.6 Acknowledgement

Financial support by the EU Commission through Project Evolution-314744 is gratefully acknowledged.

## References

- [1] Naficy, S., Brown, H.R., Razal, J.M., Spinks, G.M., Whitten, P.G., ‘Progress toward robust polymer hydrogels’, *Australian J. Chem.*, 64, 1007–1025, 2011.
- [2] Haque, M.A., Kurokawa, T., Kamita, G., Gong, J.P., ‘Lamellar bilayers as reversible sacrificial bonds to toughen hydrogel: hysteresis, self-recovery, fatigue resistance, and crack blunting’, *Macromolecules*, 44, 8916–8924, 2011.
- [3] Schexnailder P., Schmidt, G., ‘Nanocomposite polymer hydrogels’, *Colloid Polym. Sci.*, 287, 1–11, 2009.
- [4] Haraguchi, K., ‘Stimuli-responsive nanocomposite gels’, *Colloid Polym. Sci.*, 289, 455–473, 2011.
- [5] Deligkaris, K., Tadele, T.S., Olthuis, W., van den Berg, A., ‘Hydrogel-based devices for biomedical applications’, *Sensors Actuators B*, 147, 765–774, 2010.
- [6] Messing, R., Schmidt, A.M., ‘Perspectives for the mechanical manipulation of hybrid hydrogels’, *Polym. Chem.*, 2, 18–32, 2011.

- [7] Buenger, D., Topuz, F., Groll, J., ‘Hydrogels in sensing applications’, *Progr. Polym. Sci.*, 37, 1678–1719, 2012.
- [8] Qian, Z.-Y., Fu, S.-Z., Feng, S.-S., ‘Nanohydrogels as a prospective member of the nanomedicine family’, *Nanomedicine*, 8, 161–164, 2013.
- [9] Higuchi, A., Ling, Q.-D., Chang, Y., Hsu, S.-T., Umezawa, A., ‘Physical cues of biomaterials guide stem cell differentiation fate’, *Chem. Rev.*, 113, 3297–3328, 2013.
- [10] Discher, D.E., Mooney, D.J., Zandstra, P.W., ‘Growth factors, matrices, and forces combine and control stem cells’, *Science*, 324, 1673–1677, 2009.
- [11] Song, M.J., Dean, D., Knothe Tate, M.L., ‘Mechanical modulation of nascent stem cell lineage commitment in tissue engineering scaffolds’, *Biomaterials*, 34, 5766–5775, 2013.
- [12] Pelaez, D., Huang, C.-Y.C., Cheung, H.S., ‘Cyclic compression maintains viability and induces chondrogenesis of human mesenchymal stem cells in fibrin gel scaffolds’, *Stem Cells Develop.*, 18, 93–102, 2009.
- [13] Meyer, E.G., Buckley, C.T., Steward, A.J., Kelly, D.J., ‘The effect of cyclic hydrostatic pressure on the functional development of cartilaginous tissues engineered using bone marrow derived mesenchymal stem cells’, *J. Mech. Behav. Biomed. Mater.*, 4, 1257–1265, 2011.
- [14] Hong, W., Zhao, X., Zhou, J., Suo, Z., ‘A theory of coupled diffusion and large deformation in polymeric gels’, *J. Mech. Phys. Solids*, 56, 1779–1793, 2008.
- [15] Hong, W., Liu, Z., Suo, Z., ‘Inhomogeneous swelling of a gel in equilibrium with a solvent and mechanical load’, *Int. J. Solids Struct.*, 46, 3282–3289, 2009.
- [16] Duda, F.P., Souza, A.C., Fried, E., ‘A theory for species migration in finitely strained solid with application to polymer network swelling’, *J. Mech. Phys. Solids*, 58, 515–529, 2010.
- [17] Chester, S.A., Anand, L., ‘A coupled theory of fluid permeation and large deformations for elastomeric materials’, *J. Mech. Phys. Solids*, 58, 1879–1906, 2010.
- [18] Baek, S., Pence, T.J., ‘Inhomogeneous deformation of elastomer gels in equilibrium under saturated and unsaturated conditions’, *J. Mech. Phys. Solids*, 59, 561–582, 2011.
- [19] Yan, H., Jin, B., ‘Influence of microstructural parameters on mechanical behavior of polymer gels’, *Int. J. Solids Struct.*, 49, 436–444, 2012.

- [20] Drozdov, A.D., Christiansen, J.deC., 'Constitutive equations in finite elasticity of swollen elastomers', *Int. J. Solids Struct.*, 50, 1494–1504, 2013.
- [21] Drozdov, A.D., Christiansen, J.deC., 'Stress–strain relations for hydrogels under multiaxial deformation', *Int. J. Solids Struct.*, 50, 3570–3585, 2013.
- [22] Lucantonio, A., Nardinocchi, P., Teresi, L., 'Transient analysis of swelling-induced large deformations in polymer gels', *J. Mech. Phys. Solids*, 61, 205–218, 2013.
- [23] Zhao, X., Huebsch, N., Mooney, D.J., Suo, Z., 'Stress–relaxation behavior in gels with ionic and covalent crosslinks', *J. Appl. Phys.*, 107, 063509, 2010.
- [24] Chester, S.A., 'A constitutive model for coupled fluid permeation and large viscoelastic deformation in polymeric gels', *Soft Matter*, 8, 8223–8233, 2012.
- [25] Wang, X., Hong, W., 'A visco-poroelastic theory of polymeric gels', *Proc. Roy. Soc. A*, 468, 3824–3841, 2012.
- [26] Strange, D.G.T., Fletcher, T.L., Tonsomboon, K., Brawn, H., Zhao, X., Oyen, M.L., 'Separating poroviscoelastic deformation mechanisms in hydrogels', *Appl. Phys. Lett.*, 102, 031913, 2013.
- [27] Baumberger, T., Caroli, C., Martina, D., 'Solvent control of crack dynamics in a reversible hydrogel', *Nature Mater.*, 5, 552–555, 2006.
- [28] Seitz, M.E., Martina, D., Baumberger, T., Krishnan, V.R., Hui, C.-Y., Shull, K.R., 'Fracture and large strain behavior of self-assembled triblock copolymer gels', *Soft Matter*, 5, 447–456, 2009.
- [29] Kundu, S., Crosby, A.J., 'Cavitation and fracture behavior of polyacrylamide hydrogels', *Soft Matter*, 5, 3963–3968, 2009.
- [30] Wang, X., Hong, W., 'Delayed fracture in gels', *Soft Matter*, 8, 8171–8178, 2012.
- [31] Zhang, J., An, Y., Yazzie, K., Chawla, N., Jiang, H., 'Finite element simulation of swelling-induced crack healing in gels', *Soft Matter*, 8, 8107–8112, 2012.
- [32] Korchagin, V., Dowbow, J., Stepp, D., 'A theory of amorphous viscoelastic solids undergoing finite deformations with application to hydrogels', *Int. J. Solids Struct.*, 44, 3973–3997, 2007.
- [33] Wang, X., Hong, W., 'Pseudo-elasticity of a double network gel', *Soft Matter*, 7, 8576–8581, 2011.
- [34] Zhao, X., 'A theory for large deformation and damage of interpenetrating polymer networks', *J. Mech. Phys. Solids*, 60, 319–332, 2012.

- [35] Haraguchi, K., Li, H.-J., 'Mechanical properties and structure of polymer–clay nanocomposite gels with high clay content', *Macromolecules*, 39, 1989–1905, 2006.
- [36] Bakarich, S.E., Pidcock, G.C., Balding, P., Stevens, L., Calvert, P., in het Panhuis, M., 'Recovery from applied strain in interpenetrating polymer network hydrogels with ionic and covalent cross-links', *Soft Matter*, 8, 9985–9988, 2012.
- [37] Gent, A.N., 'A new constitutive relation for rubber', *Rubber Chem. Technol.*, 69, 59–61, 1996.
- [38] Wall, F.T., Flory, P.J., 'Statistical thermodynamics of rubber elasticity', *J. Chem. Phys.*, 19, 1435–1439, 1951.
- [39] Haraguchi, K., Li, H.-J., Ren, H.-J., Zhu, M., 'Modification of nanocomposite gels by irreversible rearrangement of polymer/clay network structure through drying', *Macromolecules*, 43, 9848–9853, 2010.
- [40] Carlsson, L., Rose, S., Hourdet, D., Marcellan, A., 'Nano-hybrid self-crosslinked PDMA/ silica hydrogels', *Soft Matter*, 6, 3619–3631, 2010.
- [41] Drozdov, A.D., Christiansen, J.deC., 'Thermo-viscoelastic and viscoplastic behavior of high-density polyethylene', *Int. J. Solids Struct.*, 45, 4274–4288, 2008.
- [42] Xiong, L., Hu, X., Liu, X., Tong, Z., 'Network chain density and relaxation of in situ synthesized polyacrylamide/hectorite clay nanocomposite hydrogels with ultrahigh tensibility', *Polymer*, 49, 5064–5071, 2008.

## **Regulatory Issues in Developing Advanced Therapy Medicinal Products with Stem Cells in Europe**

---

**Maria Cristina Galli, B.Sc., Ph.D.**

Department of Cell Biology and Neurosciences,  
Istituto Superiore di Sanità Roma, Italy

Corresponding author: Maria Cristina Galli <mariacristina.galli@iss.it>

Author is currently co-chair of the ATMP platform in the European infrastructure for translational medicine EATRIS-ERIC.

The views expressed in this article are author's personal views and may not be understood or quoted as being made on behalf of or reflecting the position of EMA or AIFA.

### **11.1 Introduction**

This chapter discusses European requirements for development of Advanced Therapy Medicinal Products (ATMP) based on stem cells, describing the framework for clinical trials and for marketing authorization, as well as the critical issues and challenges for developing stem cell-based ATMP.

The recent advances of biotechnologies have opened new promising perspectives for the development of ATMP, including stem cell therapy and regenerative medicine, which may potentially have a great beneficial impact on many human diseases, including among others cancer, degenerative and genetic diseases.

ATMP are based on the cutting-edge progress of biomedical research and on the use of novel and sophisticated technologies progressively aiming at patient-tailored interventions.



ATMP comprise a variety of novel therapeutic strategies, including Cell Therapy, Gene Therapy and Tissue Engineered Medicinal Products (CTMP, GTMP, TEP, respectively).

In Europe, as in most countries in the world, ATMP are considered as medicines, therefore they are covered by the pharmaceutical legislation.

## **11.2 European Regulatory Frame for ATMP**

ATMP are covered by the European legal frame for medicinal products through the EU Regulation 1394/2007 [1]. The current EU definition of GTMP and of CTMP is contained in the new Annex 1 that has been recently issued amending Directive 2001/83/EC [2], while the definition of TEP as well as of combined ATMP is contained in the EU Regulation 1394/2007.

GTMP are defined as those biological medicinal products that contain or consist of a recombinant nucleic acid used in or administered to human beings with a view to regulating, repairing, replacing, adding or deleting a genetic sequence; in addition, their therapeutic, prophylactic or diagnostic effects relate directly to the recombinant nucleic acid sequence they contain, or to the product of genetic expression of that sequence. Therefore, medicinal products such as viral or non viral vectors, plasmid or bacterial vectors, recombinant oncolytic viruses, genetically modified cells, cancer immunotherapeutics (so called “cancer vaccines”) are considered GTMP if they fulfil the current definition. It should be noted that, according to new Annex 1, vaccines for infectious diseases are no longer considered GTMP [2].

Somatic CTMP are defined as those biological medicinal products that: i) contain or consist of cells or tissues that have been subject to substantial manipulation so that their biological characteristics, physiological functions or structural properties relevant for the intended clinical use have been altered, or ii) contain or consist of cells or tissues that are not intended to be used for the same essential function(s) in the recipient and the donor, and iii) are presented as having properties for, or are used in or administered to human beings with a view to treating, preventing or diagnosing a disease through the pharmacological, immunological or metabolic action of its cells or tissues [2].

TEP are defined as those biological medicinal products that contain or consist of engineered cells or tissues; and are presented as having properties for, or are used in or administered to humans with a view of regenerating, repairing or replacing a human tissue. Cells/tissues shall be considered ‘engineered’ if they have been subject to substantial manipulation or are not

intended to be used for the same essential function(s) in the recipient and the donor [3].

Medicinal products for stem cell therapy and regenerative medicine are considered as CTMP or TEP, whereas if genetically modified they are considered as GTMP.

ATMP may also contain a medical device (MD), such as e.g. biomaterials, scaffolds, matrices. In this case, EU Regulation 1394/2007 stipulates that the combination of ATMP and MD is defined as combined ATMP and that it is handled completely under the pharmaceutical legislation. Therefore, while MD directives are applicable to the MD before it is put in the combination, the whole combined ATMP shall be subject to EMA evaluation. Any type of MD that is present in the combination shall meet the MD essential requirements; the dossier for market authorization application of the combined ATMP shall include description of MD physical characteristics, performance and design methods, as well as evidence of conformity and, where available, results of assessment by a Notified Body [4].

Through EU Regulation 1394/2007, ATMP are within the frame of EU Regulation 726/2004 according to which no medicinal product can be marketed in Europe without an approval. For biological medicines, EU-wide market authorization is granted or denied by the European Commission through the centralised procedure taking place at the European Medicine Agency (EMA) [5]. In addition to those Regulations, the main EU regulatory framework for ATMP includes also Directive 2001/20/EC regulating clinical trials [6].

In the EU Regulation 1394/2007 a specific Committee for Advanced Therapy (CAT) is created. CAT covers the scientific areas relevant to ATMP, including gene therapy, cell therapy, tissue engineering, MD, biotechnology, surgery, pharmacovigilance, risk management, ethics.

CAT is responsible for ATMP evaluation in the centralised procedure, but EMA final opinion to the European Commission is always given by the Committee for Human Medicinal Products (CHMP).

Two new procedures specific for CAT have been established in the European Regulation 1394/2007: ATMP classification [7] and certification of quality and non-clinical data [8]; the latter is available for SME only.

European Regulation 1394/2007 also contain two very important legal requirements for ATMP: i) long term follow-up of safety and efficacy, in order to build up knowledge on ATMP long term effects [9], and ii) an active traceability system enabling to track the ATMP used to the patient who received it, and vice-versa, for 30 years after ATMP expiry date [10].

Development of medicines includes basically two steps: preclinical and clinical development. The first part includes designing the substance/molecule that represents the medicine, proving its activity and testing its safety in a preclinical model, while the latter part includes translating those results into human subjects by means of clinical trials.

As for any other medicine, in Europe clinical trials with ATMP are covered by the Directive 2001/20/EC [6], that stipulates that for all medicines, clinical trial approval is the responsibility of Competent Authority in each European Member State (MS). Therefore clinical development takes place at national level. For any given clinical trial to be performed in a given MS, the EU Member State performs a separate evaluation and authorization procedure. This is also the case when a multinational trial is to be carried out, which may represent a difficult task if reviewers have divergent opinion in the different EU MS on the same clinical trial proposal. Procedures and initiatives have been put in place by EMA and national Competent Authorities to decrease the chance that such divergences occur and to facilitate an efficient translation of research discoveries into effective ATMP.

EMA and national Competent Authorities are also concerned that patients are offered SC-based medicinal products only under controlled conditions, such as e.g. in clinical trials or if market authorized. To ensure patients' safety, SC-based medicinal product development should comply with the highest standards, as for any investigational medicinal product, under the supervision of statutory regulatory bodies.

Thus a number of guidance documents (guidelines or reflection papers) describing quality, preclinical and clinical requirements for CPMP/TEP as well as for GTMP, have been produced by EMA to help applicants in developing their products. All guidance documents are available through the EMA website [11].

The main guidance documents for CTMP/TEP is the guideline on human cell-based medicinal products [12], while for GTMP it is the guideline on quality, preclinical and clinical aspects of gene transfer medicinal products [13].

Other guidance documents are available, covering aspects such as for example: risk based approach [14], chondrocyte-based CTMP [15], potency testing of cell-based immunotherapy medicinal products for the treatment of cancer [16], clinical aspects related to TEP [17], genetically modified cells [18], risk of germ-line transmission for GTMP [19], long term follow up for GTMP [20], environmental risk assessment for GTMP [21], non-clinical studies required before first clinical use of GTMP [22].

CAT has recently produced a reflection paper [23] that covers specifically stem cell (SC)-based ATMP. This reflection paper addresses all medicinal products that are presented for marketing authorization and that use any types of SC as starting material, regardless of SC differentiation status in the final product.

### 11.3 Stem Cell-Based ATMP

SC therapy holds the promise to treat degenerative diseases, cancer and repair of damaged tissues for which there are currently no or limited therapeutic options. SC-based ATMP in general can be classified as CTMP or TEP; if they are genetically modified, they are classified as GTMP. When they contain a MD, they are considered as combined ATMP.

SC-based ATMP can be obtained from adult stem cells or pluripotent stem cells, such as mesenchymal/stromal stem cells (MSC), hematopoietic stem cells (HSC), tissue-specific progenitor cells.

They can be also prepared from human embryonic stem cells (hESC) or induced pluripotent stem cells (iPSC).

Although stem cells share the same principal characteristics of potential for self-renewal and differentiation, SC-based medicinal products do not constitute a homogeneous class. Instead, they represent a spectrum of different cell-based products for which there is a variable degree of scientific knowledge and clinical experience available. For example, while MSCs or HSCs have been more extensively used for therapeutic purposes, this is not the case for hESCs or iPSCs.

Despite their clinical potential, SC-based ATMP bear also potential risks, that require a thorough evaluation before clinical use. Different levels of risk can be associated with specific types of SC. For example, the risk profile associated with iPSCs is expected to be different from those of adult SC (e.g. MSCs or HSCs) for which a substantial amount of clinical experience has already been gained.

The risk profile of SC-based ATMP depends on many risk factors, such as for example the type of stem cells, their differentiation status and proliferation capacity, *in vitro* manipulation steps, the route of administration and the intended site for clinical effect, the irreversibility of treatment or on the other hand the risk of cell loss, the long-term survival of engrafted cells.

The risks so far identified in clinical experience or the potential risks (i.e. those observed in animal studies) include tumour formation, unwanted immune responses and the transmission of adventitious agents.

Cell plasticity and product differentiation might also affect results generated during development, therefore it is expected that nonclinical and clinical studies are performed with well defined and characterized product so that results can be better interpreted.

## **11.4 Quality Issues for Stem Cell-Based Product Development**

The risk of transmitting adventitious agents, such as viruses or TSE agent, is common to all biological medicinal products.

Such risk is to be dealt with by building the safety of the final product from the safety of starting cells and raw materials. Therefore, screening of donors [24, 25] and of all reagents that are used in the production process [26] for presence of infectious agents is a mandatory activity.

Based on their characteristics of unlimited self-renewal and high proliferation rate, SC are often defined as cells able to form teratomas *in vivo*. Therefore, inherent with SC therapy is the risk of tumorigenicity. To control this risk, lineage-commitment before administration to the patient is a desirable characteristics of a SC product. To obtain the intended lineage-committed cell population, production process is critical.

Process factors (e.g. separation methods, growth factors, serum) as well as conditions and duration of *in vitro* culture can affect cell population composition and differentiation capacity *in vivo*, thus affecting also the mode of action. Therefore, impact of those factors should be carefully taken into consideration when planning and executing production process as well as quality controls. Critical manufacturing steps that are employed to reach required differentiation stage should be controlled with relevant markers to ensure the intended phenotype is maintained.

Since identity of the SC-based ATMP is defined by self renewal capacity (proliferation) and expression of specific markers, and the starting cell material (*i.e.* bone marrow, fat tissue, umbilical cord blood) is often a mixed cell populations, identity of the cell population as well as the heterogeneity profile of final product should be carefully defined and characterized. Several markers can be employed to establish identity, investigating cell type, lineage commitment, terminal differentiation and/or functionality. Whatever the test method chosen, the cell identity markers should be specific for the intended cell population and should be based on biological or molecular mechanism of therapy.

For pluripotent SC as well as somatic SC there is a risk of genomic instability in culture. Culture conditions (e.g. feeder cells and excipients) influence SC genomic stability. Therefore, to decrease such risk the presence of proliferative and pluripotent cells tolerated in the final product should be measured by means of e.g. cytogenetic analysis, telomerase activity, proliferative capacity, senescence, etc., and limited.

Biological activity (i.e. potency) of SC-based ATMP can be investigated by means of expression of relevant macromolecules, such as for example growth factors, enzymes, cytokines, and/or formation of extra cellular matrix cellular structures, and/or cell-cell interactions (e.g. immune activation/inhibition), and/or differentiation or self-renewing capacity or migration. *In vivo* functional assays may also be employed.

More probably, a combination of different assays may be needed to confirm the potency of a SC-based product. Whatever the assays chosen, they should be utilized both at quality and non-clinical level.

## 11.5 Non Clinical Issues for Stem Cell-Based Product Development

As compared to cell-based medicinal products that contain only differentiated cells, for SC-based medicinal product non-clinical evaluation may need to be more substantial.

Non clinical studies should evaluate different aspects including proof of concept, biodistribution and microenvironment (*niche*), ectopic tissue formation, *in vivo* differentiation, immune rejection and persistence, tumorigenicity. Potential inflammatory/immune response to SC product is also very important, since it underlies the risk of stem cell elimination and of long term failure of treatment.

Notwithstanding a thorough quality control program, a SC-based product may still contain cells in an undifferentiated proliferative state, that bear the potential for tumor formation.

Therefore during development appropriate tests should be carried out to minimize risk of transformation and tumor formation, in particular when using hESC or iPSC, that have a relatively higher potential risk than other types of SC.

Both tumorigenicity and chromosomal stability should be evaluated in the SC product before initial clinical use.

Traditionally, preclinical studies for testing safety of medicines are carried out in animal models.

Even though animal models reflecting the addressed disease would be ideal, in practice this can be prevented by several limitations. In fact, not only the relevant model strain may not be available, but also large animal models may be preferable for studying surgically implanted products, or for long-term evaluation of tissue regeneration and repair or in those situations where the animal size, organ physiology or immune system is relevant for the clinical effect (e.g. regeneration of tissue). Very likely, more than one animal species or strains might be needed. *In vitro* models may also provide additional and/or alternative ways to address some specific aspects.

Ideally, the human cell product should be used, thus requiring immune-suppressed animals. However, for studying aspects such as e.g. persistence or functionality, homologous animal models might provide the most relevant system, even though predictiveness of such a model may be limited because of the still limited knowledge of the similarity between animal and human SC differentiation processes.

## **11.6 Clinical Issues for Stem Cell-Based Product Development**

Ideally, nonclinical evidence on the proof-of-concept and safety of the SC-based product is expected before administration to humans.

In practice, as discussed above, there may be cases where sufficient nonclinical data cannot be obtained. In such cases the evidence should be generated in clinical studies by including additional end points for efficacy and safety, for instance to address the effect of an altered microenvironment (e.g. by inflammation, ischemia).

Clinical studies should evaluate different aspects including proof-of-concept, mode of action, dose finding, biodistribution, persistence, ectopic presence of SC product, safety and long term efficacy.

The mode of action of a SC- based product may be directly dependent on the stem cell population, on molecules secreted by the cells or on their engraftment in the host tissue.

Studies to follow the cells during the clinical studies, i.e. to assess biodistribution of SC product, may be important, depending on the SC product risk profile and its mode/site of administration. Due to a number of circulating SC higher than in physiological condition, abnormal distribution may occur leading to ectopic engraftment in non-target tissues.

On the other hand, such studies may be very imposing on the patients and in practice are hampered by the lack of suitable non invasive tracers.

Developing and validating new non-invasive methods for biodistribution studies in humans as well as markers or tracers for tracking cells in clinical studies is a highly desirable activity for future development of the field.

A specific safety concern relates to the SC ability to form teratomas. If a tumor is observed in a treated patient, then an investigation (e.g. genetic analysis) on whether it is due to SC product or to endogenous causes should be carried out.

From the clinical efficacy point of view, it is necessary to set up appropriate structural and morphological endpoints. Those should enable to study tissue regeneration, repair or replacement both at short term and at long term. It should be considered that for SC-based products impairment of efficacy is also a safety issue.

## 11.7 Conclusion

Stem cell therapy may represent great hope for many diseases and degenerative conditions, but a thorough evaluation of quality as well as safety and efficacy characteristics of the SC- based medicinal product is critical during clinical development in order to obtain a safe and efficacious SC-based ATMP. Developers of SC-based products are strongly encouraged to engage in dialogue with the CAT/EMA as well as with national Competent Authorities at an early stage of this process.

The cooperation between all the actors in the development process is crucial to contribute in the continuous effort to protect the European patients, while helping in developing safer and more efficacious SC- based ATMP.

## References

- [1] EU Regulation 1394/2007, Official Journal of the European Union L 324/121, 10/12/2007
- [2] Annex 1, part IV to Dir 2001/83/EC as amended in Directive 2009/120/EC, Official Journal of the European Union L 242/3, 15/9/2009
- [3] EU Regulation 1394/2007, art 2c
- [4] EU Regulation 1394/2007, art 2d
- [5] EU Reg. 726/2004, Official Journal of the European Union L 136/1, 30/04/2004
- [6] Directive 2001/20/EC, Official Journal of the European Communities, L121/34, 1/5/2001



- [7] EU Regulation 1394/2007, art 17
- [8] EU Regulation 1394/2007, art 18
- [9] EU Regulation 1394/2007, art 14
- [10] EU Regulation 1394/2007, art 15
- [11] <http://www.ema.europa.eu>
- [12] CHMP/410869/2006 Guideline on human cell-based medicinal products
- [13] CPMP/BWP/3088/99 Note for Guidance on quality, preclinical and clinical aspects of gene transfer medicinal products
- [14] CAT/CPWP/686637/2011 Guideline on Risk-based approach according to Annex I, part IV of Directive 2001/83/EC applied to Advanced Therapy Medicinal Products
- [15] EMA/CAT/CPWP/568181/2009 Reflection paper on *in-vitro* cultured chondrocyte containing products for cartilage repair of the knee
- [16] EMEA/CHMP/BWP/271475/2006 Guideline on potency testing of cell based immunotherapy medicinal products for the treatment of cancer
- [17] EMA/CAT/CPWP/573420/2009 Draft reflection paper on clinical aspects related to tissue- engineered products
- [18] EMA/CAT/GTWP/671639/2008 Guideline on quality, non-clinical and clinical aspects of medicinal products containing genetically modified cells
- [19] EMEA/273974/2005 Guideline on non-clinical testing for inadvertent germline transmission of gene transfer vectors
- [20] EMEA/CHMP/GTWP/60436/2007 Guideline on follow up of patients administered with gene therapy medicinal products
- [21] EMEA/CHMP/GTWP/125491/2006 Guideline on scientific requirements for the environmental risk assessment of gene therapy medicinal products
- [22] EMEA/CHMP/GTWP/125459/2006 Guideline on the non-clinical studies required before first clinical use of gene therapy medicinal products
- [23] EMA/CAT/571134/2009 Reflection paper on stem cell-based medicinal products
- [24] Directive 2004/23/EC, Official Journal of the European Communities, L102/48, 7/4/2004
- [25] Directive 2006/17/EC, Official Journal of the European Communities, L38/40, 9/2/2006
- [26] European Pharmacopoeia chapter 5.1.7 Viral Safety

---

# Index

---

## A

Antigen presenting cells 81  
Automation 98, 99, 104

## B

Bioactive 1, 2, 14, 25, 49  
Biocompatibility 1, 12, 38, 45  
Biomaterials 1, 5, 12, 37, 45  
Bioreactor 97, 98, 101  
Bone marrow 57, 80, 178  
Bypassing pluripotency 126,  
128, 129

## C

Cancer 7, 82, 107, 174  
Cancer stem cells 80, 109  
Cardiac precursor cells 26,  
27  
Cell processing facility 97, 101  
Cell sheet 97, 103, 104  
Cerium dioxide 25, 26  
Collagen 1, 15, 43, 48  
Cytokine 28, 80, 81, 179

## D

Derivation strategies 118  
Differentiation 2, 47, 53, 67, 108,  
180  
Direct reprogramming 118, 119,  
126, 127  
Drug delivery systems 1, 8, 16

## E

Embryonic stem cells 53, 80, 118,  
177  
Ethics 117, 121, 175

## F

Flexible modular platform 97,  
103, 104

## H

Hedgehog signaling 107, 110,  
112

## I

Immunosuppression 80  
iPS 53, 99, 123, 124  
iPSC 117, 118, 123, 126, 177, 179

## L

Layered silicates 1, 7, 8

## M

Manufacturing facility 97, 103  
Melanoma 82, 107, 108, 112  
Mesenchymal stem cells 57, 79,  
80, 185  
Microenvironment 29, 55, 80, 85  
Multipotency 29, 55, 80, 118

## N

Nanocomposites 1, 5, 10

**P**

Patenting 117, 124, 127, 128  
Pluripotency 55, 59, 117, 126,  
128  
Potentiality 54, 119, 125, 127

**R**

Reactive oxygen species 25,  
27, 28  
Regenerative medicine 37, 41, 53,  
97

**S**

Scaffolds 1, 25, 175  
Self-renewal 27, 70, 97, 109,  
112, 177, 178

Spermatogonial stem cells 53,  
54, 55  
Stem cells 3, 53, 59, 80,  
113

**T**

Tetraploid complementation 118,  
119, 121, 123  
Tissue engineering 1, 70, 97,  
185

---

## Editor's Biographies

---

**Mayuri Prasad** is currently a post doctorate fellow in the Haematological Research Laboratory (HRL) that was established in 2007 and is part of Department of Haematology at Aalborg University Hospital in Denmark. She has done her PhD from the Laboratory for Stem Cell Research, Department of Health Science and Technology, Aalborg University. Major field of interest include embryonic stem cell proliferation and differentiation in hypoxia, ion channels involved in mesenchymal stem cell proliferation in hypoxia, *in vitro* dose response studies of anti-neoplastic drugs, aimed at the stratification of patients with B cell malignancies.

**Paolo Di Nardo**, after his doctorate degree in Medicine and Cardiology, expanded his knowledge in basic and applied sciences in different Italian and foreign laboratories. At present, he has teaching appointments at the Medical School and at the Department of Biology of the University of Rome Tor Vergata. Furthermore, he is Vice-Head of the Cardio-respiratory Clinic of the same University. Scientific advisor of major international organizations and member of international scientific societies, he has founded the Laboratory of Cellular and Molecular Cardiology and is Scientific Director of the Centre of Space Bio-Medicine of the University of Rome Tor Vergata. He has also founded the Japanese-Italian Tissue Engineering Laboratory (JITEL) at the Tokyo Women's Medical University and the Canadian-Italian Tissue Engineering Laboratory (CITEL) at Winnipeg (Manitoba). Co-founder of the Italian Society of Cardiovascular Research and of the (Italian) National Institute for Cardiovascular Research. Member of international scientific societies, he is author of several papers published in peer-reviewed international scientific journals. Among others, in 1994, he organized the first international Congress in which the possibility of heart regeneration in mammals has been analyzed. Since then, his major interests have been in cardiac pathophysiology, myocardial effects of omega-3 fatty acids and stem cell and tissue engineering technology.